JPLCA$_T$

Volume 8, Part A-1, No. 2, February 1970

Journal of Polymer Science

Part A-1: Polymer Chemistry

Contents

(continued inside)

Published by INTERSCIENCE PUBLISHERS a division of John Wiley & Sons, Inc.

Journal of Polymer Science **Part A-1: Polymer Chemistry**

Contents (continued), Vol. 8

(continued on inside back cover)

The Journal of Polymer Science is published in four sections as follows: Part A-1, Polymer Chemistry, monthly; Part A-2, Polymer Physics, monthly; Part B, Polymer Letters, monthly; Part C, Polymer Symposia, irregular.

Published monthly by Interscience Publishers, a Division of John Wiley & Sons, Inc., covering one volume annually. Publication Office at 20th and Northampton Sts., Easton, Pa. 18042. Executive, Editorial, and Circulation Offices at 605 Third Avenue, New York, N. Y. 10016. Second-class postage paid at Easton, Pa. Subscription price, $325.00 per volume (including Parts A-2, B, and C). Foreign postage $15.00 per volume (including Parts A-2, B, and C).

JOURNAL OF POLYMER SCIENCE: PART A-1 VOL. 8, 289–293 (1970)

Chain Twisting in Long-Chain Aliphatic Compounds and Polyethylene

H. K. WELSH, *Division of Applied Physics, National Standards Laboratory, CSIRO, Sydney, Australia*

Synopsis

Rate parameters for dielectric relaxation and the thermal properties of long-chain molecular systems are shown to provide evidence for chain twisting at chain lengths shorter than previously suggested. Comparison of the temperatures of maximum absorption at 1 Hz for mechanical and dielectric relaxation suggests that the underlying motion is not the same for the two observed quantities. The evidence for relaxation in polyethylene is shown to be compatible with this suggestion.

INTRODUCTION

Several models for the motion which underlies the α_c dielectric and mechanical relaxation in chain-folded polymers have been discussed in detail by Hoffman et al.[1] The models require rotation of straight lengths of chain, coupled in some fashion, to movement of the folds between which they lie. In each model the straight lengths may behave as rigid rods or as rods with internal twisting. For rigid rods the activation energy is expected to be a linear function of the chain length, while for rods which twist a limiting energy will be approached as the chain length increases. The way in which the limit is approached may depend on the detailed shape of the potential, even for comparatively simple symmetrical double-well systems.

A guide to the importance of twisting is given by relaxation parameters of aliphatic molecular systems, regarded as short polymers. Data may be analyzed by plotting as a function of chain length either the activation energy and frequency factor or the temperature of maximum absorption at a fixed frequency. The effect of chain twisting is more obvious if the first method is used. An extensive collection[2] of relaxation rate parameters in solid solutions of polar long-chain compounds in normal paraffins and of the polar compounds in polycrystalline form provides material suitable for analysis. The second, less satisfactory method is necessary for examination of mechanical relaxation in normal paraffins which has been studied[3] only at 1 Hz over a range of temperature.

DIELECTRIC RELAXATION

Grouping data for solutions of ketones in hydrocarbons with some of the data for polycrystalline esters and ethers, Hoffman et al. conclude that

linear dependence on chain length of both activation energy and frequency factor holds for chains with at least 37 atoms (their Fig. 13). The implicit assumption that the same motion is responsible for dielectric relaxation in both types of system requires examination. In the solid solutions, the polar molecule is shorter by one atom than the nonpolar solvent. It is plausible that the solute molecule moves between two equivalent equilibrium positions related by a screw rotation of 180°, as in the α_c-B model.[3] In the molecular crystals, either screw or simple rotation necessarily gives potential minima of unequal depth. It is now established[4] that absorption in these systems is sensitive to chemical impurities and lattice perfection. The observed motion appears to be movement of host molecules near defects, which reduces the inequality in depth of potential wells, rather than the movement of impurities in the host lattice. Whether defects modify screw or simple rotation has yet to be determined. In either case, the difference in shape of the potential barrier in solutions and molecular crystals is expected to lead to different functional dependence on chain length if twisting is significant.

If the solid solution and molecular crystal data are treated separately, as in the original plot by Meakins[2] (his Fig. 12), it is clear that the activation energies for solutions of symmetrical ketones and ethers in normal paraffins approach a limit for chain lengths greater than about 30, a limit which is different for each chemical class. This conclusion is supported for ketone solutions by data for $(C_{17}H_{35})_2CO$ and $(C_{29}H_{59})_2CO$ in polyethylene, for which activation energies of 19 and 24 kcal/mole are reported.[5] Although caution is required because of the change in solvent characteristics, the activation energy for the shorter ketone agrees well with that reported for the same chain length by Meakins. It suggests that the difference between the experimental value for the longer ketone and the value about 40 kcal/mol, estimated by extrapolation of the linear plot given by Hoffman et al. is significant, indicating a considerable effect from chain twisting. It is noted that the logarithms of the frequency factor, 19 and 20, respectively, are compatible with a linear relationship to activation energy,[2] rather than to chain length,[1] a further indication of chain twisting. These results were included by Hoffman et al. in the fixed frequency analysis, where they fall in a chain length region which is not yet sensitive to chain twisting. Indeed, it appears from their Figure 12 that chain twisting has little effect for chain lengths less than 90 or 100.

Thus it is seen that, if attention is restricted to groups in which a common mechanism is expected to occur, as in the solutions, dielectric relaxation data strongly suggest the influence of chain twisting on relaxation parameters at quite short chain lengths. The precise form of the functional relation to chain length is not well defined experimentally, but there is an indication that it may depend on the chemical type of the polar solute. Further work is needed before full use can be made of the molecular crystal data which are representative of several types of ester or ether whose solid-state structural relationships are not known. Furthermore, recent work[6]

has shown that differences in absorption characteristics between polycrystalline and single crystal samples may be complex.

THERMAL PROPERTIES

As well as the effect on dynamical properties, chain twisting may influence thermal properties such as the entropy of the order–disorder transition[7] well established in paraffins. If chains behave as rigid rods, the entropy will be independent of chain length, with a value determined by the number of orientations available to each molecule. If twisting is effective, the entropy will be a function of the chain length. An indication of chain twisting of this kind is important because it shows that some chains are twisted at equilibrium and not just when crossing a barrier.

From the entropies available at the time, Hoffman and Decker[8] concluded that the transition entropy was constant for chain lengths between 20 and 30. However, if entropies are calculated from the latent heats of transition collected by Broadhurst,[9] it is apparent (Fig. 1) that, for both odd and even hydrocarbons, the entropies are strongly dependent on chain

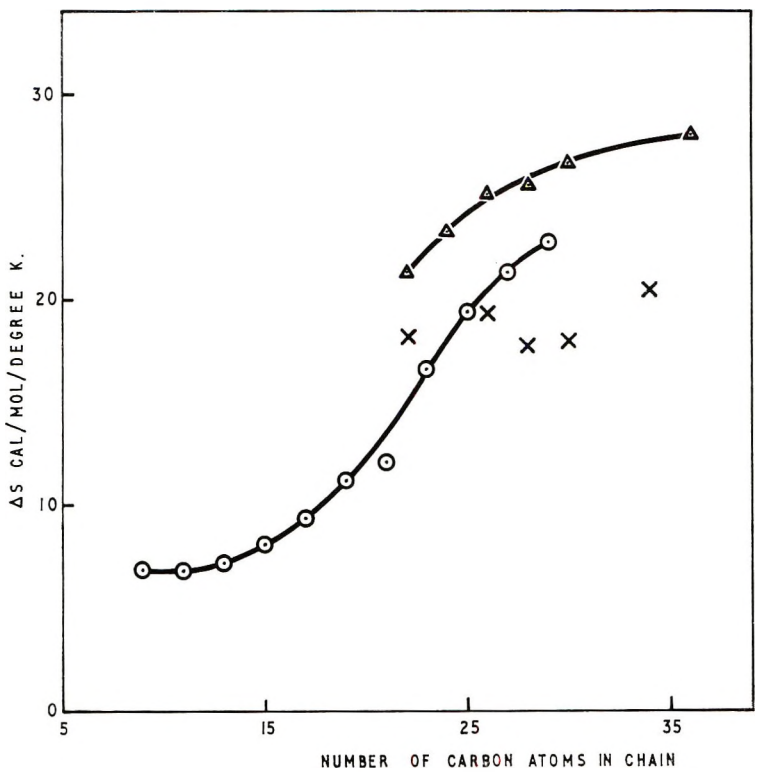

Fig. 1. Entropy of transition in normal paraffins as a function of chain length: (⊙) odd paraffins; (△) even paraffins, calculated from Broadhurst;[9] (×) even paraffins, quoted by Hoffman and Decker.[8]

length. Although detailed analysis is not possible because of the absence of necessary data, the chain length dependence appears incompatible with rigid rod behavior and supports chain twisting at short chain lengths as an equilibrium phenomenon.

COMPARISON OF MECHANICAL AND DIELECTRIC RELAXATION

The fixed frequency data for mechanical relaxation in paraffins do not show any effect from the well known[9] difference in crystal structure between the even and odd series. On reduction to the same form, the dielectric data show no distinction between solutions and molecular crystals, despite that shown in activation energies and frequency factors. Nevertheless, there is a clear difference in trend between the two sets of data, even when the dielectric data excluded by Hoffman et al. are added. It appears that this difference is not structural in origin, indicating that it is incorrect to assume that the same motion underlies both phenomena. An active dielectric process requires overall chain rotation, which the present work shows to interact with internal twisting. If the active mechanical process is not the same, it may have a different, perhaps linear, dependence of relaxation parameters on chain length which the available data are inadequate to demonstrate.

RELAXATION IN POLYMERS

The possibility that mechanical and dielectric relaxations arise from different modes of motion can be transferred reasonably from the long-chain molecular systems to polyethylene. In the dielectric case, measurements on oxidized polyethylene yield activation energies between 25 and 30 kcal/mole in single-crystal mats[10] and bulk samples,[11] with clear evidence for chain twisting in the fixed frequency analysis. By contrast, the mechanical relaxation has an activation energy quoted[1] as 43 kcal/mole in mats of single-crystal polyethylene and even higher (60 and 168 kcal/mole) in bulk samples. The temperatures of maximum absorption at 1 Hz in polymer samples are represented adequately by extrapolation from the molecular crystal data, assuming linear dependence of relaxation parameters on chain length.

The large difference between the activation energies for mechanical and dielectric relaxation supports different extrapolations of the molecular crystal fixed frequency data to the polymer systems. Together they appear to preclude identical mechanisms for both relaxations.

CONCLUSION

It is clear that proper selection of data strongly suggests that chain twisting is important at short chain lengths in dielectric relaxation. Confirma-

tion requires measurement of relaxation parameters for systems with molecular chains having about fifty carbon atoms.

Proof of the identity of mechanism in mechanical and dielectric relaxation requires measurements by both methods on the same systems at several frequencies so that activation energies may be compared.

References

1. J. D. Hoffman, G. Williams, and E. Passaglia, in *Transitions and Relaxations in Polymers* (*J. Polym. Sci. C*, **14**), R. F. Boyer, Ed., Interscience, New York, 1966, p. 173.
2. R. J. Meakins, *Progress in Dielectrics*, Vol. 3, Heywood, London, 1961, p. 153.
3. K. H. Illers, *Rheol. Acta*, **3**, 194 (1964).
4. J. S. Dryden and H. K. Welsh, *Trans. Faraday Soc.*, **60**, 2135 (1964).
5. C. A. F. Tuijnman, *Polymer*, **4**, 315 (1963).
6. H. K. Welsh, *Trans. Faraday Soc.*, **63**, 1959 (1967).
7. H. Fröhlich, *Trans. Faraday Soc.*, **40**, 498 (1944).
8. J. D. Hoffman and B. F. Decker, *J. Phys. Chem.*, **57**, 520 (1953).
9. M. G. Broadhurst, *J. Res. Nat. Bur. Stand.*, **66A**, 241 (1962).
10. Y. Ishida and K. Yamafuji, *Kolloid-Z.*, **202**, 26 (1965).
11. C. A. F. Tuijnman, *Polymer*, **4**, 259 (1963).

Received January 19, 1968

JOURNAL OF POLYMER SCIENCE: PART A-1 VOL. 8, 295–300 (1970)

Alternating Copolymerization of Polar Vinyl Monomers in the Presence of Zinc Chloride. III. NMR Study of Methyl Methacrylate–Styrene Copolymer

SHIGERU YABUMOTO, KIYOSHI ISHII, and KOICHIRO ARITA,
Central Research Laboratory, Daicel Limited, Iruma-gun, Saitama, Japan

Synopsis

The copolymer composition curve of the methyl methacrylate–styrene copolymer obtained by the copolymerization in the presence of $ZnCl_2$ has more alternating tendency than that of ordinary methyl methacrylate–styrene copolymer obtained by radical copolymerization. The fine structure of the copolymer was examined by NMR, and the mechanism of the propagation step of the copolymerization in the presence of $ZnCl_2$, which was proposed in the first report of this series, was verified.

INTRODUCTION

In the first report of this series,[1] it was shown from a kinetic point of view that the copolymerization of acrylonitrile (AN) with styrene (St) in the presence of $ZnCl_2$ has a strong alternating tendency; in a second paper[2] some properties indicative of an alternating copolymer structure were investigated.

Recently determination of the fine structure of methyl methacrylate (MMA)–St copolymer by NMR spectrometry was reported by Ito and Yamashita.[3] In the present work the MMA–St copolymer obtained by the copolymerization in the presence of $ZnCl_2$ was examined by NMR spectrometry; it was shown that monomer sequence distribution in the copolymer obtained in the presence of $ZnCl_2$ actually can be represented by apparent monomer reactivity ratios, as predicted in the first report of this series.

EXPERIMENTAL

Materials

Commercially available monomers were dried over anhydrous sodium sulfate and distilled in a stream of dry nitrogen.

$ZnCl_2$ was guaranteed reagent grade, and was used without further purification.

Copolymerization Procedure

$ZnCl_2$ was dissolved in MMA at a given concentration, and this solution and St were introduced into a glass tube in a stream of dry nitrogen. The glass tube was sealed off and maintained at a constant temperature to permit polymerization.

The resulting copolymer was purified by repeated dissolution in ethyl acetate and precipitation into methanol; elimination of $ZnCl_2$ was confirmed with an acetone solution of dithizone.

Copolymer Composition Analysis and Reactivity Ratios

All copolymerizations were carried out at less than 3% conversion. The copolymer obtained was fractionated into a cyclohexane-soluble portion and an insoluble portion. The copolymer composition was determined from the carbon content of the copolymer (F & M 185 Carbon Hydrogen Nitrogen Analyzer). Monomer reactivity ratios were determined by the line intersection method.[4]

NMR Spectra

NMR spectra were measured at 60°C with 7% solutions in carbon tetrachloride by use of a Japan Electron Optics 100MC Spectrometer (JNM-4H-100), with tetramethylsilane as an internal standard.

RESULTS AND DISCUSSION

The copolymerization of MMA with St took place easily on addition of $ZnCl_2$, and the copolymer obtained contained a cyclohexane-soluble portion and a cyclohexane-insoluble portion. It was shown by carbon content and IR spectra that the cyclohexane-soluble material was styrene homopolymer and the cyclohexane-insoluble part was the copolymer. The relative amounts of the cyclohexane-insoluable material obtained under various conditions are shown in Table I. It is obvious that cationic polymerization of styrene and thermally initiated radical copolymerization occurred simultaneously.

TABLE I
Relative Amounts of Cyclohexane-Insoluble Material

Sample	$ZnCl_2$/MMA (mole ratio)	MMA in the monomer feed, mole-%	Polymerization temperature, °C	Relative amounts of cyclohexane-insoluble material, wt-%
4ZMS10	0·21	10	60	15
4ZMS20	0·21	20	60	38
4ZMS50	0·21	50	60	33
4ZMS80	0·21	79	60	71
4ZMS90	0·21	89	60	81

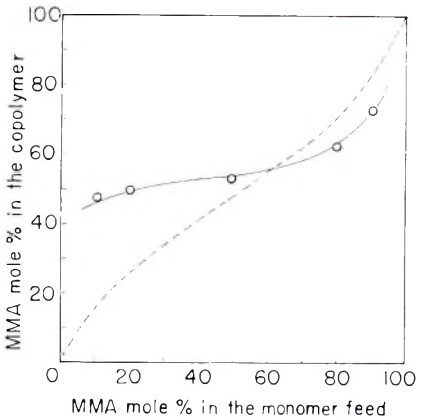

Fig. 1. Copolymer composition for MMA-St copolymerization(——) in the presence of $ZnCl_2$ at 60°C, $ZnCl_2$/MMA = 0.21 (mole ratio), r_1 = 0.19, r_2 = 0.02; (--) ordinary radical copolymerization, r_1 = 0.43, r_2 = 0.50.

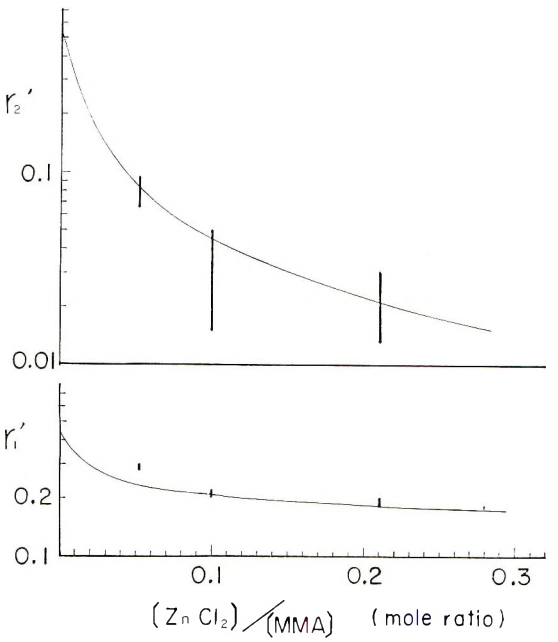

Fig. 2. Apparent monomer reactivity ratios vs. $ZnCl_2$ concentration.

Some examples of the composition of cyclohexane-insoluble part are shown in Figure 1 as a function of the monomer composition in the feed.

The composition of the copolymer indicates more alternating tendency than that of ordinary MMA–St copolymer, and the change of the apparent monomer reactivity ratios with the concentration of $ZnCl_2$ is shown in Figure 2.

The meaning of the apparent monomer reactivity ratios was discussed in detail in the first report of this series, and the equations which represent

the relation between apparent monomer reactivity ratios and the Q,e scheme were derived as follows:

$$r_1' = \frac{(1-t)^2 Q_1 \exp\{-e_1^2\} + t(1-t)(Q_2 + PQ_1) \times \exp\{-e_1e_2\} + t^2 PQ_2 \exp\{-e_2^2\}}{(1-t)Q_3 \exp\{-e_1e_3\} + tPQ_3 \exp\{-e_2e_3\}} \quad (1)$$

$$r_2' = \frac{Q_3 \exp\{-e_3^2\}}{(1-t)Q_1 \exp\{-e_1e_3\} + tQ_2 \exp\{-e_2e_3\}} \quad (2)$$

In the case of the MMA-St copolymerization in the presence of $ZnCl_2$, M_1 is MMA, M_2 is MMA·$ZnCl_2$ complex and M_3 is St, and t is defined by eq. (3):

$$t/(1-t) = [M_2]/[M_1] \quad (3)$$

The Q, e values of MMA and St are known from the literature,[5] and P, Q_2, and e_2 are unknown. These values were determined by a curve-fitting method in Figure 2 as $P = 14.8$, $Q = 13.5$, $e = 1.74$. The solid line in Figure 2 is the curve obtained from this calculation; this plot successfully explains the decrease of the apparent monomer reactivity ratios of the copolymerization with increase of the quantity of $ZnCl_2$ added. To calculate t in eq. (3) the composition of MMA·$ZnCl_2$ complex was assumed to be in a molar ratio of 2:1, on the basis of the results reported by Makishima et al.[6]

In the first report of this series it was concluded from a kinetic point of view that the monomer sequence distribution in the copolymer obtained by the copolymerization in the presence of a salt can be represented by apparent monomer reactivity ratios.

To verify this assumption an NMR study of the MMA–St copolymer obtained in the presence of $ZnCl_2$ (cyclohexane-insoluble) was carried out. A typical example of the NMR spectra is shown in Figure 3.

Recently several groups of workers[3, 7–9] reported NMR study of the MMA–St copolymer. Ito and Yamashita correlated the three peaks due to methoxy protons in the 6.4–7.8 τ region with a triad distribution along the copolymer chain, with the MMA unit as a center.

Since the peak due to methyne protons was assumed to overlap in the

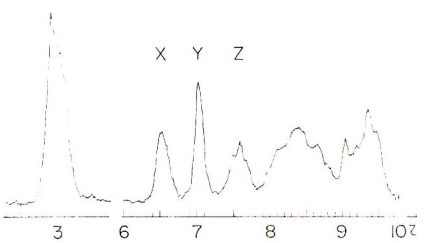

Fig. 3. NMR spectra of the MMA–St copolymer obtained in the presence of $ZnCl_2$; $ZnCl_2$/MMA = 0.30 (mole ratio), MMA/St = 1.0, 60°C.

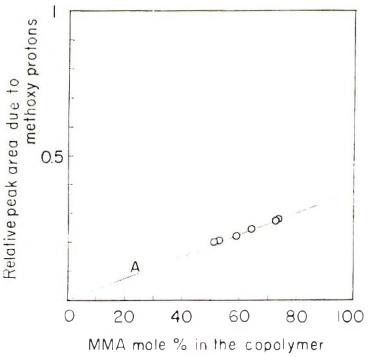

Fig. 4. Relative peak area due to methoxy protons vs. MMA content (○) calculated from carbon analysis; (——) theoretical.

peak Z in Figure 3, in calculating areas of X, Y, and Z, the area of Z was corrected by one fifth of the area of the peak of phenyl protons in the 2.8–3.2 τ region. The sum of the areas thus corrected is in good agreement with the areas for methoxy protons estimated from the carbon content in the copolymer, as shown in Figure 4.

Following the treatment by Ito and Yamashita, relative areas of X, Y, and Z are represented as follows:

$$F_X = P_3\{\mathrm{MMM}\} + 2(1 - \sigma)P_3\{\mathrm{MMS}\} + (1 - \sigma)^2 P_3\{\mathrm{SMS}\} \quad (4)$$

$$F_Y = 2\sigma P_3\{\mathrm{MMS}\} + 2\sigma(1 - \sigma)P_3\{\mathrm{SMS}\} \quad (5)$$

$$F_Z = \sigma^2 P_3\{\mathrm{SMS}\} \quad (6)$$

where M and S represent MMA and St units, respectively, $P_3\{\cdot\mathrm{M}\cdot\}$ is the mole fraction of the corresponding triad, and σ is a parameter of "co-isotacticity."[3] Each triad fraction is given by the probability of the addition of S to M radical (P_{MS}) as follows:

$$P_3\{\mathrm{MMM}\} = (1 - P_{\mathrm{MS}})^2 \quad (7)$$

$$P_3\{\mathrm{MMS}\} = P_3\{\mathrm{SMM}\} = P_{\mathrm{MS}}(1 - P_{\mathrm{MS}}) \quad (8)$$

$$P_3\{\mathrm{SMS}\} = P_{\mathrm{MS}}^2 \quad (9)$$

P_{MS} is represented by apparent monomer reactivity ratios as described in the first report:

$$P_{\mathrm{MS}} = \frac{[\mathrm{M}_3]}{[\mathrm{M}_3] + r_1'\{[\mathrm{M}_1] + [\mathrm{M}_2]\}} \quad (10)$$

F_X, F_Y, and F_Z were calculated by eqs. (4)–(10), and these values are compared with the values observed by NMR in Table II. In this calculation σ was assumed to be identical with that of the ordinary radical copolymerization of MMA with St,[3] i.e., $\sigma = 0.48$, and r_1' was estimated from the carbon content. The calculation is satisfactorily consistent with the NMR data, as shown in Table II.

TABLE II
Calculated and Observed Relative Areas of X, Y, and Z

Sample	$ZnCl_2$/MMA (mole ratio)	r_1'	Calculated from r_1'			Observed by NMR		
			F_X	F_Y	F_Z	F_X	F_Y	F_Z
1ZMS70	0.10	0.21	0.45	0.44	0.11	0.46	0.41	0.13
1ZMS90	0.10	0.21	0.68	0.29	0.03	0.70	0.26	0.04
4ZMS50	0.21	0.19	0.36	0.48	0.16	0.37	0.46	0.17
4ZMS80	0.21	0.19	0.52	0.40	0.08	0.51	0.41	0.08
4ZMS90	0.21	0.19	0.66	0.30	0.03	0.64	0.32	0.04
5ZMS50	0.30	0.18	0.35	0.48	0.17	0.37	0.45	0.18

Further, r_1' and σ were calculated from the values of F_X, F_Y, and F_Z by eqs. (4)–(10); for the 1Z series, $\sigma = 0.48$, $r_1 = 0.21$; for the 4Z series, $\sigma = 0.44$, $r_1' = 0.14$.

The r_1' values thus calculated are sufficiently consistent with the values estimated from the composition of the copolymers, and it is noteworthy that σ is almost identical with the value of ordinary radical copolymerization.

Thus it was shown that the monomer sequence distribution in the copolymer obtained by the copolymerization in the presence of a salt can be represented by apparent monomer reactivity ratios, at least in the case of the MMA-triad distribution in the MMA–St copolymer obtained in the presence of $ZnCl_2$.

The fact that the coisotacticity of the MMA–St copolymerization in the presence of $ZnCl_2$ is almost identical with that of ordinary MMA–St copolymerization indicates that steric control of the propagation step of MMA–St copolymerization by complexing with $ZnCl_2$ is invalid, as in the case with the homopolymerization of MMA in the presence of $ZnCl_2$.[11]

The authors wish to thank Daicel Limited for permission to publish this work. They also wish to thank Dr. Koichi Hatada for useful discussion and advice.

References

1. S. Yabumoto, K. Ishii, and K. Arita, *J. Polym. Sci. A-1*, **7**, 1577 (1969).
2. S. Yabumoto, K. Ishii, and K. Arita, *J. Polym. Sci. A-1*, **7**, 1683 (1969).
3. K. Ito and Y. Yamashita, *J. Polym. Sci. B*, **3**, 625 (1965).
4. F. W. Billmeyer, Jr., *Textbook of Polymer Science*, Interscience, New York, 1962, pp. 315–316.
5. G. E. Ham, *Copolymerization*, Interscience, New York, 1964, pp. 845–863.
6. S. Makishima, H. Hirai, and S. Okusawa, paper presented at the 18th Annual Congress of the Chemical Society of Japan, 1965, No. 3225.
7. F. A. Bovey, *J. Polym. Sci.*, **62**, 197 (1962).
8. A. Nishioka, Y. Kato, and N. Ashikari, *J. Polym. Sci.*, **62**, S10 (1962).
9. Y. Kato, N. Ashikari, and A. Nishioka, *Bull. Chem. Soc. Japan*, **37**, 1630 (1964).
10. H. J. Harwood and W. M. Ritchey, *J. Polym. Sci. B*, **3**, 419 (1965).
11. T. Otsu, B. Yamada, and M. Imoto, *J. Macromol. Sci.*, **A1**, 61 (1967).

Received September 5, 1968

JOURNAL OF POLYMER SCIENCE: PART A-1 VOL. 8, 301–318 (1970)

Mechanism of Cerium(IV) Oxidation of Glucose and Cellulose*

CHARLES R. POTTENGER† and DONALD C. JOHNSON,
The Institute of Paper Chemistry, Appleton, Wisconsin 54911

Synopsis

Cerium(IV) oxidations of model compounds for the hydroxylic functional groups of cellulose were conducted in 1.0*M* perchloric acid. Glucose, the model selected for the reducing end group, was oxidized 360 times faster than Schardinger β-dextrin, the model for anhydro-D-glucose repeating units. In the presence of a fourfold excess of glucose, stoichiometry indicated specific conversion to arabinose; the competitive oxidation of arabinose produced is insignificant. Specific C_1–C_2 bond cleavage was also indicated for 2-*O*-methyl-D-glucose, galactose, 2-*O*-methyl-D-galactose, and cellobiose. Anhydro-D-glucose units were oxidized predominantly by C_2–C_3 bond cleavage as shown by the identification of erythrose and glyoxal in hydrolyzates of cerium(IV) oxidized Schardinger β-dextrin and cellulose. Kinetic studies showed that chelate complexes were involved in oxidations of glucose, methyl β-D-glucopyranoside, 1,5-anhydro-D-glucitol, and Schardinger β-dextrin. The oxidations of glucose derivatives which differed with respect to substituents on C_1 and C_2 demonstrated the importance of the hemiacetal group and the presence of oxygen on C_2. For example, the relative rates of oxidation at 15°C for methyl β-D-glucopyranoside, 1,5-anhydro-D-glucitol, 2-deoxy-D-glucose, glucose, and 2-*O*-methyl-D-glucose are 1:1:12:360:1860, respectively. The mechanism of glucose oxidation is thought to involve formation of a chelate complex, disproportionation of the complex to form a free radical at either C_1 or C_2 and further rapid oxidation to 4-*O*-formyl-D-arabinose which is hydrolyzed in the reaction medium. General implications of the experimental results pertaining to initiation of vinyl graft polymerization on cellulose are discussed.

INTRODUCTION

The use of cerium(IV)–alcohol redox systems for chemical initiation of vinyl polymerizations has been studied in recent years.[1–14] Particular interest has been shown in the possible modification of cellulosic properties by grafting with selected vinyl compounds. The formation of free radicals on cellulose by cerium(IV) oxidation has been demonstrated by electron spin resonance.[13] The mechanism by which cerium(IV) generates free radicals is believed to involve the formation of a coordination complex between the oxidant and the hydroxyl groups of cellulose. The cerium(IV)–cellulose complex then disproportionates forming a free radical on

* Presented in part at the Spring Meeting of the American Chemical Society, San Francisco, Calif., April 1968.

† Present address: Potlatch Forests, Inc., Cloquet, Minnesota 55720.

the cellulose chain and cerium(III). Model compound studies of cerium(IV) oxidations of monohydric alcohols and 1,2-glycols support the postulated mechanism and suggest that the C_2–C_3 glycol and the C_6 hydroxyl of an anhydro-D-glucose unit may be preferred sites for free-radical generation.[2,9,15–17] However, other workers[6,11,12] have suggested that the reducing end groups are important sites for free radical formation.

Evidence for the formation of stable coordination complexes has been obtained by kinetic and spectrometric methods for cerium(IV) oxidations of many compounds in perchloric and nitric acids.[16–22] Complex formation in cerium(IV) oxidations in sulfuric acid solutions has been detected only in a few studies.[23–27] Reactions in sulfuric acid often follow second-order kinetics.[2,16,20,26–28] Muhammad and Rao[28] have suggested a direct oxidation mechanism for oxidations in sulfuric acid; however, Hintz and Johnson[16] point out the possibility that the oxidation proceeds through an intermediate complex where the equilibrium constant for complex formation is small.

The complex formed between cerium(IV) and a 1,2-glycol may be either a chelated or an acyclic species. When one considers the enhanced stability of chelate complexes[29–31] it seems reasonable that they will be formed when possible. Oxidations of monohydric alcohols,[16,19,21,32] which cannot form chelate intermediates, and 1,2-glycols[16,20,32] by cerium(IV) in 1.0*M* perchloric acid show that the equilibrium constants for complex formation are significantly larger for the 1,2-glycols. This increase is attributed to chelate stabilization of the cerium(IV)-1,2-glycol complexes. It was concluded[16,32] from studies of cerium(IV) oxidation of 1,2-cyclohexanediols and their monomethyl ethers that substitution of methyl for hydroxyl hydrogen apparently prevents chelate formation. However, the overall rates of oxidation for the 1,2-glycol and its monomethyl ether were about equal due to compensating differences in equilibrium constants for complex formation and disproportionation rate constants for the two compounds. In this work the course of cerium(IV) oxidations of D-glucose and other compounds related to glucose and to cellulose were evaluated by kinetic and product studies in 1.0*M* perchloric acid. The products of cellulose oxidation were also investigated.

EXPERIMENTAL

Source of Reactants

Commercially available analytical reagents were obtained when possible. D-Glucose (Mallinckrodt), Schardinger β-dextrin (Pierce), cellulose (Whatman Standard Grade), cellobiose (Eastman), D-galactose (Matheson, Coleman and Bell), D-ribose, and 2-deoxy-D-glucose (Pfanstiehl) were used without further purification. Methyl β-D-glucopyranoside (Pfanstiehl) was purified by digesting 20 min at 80°C in 1.0*M* sodium hydroxide followed by deionizing on a column of Amberlite MB-3 (Rohm and Haas) mixed anion–cation exchange resin. The methyl β-D-glucopyranoside was

recrystallized from methanol. The following compounds were prepared by literature procedures: 1,5-anhydro-D-glucitol,[33] methyl-2,3,4,6-tetra-*O*-methyl-β-D-glucopyranoside,[34] methyl-4,6-di-*O*-methyl-β-D-glucopyranoside,[35] 2,3,4,6-tetra-*O*-methyl-D-glucose,[36] 2-*O*-methyl-D-glucose,[37] and methyl β-D-galactopyranoside.[38]

Arabinose (Pfanstiehl), erythrose (K and K), erythritol (Pierce) and glyoxal (Matheson, Coleman and Bell) were used without further purification as standards in product analysis experiments.

Solutions of organic compounds were prepared by weighing out samples of pure compounds, using care to prevent absorption of moisture by hygroscopic samples. Triply distilled water was used in all solutions. All experiments were run in 1.0*M* perchloric acid. A stock solution, 0.05*M* cerium(IV) in 1.0*M* perchloric acid, was prepared by appropriate dilution of a solution of 0.5*M* cerium(IV) perchlorate in 6*M* perchloric acid (G. Frederick Smith).

Product Analysis

The stability of the glycosidic bond in the reaction medium was demonstrated. A 12.3% solution of methyl-2,3,4,6-tetra-*O*-methyl β-D-glucopyranoside in 1.0*M* perchloric acid showed no change in optical rotation after 159 hours at room temperature. Therefore, hydrolysis of glycosidic bonds did not occur under the reaction conditions used in this study.

Qualitative identifications of carbohydrate reaction products were made by paper chromatography, gas chromatography, and by preparation of derivatives. Arabinose and erythrose were identified by paper chromatography (Whatman No. 1 paper), authentic samples being used as references. The chromatographic solvents were ethyl acetate–pyridine–water (8:2:1, v/v) and ethyl acetate–acetic acid–formic acid–water (18:3:1:4, v/v). Paper chromatograms were visualized by using a three-stage dip of silver nitrate, sodium hydroxide, and sodium thiosulfate.[39]

Reaction mixtures were found to be free of suspected glyconic acids as shown by paper chromatography. Therefore, product analysis reaction mixtures were deionized on Amberlite MB-3 (Rohm & Haas) and concentrated before applying to paper chromatograms.

Glucose Oxidation

Arabinose produced by cerium(IV) oxidation of glucose was also identified by isolation of the compound by preparative paper chromatography (Whatman 3MM paper) and preparation of its diethyldithioacetal. The melting point and mixed melting point of the product diethyldithioacetal was 124–125°C (lit.[40] mp 125–125.5°C). The infrared spectrum of the product diethyldithioacetal was identical to that of authentic arabinose diethyldithioacetal.

Formic acid was qualitatively identified as a product of glucose oxidation by cerium(IV) in 1.0*M* perchloric acid. This determination was made by

collecting the distillate from room temperature evaporation of a glucose oxidation mixture and analyzing by the procedure of Feigl.[41]

The stoichiometry of glucose oxidation by cerium(IV) was established by determining the yield of arabinose. The method used to establish the yield of product involved the oxidation of 5.550×10^{-3} mole glucose by 2.775×10^{-3} mole cerium(IV) in 1.0*M* perchloric acid at 20.0°C. The reaction mixture was neutralized with potassium hydroxide, filtered to remove potassium perchlorate, and deionized using Amberlite MB-3 mixed anion-cation exchange resin. After concentrating on a rotary vacuum evaporator, the neutral solution containing arabinose and glucose was analyzed by the method of Saeman et al.[42]

Cellulose and Schardinger β-Dextrin Oxidations

Determination of products from reactions of cellulose or Schardinger β-dextrin required that the oxidized polysaccharides be hydrolyzed before analyses were made. Before hydrolysis, the oxidized polysaccharide was removed from the reaction medium. Oxidized Schardinger β-dextrin was found to form an insoluble complex with xylene. The complex was formed by adding several milliliters of xylene to the reaction solution and shaking vigorously. The xylene oxidized-Schardinger β-dextrin complex was then collected by filtration, washed with water to remove perchloric acid, and resuspended in water. The suspension was heated on a steam-bath until the solution became clear; this treatment removed the xylene destroying the complex.

Cellulose, which is insoluble in the reaction medium, was simply filtered and washed to free it of perchloric acid after oxidation.

The oxidized Schardinger β-dextrin was hydrolyzed by refluxing in approximately 0.7*N* sulfuric acid for 2 hr. The hydrolyzate was then neutralized with sodium hydroxide to pH 5 and concentrated for spotting on paper chromatograms.

Oxidized cellulose was hydrolyzed by dissolving in 72% sulfuric acid and then diluting to 9% sulfuric acid and refluxing for 4 hr.

A more complicated hydrolysis procedure was employed when studying oxidized cellulose in an attempt to establish reaction stoichiometry of the cerium(IV)-anhydro-D-glucose reaction. It has been shown[43] that the hydrolysis of periodate-oxidized starch is facilitated by the use of sulfur dioxide. In the hydrolysis of oxidized cellulose a 1-g sample was dissolved in 10 ml 72% sulfuric acid; after 20 min a solution of 17.5 g sulfur dioxide in 125 ml ice water was added to the oxidized cellulose solution in a Teflon-lined Parr Bomb.[44] The bomb was sealed and placed in an oven at 115°C. After 7 hr the bomb was removed from the oven and cooled. The sulfur dioxide was removed by low-pressure evaporation, and the solution was deionized by passing it through a column of Amberlite MB-3 mixed anion–cation exchange resin. The deionized hydrolyzate was concentrated and used to spot preparative paper chromatograms.

Hydrolysis of an unoxidized sample of Whatman Standard Grade cellu-

lose by the above procedure followed by qualitative paper chromatographic analysis showed that fructose was produced under these conditions.

Erythrose was identified by isolation of the compound from an oxidized cellulose hydrolyzate by preparative paper chromatography (Whatman 3MM paper) and gas chromatography of its trimethylsilyl derivative[45] on an SE-30 column at 135°C. After obtaining positive evidence for erythrose-TMS the sample was hydrolyzed to remove the TMS groups.[46] The erythrose was then reduced to erythritol[47] and the erythritol-TMS derivative was prepared. Positive identification of erythritol-TMS by gas chromatography provided further evidence for the presence of erythrose as a reaction product. Paper chromatography of hydrolyzates of oxidized Schardinger β-dextrin showed the presence of erythrose as was found for oxidized cellulose.

Glyoxal was qualitatively identified in hydrolyzates of oxidized cellulose and Schardinger β-dextrin by adding 10 ml of hydrolyzate to 40 ml 2*N* hydrochloric acid saturated with 2,4-dinitrophenylhydrazine. The precipitated 2,4-dinitrophenylhydrazones were analyzed by comparative thin-layer chromatography on Silica gel G (Brinkman). Analysis was conducted by use of two developers, benzene–tetrahydrofuran (93:7, v/v) and benzene–petroleum ether (3:1, v/v), and the product 2,4-dinitrophenylhydrazones were identical to the derivatives of known glyoxal.

Quantitative determination of the amount of erythrose recovered from the hydrolyzate of a cerium(IV) oxidized cellulose was accomplished using the method of Smith and Duke.[48] The hydrolyzate was separated by paper chromatography permitting isolation of glucose, fructose, and erythrose. The amounts of total hexose and erythrose were determined by oxidation with excess cerium(IV).

Rate Determinations

All kinetic experiments were run with the organic substrate in excess so that the reactions would be pseudo-first-order with respect to cerium(IV). Reaction rates were determined by following the absorbance of the reaction solution using a Cary Model 15 recording spectrophotometer. For reactions having rate constants lower than 10^{-2} sec^{-1}, the procedure previously described[16] was used. Reactions with rate constants greater than 10^{-2} sec^{-1} were determined using a technique where the reactants were mixed within the spectrophotometer cell. The required amount of oxygen-free oxidant solution, up to 0.25 ml of 0.05*M* cerium(IV) in 1.0*M* perchloric acid, was placed in the 1 × 1 cm spectrophotometer cell; then a glass tube of 1.5-mm inside diameter, bent as shown in Figure 1, was placed in the cell and the cell was placed in the spectrophotometer cell holder. A length of 1.5-mm outside diameter polyethylene tubing extended from the glass tube to a syringe outside of the cell compartment. The syringe was held in a special brass water jacket which permitted accurate temperature control of the substrate solution. Reactions were initiated by rapidly depressing the syringe plunger. Approximate mixing time for a 2.75-ml sample was

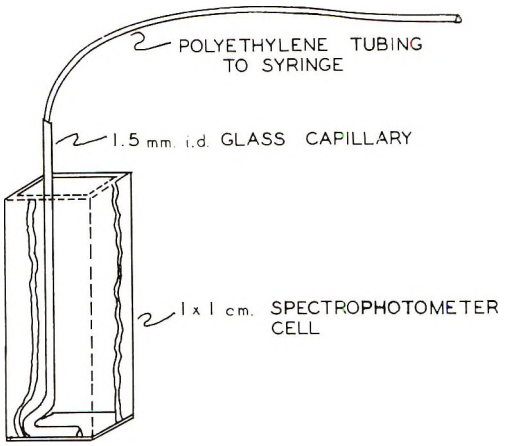

Fig. 1. Schematic view of mixing tube used for kinetic studies of rapid reactions in the Cary recording spectrophotometer.

1 sec. Temperature for all experiments was maintained constant by using a constant temperature bath. Water from the bath was circulated through the cell holder, cell compartment, and the syringe holder. Reaction temperatures reported are the mean of temperatures measured at the inlet and outlet of the cell jacket. Temperature fluctuations were less than $\pm 0.03°C$, and the reaction temperatures are conservatively estimated to be accurate to $\pm 0.1°C$.

The wavelength at which absorbance was followed was chosen to give a reasonably large initial absorbance. The magnitude of the initial absorbance is determined by the absorbance of the cerium(IV)-substrate complex. For reactions of Schardinger β-dextrin the wavelength used was 390 mμ; 425 mμ was used for all other compounds.

Pseudo-first-order rate constants were calculated from the slopes of the logarithm of absorbance *versus* time. All reactions of D-glucose and methyl β-D-glucopyranoside were run in duplicate, and the maximum deviation from the mean of the rate constants was 3.3%. Reactions of Schardinger β-dextrin and 1,5-anhydro-D-glucitol were not duplicated at all substrate concentrations, but at 0.040*M* substrate the reproducibility was 2.1 and 1.9%, respectively.

Since Hintz and Johnson[16] reported serious deviations from pseudo-first-order behavior in cerium(IV) oxidations of 1,2-cyclohexanediols in 1.0*M* perchloric acid when dissolved oxygen was present, all reactant solutions for this study were purged with nitrogen before mixing.

RESULTS AND DISCUSSION

Model Compounds for Cellulose

D-Glucose was selected as a model for the reducing endgroup of cellulose; methyl β-D-glucopyranoside and 1,5-anhydro-D-glucitol were selected as

models for the nonreducing endgroup. Schardinger β-dextrin (cycloheptaamylose) was chosen as the model for the anhydro-D-glucose repeating unit of cellulose. Kinetic studies of the cerium(IV) oxidations of these compounds were used to estimate the relative reactivity of the various hydroxyl groups occurring in cellulose. Further information concerning the reactivity of the C_1 group in aldoses was obtained by kinetic studies of D-galactose, cellobiose, 2,3,4,6-tetra-*O*-methyl-D-glucose, 2-*O*-methyl-D-glucose, 2-*O*-methyl-D-galactose, 2-deoxy-D-glucose and methyl β-D-galactopyranoside.

Product Analysis

The products obtained from the oxidation of glucose by cerium(IV) in 1.0*M* perchloric acid at 20.0°C are arabinose and formic acid. The yield of arabinose was determined and found to agree with calculations based on an assumed stoichiometry of 1 mole of arabinose formed per 2 moles of cerium(IV) reduced. The results are summarized in Table I. The actual difference from theory may be due to loss of a small amount of glucose by isomerization to fructose. Paper chromatography of oxidation mixtures supported this explanation.

Qualitative paper chromatography of 2-*O*-methyl-D-glucose oxidation products showed that the only detectable product was arabinose indicating that the C_1 group is involved in the oxidation even when C_2 contains a methoxyl group. This behavior was confirmed by studies of D-galactose and 2-*O*-methyl-D-galactose which yielded xylose on cerium(IV) oxidation. Cellobiose also yielded a disaccharide product, presumed to be 3-*O*-glucosyl-D-arabinose, which yielded glucose and arabinose on acid hydrolysis indicating that the oxidation involved attack at C_1 resulting in rupture of the C_1–C_2 bond.

Qualitative paper chromatography of the products of methyl β-D-glucopyranoside reactions showed the presence of erythrose and erythronic or glyoxylic acids.

The products obtained from hydrolyzates of cerium(IV)-oxidized cellulose and Schardinger β-dextrin are erythrose and glyoxal. Erythrose was identified by paper chromatography and by gas chromatography of its TMS-derivative. Glyoxal was identified by the isolation of its 2,4-dinitrophenylhydrazone from the hydrolyzates. Table I shows that the recovery

TABLE I
Determination of Reaction Products[a]

Substrate	Substrate concn, *M*	Ce(IV) concn, *M*	Products	Yield, %[b]
Glucose	0.070	0.035	Arabinose	109
Cellulose[c]	0.070	0.035	Erythrose	41

[a] All reactions run at 20.0°C in 1.0*M* perchloric acid.
[b] Assuming 2 moles cerium(IV) consumed per mole substrate oxidized.
[c] Concentration expressed on basis of anhydro-D-glucose units.

of erythrose was not in agreement with the assumed consumption of 2 moles of cerium(IV) per mole of 1,2-glycol oxidized. However, since no oxidation products other than erythrose and glyoxal were detected in these hydrolyzates, it seems reasonable to conclude that cleavage of the C_2–C_3 bond of anhydro-D-glucose units is the predominant reaction.

Complex Formation

Oxidations of organic substrates are generally believed to involve direct transfer of a single electron. It is clear that the reaction mechanism will include an interaction between the cerium(IV) and the organic substrate. Two types of mechanisms can be distinguished depending on the nature of this interaction. In the first mechanism a stable coordination complex is formed between the cerium(IV) and the organic substrate, S, in a rapid preliminary equilibrium step. The intermediate complex then disproportionates, unimolecularly, in the rate-determining step forming cerium(III) and a free radical, S·.

$$\mathrm{Ce(IV)} + \mathrm{S} \overset{K}{\rightleftarrows} \mathrm{Complex} \xrightarrow[\text{slow}]{k} \mathrm{Ce(III)} + \mathrm{S}\cdot + \mathrm{H}^+$$

The free radical is rapidly oxidized by a second mole of cerium(IV).

$$\mathrm{Ce(IV)} + \mathrm{S}\cdot \xrightarrow{\text{fast}} \mathrm{Ce(III)} + \mathrm{Product} + \mathrm{H}^+$$

The second mechanism assumes that the substrate is oxidized directly by cerium(IV). In this case the interaction takes place in the transition state:

$$\mathrm{Ce(IV)} + \mathrm{S} \rightarrow \{\mathrm{Ce(IV)}\text{---}\mathrm{S}\} \rightarrow \mathrm{Ce(III)} + \mathrm{S}\cdot + \mathrm{H}^+$$

As in the first mechanism, the free radical is rapidly oxidized by a second mole of cerium(IV).

The participation of intermediate complexes in the reaction mechanism can be evaluated from kinetic data. Duke[49] originally derived the general theory for oxidations involving coordination complexes and was the first to apply it to cerium(IV) oxidation.[17, 18] This theory was also discussed in detail more recently,[16] so only general considerations are necessary here. In particular, it is important to point out that both the coordination complex and the direct-bimolecular reactions predict pseudo-first-order behavior with respect to cerium(IV). However, the dependence of the pseudo-first-order rate constant on substrate concentration is different for the two alternate mechanisms. The coordination-complex mechanism predicts that a plot of the pseudo-first-order rate constant k' versus S will be nonlinear, concave downward, and pass through the origin. The direct-bimolecular mechanism predicts a linear relationship between k' and S.

It can be shown[16, 49] that if the coordination-complex theory applies, then the pseudo-first-order rate constant k' is related to the equilibrium constant for complex formation k and the rate constant for complex disproportionation k by the expression

$$1/k' = (1/k) + (1/kK\,[\mathrm{S}])$$

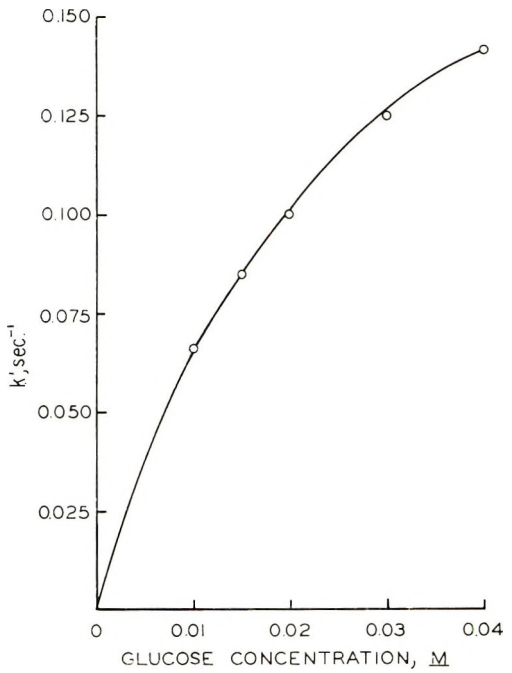

Fig. 2. Effect of glucose concentration on the pseudo-first-order rate constant at 20.0°C. Initial cerium concentration, 0.002*M*.

Therefore, further evidence for complex formation is obtained if a plot of $1/k'$ versus $1/[S]$ is linear with a positive intercept. From the values of the slope and intercept of such a reciprocal plot the equilibrium constant for complex formation, K, and the disproportionation rate constant, k, can be calculated.

The reactions of D-glucose, Schardinger β-dextrin, methyl β-D-glucopyranoside, and 1,5-anhydro-D-glucitol were studied in 1.0*M* perchloric acid at 20.0°C. The results are summarized in Table II. In each case, pseudo-first-order kinetics were observed. The pseudo-first-order rate constant was found to be independent of cerium(IV) concentration in a number of glucose oxidations. The plots of k' versus [S] for these reactions were definite curves indicating complex formation between cerium(IV) and these substrates. The reciprocal plots were linear, and equilibrium constants for complex formation and disproportionation rate constants were calculated from the slopes and intercepts of these plots. In Figures 2 and 3 the results for glucose are illustrated, and in Table III the values calculated for K and k are summarized.

In perchloric acid, complex formation with alcohols is indicated by a change of the normally yellow cerium(IV) solution to a red-brown. Ardon[19] developed a method for relating this color change to the equilibrium constant for complex formation for reactions proceeding through a 1:1 complex. It can be shown[16, 19] that the difference between the observed

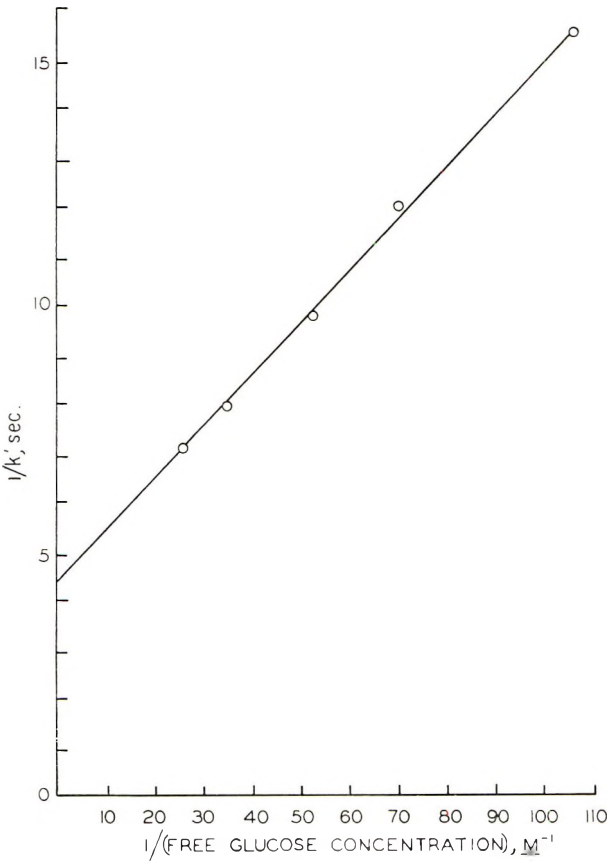

Fig. 3. Reciprocal plot for reaction of glucose with cerium(IV) in 1.0M perchloric acid at 20.0°C.

initial absorbance, A_0, and the absorbance, A_b, observed for a cerium(IV) solution of the same concentration without the organic substrate is related to the equilibrium constant for complex formation by the expression

$$1/(A_0 - A_b) = 1/\Delta\epsilon[\mathrm{Ce(IV)}]_0 + 1/\Delta\epsilon[\mathrm{Ce(IV)}]_0 K[\mathrm{S}]$$

where $[\mathrm{Ce(IV)}]_0$ is the initial cerium(IV) concentration and $\Delta\epsilon$ is the difference in the molar absorptivities of the complex and cerium(IV).

The equilibrium constant for complex formation can be calculated from the slope and intercept of a plot of $1/(A_0 - A_b)$ versus $1/[\mathrm{S}]$. The plots of $1/(A_0 - A_b)$ versus $1/[\mathrm{S}]$ are shown in Figure 4. Reliable data for glucose could not be obtained because of its high reactivity. The equilibrium constants obtained by this spectrometric method are given in Table III. These values agree reasonably well with the equilibrium constants obtained by the kinetic method and confirm the existence of the 1:1 complex.

The equilibrium constants for complex formation given in Table III can be compared to those obtained for other α-glycols and monohydric alcohols

TABLE II
Effect of Substrate Concentration for Reactions in 1.0*M* Perchloric Acid at 20.0°C[a]

Substrate	Substrate concn, *M*	$10^4 k'$, sec^{-1}	$A_0 - A_b$
Glucose	0.040	1469.0	
	0.030	1250.0	
	0.020	997.0	
	0.015	847.0	
	0.010	666.0	
Schardinger β-dextrin[b]	0.100	8.37	0.662
	0.080	7.36	0.464
	0.060	5.89	0.461
	0.050	4.96	0.407
	0.040	4.26	0.338
	0.030	3.53	0.304
	0.020	2.50	0.205
	0.015	2.07	0.157
Methyl β-D-glucopyranoside	0.080	9.73	0.680
	0.060	7.15	0.571
	0.040	5.56	0.450
	0.030	3.82	0.355
	0.020	3.06	0.179
1,5-Anhydro-D-glucitol	0.080	10.25	0.874
	0.040	6.64	0.598
	0.030	5.56	0.472
	0.020	4.07	0.371

[a] Initial cerium(IV) concentration 0.00196*M*.

[b] Model for anhydro-D-glucose units. Concentration calculated on an anhydro-D-glucose unit basis.

TABLE III
Evidence for Complex Formation in 1.0*M* Perchloric Acid. Complex Formation Constants and Rate Constants for Complex Disproportionation at 20.0°C

Substrate	Complex formation constant *K*, M^{-1}		Disproportionation rate constant *k*, min^{-1}
	Spectrometric data	Kinetic data	
Glucose	—	39.4	14.04
Schardinger β-dextrin	9.0	10.3	0.09
Methyl β-D-glucopyranoside	9.4	6.2	0.16
1,5-Anhydro-D-glucitol	12.7	12.7	0.12

which have been studied under similar conditions. Some literature results for equilibrium constants in 1.0*M* perchloric acid at 20.0°C for methanol, ethanol, and glycerol are 1.5,[21] 4.3,[19] and 25.0,[20] respectively. For the cyclic alcohols, *cis*- and *trans*-1,2-cyclohexanediols, 2-methoxycyclohexanol, and cyclohexanol in 1.0*M* perchloric acid at 15.0°C the equilibrium constants were 29.0, 18.0, 2.1, and 2.9, respectively.[16] The greater stability, as indicated by larger equilibrium constants, of the 1,2-glycol containing

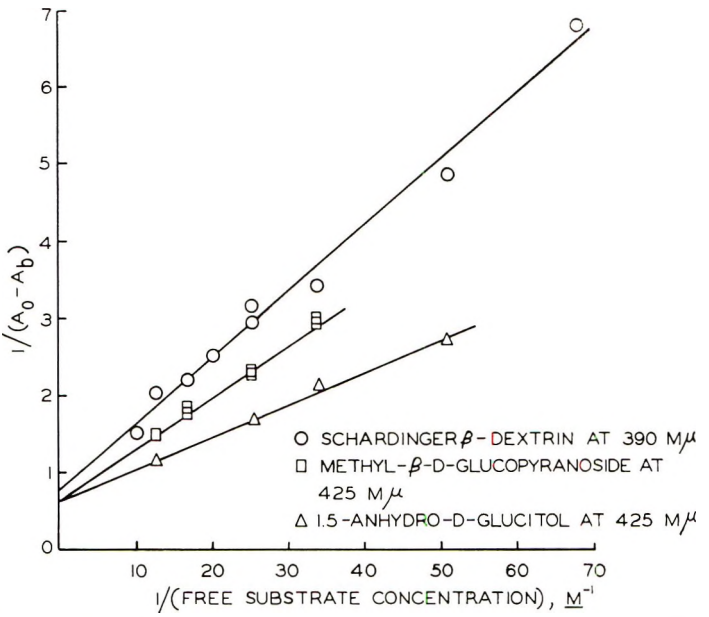

Fig. 4. Reciprocal plots of spectrophotometric data for reactions in 1.0*M* perchloric acid at 20.0°C.

compounds indicates that these compounds form chelate complexes with cerium(IV).

All of the compounds for which equilibrium constants were determined in this study contained α-glycol groups. The magnitudes of the equilibrium constants (Table III) suggest that in all cases the complexes involved are more stable than known complexes involving coordination of single hydroxyl groups. The increase in complex stability suggests chelate complexes are formed between these compounds and cerium(IV) in perchloric acid solution.

The high equilibrium constant for complex formation obtained for glucose oxidations in 1.0*M* perchloric acid predicts that nearly all of the oxidant will be involved in cerium(IV)–glucose complexes when glucose is present in excess. This explains why the potentially reactive product, arabinose, is not oxidized further, since the oxidant is not readily available for reaction. In fact, arabinose and glucose must compete with the reactive free radical for uncoordinated cerium(IV) made available by dissociation of the complex.

Structural Influences on Reactivity

In Table IV are given the results of kinetic studies with a variety of carbohydrate systems. Completely methylated glucose was oxidized at a rate one-fifteenth the rate of oxidation of methyl-4,6-di-*O*-methyl-β-D-glucopyranoside. Since it has been shown that the glucosidic bond is not hydrolyzed under the reaction conditions, this result shows that hydroxyl

TABLE IV
Reaction Rates of Selected Carbohydrate Derivatives with Cerium(IV) in 1.0*M* Perchloric Acid at 15.0°C

Compound[a]	$10^4\ k'$, sec^{-1}	Relative rate
Methyl-2,3,4,6-tetra-*O*-methyl-β-D-glucopyranoside	0.113	0.048
Methyl-4,6-di-*O*-methyl-β-D-glucopyranoside	1.64	0.7
Methyl β-D-glucopyranoside	2.37	1
Schardinger β-dextrin[b]	2.36	1
2-*O*-Methyl-D-glucose	4310	1860
2-Deoxy-D-glucose	2.94	12.4
Glucose	855.0	360
Galactose	1750	736
2-*O*-Methyl-D-galactose	3230	1370
Cellobiose	501	212
Ribose	1670	705

[a] Substrate concentration 0.040*M* in all cases, cerium(IV) concentration, 0.00196*M*.
[b] Concentration based on anhydro-D-glucose units.

groups are not essential for oxidation to occur. The similarity in overall rates of cerium(IV) oxidations of methyl β-D-glucopyranoside, methyl-4,6-di-*O*-methyl-β-D-glucopyranoside, and Schardinger β-dextrin suggests that these glycosides all react via chelate complexes involving α-glycols. Aldoses, on the other hand, are oxidized much more rapidly than the glycosides. However, the presence of oxygen on C_2 is important as indicated by the decreased rate of oxidation found for 2-deoxy-D-glucose.

The rate of 2-*O*-methyl-D-glucose oxidation (Table IV) is greater than the rate of glucose oxidation; however, it has been shown that both compounds yield arabinose as the initial reaction product demonstrating that the reaction breaks the C_1–C_2 bond. The situation is similar to that found for *trans*-2-methoxy-cyclohexanol and *trans*-1,2-cyclohexanediol,[16] which are oxidized at about the same overall rates, and both give adipaldehyde. The equilibrium constant for complex formation with *trans*-1,2-cyclohexanediol was significantly larger than that for *trans*-2-methoxycyclohexanol, while the reverse was true for the disproportionation rate constants.

Mechanism of Glucose Oxidation by Cerium(IV)

As described in previous sections, glucose is oxidized by cerium(IV) in perchloric acid to produce arabinose, formic acid, and cerium(III). The kinetics of this reaction showed that glucose and cerium(IV) interact in an equilibrium step to form an intermediate complex which is assumed to disproportionate forming a free radical and reduced cerium(III). The free radical is then further oxidized in a rapid second attack by cerium(IV) to form the product and a second mole of cerium(III).

The nature of the intermediate complex, as deduced from the magnitude of the equilibrium constant (Table III) and the reactivity of 2-deoxy-D-

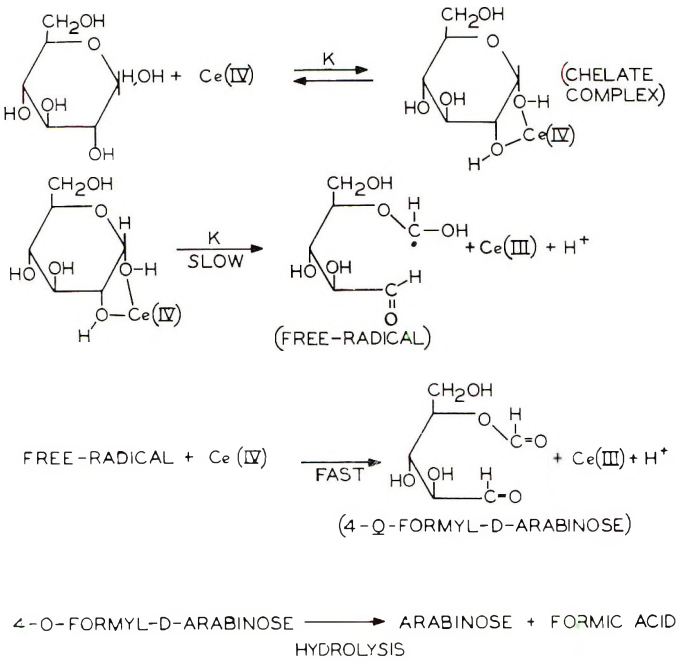

Scheme I.

glucose (Table IV), is believed to involve both the C_1 and C_2 hydroxyls in a chelate complex. In Scheme I is depicted the reaction mechanism described above which can explain the products and kinetics of glucose oxidation by cerium(IV).* It is to be noted that the formation of formate esters has been established in periodate and lead tetraacetate oxidations of glucose.[50] Such formate esters are expected to be hydrolyzed under the conditions used for the present studies. An alternate mechanism can also be proposed (Scheme II) which produces arabinose and formic acid directly. However, studies of cerium(IV) oxidations of ribose (Table IV), which has about 10% free aldehyde in aqueous solution[51] as compared to 0.012% for glucose, showed no significant increase in rate; so it seems probable that the mechanism involves the pyranose form of glucose.

Radical formation at C-1 (as shown in Scheme I) might well be preferred because of the greater resonance stabilization expected for such a radical. The data in Table III show that the overall difference in the reactivities of glucose and the other compounds is primarily due to the greater ease of radical formation from the glucose complex. Further work is necessary to answer this question.

The site of radical formation may have considerable relevance to the efficiency of graft polymerization onto cellulose. It is clear that initiation of a graft could occur by combination of a monomer with a C-1 radical at a reducing end of cellulose. The linkage formed, however, would be a highly

* It should be understood that there are two possible radical sites for the free radicals in Schemes I–III.

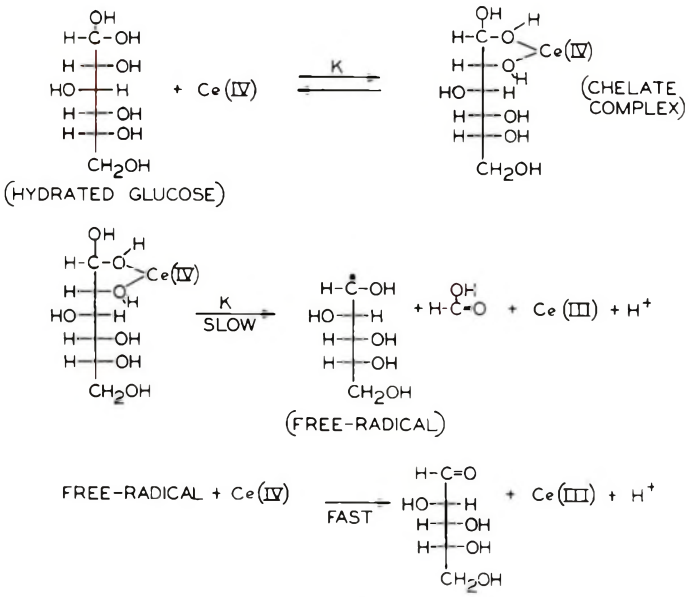

Scheme II.

unstable hemiacetal. True grafting would thus be prevented at the reducing ends. A recent study[52] has revealed that grafting of methyl methacrylate onto cellulose becomes markedly less efficient as the aldehyde content of the cellulose increases.

Mechanism of Anhydro-D-glucose Oxidation by Cerium(IV)

The products and kinetics of reactions of Schardinger β-dextrin (cycloheptaamylose) and cellulose may be rationalized by the mechanism shown in Scheme III. This is essentially the same pathway suggested by

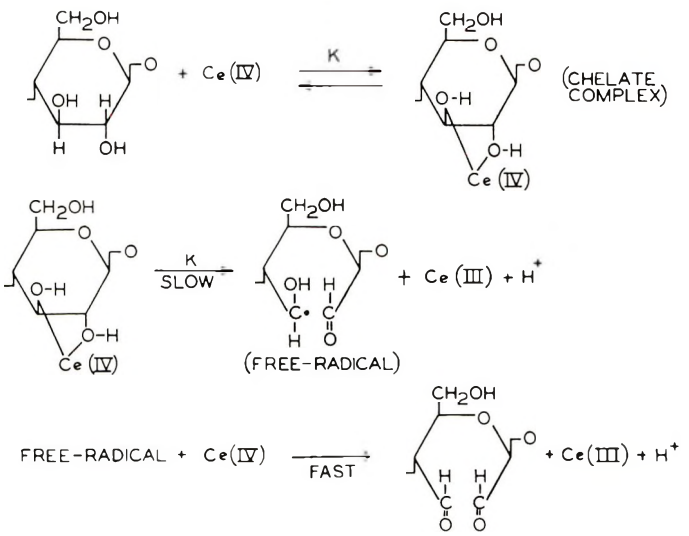

Scheme III.

others.[13] The hydroxyl groups at C_2 and C_3 of an anhydro-D-glucose unit form a chelate complex with cerium(IV). The complex disproportionates forming a free radical which is rapidly oxidized by a second mole of cerium(IV). In the presence of monomer, the intermediate radical could then generate a stable graft.

Oxidations of Cellulose Model Compounds

In the Introduction, it was pointed out that the suggested sites of cerium(IV) oxidation of cellulose are the C_2–C_3 diol or C_6 hydroxyl of an anhydro-D-glucose unit of the reducing end group. Hintz[16] compared the relative rates of oxidation of *trans*-1,2-cyclohexanediol, cyclohexanemethanol, and tetrahydropyran-2-methanol as models for the C_2–C_3 glycol and C_6 hydroxyl groups and predicted that the diol group of cellulose would be oxidized about six times faster than the C_6 hydroxyl.

The results of this study show that, using carbohydrate compounds as models for cellulose, the reducing function is 360 times as reactive as an anhydro-D-glucose repeating group (Table V). Furthermore, no evidence was obtained which indicated significant reaction of the C_6 hydroxyl under the conditions used.

Product analysis studies with the kinetic model for anhydro-D-glucose, Schardinger β-dextrin, and with authentic cellulose showed the presence of erythrose and glyoxal in hydrolyzates of the oxidized polysaccharides. This evidence suggests preferential cleavage of the C_2–C_3 bonds of anhydro-D-glucose as was originally expected.

Based on the results of this study it seems reasonable to predict that cellulose oxidation takes place predominantly at either the C_2–C_3 diol or at the reducing endgroup. The relative importance of oxidations at the two sites will depend to a great extent on degree of polymerization and accessibility of reducing endgroups.

TABLE V
Oxidations of Cellulose Model Compounds in 1.0*M* Perchloric Acid at 15.0°C

Substrate	Relative rate
Glucose	360
Schardinger β-dextrin[a]	1
Methyl β-D-glucopyranoside	1
1,5-Anhydro-D-glucitol	1.5

[a] Concentration based on anhydro-D-glucose units.

CONCLUSIONS

Cerium(IV) oxidations of glucose, Schardinger β-dextrin (anhydro-D-glucose units), methyl β-D-glucopyranoside, and 1,5-anhydro-D-glucitol proceed via chelate intermediate complexes, as indicated by the magnitude of the equilibrium constants determined by kinetic and spectrometric techniques. Glucose is oxidized by the formation of a coordination complex

involving the C_1 and C_2 hydroxyl groups and cerium(IV) which disproportionates, breaking the C_1–C_2 bond, and forms a free radical on C_1 or C_2. The free radical is oxidized by a second mole of cerium(IV).

Oxidation of excess glucose by cerium(IV) in 1.0*M* perchloric acid gives a quantitative yield of arabinose. This controlled degradation of reducing sugars may have synthetic applications. It appears to be successful with glucose, 2-*O*-methyl-D-glucose, galactose, 2-*O*-methyl-D-galactose, and cellobiose.

Consideration of the relative rates of oxidation of the cellulose model compounds used in this study suggests that the reducing endgroup is 360 times as reactive as the anhydro-D-glucose repeating unit or the nonreducing endgroup. Assuming equal accessibility in a cellulose of normal degree of polymerization the high relative concentration of anhydro-D-glucose units predicts that most oxidative attacks will involve cleavage of a C_2–C_3 bond. However, for celluloses of low degree of polymerization, oligomers, or samples in which endgroups are more accessible, the reactivity of the reducing endgroup will predominate and attack will occur primarily by C_1–C_2 cleavage.

This paper is taken from the thesis submitted by C. R. Pottenger in partial fulfillment of the requirements of The Institute of Paper Chemistry for the degree of Doctor of Philosophy from Lawrence University, Appleton, Wisc. June 1968.

The authors wish to thank Drs. P. A. Seib and K. Ward, Jr. for their comments and suggestions. Particular thanks are due to Dr. P. A. Seib for preparing and contributing the sample of 2-*O*-methyl-D-glucose used in this study.

References

1. G. Mino and S. Kaizerman, *J. Polym. Sci.*, **31**, 242 (1958).
2. G. Mino, S. Kaizerman, and E. Rasmussen, *J. Amer. Chem. Soc.*, **81**, 1494 (1959).
3. G. Mino, S. Kaizerman, and E. Rasmussen, *J. Polym. Sci.*, **38**, 393 (1959).
4. F. K. Guthrie, *Tappi*, **46**, 656 (1963).
5. R. H. Cornell, *Tappi*, **45**, 145A (1962).
6. I. Terasaki and M. Matsuki, *Sen-i-Gakkaishi*, **18**, 147 (1962).
7. H. Yashuda, J. A. Wray, and V. Stannett, in *Fourth Cellulose Conference* (*J. Polym. Sci. C*, **2**), R. H. Marchessault, Ed., Interscience, New York, 1963, p. 387.
8. A. A. Katai, V. K. Kulshrestha, and R. H. Marchessault, in *Fourth Cellulose Conference* (*J. Polym. Sci. C*, **2**), R. H. Marchessault, Ed., Interscience, New York, 1963, p. 403.
9. Y. Iwakura, T. Kurosaki, and K. Imai, *J. Polym. Sci. A*, **3**, 1185 (1965).
10. R. M. Livshits, V. P. Alachev, E. V. A. Prokof, and Z. A. Rogovin, *Vysokomol. Soedin.*, **6**, 655 (1964); Abstr. Bull. Inst. Paper Chem., **35**, 1564.
11. L. Neimo and H. Sihtola, *Paperi Puu*, **6**, 369 (1965).
12. R. A. Wallace and D. G. Young, *J. Polym. Sci. A-1*, **4**, 1179 (1966).
13. J. C. Arthur, Jr., P. J. Baugh, and O. Hinojosa, *J. Appl. Polymer Sci.*, **10**, 1591 (1966).
14. Z. Reyes, C. E. Rist, and C. R. Russell, *J. Polymer Sci. A-1*, **4**, 1031 (1966).
15. R. J. E. Cumberbirch and J. R. Holker, *J. Soc. Dyers Colourists*, **82**, 59 (1966).
16. H. L. Hintz and D. C. Johnson, *J. Org. Chem.*, **32**, 556 (1967).
17. F. R. Duke and A. A. Forist, *J. Amer. Chem. Soc.*, **71**, 2790 (1949).
18. F. R. Duke and R. F. Bremer, *J. Amer. Chem. Soc.*, **73**, 5179 (1951).
19. M. Ardon, *J. Chem. Soc.*, **1957**, 1811.

20. G. G. Guilbault and W. H. McCurdy, Jr., *J. Phys. Chem.*, **67**, 283 (1963).
21. S. S. Muhammad and K. V. Rao, *Bull. Chem. Soc., Japan*, **36**, 943 (1963).
22. S. Venkatakrishnan and M. Santappa, *Z. Physik. Chem.* (Frankfurt), **16**, 73 (1958).
23. K. P. Bhargava, R. Shanker, and S. N. Joshi, *J. Sci. Ind. Res. (India)*, **21B**, 573 (1962).
24. J. S. Littler, *J. Chem. Soc.*, **1959**, 4135.
25. Y. A. El-Tantawy and G. A. Rechnitz, *Anal. Chem.*, **36**, 1774 (1964).
26. R. N. Mehrotra, *Z. Physik. Chem.*, (Leipzig), **230**, 221 (1965).
27. A. McAuley, *J. Chem. Soc.*, **1965**, 4054.
28. S. S. Muhammad and K. V. Rao, *Bull. Chem. Soc., Japan*, **36**, 949 (1963).
29. J. C. Bailar, Ed., *The Chemistry of Coordination Compounds*, Reinhold, New York, 1956, p. 221.
30. F. A. Cotton and G. Wilkinson, *Advanced Inorganic Chemistry*, Interscience, New York, 1962, p. 547.
31. S. Chaberek and A. Martell, *Organic Sequestering Agents*, Wiley, New York, 1959, p. 140.
32. H. L. Hintz, Dissertation, The Institute of Paper Chemistry, Appleton, Wisc., 1966.
33. R. K. Ness, H. G. Fletcher, Jr., and C. S. Hudson, *J. Amer. Chem. Soc.*, **72**, 4547 (1950).
34. E. L. Falconer and G. A. Adams, *Can. J. Chem.*, **34**, 338 (1956).
35. G. N. Bollenbach, *Methyl Glucoside*, Academic Press, New York, 1958, p. 219.
36. H. G. Walker, M. Gee, and R. M. McCready, *J. Org. Chem.*, **27**, 2100 (1962).
37. I. O. Mastronardi, S. M. Flematti, J. O. Deferrari, and E. G. Gros, *Carbohyd. Res.*, **3**, 177 (1966).
38. J. K. Bott, W. N. Haworth, and E. L. Hirst, *J. Chem. Soc.*, **1930**, 2653.
39. W. E. Trevelyn, D. P. Proctor, and J. S. Harrison, *Nature*, **166**, 444 (1950).
40. H. Zinner, *Chem. Ber.*, **84**, 780 (1951).
41. F. Feigl, *Spot Tests, Vol. II*, Elsevier, Amsterdam, 1954.
42. J. F. Saeman, W. E. Moore, R. L. Mitchell, and M. A. Millett, *Tappi*, **37**, 336 (1954).
43. J. D. Moyer and H. S. Isbell, *Anal. Chem.*, **29**, 1862 (1957).
44. C. A. Wilham, T. A. McGuire, J. W. VanCleve, F. H. Otey, and C. L. Mehltretter, *Ind. Eng. Chem. Prod. Res. Develop.*, **1**, 62 (1962).
45. C. C. Sweeley, R. Bently, M. Makita, and W. W. Wells, *J. Amer. Chem. Soc.*, **85**, 2497 (1963).
46. E. J. Reist and G. L. Holton, *Carbohyd. Res.*, **2**, 181 (1966).
47. E. P. Crowell and B. B. Burnett, *Anal. Chem.*, **39**, 121 (1967).
48. G. F. Smith and F. R. Duke, *Ind. Eng. Chem. Anal. Ed.*, **15**, 120 (1943).
49. F. R. Duke, *J. Amer. Chem. Soc.*, **69**, 2885 (1947).
50. W. Mackie and A. S. Perlin, *Can. J. Chem.*, **43**, 2645 (1965).
51. S. M. Cantor, and Q. P. Peniston, *J. Amer. Chem. Soc.*, **62**, 2113 (1940).
52. Y. Ogiwara, Y. Ogiwara, and H. Kubota, *J. Polymer Sci. A-1*, **5**, 2791 (1967).

Received September 25, 1968
Revised November 11, 1968

JOURNAL OF POLYMER SCIENCE: PART A-1 VOL. 8, 319–328 (1970)

Stereoregular Poly(methacrylic Acids)

N. N. AYLWARD, *The Chemistry Department, Aberdeen University, Old Aberdeen, Scotland*

Synopsis

A convenient method is described for the preparation of isotactic and syndiotactic poly(trimethylsilyl methacrylates) by using the monomer trimethyl silyl methacrylate and butyllithium initiation in toluene and tetrahydrofuran, respectively. The structure of these polymers enables complete hydrolysis to the corresponding poly(methacrylic acids), which were characterized with respect to tacticity and molecular weight. The asymmetric induction in toluene produced 89% isotactic polymer, while that in tetrahydrofuran gave polymer >90% syndiotactic and heterotactic in terms of triads. A method of fractionation of the polyelectrolytes by gel-permeation chromatography on a preparative scale was shown to be applicable.

INTRODUCTION

With the increasing interest in the dimensions and conformational transitions of atactic[1,2] and stereoregular poly(methacrylic acids),[3,4] alternate methods have been sought for the preparation and fractionation of the isotactic and syndiotactic polyacids which would give suitably high tacticity and molecular weights.

Isotactic PMA is usually made by the sulfuric acid hydrolysis of isotactic PMMA which can be produced by butyllithium or phenylmagnesium bromide initiation in hydrocarbon solvent.[5–7] While acid and also alkaline hydrolysis can be made to go to completion, the polyacid is seemingly always discolored but not appreciably degraded. Syndiotactic PMMA is readily obtainable in high tacticity,[8] but it has not been completely hydrolyzed.[6]

Compared with these indirect methods, syndiotactic PMA of only about 85% syndiotactic triads has been made by the low-temperature polymerization of methacrylic acid by γ-rays from a ^{60}Co source,[9] and by the free-radical polymerization of sodium methacrylate at high pH in aqueous medium.[8]

In this work the monomer trimethyl silyl methacrylate was examined as being one of the best starting materials for the synthesis of these polyacids. It has previously been polymerized with various initiators and the polymers shown to be easily hydrolyzed,[10,11] but the tacticity was not quantitatively determined, and no yield was recorded for butyllithium initiation. Contrarily, we find on conducting polymerizations in toluene and tetrahydro-

furan that isotactic and predominantly syudiotactic/heterotactic poly(trimethylsilyl methacrylates) are produced.

The general features of the anionic polymerizations of esters of methacrylic acid are well documented.[12] Of the two general methods of producing isotactic polymer from α-substituted monoenes, namely, constant mode of attack and constant bond opening, or alternating attack and alternating bond opening,[13] the former, with *trans* opening of the double bond, is the basis of a mechanism[14–16] involving coordinated ionic polymerization[17] by a contact ion-pair.[12] This has been unequivocally demonstrated by the formation of threo-meso poly(ethyl methacrylate-d_1) when ethyl *cis*-β-d_1-methacrylate was polymerized by butyllithium in toluene.[12]

For the polymerizations in tetrahydrofuran, studies of lithium poly(ethyl methacrylate)[18] have shown there are essentially no free ions and a solvent-separated ion-pair is responsible for propagation. With this species the monomer does not coordinate before reaction, but approaches the anion in the syndiotactic sense which is sterically preferred because of the usual nonbonded interactions.[19–21] Polymerization will thus proceed as from a single propagating species, but the mechanism could be more complicated to some degree.[22]

EXPERIMENTAL

Materials

Analar grade toluene and reagent-grade tetrahydrofuran were used. These were refluxed over sodium and distilled. They were then stirred and refluxed over calcium hydride and distilled in an argon atmosphere. The toluene fraction boiling at 110.0–110.5°C and the tetrahydrofuran fraction boiling at 66.3°C were collected and used in polymerization work. Final purification and drying of solvents was achieved by using a high vacuum grid to enable distillation of the solvents into vessels containing small quantities of outgassed butyllithium.

Prepurified grade argon was used as the inert atmosphere in all reactions.

***n*-Butyllithium.** *n*-Butyllithium was prepared from *n*-butyl chloride and a slight excess of lithium wire in low-boiling petroleum ether as the solvent.[23] The reaction mixture was centrifuged under argon, and the supernatant liquid withdrawn with a syringe and stored in serum-capped bottles at −20°C under argon. Several preparations, ranging in molarity from about 3.0 to 4.0*M*, were employed.

Trimethylsilyl Methacrylate. This monomer has been synthesized by the reaction[11]

$$CH_2{=}\underset{\displaystyle CH_3}{\underset{|}{C}}{-}CO_2Ag + (CH_3)_3SiCl \rightarrow CH_2{=}\underset{\displaystyle CH_3}{\underset{|}{C}}{-}CO_2Si(CH_3)_3 + AgCl \qquad (1)$$

but to prepare large quantities the base-catalyzed reaction (2) was found to be preferable.

$$CH_2{=}\underset{\displaystyle CH_3}{\overset{\displaystyle |}{C}}{-}CO_2H + (CH_3)_3SiCl \xrightarrow{C_6H_5N(CH_3)_2} CH_2{=}\underset{\displaystyle CH_3}{\overset{\displaystyle |}{C}}{-}CO_2Si(CH_3)_3 + C_6H_5\overset{+}{N}H(CH_3)_2Cl^- \quad (2)$$

After phase separation of the lightly refluxing mixture the monomer was collected in the ether layer, washed with water and dried. It was normally kept over calcium hydride. By distillation under reduced pressure the monomer was collected in several fractions; yield, 60%; bp, 52°C/20 mm Hg; $n_D^{25°} = 1.407$.

The structure of the product was determined from the infrared spectra of the liquid examined as a smear between KBr disks: C=O at 1710, C=C at 1640, SiMe at 1260 cm^{-1}. The nuclear magnetic resonance spectrum was taken in deuterochloroform with tetramethylsilane as internal standard. The proton resonance of the SiMe group was at 9.74 τ, Me at 8.13, 8.16 and the methylene resonances, which were complex, at 4.48 and 3.94 τ.

Polymerizations

The Pyrex glass reaction vessel used for the polymerizations constituted part of a high vacuum grid maintained at $<10^{-5}$ mm Hg and monitored with a Vacustat pressure gauge. The vessel could therefore be flamed out under high vacuum and the monomer and solvent distilled in from vessels containing sodium films. Condensation of the vapors was effected by the use of liquid nitrogen. The polymerization vessel, which contained a serum cap, was then isolated from the grid and connected by way of a tap and the serum cap to an argon line which entered the vessel by means of a hypodermic needle through the serum cap. By these techniques the advantages of high-vacuum operations and the ease of using rubber seals were combined. Initiator could then be added by syringe through the same serum cap. In addition the vessel was kept at −70°C by a bath of methanol and solid carbon dioxide. Stirring was effected by an internal PTFE-coated stirrer operated magnetically from below.

The polymerization was carried out by distilling pure toluene (CaH_2- and BuLi-dried) and monomer (CaH_2- and Na-dried), 10% v/v, into the reaction vessel which was subsequently held at −70°C. On the addition of 3 mole-% of butyllithium the solution turned light yellow. Polymerization was rapid and left for 6 hr to complete reaction. The yield was essentially quantitative, being governed only by the very high viscosity of the solution. The poly-(trimethylsilyl methacrylate) was terminated by exposure to water vapor and the solvent was removed under reduced pressure to yield translucent polymer. This was insoluble in most organic solvents.

Analysis of some elements of the polymer gave C 51.9%, H 8.8%, in comparison with the calculated values of C 53.1%, H 8.9%.

To hydrolyze this polymer to poly(methacrylic acid), 1 g of polymer was suspended in 100 ml of 20% sodium hydroxide and the solution refluxed for 12 hrs. The solution was filtered and the polyacid precipitated with hydrochloric acid, washed with distilled water, and dried at 60°C in a vacuum oven. Hydrolysis was shown to be definitely complete at the end of this time by the absence of the proton resonance of the Si-Me group in the NMR spectrum and the similarity of the infrared spectrum to published examples.[3] The material was very similar to that from the hydrolysis of isotactic PMMA as it had an extremely small solubility in water, but was soluble in dimethylformamide, dimethyl sulfoxide, propylene carbonate, and sodium hydroxide, from which it may be further purified.

The procedure for the polymerization of trimethylsilyl methacrylate to the syndiotactic polymer was to distill tetrahydrofuran (Na-, CaH_2-, and BuLi-dried) and monomer (CaH_2- and Na-dried), 10% v/v into the reaction vessel which was held at −70°C. Addition of 3 mole-% of butyllithium to the solution caused considerable polymerization in about 10 min and an almost quantitative yield after having been left for 6 hr to complete the reaction. The poly(trimethylsilyl methacrylate) was terminated by exposure to water vapor and the solvent was removed under reduced pressure to yield translucent polymer which was insoluble in most organic solvents.

Analysis of some elements of the polymer gave C 53.0%, H 8.4%, in comparison with the calculated values of C 53.1%, H 8.9%.

The same procedure was used in the hydrolysis of this polymer as for the first poly(trimethylsilyl methacrylate), except that a reflux time of $2^1/_2$ days was taken. The NMR spectrum from an aqueous alkaline solution of the polyacid, and the infrared spectrum taken from KBr disk indicated that hydrolysis was definitely complete at the end of this time.

$$-(CH_2-\underset{\displaystyle CO_2Si(CH_3)_3}{\overset{\displaystyle CH_3}{\overset{|}{\underset{|}{C}}}}-)_n + n\mathrm{NaOH} \rightarrow -(CH_2-\underset{\displaystyle CO_2^-Na^+}{\overset{\displaystyle CH_3}{\overset{|}{\underset{|}{C}}}}-)_n + n(CH_3)_3SiOH \qquad (3)$$

This polyacid was sparingly soluble in water but was soluble in sodium hydroxide.

Characterization of the Products

High-resolution nuclear magnetic resonance spectroscopy of polymers in solution is normally the most informative, quantitative technique for determining stereochemical configuration,[24] while useful information can often be obtained from x-ray diagrams and empirical infrared absorption measurements.

Isotactic Poly(trimethylsilyl Methacrylate)

NMR Measurements. Polymer solutions were normally 10% w/v with 1% of internal standard. Standards were either tetramethylsilane or 3-trimethylsilylpropane-1-sulfonate, depending on their solubility in

the solvent being used. The Varian 60 Mcps instrument was operated at 30°C.

The NMR of poly(trimethylsilyl methacrylate) from the first polymerization could be determined as the polymer had a slight solubility in dimethylformamide. Good isotacticity, but with poor resolution was indicated by the position of the C-Me resonance at 8.78 τ, the same as for isotactic PMMA.[25] The proton resonance of Si-Me was at $\simeq$9.81 τ.

The NMR of the polyacid from the first preparation gave a C-Me resonance at 8.84 τ, indicating at least 75% isotactic content. This NMR was identical with that given by isotactic PMA from the hydrolysis of isotactic PMMA.

To characterize this polyacid further it was methylated in benzene according to the method of Katchalsky and Eisenberg.[26] The PMMA from this process was shown from NMR to consist of 89% *I*, 8% *H*, and 3% *S* in terms of triads. The error is 5% in these values. The corresponding *J* value,[27] which is an empirical measure, based at 1062 cm^{-1} on the disappearance of a zigzag planar vibration[28] and at 1483 cm^{-1} on the reduction in intensity of the asymmetric deformation of the α-CH_3 group,[29] yielded values of 28.3 and 19.1, respectively, giving an average value of 23.7. This is slightly below the normal range of values[27] and strongly supports the high isotactic content of this polymer.

Infrared and X-Ray Characterization. Insoluble polymers were ground with dry KBr and made into a disk. The infrared spectrum of the isotactic PMA was identical to that of a sample from the hydrolysis of isotactic PMMA and to published spectra.[3] In particular, only one peak is observed between 900 and 1000 cm^{-1}, which has been interpreted by Tsuruta et al.[7] as indicative of a high degree of isotacticity.

The x-ray analysis of powdered samples by use of a Debye-Scherrer camera did not give sharp diffraction cones, but differential thermal analysis with the Du Pont 900 differential thermal analyzer was sufficiently sensitive to detect two transitions on the thermogram. The sample (2 mg) was kept under high vacuum and subjected to a 15°C/min heating rate, with the instrument adjusted to obtain a horizontal base line.[30] Under these conditions second-order and first-order transitions may be differentiated with suitable polymers. A very weakly endothermic transition at 68°C was assigned to a glass transition, while the endothermic peak at 183°C indicated a melting point.

Molecular Weight Determinations. By determining the limiting viscosity number of methylated isotactic PMA, approximate molecular weights were obtained from the relationship

$$[\eta] = 3.4 \times 10^{-5} \bar{M}_w^{0.83}$$

which was derived from measurements on conventional PMMA.[31] Measurements were taken at 25 $\pm$ 0.01°C in chloroform as this is one of the most powerful solvents for PMMA. The molecular weight was normally of the order of 8.4×10^4 which was suitable for physical experiments.

Syndiotactic Poly(trimethylsilyl Methacrylate)

NMR Measurements. Considerable difficulty was experienced in attempts to characterize this polymer as a result of its extreme insolubility in most solvents. For this reason the NMR of the polymer could not be taken.

The α-Me proton resonance of the lithium salt of this polyacid occurred at 9.02 τ, which is considerably above that for the isotactic acid. This allowed the isotactic content to be estimated at no more than 10% in terms of triads.

A sample expected to be highly syndiotactic also had this resonance at 9.02 τ (this had been produced by UV irradiation of sodium methacrylate at 0°C by using benzoin as photosensitizer and a methanol–water mixture as solvent at pH $\simeq$ 10). Atactic lithium polymethacrylate had this resonance at $\simeq$9.0 τ. It is therefore certain that the polymer derived from poly(trimethylsilyl methacrylate) is substantially heterotactic/syndiotactic.

To characterize the PMA further it was subjected to methylation in dimethyl sulfoxide, benzene, and chloroform under various conditions, but complete solution of the polyacid was never achieved. Difficulty in obtaining a truly representative sample of soluble PMMA from this methylation has previously been found.[32] The J value of this insoluble polymer was 96.2, which is below the 100–115 recorded for syndiotactic PMMA.[27] This polyacid could not be adequately methylated in our experience, while atactic samples were easily methylated and solubilized within 30 min.

Differential Thermal Analysis and Infrared Characterization. Differential thermal analysis of the poly(trimethylsilyl methacrylate) under the same conditions as for the isotactic polymer gave a thermogram depicting two transitions; a weak endotherm at 127°C and an endothermic peak at 224°C. These are most easily assigned to a glass transition and the melting point. The latter would agree with the changing appearance of the material at 224°C.

The infrared spectrum of this polymer was very similar to that recorded for the isotactic polymer, except that there appeared to be more of a doublet between 900 and 1000 cm.$^{-1}$ Some small differences between 1400 and 1500 cm^{-1} were also apparent. Also, a weak shoulder appears at 797 cm.$^{-1}$

The infrared spectrum of the poly(methacrylic acid) was almost identical with published data,[3] but with less resolution.

Molecular Weight Determinations. Some preparations of the heterotactic/syndiotactic PMA were completely soluble in water, so that the number-average molecular weight could be determined by osmometry with the use of the Mechrolab Model 501 high-speed membrane osmometer. The instrument was operated at 37°C 0.005N hydrochloric acid being used as the solvent. As solutions of this polyacid normally kept at pH $\simeq$ 6.0, it is unlikely that they are ionized in 0.005N hydrochloric acid. The

molecular weight was then determined as for neutral polymers. Plots of π/c against c were reasonably straight and the molecular weight was often of the order of 2.9×10^4.

Fractionation of Poly(methacrylic Acids)

Gel-permeation chromatography was used, as this is at present the most convenient and rapid technique for the fractionation of polymers on an analytical and preparative scale. Details of this method and of the instrumentation have been presented in the literature.[33,34] The technique fractionates polymers and permits determination of their molecular weight distribution. Material is separated according to molecular size, based on the depth to which each molecular species is able to diffuse into the gel network. Accordingly, the largest molecular species should penetrate the crosslinked polymer gel the least and be eluted first.

As the polyacids corresponded to the correct empirical formula, and branching and crosslinking seemed very unlikely, fractionation was expected to separate according to molecular weight, with possibly some effect of tacticity superimposed. Preliminary work centred on fractionating the isotactic polyacid in the un-ionized form, but the Biogel resin (a copolymer of acrylamide and methylenebisacrylamide) would not swell sufficiently in dimethyl-formamide or propylene carbonate. Also, dimethyl sulfoxide at a temperature of 50°C seemed suitable, but led to rather low flow times.

However, when the polyacids were converted to their sodium salts it was found possible to elute them from a column of Biogel maintained in 0.1*M* borax as a buffer. An appropriate apparatus consisted of a column 5 cm in diameter and 1 liter volume fitted with a coarse grade 1 sinter at the lower end, where a small "dead volume" was formed by rapidly tapering the column. The Biogel was P-300 with an exclusion limit of 300000 molecular weight (substances of MW 300 000 will have an R_f of approximately 0.9), previously swollen in 0.1*M* borax and poured into the column as a slurry in the normal manner. Samples of the polyacids ($^1/_2$ or 1 g), neutralized with sodium hydroxide and held in 0.1*M* borax, were adsorbed to the top of the column. Elution was conducted over a period of about 18 hr at room temperature ($\simeq$20°C). An automatic siphoning device collected 20-ml samples. The polyacid was precipitated in each fraction by the addition of concentrated hydrochloric acid and boiling. The fractions were filtered, washed with distilled water until neutral and dried to constant weight in a vacuum oven at 70°C. Assuming that the fractionation was successful, the weight distribution of material indicated a very heterogeneous sample.

Of equal importance in any fractionation procedure is a method for monitoring its success or failure. For this purpose we have used limiting viscosity number to indicate any fractionation and the analytical ultracentrifuge to give a qualitative idea of the monodispersity of the fractions.

TABLE I
The Variation of Limiting Viscosity Number with Fraction

Fraction	$(\eta_{sp}/c)_{C=0}$	Wt. of recovered polymer, mg/20 ml
1	0.84	42.9
2	0.77	53.9
3	0.68	42.4
4	0.63	51.3
5	0.56	41.3
6	0.55	45.7
7	0.53	26.8
8	0.48	24.2
9	0.49	17.8
10	0.36	16.9

To eliminate difficulties due to the polyelectrolytic nature of the material or the region of their conformational transitions viscosity measurements were conducted in 2*N* sodium hydroxide at 30°C. This enabled the determination of the limiting viscosity number by dilution with 2*N* sodium hydroxide. Initial concentrations of polyacid were 2.0 g/l. Repeated runs always gave limiting viscosity numbers of >0.80 and <0.35 for the first and last fractions, as shown in Table I for isotactic PMA.

To study the monodispersity of the fractions, 1% solutions of the isotactic polyacid were made in dimethylformamide, which is one of the few available solvents for material of high tacticity. The ultracentrifuge was run at 25°C at 60000 rpm with initial and final fractions from the column. The high molecular weight material appeared to give as sharp a peak as is obtained from monodisperse polystyrene using Schlieren optics. The lower molecular weight fractions were definitely broader, but it is uncertain if this was only due to diffusion. A large difference in sedimentation coefficients was noted, and no fractions appeared bimodal. Similar results were obtained for the heterotactic/syndiotactic polyacid fractions in dilute sodium hydroxide.

It must be remembered that fractionation above a molecular weight of 300,000 cannot be expected, and also some fractionation due to tacticity may result.

DISCUSSION

The anionic polymerizations in toluene and tetrahydrofuran of the monomer, trimethylsilyl methacrylate, provide another example of this method of producing high molecular weight stereoregular polymers, which was first used by Fox et al.[35–37] in 1958 to produce several crystalline poly(methyl methacrylates). It is to be expected that the mechanisms of polymerization of this methacrylate are similar. Thus the large initiator requirement for propagation, the broad molecular weight distributions, and the reasonably high molecular weights of the polymers, are almost certainly a result

of a combination of attack on carbonyl,[38] pseudo-termination,[39] and varying rates of growth of the propagating chains,[40, 41] as found for other esters.

There is also a similarity in the physical constants of the two sets of polymers. The glass temperatures and melting points of the isotactic and syndiotactic poly(trimethylsilyl methacrylates) being 68 and 183°C, 127 and 224°C, respectively, compared with the values of 45 and 160°C and 115 and >200°C, respectively, for the corresponding poly(methyl methacrylates).[35]

The hydrolysis of the two sets of polymers shows a large difference. The poly(methyl methacrylates) are hydrolyzed only under drastic conditions, and this is never complete for the syndiotactic polymer. The preferential nucleophilic attack on the silicon[42] of the poly(trimethylsilyl methacrylates) allows complete hydrolysis and the production of good white polyacids.

That the two asymmetric syntheses had produced dissimilar tactic polymers is clearly shown in the attempts to determine quantitatively the microtacticity of the polymers. The isotactic polymer is well characterized at 89% isotactic triads, but the polymer from the second synthesis is only determined as 90% heterotactic/syndiotactic triads. However, comparison of the NMR of the salt of this polymer with that from the photosensitized polymerization of sodium methacrylate did not show any differences. As the latter should have been about 75% syndiotactic triads,[8] it is unnecessary to assume that the heterotactic content of the poly(trimethylsilyl methacrylate) from the second synthesis is greater than 15%.

I thank Professor G. M. Burnett, Dr. P. Meares, Dr. J. P. Hermans, the Technical Staff, and Aberdeen University.

References

1. S. S. Urazovskii and I. T. Slyusarov, *Vysokomol. Soedin.*, **3**, 420 (1961).
2. A. R. Mathieson, J. V. McLaren, and R. T. Shet, *Europ. Polym. J.*, **3**, 399 (1967).
3. G. Barone, V. Crescenzi, and F. Quadrifoglio, *Ric. Sci. Rend.*, **A8**, 1069 (1965).
4. M. Nagasawa, T. Murase, and K. Kondo, *J. Phys. Chem.*, **69**, 4005 (1965).
5. E. M. Loebl and J. J. O'Neill, *J. Polym. Sci.*, **45**, 538 (1960).
6. J. J. O'Neill, E. M. Loebl, A. Y. Kandanian, and H. Morawetz, *J. Polym. Sci. A*, **3**, 4201 (1965).
7. T. Tsuruta, T. Makimoto, and H. Kanai, *J. Macromol. Chem.*, **1**, 31 (1966).
8. F. A. Bovey and G. V. D. Tiers, *Fortschr. Hochpolym.-Forsch.*, **3**, 139 (1963).
9. E. M. Loebl and J. J. O'Neill, *J. Polym. Sci. B, B1*, 27 (1963).
10. T. Tsuruta, T. Jinda, and J. Furukawa, *Kogyo Kagaku Zasshi*, **66**, 92 (1963).
11. T. Tsuruta and J. Furukawa, *Bull. Inst. Chem. Res. Kyoto Univ.*, **40**, 151 (1962).
12. W. Fowells, C. Schuerch, F. A. Bovey, and F. P. Hood, *J. Amer. Chem. Soc.*, **89**, 1396 (1967).
13. G. Natta, M. Peraldo, M. Farina, and G. Bressan, *Makromol. Chem.*, **55**, 139 (1962).
14. D. J. Cram and K. R. Kopecky, *J. Amer. Chem. Soc.*, **81**, 2748 (1959).
15. W. E. Goode, F. H. Owens, and W. L. Myers, *J. Polym. Sci.*, **47**, 75 (1960).
16. C. E. H. Bawn and A. Ledwith, *Quart. Rev.* (London), **16**, 361 (1962).
17. J. Furukawa, *Bull. Inst. Chem. Res. Kyoto Univ.*, **40**, 130 (1962).
18. T. E. Hogen-Esch and J. Smid, *J. Amer. Chem. Soc.*, **88**, 307 (1966); *ibid.*, **88**, 318 (1966).

19. L. L. Ferstandig and F. C. Goodrich, *J. Polym. Sci.*, **43**, 373 (1960).
20. J. W. L. Fordham, *J. Polym. Sci.*, **39**, 321 (1959).
21. C. E. H. Bawn, W. H. Janes, and A. M. North, in *Macromolecular Chemistry, Paris, 1963*, (*J. Polym. Sci. C*, **4**), M. Magat, Ed., Interscience, New York, 1963, p. 427.
22. K. Hatada, K. Ota, and H. Yuki, *J. Polym. Sci. B*, **5**, 225 (1967).
23. H. Gilman, W. Langham, and F. W. Moore, *J. Amer. Chem. Soc.*, **62**, 2327 (1940).
24. F. A. Bovey, *Pure Appl. Chem.*, **12**, 525 (1966).
25. F. A. Bovey and G. V. D. Tiers, *J. Polym. Sci.*, **44**, 173 (1960).
26. A. Katchalsky and H. Eisenberg, *J. Polym. Sci.*, **6**, 145 (1951).
27. W. E. Goode, F. H. Owens, R. P. Fellman, W. H. Snyder, and J. E. Moore, *J. Polym. Sci.*, **46**, 317 (1960).
28. S. Havriliak and N. Roman, *Polymer*, **7**, 387 (1966).
29. H. Nagai, H. Watanabe, and A. Nishioka, *J. Polym. Sci.*, **62**, 895 (1962).
30. E. I. Du Pont de Nemours & Co. (Inc.), Wilmington, Del. 19898. Du Pont 900 Differential Thermal Analyzer Instruction Manual, 1967.
31. S. N. Chinai, J. D. Matlack, A. L. Resnick, and R. J. Samuels, *J. Polym. Sci.*, **17**, 391 (1955).
32. W. L. Miller, W. S. Brey, and G. B. Butler, *J. Polym. Sci.*, **54**, 329 (1961).
33. J. C. Moore, *J. Polym. Sci. A*, **2**, 835 (1964).
34. G. D. Edwards, *J. Appl. Polym. Sci.*, **9**, 3845 (1965).
35. T. G. Fox, B. S. Garrett, W. E. Goode, S. Gratch, J. F. Kincaid, A. Spell, and J. D. Stroupe, *J. Amer. Chem. Soc.*, **80**, 1768 (1958).
36. B. S. Garrett, W. E. Goode, S. Gratch, J. F. Kincaid, C. L. Levesque, A. Spell, J. D. Stroupe, and W. H. Watanabe, *J. Amer. Chem. Soc.*, **81**, 1007 (1958).
37. J. D. Stroupe and R. E. Hughes, *J. Amer. Chem. Soc.*, **80**, 2341 (1958).
38. D. M. Wiles and S. Bywater, *Trans. Faraday Soc.*, **61**, 150 (1965).
39. D. L. Glusker, I. Lysloff, and E. Stiles, *J. Polym. Sci.*, **49**, 315 (1961).
40. B. J. Cottam, D. M. Wiles, and S. Bywater, *Can. J. Chem.*, **41**, 1905 (1963).
41. C. F. Ryan and P. C. Fleischer, *J. Phys. Chem.*, **69**, 3384 (1965).
42. L. H. Sommer, *Stereochemistry, Mechanism, and Silicon*, McGraw-Hill, New York, 1965, p. 66.

Received August 21, 1968
Revised November 13, 1968

JOURNAL OF POLYMER SCIENCE: PART A-1 VOL. 8, 329–334 (1970)

Transient Analysis of a Viscoelastic Torsion Pendulum

R. D. GLAUZ, *Department of Mathematics, University of California Davis, California 95616*

Synopsis

The transient torsion pendulum of arbitrary cross section is analyzed as a device for obtaining physical properties of a viscoelastic material. The damped sinusoidal motion yields a damping factor and frequency from which the complex modulus is computed. The particular cases of circular and rectangular cross section are considered with tables and approximations simplifying the practical application of the method.

INTRODUCTION

The torsion pendulum has been analyzed by Elder,[1] Kostyrko,[2] Nielsen,[3] and Tschoegl.[4] The various approximations made by Nielsen and Tschoegl indicated the need for an analysis considering the torsion pendulum as a damped oscillation of a finite bar of material by using the dynamic torsional equations such as in Love.[5] The complete analysis was done by Kostyrko.[2] This analysis was later extended by Elder[1] to the consideration of additional eigenvalues.

ANALYSIS

This analysis studies the free oscillation of a torsion pendulum as a means of obtaining the physical properties of a viscoelastic material. The torsion pendulum is of arbitrary cross section whose motion may be represented by the differential equation:[5]

$$\rho P\left[I_p(\partial^2\theta/\partial t^2) - \int \phi^2 dA\,(\partial^4\theta/\partial x^2\partial t^2)\right] = \kappa Q(\partial^2\theta/\partial x^2) \qquad (1)$$

in which P and Q represent the differential operators in the linear time-dependent stress–strain law, [eq. (2)], ρ is density, θ is relative angular displacement (radians), t is time (seconds), x is the coordinate along axis, I_p is the polar moment of inertia of cross section, κ is the torsional constant, and ϕ is the torsion function.

$$P(\tau) = Q(\gamma) \qquad (2)$$

The second term of eq. (1) yields a contribution from the out-of-plane warping of a noncircular cross section.

The boundary condition at the clamped end is zero displacement. The free end has a mass attached with a moment of inertia. Thus

$$\begin{aligned} \theta(0) &= 0 \\ [I_1 P(\partial^2\theta/\partial t^2) &= -\kappa Q(\partial\theta/\partial x)]_{x=l} \end{aligned} \tag{3}$$

The special case of a perfectly elastic torsion pendulum would oscillate continuously with zero change in amplitude

$$\theta(x,t) = H(x)e^{i\omega t} \tag{4}$$

where ω is the frequency of vibration. The effect of internal viscosity as exhibited by viscoelastic materials is a damping which causes a decrease in amplitude with time. This may be represented by the addition of an exponential damping factor $e^{-\lambda t}$ to eq. (4) resulting in

$$\theta(x,t) = H(x)e^{i\omega t}e^{-\lambda t} \tag{5}$$

Elder[1] considers the complete set of eigenvalues λ_i and shows that after an initial transient period the first or smallest eigenvalue predominates.

Substitution of eq. (5) into the partial differential eq. (1) and boundary condition eqs. (3) yields the determining equations for $H(x)$ as

$$\begin{aligned} H''(x) + (\psi/l)^2 H(x) &= 0 \\ H(0) &= 0 \\ H'(l) - (\psi^2/\alpha l)H(l) &= 0 \end{aligned} \tag{6}$$

where we have defined ψ, α by

$$\left(\frac{\psi}{l}\right)^2 = -\frac{-\rho I_p(i\omega-\lambda)^2 P(i\omega-\lambda)}{\kappa Q(i\omega-\lambda) + \rho(i\omega-\lambda)^2 P(i\omega-\lambda)\int \phi^2 d\Lambda} \tag{7}$$

$$\frac{1}{\alpha}\frac{\psi^2}{l} = \frac{-I_1(i\omega-\lambda)^2 P(i\omega-\lambda)}{\kappa Q(i\omega-\lambda)} \tag{8}$$

where l is the pendulum length and I_1 is the mass moment of inertia of the pendulum bob.

The solution of eq. (6) is given by

$$H(x) = C_1 \sin(\psi/l)x + C_2 \cos(\psi/l)x \tag{9}$$

The boundary conditions become relations determining C_1, C_2:

$$\begin{aligned} C_2 &= 0 \\ C_1(\alpha\cos\psi - \psi\sin\psi) - C_2(\alpha\sin\psi + \psi\cos\psi) &= 0 \end{aligned} \tag{10}$$

In order for this pair of homogeneous equations to have a nontrivial solution for C_1, C_2, the determinant of their coefficients must vanish, yielding

$$\alpha\cos\psi - \psi\sin\psi = 0 \tag{11}$$

with α obtainable from eqs (7); (8) in the form

$$\alpha = (\rho I_p l/I_1)\left[1 + (\psi^2/I_p l^2)\int \phi^2 dA\right] \tag{12}$$

Separating eq. (7) defining $(\psi/l)^2$ into real and imaginary parts yields the two equations:

$$G_1 = \frac{\rho(\omega^2 - \lambda^2)I_p l^2}{\psi^2 \kappa}\left(1 + \frac{\psi^2}{I_p l^2}\int \phi^2 dA\right) \tag{13}$$

$$G_2 = \frac{2\rho\omega\lambda I_p l^2}{\psi^2 \kappa}\left(1 + \frac{\psi^2}{I_p l^2}\int \phi^2 dA\right) \tag{14}$$

with the complex shear modulus defined by

$$G_1 + iG_2 = [Q(i\omega - \lambda)/P(i\omega - \lambda)] \tag{15}$$

COMPUTATION OF ψ

Equation (11) has only real roots ψ for real values of α. This can be proved by assuming a complex ψ and showing that the imaginary part must be zero using a sign argument.

Equations (12), (13), (14) in which ψ occurs involve ψ^2 terms only so that a method of evaluation for ψ^2 will be given. By reversion of series eq. (11) is solved for ψ^2 as a function of α:[6]

$$\psi^2 = \alpha - \frac{1}{3}\alpha^2 + \frac{4}{45}\alpha^3 - \frac{16}{945}\alpha^4 + \frac{16}{14175}\alpha^5 + \cdots \tag{16}$$

This approximation will yield accurate values of ψ^2 for most test conditions. If the value of α is such that a more accurate method is required, one of the standard methods for the numerical solution of nonlinear equations can be utilized.[7] The accuracy of eq. (16) for five terms is better than three significant digits at $\alpha = 1.00$ and rapidly improves to six significant digits for $\alpha = 0.25$. For very small α (e.g., Elder's example[1] $\alpha = 10^{-4}$), a correspondingly smaller number of terms may be sufficient.

The presence of ψ^2 in eq. (12) can be included in eq. (16) at the expense of considerable complexity. From a computational standpoint it is more economical to iterate between eqs. (12) and (16) because of the small size of the ψ^2 term in eq. (12).

CIRCULAR CROSS SECTION

For a circular cross section of radius r the equations simplify to

$$I_p = \pi r^4/2 \tag{17}$$

$$\kappa = \pi r^4/2 \tag{18}$$

$$\phi = 0 \tag{19}$$

$$\alpha = \rho I_p l/I_1 \tag{20}$$

$$G_1 = \rho(\omega^2 - \lambda^2)l^2/\psi^2 \tag{21}$$

$$G_2 = 2\rho\omega\lambda l^2/\psi^2 \tag{22}$$

RECTANGULAR CROSS SECTION

The rectangular cross section is useful in the testing environment because of its relative ease of fabrication. Let the cross section be of thickness $2b$ and width $2a$. In a cartesian coordinate system the physical boundaries would be the lines $x = \pm a$, $y = \pm b$. The thickness $2b$ is assumed to be smaller than the width $2a$. Then

$$I_p = 4/3\ a^4\ (b/a)\ [1 + (b/a)^2] \tag{23}$$

$$= a^4 I_{p_1}$$

$$\kappa = a^4\left[\frac{16}{3}\left(\frac{b}{a}\right)^3 - \left(\frac{b}{a}\right)^4\left(\frac{4}{\pi}\right)^5 \sum_{n=0}^{\infty} \frac{1}{(2n+1)^5} \tanh\frac{(2n+1)\pi a}{2b}\right] \tag{24}$$

$$= a^4\kappa_1$$

$$\phi = -xy + 4b^2\left(\frac{2}{\pi}\right)^3 \sum_{n=0}^{\infty} \frac{(-1)^n \sinh[(2n+1)\pi x/2b]}{(2n+1)^3 \cosh[(2n+1)\pi a/2b]} \times \sin\frac{(2n+1)\pi y}{2b}\Bigg] \tag{25}$$

From (25) the integral occurring in several equations can be obtained as

$$\int \phi^2 dA = a^6\left\{\frac{4}{9}\left(\frac{b}{a}\right)^3 - \frac{16}{5}\left(\frac{b}{a}\right)^5 + \frac{1024}{\pi^6}\left(\frac{b}{a}\right)^5 \times \sum_{n=0}^{\infty} \frac{1}{(2n+1)^6} \tanh\frac{(2n+1)\pi a}{2b} \times \left[\left(\frac{b}{a}\right)\frac{6}{\pi(2n+1)} + \tanh\frac{(2n+1)\pi a}{2b}\right]\right\} \tag{26}$$

$$= a^6 I_{\phi_1}$$

These values are tabulated for various b/a ratios in Table I.

The effect of the out-of-plane warping is measured by the size of the term

$$(\psi^2/I_p l^2) \int \phi^2 dA \tag{27}$$

relative to 1. For the circular cross section the term vanishes, and for the rectangular cross section the term can be written

$$(\psi^2/I_p l^2) \int \phi^2 dA = \psi^2 (a/l)^2\ (I_{\phi_1}/I_{p_1}) \tag{28}$$

TABLE I

b/a	I_{p_1}	κ_1	I_{ϕ_1}
0.1	0.134667	0.004997	0.000425
0.2	0.277333	0.037289	0.003003
0.3	0.436000	0.116775	0.008299
0.4	0.618667	0.255350	0.014912
0.5	0.833333	0.457363	0.020323
0.6	1.088000	0.720963	0.022317
0.7	1.390667	1.040144	0.020140
0.8	1.749333	1.406833	0.014958
0.9	2.172000	1.812513	0.009707
1.0	2.666667	2.249234	0.008602

The ratio I_ϕ/I_{p_1} has been computed for various b/a ratios as shown in Figure 1. For many testing conditions the out-of-plane warping effect is thus negligible.

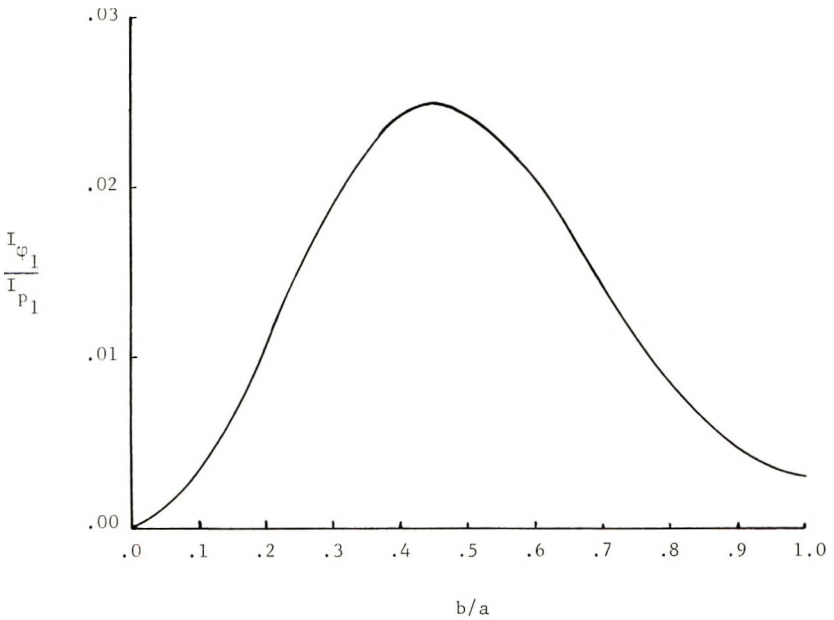

Figure 1.

TEST DATA ANALYSIS

In analyzing a typical test the position of the pendulum is recorded versus time. The resulting trace is analyzed to obtain the frequency ω from time between successive crossings of the axis. The damping factor is obtained from a fitting of the log of the amplitude versus time. The slope is the damping factor.

References

1. A. S. Elder, *Trans. Soc. Rheol.*, **9: 2,** 187 (1965).
2. G. J. Kostyrko, M.S. Thesis, Sacramento State College, 1963.
3. L. E. Nielsen, *Rev. Sci. Instr.*, **22,** 690 (1951).
4. N. W. Tschoegl, *J. Appl. Phys.*, **32,** 1794 (1961).
5. A. E. H. Love, *A Treatise on the Mathematical Theory of Elasticity*, Dover, New York, 1944, p. 429.
6. J. B. Scarborough, *Numerical Mathematical Analysis*, Johns Hopkins Press, Baltimore, 1962, p. 96.
7. S. D. Conte, *Elementary Numerical Analysis an Algorithmic Approach*, McGraw-Hill, New York, 1965.

Received November 26, 1968

JOURNAL OF POLYMER SCIENCE: PART A-1 VOL. 8, 335–349 (1970)

Hydrolytic Polymerization of Caprolactam. I. Hydrolysis—Polycondensation Kinetics

C. GIORI* and B. T. HAYES, *Allied Chemical, Fibers Division, Petersburg, Virginia 23803*

Synopsis

In a study aimed at process optimization of caprolactam polymerization, particular reference has been paid to the competing role of water in caprolactam hydrolysis and endgroup polycondensation. The dependence of the apparent equilibrium constant for polycondensation on water concentration indicated that there is a strong effect of the medium on the activities of the reacting species which can not be neglected in a kinetic study of the polycondensation reaction. The effect of a variation of the medium was taken into account by using a polycondensation rate constant which included a function of the water present at any given time. With the aid of analog computer curve-fitting techniques, good agreement with second-order kinetics was found. The validity of a second-order mechanism was confirmed in a kinetic study of the chain amide linkage hydrolysis. The hydrolysis of caprolactam follows substantially different kinetics, where the generation of carboxyl groups reduces the activation energy of the reaction, which follows predominantly a third-order mechanism.

INTRODUCTION

The kinetics of hydrolytic polymerization of caprolactam have been widely investigated by a Dutch group of workers,[1–3] by Wiloth,[4,5] by Skuratov and co-workers,[6] and by Wyness.[7] Three main equilibrium reactions were distinguished: hydrolysis of caprolactam (CL) to ϵ-aminocaproic acid (ACA) [eq. (1)],

$$\mathrm{CL} + \mathrm{H_2O} \rightleftarrows \mathrm{ACA} \tag{1}$$

stepwise addition of caprolactam units to the polymer chains [eq. (2)]

$$\mathrm{CL} + n\text{-mer} \rightleftarrows (n+1)\text{-mer} \tag{2}$$

and condensation of amine and carboxyl groups with formation of an amide group and a molecule of water [eq. (3)].

$$\mathrm{—COOH} + \mathrm{NH_2} \rightleftarrows \mathrm{—CO—NH—} + \mathrm{H_2O} \tag{3}$$

The stepwise addition of caprolactam was recognized to be the predominating polymerization reaction and has been investigated in considerable detail.[8] However, in a polymerization process, reactions (1) and (3) appear to be more important as far as the overall rate of polymerization is

* Present address: Research Institute, Illinois Institute of Technology, Chicago, Illinois 60616.

concerned. In fact, the final degree of polymerization is determined by the equilibrium reaction (3) which, in turn, is promoted by the endgroup generation from reaction (1). The rate of reactions (1) and (3) and their contribution to the overall polymerization can be increased by controlling the water content during the course of the process. Since water plays a competitive role on reactions (1) and (3), a knowledge of the kinetics of these reactions is essential.

The object of the present work is to study the hydrolysis-polycondensation kinetics in a caprolactam polymerization. The study of the polycondensation kinetics requires a knowledge of the equilibrium constant of reaction (3). Since data in the literature describing such equilibrium in systems with low water content are uncertain,[9,10] we felt that a reevaluation of the polycondensation equilibrium was necessary.

EXPERIMENTAL

Materials

ε-Caprolactam (Allied Chemical, Plastics Division) was distilled under vacuum before use and the intermediate fraction collected. The moisture present in the distillate was analyzed and taken into account when further addition of water was made.

Nylon 6 was prepared in a 3000-cc reactor with agitation under a nitrogen stream of 50 cc/min. ε-Aminocaproic acid, 5%, was added to the lactam. The temperature was raised to 255°C in 1 hr. The polymerization was continued at 255°C for 15 min for preparation of low molecular weight polymer (to be used in polycondensation experiments). The polymer samples were repeatedly washed with boiling water until no extractables were present, then dried at 100°C under vacuum (0.1 mm Hg) for 20 hr. The moisture content after drying was 0.01%. The carboxyl group concentration was 146 eq/10^6 g.

Nylon 7 was prepared by polymerization of enantholactam (Aldrich Chemical Co.) as described in the literature.[11] The very low equilibrium monomer content was eliminated by extraction, as described for nylon 6. After drying, the carboxyl group concentration was 45 eq/10^6 g. This polymer was used in chain amide hydrolysis experiments.

Analyses

COOH Groups. The method was based on the procedure of Waltz and Taylor[12] of titration against KOH in benzyl alcohol. The accuracy of this analysis was of extreme importance, since carboxyl group concentration appears in the equilibrium constant of polycondensation (K_{III}) in the second power ([COOH] = [NH_2] in absence of terminators). Particularly in systems with low water content, a small variation in the number of end groups will give a large change in K_{III}. The method of analysis was very accurate, yielding an estimated error in K_{III} never higher than 5%.

Per Cent Extractables. A sample of polymer was placed in boiling water under reflux for 2 hr. After filtering, the water-soluble content of the solution was determined by differential refractometry.[13]

Per Cent Moisture in Nylon 6. The moisture content was determined by using a manometric method. The polymer sample was heated at 185°C in a closed system under vacuum. The percentage of moisture in the sample was determined by measuring the pressure generated by the water vapor by using a calibrated oil manometer.

Per Cent Moisture in Caprolactam. The moisture content of caprolactam was determined by titrating a sample of molten caprolactam with Karl Fischer reagent with the use of a Beckman KF-3 aquameter.

Per Cent Caprolactam in Nylon 6. This was determined by gas chromatography (F & M Model 1609) on the aqueous solution of extractables.

Procedures

Reaction vessels were made from $^3/_4$-in. stainless tubes, 8 in. long, having walls $^1/_{16}$ in. thick. The tubes were sealed at each end with Swagelock caps. A salt bath controlled at ± 1°C was employed for heating the tubes. The tubes were purged with nitrogen and fully charged with the reactants. The free volume left was very small, and the water content of the melt was assumed equal to the total water present. The results of a study of the vapor–liquid equilibrium of water in molten nylon 6 indicated that for high melt-to-vapor volume ratios this is a valid assumption.[14]

The prewarmed tubes were lowered into the salt bath set to a temperature which reached the desired value within 3 min. In the case of nylon 7 hydrolysis experiments, in which high molecular weight polymer was used, 10 min was allowed for melting the polymer and reaching the desired temperature. The tubes were removed and quenched in cold water after the desired reaction time.

The polycondensation equilibria were determined as follows. Caprolactam containing different amounts of added water was reacted in sealed tubes as described at 240 and 260°C for 20 hr (preliminary experiments indicated that at both temperatures equilibrium was reached after 20 hr and that no endgroup change occurred on prolonged heating up to 60 hr). From the analysis of the reaction products the value of the equilibrium constants was calculated. The following symbols and relations have been used: K_{III} = equilibrium constant for polycondensation; W_0, W_t = initial and equilibrium water concentration (moles/10^6 g); C = concentration of carboxyl groups in the polymer (eq/10^6 g); C_{WD} = concentration of carboxyl groups in the polymer extracted with water and dried (eq/10^6 g); Z = concentration of chain amide linkages (eq/10^6 g); E = percentage by weight of water-extractable materials (caprolactam and water-soluble oligomers); M = concentration of caprolactam in the polymer (moles/10^6 g).

$$K_{III} = Z\,W_t/C^2 \tag{4}$$

$$W_t = W_0 - C \tag{5}$$

$$Z = [(10^6/113) - C_{WD}]\,[100 - E - (18\,W_t \times 10^{-4})]/100 \tag{6}$$

$$Z = [(10^6 - 113\,M - 18\,W_t)/113] - C \tag{7}$$

In the expression for K_{III}, the square of carboxyl group concentration was used instead of the product (carboxyl × amine groups), since in absence of terminators the concentration of carboxyl and amine groups is the same. In the evaluation of Z (concentration of amide linkages belonging to linear molecules), both eqs. (6) and (7) can be used, depending on whether the polymer is analyzed for caprolactam or water extractables. When eq. (6) is used, the amide linkages present in linear oligomers are neglected; when eq. (7) is used, the amide linkages present in cyclic oligomers are included in Z. Either way, the errors involved are extremely small.

Rate constants were derived from kinetic data by using concentration units of moles/10^6 g. The more proper volume concentrations were introduced by correcting the rate constants obtained in polycondensation experiments by using eq. (8) for the density of molten nylon 6 as a function of temperature (centigrade) T:[15]

$$d = 1.130 - 0.00052T \tag{8}$$

Since the density of molten nylon 6 is practically independent of the molecular weight, there was no density change during the polycondensation experiments. The rate constants for caprolactam hydrolysis at 2% water concentration were corrected for the density by using the relationship of caprolactam density as a function of temperature given by Majury:[16]

$$d = 1.097 - 0.000902T \tag{9}$$

Also in this case, since the caprolactam content in the range of conversions considered was always high (>80%), the density of the system was assumed to be constant during the course of reaction. The density of systems containing high water concentrations (10 g water/100 g nylon 7) was not determined.

RESULTS AND DISCUSSION

Polycondensation Equilibrium

The results of the polycondensation equilibrium study are shown in Table I. In Figure 1 the calculated values of the equilibrium constants at 240 and 260°C are plotted against the equilibrium water content. It can be observed that at both temperatures the calculated equilibrium constants depend on the composition of the system: they increase with increasing water concentration but decrease after a maximum is reached at about 1.5% water. A constant value is obtained for water concentrations higher than 7%. It can also be observed that higher values of equilibrium con-

stants are obtained at 240°C than at 260°C because of the exothermic nature of the condensation reaction. However, the discrepancy between the two curves becomes smaller and smaller with reducing water content, and at very low water concentration there is little or no effect of temperature on the equilibrium. This behavior indicates a very complex influence of activity coefficients.

TABLE I
Equilibrium Data Relating to Polycondensation

T, °C	Initial water concentration, g H_2O/100 g CL	[COOH], eq/10^6 g	[COOH] after extraction, eq/10^6 g	Extractables, wt-%	K_{III}
240	0.2	41	45	7.9	340
	0.3	48	53	7.9	410
	0.4	51	56	8.7	530
	0.5	56	59	8.2	560
	1.0	73	77	9.1	710
	1.5	84	89	9.6	820
	2.0	97	102	9.7	820
	4.0	145	151	10.1	710
	6.0	191	188	11.5	580
	8.0	230	218	12.8	510
	10.0	253	235	13.0	510
260	0.2	42	48	9.4	310
	0.3	50	56	9.8	370
	0.4	54	58	9.8	460
	0.5	59	65	9.9	490
	1.0	79	90	10.2	590
	1.5	95	106	10.6	620
	2.0	110	120	11.6	610
	4.0	167	161	12.2	520
	6.0	220	207	13.4	420
	8.0	253	233	14.9	410
	10.0	278	260	15.1	410

The nature of the system suggests that a variation of both water and endgroup activity coefficients is to be expected by changing water content. End-groups in nylon 6 are partially ionized, and the ionization constant K_i

$$K_i = \frac{[NH_3^+ \sim\!\sim COO^-]}{[NH_2 \sim\!\sim COOH]} \tag{10}$$

depends on the dielectric constant of the medium.[8]

With increasing water content the dielectric constant of the medium and the degree of endgroup ionization will increase. This is likely to affect endgroup activity coefficients, depending on whether the polycondensation reaction involves preferably condensation of neutral species or ionized species.

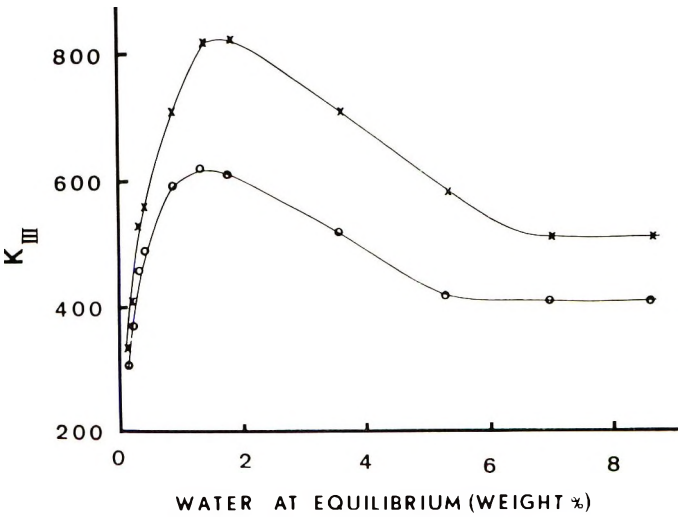

Fig. 1. Equilibrium constants for polycondensation vs. equilibrium water content: (×) 240°C; (○) 260°C.

The water activity coefficient can also affect the polycondensation equilibrium, because the system water–molten nylon 6 is not ideal, and the activity coefficient of water will change with changing water content. Furthermore, since an increase in water concentration shifts the equilibrium to lower molecular weights, the dependence of water activity coefficient on water concentration could be also affected by the change in chain length involved.

The activity coefficients of water can be determined by studying the vapor–liquid equilibrium of water in molten nylon 6.[14] In this work, the concentrations are used instead of the activities for all the reacting species, and the kinetics are expressed in terms of apparent rate and equilibrium constants.

Kinetics of Polycondensation Reaction

The kinetics of the polycondensation reaction were studied on various polyamides by different authors. However, the studies published are discordant on the question of the order of the reaction, which has never been definitely clarified. Heikens *et al.*,[17] by analogy with the kinetics of caprolactam hydrolysis, concluded that presumably also in polycondensation a second-order uncatalyzed reaction and a third-order reaction catalyzed by the carboxyl group both occur. Wiloth was of the same opinion and supported the thesis of a mixed-order reaction by kinetic measurements on the endgroup condensation of poly(ε-aminocaproic acid) and poly(7-aminoheptanoic acid).[18] Champetier and Vergoz[19] studied the polycondensation of 11-aminoundecanoic acid concluding that the reaction follows a bimolecular mechanism with a second order rate constant which decreases

exponentially with time. Ogata[20] studied the condensation of poly(hexamethylene adipamide) concluding that the reaction follows a second-order mechanism.

It seems logical to ascribe the uncertainties in the order of the reaction to the effect of a variable medium on the reactivity of end groups, which does not allow a clear determination of the reaction order. This would not indicate necessarily that the Flory principle of equal reactivity is not observed. On the basis of our observations on the condensation equilibrium, a variation in endgroup reactivity during the course of polycondensation can be ascribed to the effect of a variation of water content on the dielectric constant of the medium, the reactivity of molecules of different length being the same at any given time.

Under conditions of rapid and complete water removal this effect would be excluded, but the effect of the rate of water removal would introduce a new source of uncertainty, since the complete elimination of the reverse reaction can not be attained with certainty. Kinetic measurements are better made by using sealed reaction systems, in which the reverse reaction is fully taken into account.

In order to ascertain the order of the polycondensation reaction, we approached the problem in a different way. Since the polycondensation reaction is related to the reaction of hydrolysis of the amide linkage by the equilibrium (3), we studied the kinetics of hydrolysis of the chain amide linkage. Since the regeneration of caprolactam monomer from nylon 6 (reverse of the polyaddition reaction) followed by hydrolysis of caprolactam could constitute a disturbing side reaction in the study of polyamide hydrolysis, we preferred to study such reaction on nylon 7. As a result of the difficulty of forming eight-membered rings, the regeneration of lactam from nylon 7 is insignificant, and the reverse of the polyaddition reaction followed by hydrolysis of enantholactam can be neglected.[21]

TABLE II
Data Relating to Nylon 7 Hydrolysis[a]

t, min	[COOH], eq/10^6 g
10	62
20	97
40	152
60	196
80	216

[a] Initial water concentration, 10 g/100 g polyamide; T = 240°C.

The reaction of nylon 7 hydrolysis was studied in sealed tubes at 240°C by following the rate of carboxyl group generation from 10 to 80 min reaction time (Table II). The water consumed by hydrolysis was only a negligible portion of the initial water present (10 g H_2O/100 g polyamide), and no effect of a variation of water content on the medium is to be expected. In the kinetic analysis of the hydrolysis data, the reverse reac-

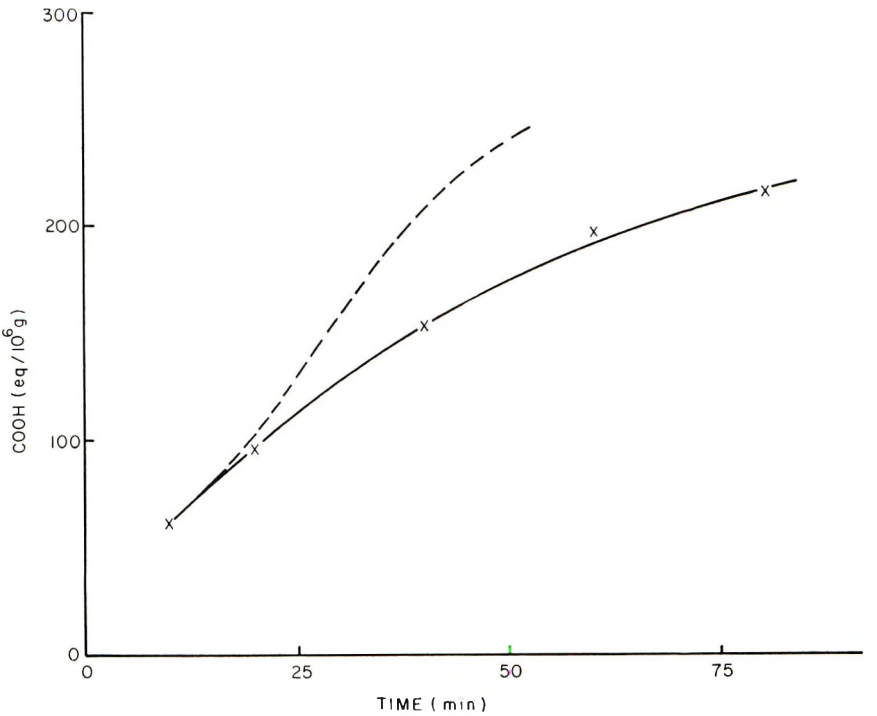

Fig. 2. Carboxyl group generation by hydrolysis of nylon 7: curve fittings for (——) second-order kinetics and (- -) for third-order kinetics (dotted line). T = 240°C; initial water concentration, 10 g/100 g polyamide.

tion (polycondensation) was taken into account and the order of the reaction was determined by using the kinetic equation (11):

$$d[\mathrm{COOH}]/dt = h[\mathrm{COOH}]^x[\mathrm{CO{-}NH}][\mathrm{H_2O}] - hK_{\mathrm{III}}[\mathrm{COOH}]^x[\mathrm{COOH}][\mathrm{NH_2}] \quad (11)$$

where h = rate constant of the hydrolysis reaction, k = rate constant of the polycondensation reaction. Since $[\mathrm{COOH}] = [\mathrm{NH_2}]$,

$$d[\mathrm{COOH}]/dt = h[\mathrm{COOH}]^x([\mathrm{CO{-}NH}][\mathrm{H_2O}] - K_{\mathrm{III}}[\mathrm{COOH}]^2) \quad (12)$$

The equilibrium constant K_{III} was taken from nylon 6 equilibrium data at the same temperature and water content (K_{III} = 510, which is a "true" constant in the range of water content of this study). The reaction rates $d[\mathrm{COOH}]/dt$ were determined graphically at various times, and the value of x yielding a constant h was determined by trial calculation. It was found that h is constant when c = 0, which indicates a second-order mechanism. This is shown in Figure 2, where it can be seen that the experimental points fit perfectly with the curve calculated for a second-order mechanism [x = 0 in eq. (12)]. For comparison, a fitting for a third-order mechanism (x = 1) is also shown, which deviates considerably from the experimental points.

Based on the knowledge of the order of reaction (3) determined from chain hydrolysis experiments, we studied the more complex polycondensa-

tion reaction at low water content. As indicated by the behavior of K_{III}, at low water content small changes in water concentration have a strong effect on the medium. The kinetics of polycondensation were studied on low molecular weight nylon 6 previously extracted and dried to a low water content (0.01% by weight). Regeneration of caprolactam followed by hydrolysis can be neglected in this case, because of the small amount of water present. The reaction was carried out in sealed tubes at 240 and 260°C. The variation of the medium associated with the increase of water content in the system during reaction (from 0.01 to approximately 0.18% by weight) was taken into account by using a rate constant which included a function of the water present at any given time.

In the range of low water contents (<0.4% by weight at equilibrium) the apparent equilibrium constants for polycondensation depend linearly on water concentration according to eqs. (13) and (14) at 240°C and 260°C, respectively,

$$K_{III} = 1.6[H_2O] + 220 \tag{13}$$

$$K_{III} = 1.5[H_2O] + 200 \tag{14}$$

where $[H_2O]$ is in moles/10^6 g.

As reported by Fukumoto,[22] in this range of low water contents, water follows Henry's law; hence the dependence of K_{III} on $[H_2O]$ must reflect a variation in endgroup activity coefficients.

As a consequence, referring to the concentrations of the reacting species, in the relationship $K_{III} = k/h$, where k is the apparent rate constant of the forward reaction (condensation) and h the apparent rate constant of the reverse reaction (hydrolysis), the variation of K_{III} reflects a variation of k, h being a constant.

k can therefore be expressed as a function of the water present according to the relationships:

$$k = h(1.6[H_2O] + 220) \tag{15}$$

$$k = h(1.5[H_2O] + 200) \tag{16}$$

at 240 and 260°C, respectively.

The second-order kinetic equations for polycondensation limited by the reverse reaction at 240 and 260°C become:

$$-d[COOH]/dt = h(1.6[H_2O] + 220)[COOH]^2 - h[CONH][H_2O] \tag{17}$$

$$-d[COOH]/dt = h(1.5[H_2O] + 200)[COOH]^2 - h[CONH][H_2O] \tag{18}$$

at 240 and 260°C, respectively.

The integration of these equations was simply performed on an analog computer using the curve fitting technique. The kinetic data are listed in Table III. In Figure 3 a comparison of the experimental points with the computer output is given. The agreement is satisfactory, indicating that the kinetic equations written above describe well the polycondensation reaction.

TABLE III
Data of Polycondensation Limited by Reverse Reaction

t, min	[COOH], eq/10^6 g 240°C	260°C
0	146	146
15	119	102
25	108	89
35	97	78
45	90	70
70	77	63
120	63	52
180	55	47

The values of h obtained at 240 and 260°C were 0.37×10^{-3} and 1.5×10^{-3} l./mole-min, respectively.

The values of k can be calculated as the product hK_{III} at any water content in the range considered.

Kinetics of Caprolactam Hydrolysis

The kinetics of caprolactam hydrolysis have been studied by Hermans et al.[1,2] and Wiloth,[4,5] respectively, at 221.5 and 220°C. We studied the reaction kinetics in the range between 235 and 265°C. The caprolactam hydrolysis was simply studied at 2% by weight water concentration in sealed tubes at short reaction times, when the end group condensation can be reasonably neglected. Also the reverse reaction of aminocaproic acid cyclization was neglected, since over the range of conversion considered the amount of caprolactam present was always large (above 80%).

While the rate of caprolactam disappearance is inclusive of the addition of caprolactam to the endgroups, this reaction does not affect the endgroup

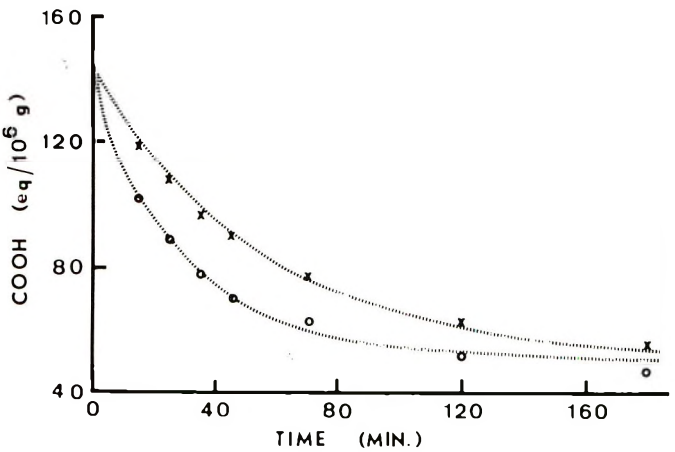

Fig. 3. Course of polycondensation limited by reverse reaction: (×) 240°C; (○) 260°C. Fit of experimental points with computer output.

TABLE IV
Data Relating to CL Hydrolysis[a]

	235°C		245°C		255°C		265°C	
t, min	[COOH], eq/10^6 g	[CL], wt-%	[COOH], eq/10^6 g	[CL], wt-%	[COOH], eq/10^6 g	[CL], wt-%	[COOH], eq/10^6 g	[CL], wt-%
10	3	98	3	98	4	98	14	98
15							24	96
20	8	97	11	97	20	97	42	94
25							65	90
30	16	96	23	95	44	93	103	85
40	27	95	42	94	85	87		
50	41	94	69	94	147	80		

[a] Initial water concentration, 2 wt. %.

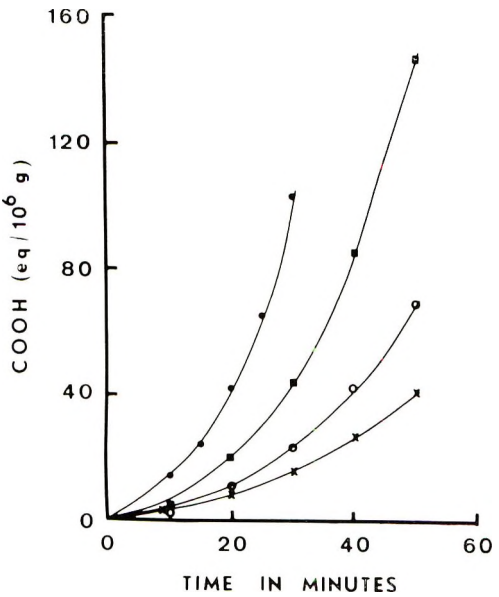

Fig. 4. Course of carboxyl group generation by hydrolysis of caprolactam: (×) 235°C; (○) 245°C; (■) 255°C; (●) 265°C. Initial water concentration, 2 wt-%.

total number; hence the rate of caprolactam hydrolysis can be conveniently followed by measuring the rate of carboxyl group generation. Kinetic data at different temperatures are listed in Table IV and in Figure 4 the carboxyl group concentration is plotted versus time. The reaction is autocatalytic, and the catalysis was shown[17] to be due to the carboxyl group.

As previously reported by Hermans[1,2] and Wiloth[4,5] we also found that uncatalyzed hydrolysis and hydrolysis catalyzed by carboxyl groups both occur, the reaction kinetics being conveniently represented by a mixed order. Indicating with k and k_c respectively the rate constants for the uncatalyzed and catalyzed hydrolysis, the following kinetic equation (19) applies:

$$d[\mathrm{COOH}]/dt = k[\mathrm{CL}][\mathrm{H_2O}] + k_c[\mathrm{CL}][\mathrm{H_2O}][\mathrm{COOH}] \tag{19}$$

which may be written:

$$\frac{d[\mathrm{COOH}]/dt}{[\mathrm{CL}][\mathrm{H_2O}]} = k + k_c[\mathrm{COOH}] \tag{20}$$

The reaction rates $d[\mathrm{COOH}]/dt$ were graphically determined from Figure 4. The water concentrations $[\mathrm{H_2O}]$ were calculated from the difference between initial water and carboxyl group concentration at any given time. Rate constants were evaluated by plotting $(d[\mathrm{COOH}]/dt)/[\mathrm{CL}][\mathrm{H_2O}]$ versus $[\mathrm{COOH}]$ (Fig. 5), the intercept and the slope of the lines yielding respectively the values of k and k_c. The rate constant values at various temperatures are reported in Table V. The contribution of catalyzed hydrolysis to

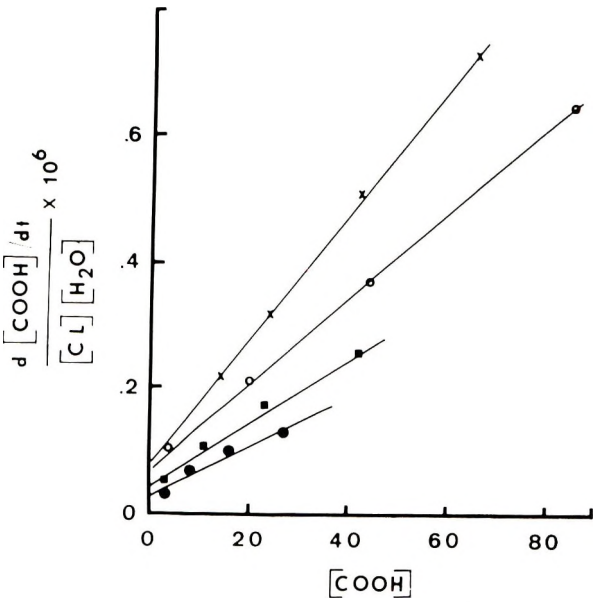

Fig. 5. Evaluation of rate constants in caprolactam hydrolysis by differential method: (●) 235°C; (■) 245°C; (○) 255°C; (×) 265°C. Concentrations are expressed in moles/10^6 g.

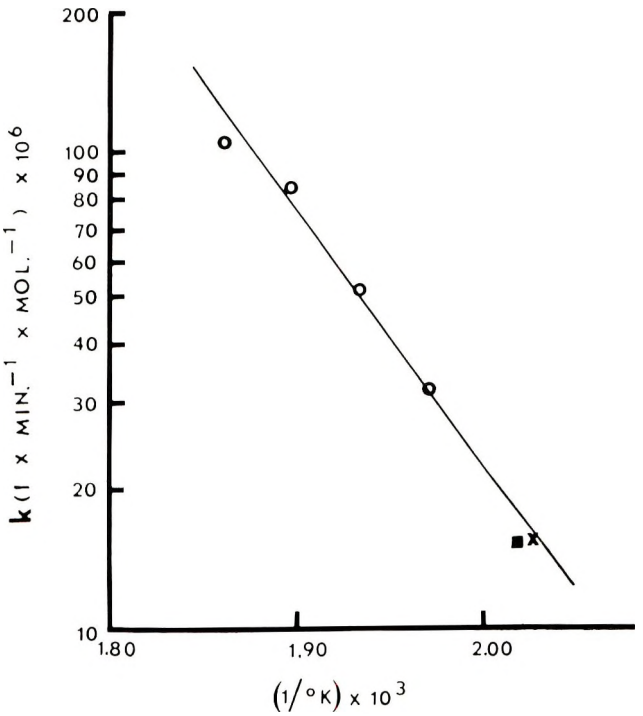

Fig. 6. Arrhenius plot for uncatalyzed caprolactam hydrolysis: (×) data of Wiloth;[4,6] (■) data of Hermans;[1,2] (○) this work.

TABLE V
Rate Constants for the Uncatalyzed and Catalyzed Caprolactam Hydrolysis

T, °C	k, l./min-mole $\times 10^6$	k_c, l.²/min-mole² $\times 10^4$
235	32	52
245	52	66
255	85	90
265	105	134

the overall reaction is by far more important than uncatalyzed hydrolysis. In Figures 6 and 7 the uncatalyzed and catalyzed rate constants are plotted versus the reverse of temperature (1/°K). By extrapolation at lower temperature, a good agreement is found with the rate constants previously published by Hermans and Wiloth. The activation energies were found to be: E = 26 kcal/mole (second-order, uncatalyzed reaction) and E = 15 kcal/mole (third order, COOH group-catalyzed reaction). The generation of carboxyl groups allows the reaction to take place by a catalyzed mechanism requiring a lower activation energy.

The authors wish to thank Mr. T. P. Moore who developed a computer program for the polycondensation reaction simulation.

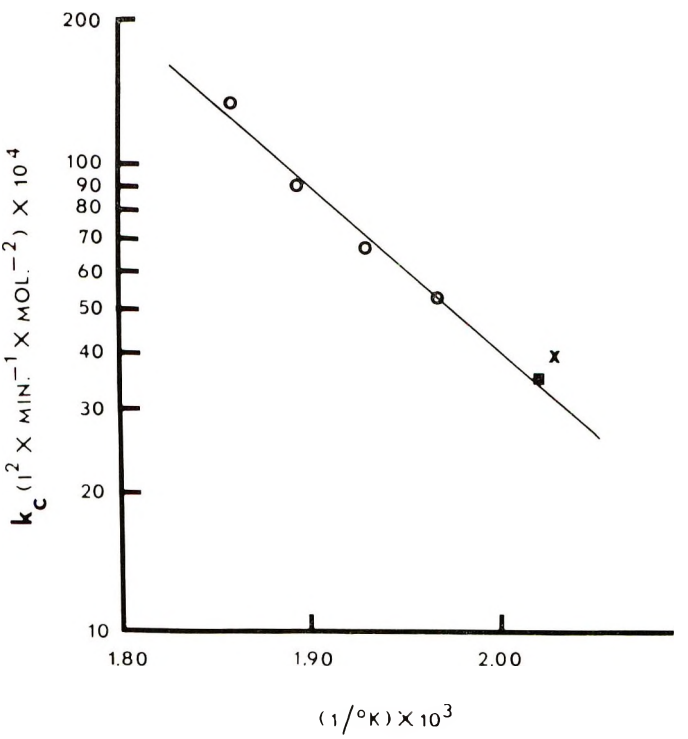

Fig. 7. Arrhenius plot for catalyzed caprolactam hydrolysis: (×) data of Wiloth;[1,2] (■) data of Hermans;[1,2] (○) this work.

References

1. P. H. Hermans, D. Heikens, and P. F. Van Velden, *J. Polym. Sci.*, **30**, 81 (1958).
2. D. Heikens and P. H. Hermans, *J. Polym. Sci.*, **44**, 429 (1960).
3. Ch. A. Kruissink, G. M. Van der Want, and A. J. Staverman, *J. Polym. Sci.* **30**, 67 (1958).
4. F. Wiloth, *Z. Physik. Chem.*, **11**, 78 (1957).
5. F. Wiloth, *Makromol. Chem.*, **30**, 189 (1959).
6. S. M. Skuratov, N. S. Enikolopyan, A. K. Bonetskaya, and V. V. Voevodskii, *Vysokomol. Soedin.*, **4**, 1770 (1962).
7. K. G. Wyness, *Makromol. Chem.*, **38**, 189 (1960).
8. Ch. A. Kruissink, paper presented at IUPAC Symposium on Macromolecules, Wiesbaden, 1959.
9. F. Wiloth, *Z. Physik. Chem.*, **5**, 66 (1955).
10. P. F. Van Velden, G. M. van der Want, D. Heikens, C. A. Kruissink, P. H. Hermans, and A. J. Staverman, *Rec. Trav. Chim.*, **74**, 1376 (1955).
11. D. D. Coffman, N. L. Cox, E. L. Martin, W. E. Mochel, and F. J. Van Natta, *J. Polym. Sci.*, **3**, 85 (1948).
12. J. E. Waltz and G. B. Taylor, *Anal. Chem.*, **19**, 448 (1947).
13. G. C. Ongermach, V. A. Dorman-Smith, and W. E. Beier, *Anal. Chem.*, **38**, 123 (1966).
14. C. Giori and B. T. Hayes, *J. Polym. Sci. A-1*, in press.
15. A. M. Kotliar, private communication.
16. T. G. Majury, *J. Polym. Sci.*, **31**, 383 (1958).
17. D. Heikens, P. H. Hermans, and G. M. Van der Want, *J. Polym. Sci.*, **44**, 437 (1960).
18. F. Wiloth, *Kolloid Z.*, **160**, 48 (1958).
19. G. Champetier and R. Vergoz, *Rec. Trav. Chim.*, **69**, 85 (1950).
20. N. Ogata, *Makromol. Chem.*, **43**, 117 (1961).
21. R. C. P. Cubbon, *Polymer*, **4**, 545 (1963).
22. O. Fukumoto, *J. Polym. Sci.*, **22**, 263 (1956).

Received February 18, 1969
Revised June 24, 1969

JOURNAL OF POLYMER SCIENCE: PART A-1 VOL. 8, 351-358 (1970)

Hydrolytic Polymerization of Caprolactam. II. Vapor–Liquid Equilibria

C. GIORI* and B. T. HAYES, *Allied Chemical, Fibers Division, Petersburg, Virginia 23803*

Synopsis

The system water–caprolactam–polymer at equilibrium is regarded as a solution consisting of two solvents (water and caprolactam) and one solute (polymer). The activities of water and caprolactam in equilibrium at 270°C in the range of 2–10 wt-% total water content have been determined by vapor-pressure measurements. Water shows large negative deviations from Raoult's law, as a consequence of the different size of water and polymer molecules. The partial molar free energies of mixing are compared with the expressions derived from the Flory-Huggins theory of polymer solutions; the results are not conclusive, but seem to indicate a qualitative agreement with the theory. The increase in vapor pressure during polymerization in sealed systems and the water dependence of the polycondensation equilibrium are discussed and explained in terms of water activity changes.

INTRODUCTION

At any temperature, the concentration of water and caprolactam in molten nylon 6 is determined by an equilibrium with water and caprolactam in the vapor phase, and the degree of polymerization is in turn determined by a chemical equilibrium with the water present in the liquid phase.

The system water–caprolactam–polymer can be considered as a solution consisting of two solvents (water and caprolactam) and one solute (polymer). This paper deals with the vapor–liquid equilibria of water and caprolactam in molten nylon 6.

EXPERIMENTAL

Materials and Analyses

Caprolactam purification and analytical techniques have been described in the previous paper.[1]

Procedures

Caprolactam (20 g) and the desired amount of water were charged in a stainless steel reactor (total volume 77 cc). The system was purged with nitrogen. The polymerization was carried out in a salt bath, whose tem-

* Present address: Research Institute, Illinois Institute of Technology, Chicago, Illinois 60616.

perature was controlled to ±1°C, into which the reactor was completely submerged. The desired temperature inside the reactor (270°C) was reached within 3 min. The pressure indicating device was a Bourdon-type gage thermally insulated provided with a grease fitting valve to prevent the condensation of the vapors in the Bourdon tube. After the equilibrium pressure was reached, the reactor was removed from the bath, the vapor phase rapidly condensed in a side-arm of the reactor, and the polymer quenched. Long heating periods were avoided, since they may give rise to measurable quantities of degradation products in the vapor phase.

On the condensate, the relative proportion of water and caprolactam present was determined by refractive index at 25°C with a Bausch & Lomb refractometer. The carboxyl group concentration and caprolactam content of the polymer were determined. In some experiments the composition of the vapor phase was also determined after 10 min reaction time. Measurements at initial water content below 2 wt-% were not carried out because sufficient condensate for analysis could not be collected.

The pressure due to the nitrogen present was subtracted from the total, the pseudo-compressibility factor for the vapor was determined (the critical temperature and critical pressure for caprolactam were derived by using Lydersen's empirical equation[2]) and the total number of moles present in the vapor was calculated. By knowledge of the composition of the vapor phase, the number of moles of caprolactam and water in the vapor and their partial pressures were also calculated. The amount of water present in the liquid phase at equilibrium was determined by difference, from a knowledge of the water introduced, the water present in the vapor phase, and the water consumed in end group generation. The method of calculation of the equilibrium constant K_{III} was described in a previous paper.[1]

RESULTS AND DISCUSSION

The vapor–liquid equilibrium of water in molten nylon 6 was studied at 270°C for initial water contents varying from 2 to 10 g H_2O/100 g caprolactam.

The results of these experiments are summarized in Table I. In Figure 1, $P_{H_2O}/P^0_{H_2O}$ (which is equal to the activity of water a_{H_2O}) is plotted versus the molar fraction of water in the liquid phase (x_{H_2O}).* The curve shows a large negative deviation from Raoult's law ($a_{H_2O} = x_{H_2O}$). The deviation is mostly due to the different size of polymer and water molecules. Large negative deviations are always observed in the study of polymer solutions, because even small amounts by weight of solvent make the solvent molar fraction very high. In these cases a better correlation is sometimes observed if the volume fractions are substituted for the molar fractions.

* For greater accuracy the fugacities could be calculated (i.e., by applying the Lewis-Randall rule for gas mixtures and by calculating the fugacity coefficient using the principle of corresponding states) and substituted for the vapor pressures.

TABLE I
Vapor–Liquid Equilibrium Data, $T = 270°C$

Initial water, g H_2O/100 g CL	Gage reading, psig	CL in liquid phase, wt-%	H_2O in liquid phase, wt-%	[COOH], eq/10^6 g	H_2O in vapor phase, wt-%	P_{H_2O} atm	P_{CL}, atm	Compressibility factor
2	95	9.6	1.19	97	73.5	5.33	0.31	0.980
4	160	9.7	2.49	159	85.0	9.78	0.28	0.970
6	215	9.9	3.87	196	88.6	13.53	0.28	0.955
8	277	10.1	5.15	239	89.0	17.68	0.35	0.940
10	325	10.6	6.50	273	91.0	20.95	0.33	0.930

TABLE II
Initial Vapor Pressures of Caprolactam and Water, T = 270°C

Initial water, g H_2O/100 g CL	P_{CL}, atm	P_{H_2O}, atm
2	0.73	2.93
4	0.83	6.51
6	0.73	9.33
8	0.72	10.35
10	0.58	13.57

In Figure 2 the activities of water $P_{H_2O}/P^0_{H_2O}$ are plotted versus the volume fractions of water. The upper curve represents the Raoult's law, the lower line represents the arbitrary relationship $a_{H_2O} = v_{H_2O}$ (activity = volume fraction). The experimental curve lies between these two curves.

The partial molar free energies of mixing for water and caprolactam in molten nylon can be easily calculated from vapor pressure data. It is interesting to compare the $\overline{\Delta F}$ values with the expressions derived from the

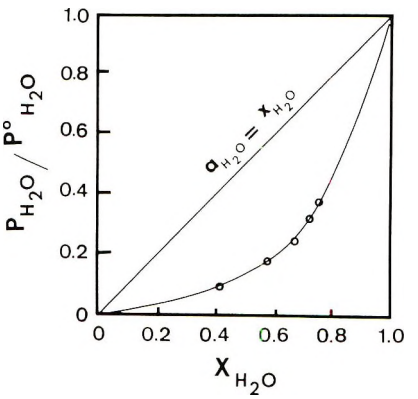

Fig. 1. Activity of water in nylon 6 at equilibrium vs. water molar fraction; T = 270°C.

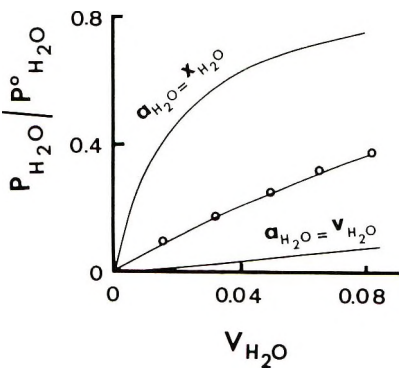

Fig. 2. Activity of water in nylon 6 at equilibrium vs. water volume fraction; T = 270°C.

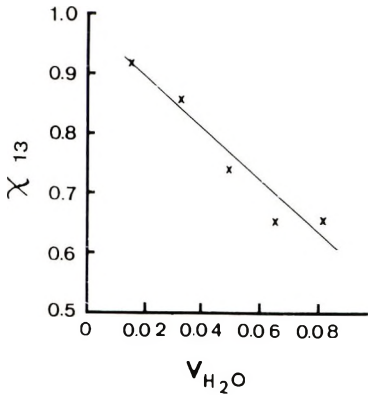

Fig. 3. Flory-Huggins interaction parameter χ_{13} vs. water volume fraction in nylon 6 at equilibrium. $T = 270°C$.

Flory-Huggins theory of polymer solutions, for the case of a ternary system consisting of a polymer in a binary solvent mixture:

$$\overline{\Delta F_1} = RT[\ln v_1 + (1 - v_1) - (v_2/x_2) - (v_3/x_3) + (\chi_{12}v_2 + \chi_{13}v_3)(v_2 + v_3) - (\chi_{23}/x_2)v_2v_3]$$

$$\overline{\Delta F_2} = RT[\ln v_2 + (1 - v_2) - v_1x_2 - v_3(x_2/x_3) + (\chi_{21}v_1 + \chi_{23}v_3)(v_1 + v_3) - \chi_{13}x_2v_1v_3]$$

Subscripts 1, 2, 3 refer respectively to water, caprolactam, and polymer. x_2, x_3 represent the ratios of the molar volumes, calculated assuming no volume change on mixing:

$$x_2 = Vm_2/Vm_1$$

$$x_3 = Vm_3/Vm_1$$

v_1, v_2, v_3, are the volume fractions of 1, 2, 3 defined as:

$$v_1 = n_1/(n_1 + n_2x_2 + n_3x_3)$$

$$v_2 = n_2x_2/(n_1 + n_2x_2 + n_3x_3)$$

$$v_3 = n_3x_3/(n_1 + n_2x_2 + n_3x_3)$$

χ_{12}, χ_{13}, χ_{23} are the Flory-Huggins interaction parameters. These equations were solved taking χ_{23} equal to zero (this is a reasonable assumption because caprolactam and polymer have a similar chemical structure). A comparison with the theory can be made by calculating the parameters χ_{12} and χ_{13} which according to the theory should be constant in all the composition range. Polar systems, however, are known to deviate from the Flory-Huggins theory, and a quantitative agreement is not expected. χ_{13} is not constant, and decreases with increasing water content (Fig. 3). However, the slope of the line shows that χ_{13} reaches values lower than 0.5 (as should be expected, because solutions of water and molten nylon at

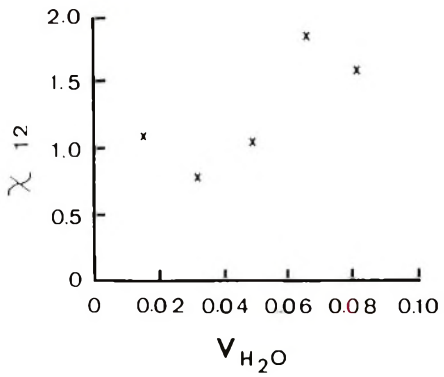

Fig. 4. Flory-Huggins interaction parameter χ_{12} vs. water volume fraction in nylon 6 at equilibrium; T = 270°C.

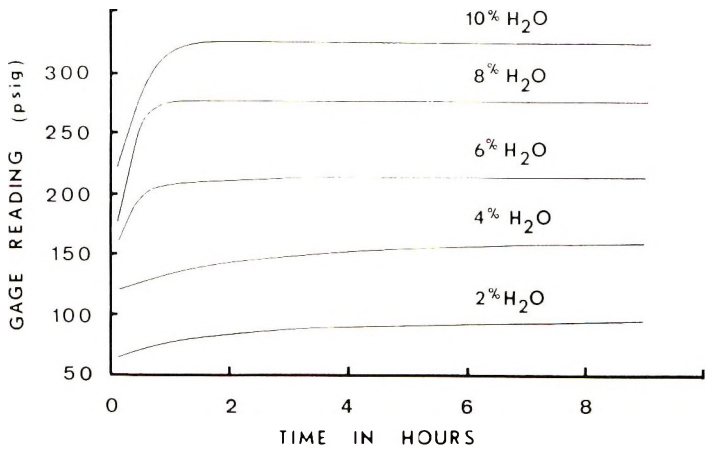

Fig. 5. Course or vapor pressure during polymerization; T = 270°C.

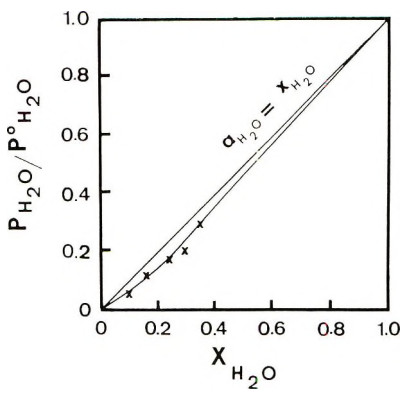

Fig. 6. Activity of water in caprolactam vs. water molar fraction; T = 270°C.

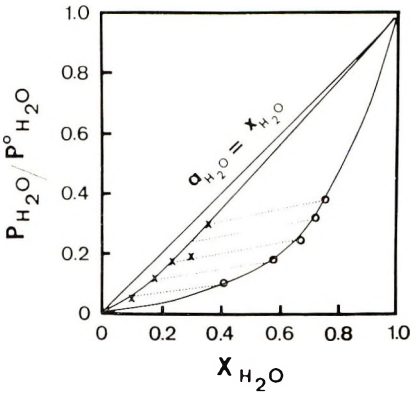

Fig. 7. Activity of water (×) in caprolactam and (○) in nylon 6 at equilibrium vs. water molar fraction; T = 270°C.

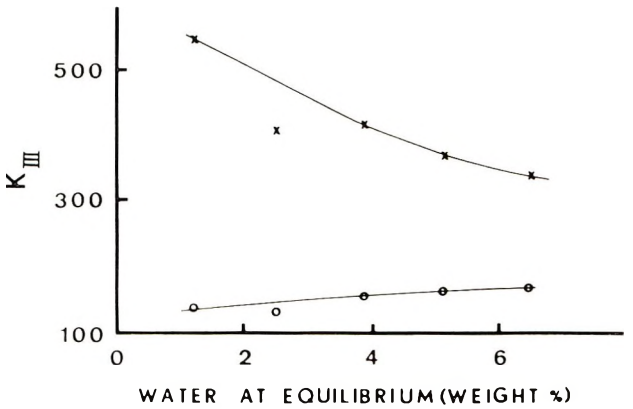

Fig. 8. Equilibrium constants for nylon 6 polycondensation vs. equilibrium water content: (×) apparent equilibrium constants; (○) equilibrium constants corrected for the water activity coefficient. T = 270°C.

equilibrium do not separate into two phases). χ_{12} values are scattered (Fig. 4), but all the values are lower than 2 (as should be expected for solvents completely miscible). These results are not conclusive, but seem to indicate a qualitative agreement with the theoretical predictions of Flory-Huggins theory.

It is interesting to observe the course of the pressure during polymerization (Fig. 5). The pressure increases continuously during polymerization, until the equilibrium value is reached. This may appear strange, because the amount of volatile materials present (water and caprolactam) decreases during polymerization. The reason for this behavior has been explained. The phase equilibria in the system caprolactam–water were studied at 270°C by determining the vapor-phase composition and calculating the vapor pressures of water and caprolactam after 10 min heating time, when the conversion of caprolactam in polymer is still negligible. The behavior

of water is shown in Figure 6. It can be seen that there is a negative deviation from ideal behavior (very uncommon case in aqueous systems, which indicates strong hydrogen bond formation between caprolactam and water).

The vapor pressures of water and caprolactam are reported in Table II. By comparison with the equilibrium vapor pressures reported in Table I, it can be seen that the contribution of caprolactam vapor pressure to the total pressure is small, and decreases during polymerization.

The increase in total pressure is therefore due to the increase in water partial pressure. In Figure 7 we plotted in the same graph the activity of water $P_{H_2O}/P^0_{H_2O}$ versus its molar fraction x_{H_2O} in caprolactam (initial conditions) and in molten nylon at equilibrium (final conditions). The partial pressure of water increases because the molar fraction of water increases, in spite of the decrease of the actual amount of water present in solution, and in spite of the much more negative deviations from ideal behavior in molten nylon. The variation of $P_{H_2O}/P^0_{H_2O}$ and x_{H_2O} from initial to final conditions is shown by the lines drawn from one curve to the other.

A knowledge of the composition of this melt at equilibrium allows one to calculate the equilibrium constant for the polycondensation reaction:

$$K_{III} = [CO—NH][H_2O]/[COOH][NH_2]$$

It was shown[1] that, due to a variation of activity coefficients, the value of the apparent equilibrium constant K_{III} depends on the water present at equilibrium. In Figure 8 the apparent equilibrium constant and the equilibrium constant obtained by substituting the water activities for the water molar fractions are plotted versus the water content at equilibrium. The activity coefficient of water increases with increasing water content and offsets the decrease of the apparent equilibrium constant. The remaining effect of a variation of end group activity coefficients is small, yielding a K_{III} which increases slightly with increasing water content. At lower water contents, however, the variation of water activity coefficient is small and the variation of end group activity coefficients very pronounced: the increase of the apparent equilibrium constant shown to occur at water contents lower than 1.5%[1] is to be ascribed to an increase of end group activity coefficients with increasing water content. This seems to indicate that the polycondensation reaction involves preferably ionized end groups.

The authors wish to thank Mr. T. P. Moore who developed a computer program for the mathematical development of the data.

References

1. C. Giori and B. T. Hayes, *J. Polym. Sci. A-1*, in press.
2. W. R. Gambill, *Chem. Eng.*, **66**, No. 12, 182 (1959).

Received February 18, 1969
Revised June 24, 1969

JOURNAL OF POLYMER SCIENCE: PART A-1 VOL. 8, 359–376 (1970)

Synthesis and Reactions of Polyvinylcyclopropane

C. G. OVERBERGER* and G. W. HALEK,† *Department of Chemistry, Institute of Polymer Research, Polytechnic Institute of Brooklyn, Brooklyn, New York*

Synopsis

Vinylcyclopropane was polymerized with a catalyst of diethylaluminum chloride and titanium trichloride and fractionated to yield isotactic, atactic, and stereoblock fractions, as shown by a combination of physical and chemical evidence. The atactic fraction contained a significant portion of product from 1,5-polymerization as well as the usual 1,2-polymerization, and this occurrence is explained by modifications in a mechanism for normal 1,2-coordination polymerization such that abnormal alkylations occur during the propagation step in the coordination sphere of the catalyst surface. Addition of hydrogen bromide to the isotactic fraction yielded predominantly poly-3-bromo pentene-1 and in-chain cyclohexane and vinylidene structures. A mechanism is proposed for these occurrences involving a hydride shift and various reactions of the initially generated carbonium ion with neighboring cyclopropyl rings. Addition of acetic acid yielded 25% addition and 25% cyclization and crosslinking. Hydrogen sulfide did not add to the cyclopropyl ring. Hydrogenation of the atactic fraction yielded poly-3-methylbutene-1 quantitatively, demonstrating that the polymeric environment did not affect the direction of ring opening but that the state of crystallinity as compared to the isotactic polymer did affect the extent of reaction. In general, the cyclopropyl ring in a polymeric environment underwent its usual reactions but was subject to reactions with neighboring groups resulting from its fixation in a polymer chain.

INTRODUCTION

In a previous study,[1] vinylcyclopropane was prepared and polymerized by a Ziegler-Natta catalyst to yield a product that was crystalline and presumed to be isotactic. Attempts were made to alter the crystalline polymer by ring opening to produce a crystalline polymer bearing pendent polar groups, but these were unsuccessful. The reasons for the failure of these reactions to yield crystalline derivatives remained to be determined. It is the purpose of this paper to report the preparation and characterization of stereoregular polyvinylcyclopropane and describe its behavior toward ring-opening reagents to elucidate the factors affecting the fate of the cyclopropyl ring in a polymeric environment.

* Present address: the University of Michigan, Ann Arbor, Michigan.

† Present address: Celanese Plastics Company Research and Development Center, Clark, New Jersey.

RESULTS AND DISCUSSION

Polymer Preparation

Pure vinylcyclopropane was prepared from the thermal decomposition of the phenylurethane of 1-cyclopropylethanol by an adaptation of a method first described by Strauss.[2] It was polymerized with a catalyst of diethylaluminum chloride and titanium trichloride (3:1) in heptane in a sealed tube at 25°C for 5 days to a 26% conversion. An x-ray diffraction study showed it was partially crystalline, and the infrared spectrum by absorptions at 3080 and 1020 cm^{-1}, showed the cyclopropane ring had survived. It was exhaustively extracted in a Soxhlet extractor by a series of solvents to give the following soluble fractions: ether (16%), heptane (4%), octane (1%), nonane (1%), and insolubles (79%).

Properties of Fractions

The ether-soluble fraction melted at 70°C on a hot stage and did not exhibit birefringence in polarized light. The x-ray diffraction patterns on powdered samples and on annealed fibers were completely amorphous halos. The density of a fiber drawn from the melt was 0.964 g/cc, as determined in a density-gradient column. All of these observations supported the conclusion that the ether soluble fraction was completely amorphous.

The infrared spectrum of this fraction exhibited strong absorptions assigned to the cyclopropyl group at 3080 and 1020 cm^{-1}. In addition, a weak-medium absorption peak was observed at 965 cm^{-1} assigned to a *trans* double bond. This spectrum was visibly similar to that reported[3] for the polymerization of vinylcyclopropane by the nonstereospecific catalysts $SnCl_4$ and $AlBr_3$, which was assumed to proceed by occurrence of 1,5-polymerization. Thus, in our polymerizations with the Ziegler-Natta catalyst, the amorphous portion representing 16–25% of the product, in addition to being nonstereoregular, appears to contain a significant portion of polymer units resulting from 1,5-polymerization. The occurrence of 1,5-polymerization when $SnCl_4$ was used, as reported above, was proposed to proceed by rearrangement of the initially generated secondary carbonium ion to a terminal primary carbonium ion:

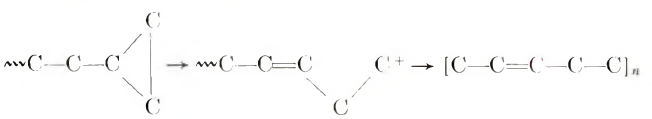

An explanation for the occurrence of 1,5-polymerization in our experiments, which does not involve a free cationic center but rather a rearrangement of electrons under the driving force of attack on the cyclopropyl ring by an electron pair within a coordination complex, can be illustrated as in Figure 1, by a mechanism patterned after a general mechanism[4–6] for the polymerization of α-olefins with Ziegler-Natta catalysts. In this mechanism, the active center of the catalyst is proposed to be an essentially

octahedrally coordinated titanium ion I with empty t_{2g} orbitals carrying in its coordination sphere one alkyl group (R) (or growing polymer chain) and having one vacant octahedral position. The monomeric vinylcyclopropane then coordinates in the vacant position through its π bond. During the act of coordination of the olefin with the titanium ion, the coordination between R and the titanium ion is reduced and the R group is expelled to attach itself in a concerted process to the nearest carbon atom of the

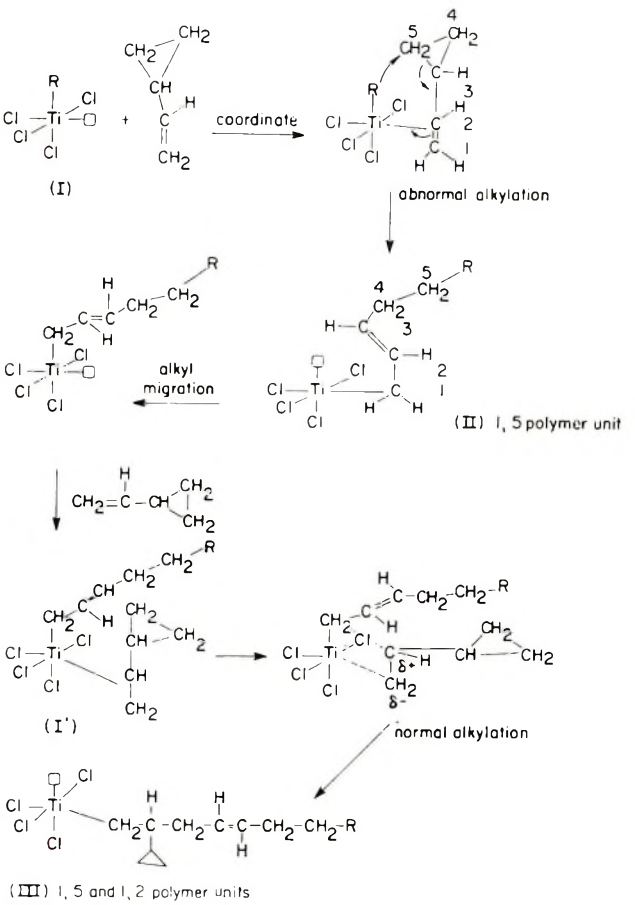

Fig. 1. Mechanism for normal and abnormal polymerization of vinylcyclopropane to yield 1,2- and 1,5-product.

olefin while the terminal carbon atom of the olefin attaches itself to the titanium ion. For reasons involved with the geometry of the crystal surface in which the active center is imbedded, the new alkyl group (growing polymer chain) must then migrate to the coordination position initially held by R, leaving the vacant octahedral position in its initial location. This final state is labeled I′. Propagation consists of repetition of these steps.

If one employs this mechanism, it is possible to modify it suitably to explain the occurrence of 1,2- and 1,5-polymerization by postulating an occasional "abnormal" alkylation of the monomer. This is illustrated in Figure 1. The active center is labeled (I) and the olefin is shown making its approach to coordinate in the vacant position through a π bond. However, during the concerted process of electron shifting, the R group (or polymer chain) attacks carbon 5, while the electron pair between carbon 5 and carbon 3 shifts into position between carbon 3 and carbon 2 and the pair between carbon 2 and carbon 1 forms a bond to the titanium ion, yielding the 1,5 polymer unit, II. After alkyl migration to form I′ and continuance of the propagation step by the "normal" mechanism, the polymer containing units of 1,2- and 1,5-polymerization (III) is formed.

The heptane-soluble fraction exhibited a crystalline melting point of 187–192°C. An x-ray powder diagram on the sample showed a moderate amount of crystallinity which increased considerably after annealing at 190°C for several hours. Infrared examination showed strong absorptions for the cyclopropyl ring at 3080 and 1020 cm^{-1} and no *trans* unsaturation. Comparison of the spectrum with that published by Natta[7] for fused and crystallized isotactic polyvinylcyclopropane showed it was identical, except that the absorptions at several peaks sensitive to crystallinity were somewhat diminished. It may be concluded that this fraction represents stereoblock polymer on the basis of its lower melting point (see below; isotactic polymer melts at 230°C) and diminished, but still considerable, crystallinity. The octane—soluble fraction exhibited a crystalline melting point of 180–190°C. Its x-ray powder diagram was quite typical of crystalline material. The infrared spectrum showed crystallinity similar to that of the heptane–soluble fraction.

The nonane-soluble fraction melted at 180–205°C. Its x-ray powder diagram was indicative of highly crystalline material. The infrared spectrum exhibited a crystallinity somewhat higher than that of the two previous fractions. It appears that these fractions also represented stereoblock polymer of longer runs of isotactic polymer.

The polymer residue resulting from the fractionation series was a hard, white powder that had a crystalline melting point of 228–232°C (lit.[7] mp 228–230°C). Upon annealing on the hot stage under nitrogen, large sperulites developed. A photomicrograph of these sperulites showed that they were negatively birefringent.

A strong fiber was drawn from the polymer in the molten state and annealed at 195°C. Its density was 0.9752 g/cc. The x-ray diffraction diagrams were very sharp and permitted determination of the unit cell, as described elsewhere.[8] Its infrared spectrum was similar to that published for isotactic polyvinylcyclopropane.[7,9]

The high-resolution NMR spectrum of this fraction exhibited absorptions at τ values of 8.53, 9.53, and 9.73 with relative peak areas of 1:1:2. Resolution was not sufficiently clear to permit distinguishing between doublet and triplets to aid in assignment of these peaks. However, on the

basis that the peaks exhibited area ratios of 1:1:2, and the polymer contained two methine protons, two chain-methylene protons, and four cyclopropyl methylenes, the 9.73 absorption may be assigned to the methylene protons on the cyclopropyl ring. This high upfield shift is in agreement with that observed for cyclopropane protons e.g., 9.7 for the cyclopropane ring.[10] The 8.53 absorption may be ascribed to the methine protons on the basis of its somewhat broader and more complex pattern and the evidence that the order of downfield shift in hydrocarbons is ordinarily $CH_3 > CH_2 > CH$,[10,11a] and that methine protons in saturated hydrocarbons normally absorb at 8.5. The remaining absorption at 9.53 may then be assigned to the chain methylene protons. This is within the range usually assigned to methylene protons in acyclic hydrocarbons, although at the high end.[12]

Hydrogen Bromide Addition

The addition of hydrogen bromide was carried out with the isotactic polyvinylcyclopropane residue resulting from extraction of the initial polymer with the solvent series described above. The polymer was swollen in decalin and then treated in sealed tubes with anhydrous hydrogen bromide and also with hydrogen bromide dissolved in glacial acetic acid. Both methods resulted in high yields of the brominated products (81 and 97% based on subsequent elemental analyses and material balances). The products melted at 140°C with decomposition. The x-ray diffraction patterns on powdered samples exhibited only amorphous halos, even after annealing at 130°C. It was clear that the crystallinity of the initial polymer had been altered. Furthermore, although forcing conditions had been employed, elemental analysis for Br, showed the addition had stopped at only 80 and 84% of the theoretical for polyvinylcyclopropane. Infrared analysis of the products showed complete disappearance of the cyclopropyl absorptions.

On the basis of the evidence obtained by a combination of infrared spectra high-resolution NMR spectra, and the elemental analyses and a consideration of the mechanism of reaction of the cyclopropyl ring, it can be concluded that the addition of HBr to polyvinylcyclopropane yielded predominantly poly-3-bromopentene-1. There was also evidence for cyclization and the presence of in-chain cyclohexane and vinylidene unsaturated structures in the product. The arguments for these conclusions are described below.

The addition of HBr to polyvinylcyclopropane would be expected to proceed by protonation of the ring to form a tertiary carbonium ion, followed by addition of bromide ion. The expected features of the product would be loss of the cyclopropyl ring and appearance of $-CHBr-CH_2-CH_3$. Evidence for this conversion was apparent in a comparison of the infrared spectra of the starting polymer and the product. The 3080 cm^{-1} absorption ascribed to the cyclopropyl ring disappeared, and the absorption due to CH_3-C- appeared at 1455 and 1380 cm^{-1}. A strong, broad absorption

centered around 795 cm^{-1} was similar to that exhibited by 2-bromobutane[13] and is attributed to the CH_3–CH_2–CHBr group extending from the polymer backbone.

The high-resolution NMR spectrum of the product also supported this predominant structure. This structure would be expected to exhibit three methyl and four methylene protons and one lone methinyl proton shifted downfield by the electronegative bromine attached to the same carbon. Absorptions were found at the following τ values: 8.88, 8.25, 5.85.

The downfield absorption at 5.85 was undoubtedly that due to the proton attached to the carbon bearing the bromine atom. Its location shows it is of the type $-\overset{H}{\overset{|}{C}}-Br$. The literature[11a] shows a value of 5.90 for $-\overset{H}{\overset{|}{C}}-Br$. The 8.88 absorption can be ascribed to the protons on the methyl group. Methyl protons in saturated hydrocarbons normally absorb at 9.10, but attachment of a $-CH_2-C-Br$ group causes slight deshielding of the methyl group and drops the absorption to the region 8.9–9.1.[11b] This combination of structures, CH_3-CH_2-C-Br, is further substantiated by the fact that the 8.88 methyl proton absorption is a triplet, as expected due to the two methylene protons adjacent to CH_3–.

The 8.25 absorption is also clearly due to the methylene groups. Actually, this absorption is a broad envelope typical of methylene protons due to much splitting, and extends over the range 8–8.8. Methylene protons normally absorb at 8.75 and, when attached to a carbon adjacent to a carbon bearing a bromine atom, drop to the range 8.1–8.5.[11b] A structure such as the proposed one would thus exhibit a composite absorption for the backbone and the side-chain methylene protons over the range actually found. The intensities of the absorptions observed further bolster the conclusion for a poly-3-bromopentene-1, because the expected ratio of 3:4:1 for the methyl protons, methylene protons, and the methinyl proton was actually observed. Thus the infrared and NMR data support the conclusion for the poly-3-bromo-pentene-1 structure expected from mechanistic considerations.

An explanation for the occurrence of a minor degree of other reactions during the addition of HBr is required by the two experimental facts that only 80–84% of the theoretical amount of HBr is accounted for in the elemental analysis of the addition products and yet no residual cyclopropyl ring was found in the infrared spectra.

Possible explanations for this combination of facts would be (a) presence of only 84% of cyclopropyl ring in the initial polymer, (b) the occurrence of an elimination reaction leading to loss of some 15–20% of the added HBr, and (c) cyclization between adjacent cyclopropane rings. These possibilities had been suggested previously,[1] but the experimental data did not permit a choice among them at that time. The current evidence would now support a combination of (b) and (c).

Possibility (a) can be eliminated, since the x-ray study of the isotactic raction employed in this reaction showed it to be highly crystalline and

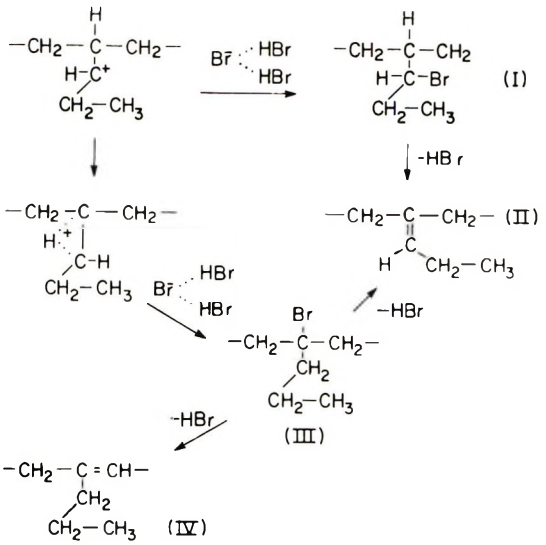

Fig. 2. Mechanism for the elimination of HBr from the addition product of HBr and polyvinylcyclopropane.

permitted a determination of the unit cell dimensions and calculations of the theoretical density. Density measurements on the polymer agreed closely with this calculated density (0.975 g/cc compared to 0.9805 g/cc calculated). This would indicate a high degree of crystallinity for this fraction and would rule out the presence of only 85% of the theoretical amount of cyclopropyl rings.

Possibility (b), the elimination of HBr from the addition product, would yield substituted vinylidenes according to the scheme shown in Figure 2.

The secondary carbonium ion resulting from protonation and opening of the cyclopropane ring could react with Br^- to yield product III, which could dehydrohalogenate to II or IV.

Product II would have an NMR pattern that would fit the experimental finding of three methyl and four methylene protons and a small amount of lone methinyl proton that might not be distinguishable from the main product, poly 3-bromopentene-1. However, occurrence of an appreciable amount of this product would yield an infrared absorption in the region of 815 cm^{-1} manyfold stronger than was actually observed. If this were the predominant side reaction, it would have to result in 16–20% vinylidene. There was an absorption at 820 cm^{-1}, but if calculated as an acyclic substituted vinylidene, it would amount to about 2–8%. The same interpretation limits the amount of product IV to a minor amount also. The occurrence of structure III as a final product would be ruled out on the basis of an NMR pattern calling for three methyl protons, six methylene protons, and no methinyl protons.

The remainder of the addition product can most satisfactorily be explained on the basis of a cyclization reaction between adjacent cyclopropyl

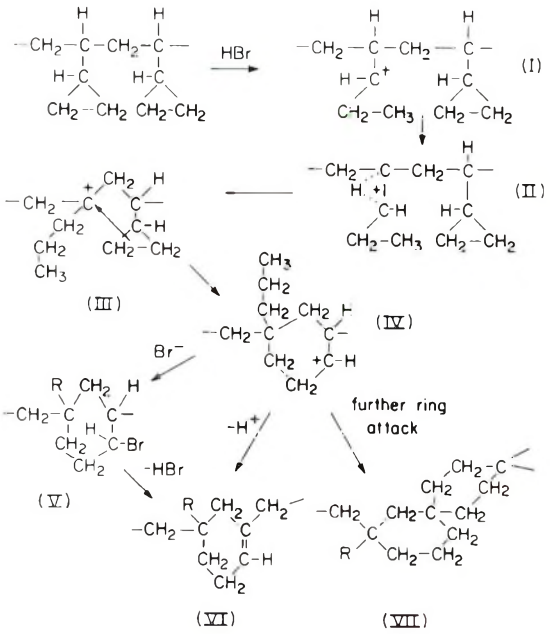

Fig. 3. Mechanism for cyclization in the addition of HBr to polyvinylcyclopropane.

rings. Evidence for intramolecular ring closures in polymers promoted by acidic catalysts has existed for some time and has been well summarized for polyenes by Cooper[14] in 1963. Recent reports have added significant infrared and NMR data to the interpretation of the problem in studies of the cyclohydrochlorination of 3,4-polyisoprene,[15] polymers containing the cyclopentyl and cyclohexyl groups,[16] cyclo and cyclized diene polymers resulting from the polymerization of conjugated dienes to ladder cyclopolymers with complex catalysts,[17] infrared absorptions of the cyclization of *cis*-1,4, *trans*-1,4, and 3,4-polyisoprenes,[18] the cationic polymerization of 4-methyl-1-pentene,[19] intramolecular hydride shift polymerization by a cationic mechanism in the case of poly-3-methylbutene-1.[20]

The cyclization reaction in the case of polyvinylcyclopropane would occur as shown in Figure 3. Here, the secondary carbonium ion (I) resulting from protonation and opening of the cyclopropane ring undergoes a hydride shift (II), to yield a tertiary carbonium ion which then forms an intermediate (III) resulting from overlap of the π-electrons of the cyclopropyl ring and the tertiary backbone carbon carbonium ion. Collapse of this intermediate then yields the cyclic carbonium ion (IV). IV can then undergo combination with bromide ion to give the bromocyclohexane (V), which can then undergo dehydrohalogenation to give the cyclohexene (VI). Alternatively, IV could undergo deprotonation to yield VI. IV could also participate in a further ring attack to form the spirane structure, VII.

The literature contains several precedents for this cyclization reaction. For example, the cyclohydrochlorination of 3,4-polyisoprene[15] is depicted

TABLE I
Infrared Absorptions of Isotactic Polyvinylcyclopropane and Addition Products

Frequency, cm^{-1}		
Starting polymer	HBr product	$HOAc–H_2SO_4$ product
3410	3410	3410
3080		3090
3000		3020
	2980	2970
2920	2920	2930
2860	2880	2860
2050	2830	
		2050
1920		1920
1715	1705	1745
1635	1625	1637
	1480	1480
		1475
1465	1465	1465
	1455	1450
	1445	
1442	1440	
1430	1435	1435
1390	1392	1392
		1387
	1380	1380
	1370	1370
1345		1345
1315		1315
1280	1280	1298
1260		
1240		1242
		1235
	1217	
1194	1190	1195
	1183	
1170	1180	1165
	1130	
1105	1105	1105
1090	1090	
1045	1045	1045
1015	1018	1018
		1010
	970	970
950		948
925		925
915		915
880	870	875
	832	
818	820	818
792	797	
763	773	
745		
730		730
650		650

as involving an attack of a tertiary carbonium ion with an adjacent double bond to form a cyclic carbonium ion which then undergoes consummation with the chloride ion, to leave a six-membered ring. Further, the cyclic carbonium ion (IV of Fig. 3) is similar to the cyclic carbonium ion proposed for the cyclization of rubber[21] with H_2SO_4–acetic acid. In the former case, deprotonation was shown to be competitive with combination with anion.[22]

The mechanism proposed for polyvinylcyclopropane cyclization in Figure 3 would consume two cyclopropyl rings per occurrence and would require formation of only 8–10% of a substituted vinylidene structure to account for the missing 16–20% HBr indicated by elemental analyses for our experimental products. Occasional involvement of additional cyclopropyl rings to yield the spirane structure would reduce these requirements even further. Examination of the infrared spectra of the HBr addition products did show the absorptions expected for these structures, namely, substituted vinylidene[23] at 820 cm^{-1}; quaternary carbon skeletal vibrations[20] at 1217, 1190, and 905 cm^{-1}; cyclohexane[24] at 1018 and 970 cm^{-1}. The absorption for the substituted vinylidene structure was rather weak in our products but it has been noted[18] that the exact position and intensity of the substituted vinylidene structure is significantly affected by being part of a "hard" structure such as in-chain cyclics. Further,[18] its optical density is lower in a KBr disk (the method we used) than in solution, which further accounts for the weakness of the absorption actually observed.

A full tabulation of absorptions is shown in Table I, which compares the HBr addition product with the starting polyvinylcyclopropane. The table also includes infrared absorptions exhibited by products resulting from the addition of acetic acid–H_2SO_4 to polyvinylcyclopropane, as described in the next section.

It is interesting to note that there are very weak absorptions in the HBr addition product (not listed in Table I because of weakness of absorptions) found common to all cyclized products formed from polyisoprenes and to copolymers from isoprene[18] at 2870, 1265, 1200, 1040, and 810 cm^{-1} and for the hydrochlorination product from 3,4-polyisoprene[15] at 1205, 1110, and 1025 cm^{-1}. These data further support a cyclic mechanism operating to some extent in our case.

The NMR spectrum expected of the cyclized portion of the HBr addition product would differ somewhat from that for the predominant product, poly-3-bromopentene-1, by having a proton distribution of 3:12:1 for the groups CH_3, CH_2, and CH, respectively. However, the effect on the overall results would be small and could not be detected. This is seen in the following calculation for 84% poly-3-bromopentene-1 and 16% of the cyclohexane structure:

$$CH_3 \text{ protons} = 0.84\ (3/8) + 0.16\ (3/16) = 34.5\%\ (36.0\%\ \text{found})$$

$$CH_2 \text{ protons} = 0.84\ (4/8) + 0.16\ (12/16) = 54.0\%\ (51.5\%\ \text{found})$$

$$CH \text{ protons} = 0.84\ (1/8) + 0.16\ (1/16) = 11.5\%\ (12.5\%\ \text{found})$$

One further point of interest is that the mechanism for the cyclization reaction shown in Figure 3 shows a hydride shift to yield a tertiary carbonium ion before attack on the adjacent ring (III), rather than attack on the ring by the initial secondary carbonium ion (I). This is likely in view of the greater stability of the tertiary carbonium ion. If attack by the secondary carbonium ion had occurred, it would have yielded a cycloheptyl ring with an absorption at 730 cm^{-1}.[25] No absorption was found in that region.

The possibility of an attack by the tertiary carbonium ion to give a cyclopentane ring was also taken into consideration, but since this would leave an energetically unfavorable carbonium ion, it appears unlikely.

Acetic Acid Addition

Several attempts were made to add acetic acid, catalyzed by sulfuric acid, to isotactic polyvinylcyclopropane in acetic acid and also in decalin. The products, which were hard black granules that no longer exhibited birefringence under the polarizing microscope, were infusible up to 350°C. Infrared examination showed they consisted predominantly of unreacted cyclopropyl rings but with a significant amount of acetylation and sulfanation product, along with the occurrence of unsaturation and cyclization. The cyclopropyl absorption was observed at 3090 cm^{-1}, although diminished to somewhat above 50%. A strong absorption for acetate was present at 1742 and 1242 cm^{-1}. Absorptions for the $-OSO_3H$ group that would be expected to appear at 1230–1150 cm^{-1} and 1440–1350 cm^{-1} could not be detected because of strong absorptions for acetate and for CH_3–C in those regions. However, on the basis of the elemental analysis of a sample of thoroughly washed and exhaustively extracted product, it was possible to calculate the presence of 5.6% H_2SO_4 and 13.0% CH_3COOH. This would correspond to addition of CH_3COOH to 20% of the initial cyclopropyl rings and addition of H_2SO_4 to 5% of the initial cyclopropyl rings. The appearance of a strong 1380 cm^{-1} absorption for CH_3–C– indicated that the addition proceeded in normal Markovnikov fashion and resulted in poly-3-substituted pentene-1 structures as in the case of the HBr addition.

The infrared spectrum also showed a moderate absorption centered at 1637 cm^{-1}, indicating C=C stretching in a nonconjugated system and an absorption at 970 cm^{-1} similar to, but twice as intense as, that ascribed to the occurrence of 8–10% of cyclization in the product from HBr addition. Unfortunately, absorptions that would confirm this (particularly at 1018 cm^{-1}) were obscured by similar absorptions remaining from the starting material. However, these addition product absorptions are similar to those observed[26] in the crude reaction mixture resulting from the addition of acetic acid, catalyzed by sulfuric acid, to the cyclopropyl ring of 2,3-methano-*trans* decalin, namely, unsaturation at 1637 cm^{-1} and absorptions at 1018 and 972 cm^{-1}. It was reported[26] that the addition resulted in a mixture of 40% acetates and 58% of product containing unsaturation

within the decalin ring as a result of deprotonation of the initially protonated product by nucleophilic attack on hydrogen by solvent. Since it was reported that no starting material remained in the reaction mixture, it would appear that the 1018 and 972 cm^{-1} absorptions are connected with unsaturation in a substituted cyclohexene ring and are not those due to the initial cyclopropyl ring.

The infusibility (>350°C) and insolubility of the polymeric addition product indicates that considerable crosslinking occurred, probably by interchain ring attacks.

Hydrogen Sulfide Addition

Attempts to add H_2S catalyzed by H_2SO_4 to isotactic polyvinyl-cyclopropane did not succeed; only unconverted polymer was recovered after reaction under forcing conditions. It is possible that a reaction catalyzed by H_2SO_4 was not actually involved, since the H_2SO_4 could be reduced to sulfur by the H_2S which would still be in excess and sufficient for reaction with the cyclopropyl ring. A reaction catalyzed by BF_3 dihydrate was tried next, but it also yielded only unchanged polymer. BF_3 dihydrate was reported to yield 80% conversions with olefins[27] under the conditions employed in our experiment. It is apparent that H_2S was not sufficiently acidic to add to the cyclopropyl ring. It was reported[28] that the presence of strong acid was required for opening of the cyclopropyl ring, since a mixture of glacial acetic acid and bicyclo(3.1.0)hexane yielded only the starting materials unchanged after 41 hours at 48°C. The same treatment in the presence of 0.07*M* *p*-toluenesulfonic acid resulted in ring opening and formation of a mixture of acetates and olefins. An extensive search of the literature did not reveal any cases of the addition of H_2S to a cyclopropyl ring.

Hydrogenation of Atactic Polymer

A portion of the atactic fraction resulting from the extraction of stereoregular polyvinylcyclopropane was subjected to hydrogenation with Raney nickel under pressure in solution. The hydrogenation experiment was carried out to learn the effect of tacticity and resulting crystallinity on the behavior of the polymer toward ring opening reagents. The hydrogenation of isotactic polyvinylcyclopropane with Raney nickel catalyst to a product that could be separated into two fractions has been reported by Natta et al.[7] One fraction, consisting of 25% of the product, was soluble in boiling heptane. It was characterized by infrared spectroscopy and was shown to be equivalent to a partially crystalline poly-3-methylbutene-1. The insoluble fraction was similarly characterized and reported to contain a mixture of 3-methylbutene-1 and nonhydrogenated structures. No evidence was found for the presence of *n*-propyl groups, and it was concluded that the hydrogenation, to the extent that it occurred, occurred between the two methylene groups of the cyclopropyl ring.

As part of our general study of the opening of the cyclopropyl ring in polyvinylcyclopropane, it was of interest to see why the hydrogenation

proceeded as it did. Opening of the ring between the two methylene groups could be inherent in the cyclopropyl ring itself or it could be due to an effect of crystallinity on the contact with the hydrogenation catalyst surface. For example, relatively forcing conditions had been employed by Natta, yet the reaction was not complete. This could result from incomplete solution of the polymer which could favor the result obtained just from the physical aspect of getting the ring in contact with the hydrogenation surface. Recent evidence on cyclopropane hydrogenation indicates chemisorption of the cyclopropane ring occurs during hydrogenation on a nickel surface.[29] An atactic polyvinylcyclopropane, which was completely soluble in the reaction medium would not present the complication of a crystallinity effect and would yield an answer to the influence of the cyclopropyl ring itself on the direction of ring opening. Accordingly, atactic polyvinylcyclopropane was subjected to the very same hydrogenation conditions employed by Natta, namely 180°C, 170 atm, for 18 hr in heptane. The product was recovered quantitatively. Whereas the starting polymer softened at 70°C, the product softened at 160–190°C. Comparison of the infrared spectrum of this product and that of the atactic polyvinylcyclopropane showed complete absence in the former of the cyclopropyl ring at 3080 and 1030 cm^{-1}. A strong isopropyl group doublet appeared at 1385 and 1365 cm^{-1} and also at 1175 cm^{-1}. Comparison with the spectrum of amorphous poly 3-methylbutene-1 from hydrogenated amorphous poly-3,4-isoprene reported by Kennedy et al.[20] showed the same general features, except that the isopropyl absorption was found at its usual position at 1175 cm^{-1} and not shifted to 1185 cm^{-1}. We do concur with them in the equal intensities of the 1388 and 1370 cm^{-1} absorptions and the absence of a 1297 cm^{-1} absorption which distinguishes the poly 3-methylbutene-1 structure from the rearranged product resulting from the low-temperature cationic polymerization of 3-methylbutene-1. Thus, hydrogenation of atactic polyvinylcyclopropane yielded a quantitative conversion to atactic poly-3-methyl butene-1. Our results are thus in accord with the direction of opening of the cyclopropyl ring between the two methylene groups as being an inherent property rather than one influenced by crystallinity. The completeness of our reaction does indicate some interference occurring in the isotactic case reported by Natta.

EXPERIMENTAL

Isotactic Polyvinylcyclopropane

Polymerization. A 125-ml glass reaction tube of 1 in. diameter, fitted with a ground-glass stopper and a sidearm closed with a stopcock, was flamed while being deaerated several times with argon through the sidearm. To it was added 20 ml of *n*-heptane, dried over Linde 4A sieves. From an argon-purged hypodermic syringe fitted with a Luer-Lok, 0.4 g. (2.5 mmole) of aluminum-activated titanium trichloride powder was blown in under argon from a storage flask weighed by difference. A 3-ml portion

of 2.5*M* diethylaluminum chloride (7.5 mmoles) was then added from an argon-purged syringe. Finally, 10.0 g (0.147 mole) of vinylcyclopropane (99.8% pure; prepared via decomposition of the phenylurethane of methyl cyclopropyl carbinol, bp 40.0°C/740 mm; n_D^{25} 1.4095; D_4^{20} 0.721), was added by syringe. The tube was sealed and allowed to stand at 25°C for 120 hr. The contents were poured into 500 ml methanol, stirred $^1/_2$ hr, and filtered. The polymer was boiled for 2 hr with a solution of butanol–methanol–HCl (3:1:5% by volume) and filtered. It was further digested in the same mixture for 24 hr, then soaked twice in 50–50 methanol–H_2O, filtered, and dried 18 hr at 70°C in a vacuum oven. The dry weight was 2.6 g (26%); this was polymer sample A.

Another portion of vinylcyclopropane (6.4 g, 0.094 mole) was polymerized by the same procedure at the following conditions: 10 ml *n*-heptane 12 mmole $TiCl_3$, 30 mmole diethylaluminum chloride, 25°C, 68 hr. The dry weight of polymer was 2.82 g (44%); polymer sample B.

Fractionation. Polymer A (2.52 g.) was extracted in a micro-Soxhlet apparatus with diethyl ether for 7 hr. The ether-soluble fraction was isolated by removal of the ether by distillation and, after drying to constant weight in a vacuum oven, amounted to 16.3%.

The residue from the ether extraction was extracted similarly with *n*-heptane for 20 hr to yield a soluble fraction amounting to 4.0%. The heptane-insoluble residue amounted to 79.7%.

Further extraction in a similar manner with octane and then with nonane removed only a few milligrams of material.

Similar extraction of polymer B yielded an ether-soluble fraction (25%), a heptane-soluble fraction (0.7%), and an insoluble residue (74.3%).

Characterization of Fractions

General. Infrared analyses were carried out an a Perkin-Elmer Model 21 spectrometer with NaCl prisms on samples consisting of 8 mg/400 mg KBr. The x-ray patterns were obtained with nickel-filtered CuKα radiation, by use of powder cameras for both powder and fibers, and both flat plate and cylindrical cameras with 28.7, 30, and 57.3 mm. radii. Crystalline melting points were determined on a Kofler hot stage with a thermometer specially calibrated for that hot stage. The melting point was recorded as the point at which birefringence disappeared when the sample was viewed in polarized light under crossed nicol prisms. Density was determined on fibers or on compression-molded disks equilibrated in a density-gradient column calibrated directly with National Bureau of Standards calibrated glass beads.

Ether-Soluble Fractions. Both samples A and B flowed at 70°C on the hot stage; no birefringence was observed. Density on a fiber drawn from a melt was 0.964 g/cc. The x-ray diffraction patterns on powdered samples and on annealed fibers were completely amorphous. Infrared absorptions showed the presence of the cyclopropyl ring at 3.25 and 9.85 μ.

Heptane-Soluble Fractions. Both samples A and B exhibited birefringence under polarized light after being melted and annealed on the

hot stage. Sample A exhibited a crystalline melting point of 187–192°C; sample B melted at 170–175°C. The x-ray diffraction patterns showed both samples to be partially crystalline. Infrared absorptions showed the presence of the cyclopropyl ring at 3.25 and 9.85 μ.

Insoluble Residues. Both samples A and B were highly crystalline. Sample A exhibited birefringence under polarized light which disappeared at 228–232°C; sample B melted at 227–230°C and crystallized with less difficulty than sample A. A strong fiber was drawn and annealed from sample A and had a density of 0.975 g/cc. The x-ray diffraction showed very sharp rings and permitted determination of a unit cell as described elsewhere.[8] Infrared absorptions showed the presence of the cyclopropyl ring at 3.25 and 9.85 μ. NMR analysis was carried out on a 3% solution in *o*-dichlorobenzene at 160°C with a tetramethylsilane internal standard at 60 Mcps. Absorptions were exhibited at the following τ values and relative peak areas: 8.53 (1), 9.53 (1), 9.73 (2).

Hydrogen Bromide Addition to Isotactic Polyvinylcyclopropane

In Glacial Acetic Acid and Decalin. Isotactic polyvinylcyclopropane, 0.203 g (3 mmole, based on the molecular weight of the polymer base unit; mp 230°C) in a 200 × 15 mm glass tube was swollen in 10 ml dry, distilled decalin by heating at 180°C for 4 hr till clear. It was then cooled to room temperature and treated with 0.62 g (7.5 mmole) of HBr in 1.5 ml of HBr–glacial acetic acid solution. The system was entirely miscible. The reaction was sealed in the tube and rotated in the dark for 44 hr at 65°C. The product was then recovered by precipitation in a mixture of 100 ml methanol and 100 ml of ethanol. After filtration and drying to constant weight in a vacuum oven at 40°C it amounted to 0.386 g (97%) of a tan powder that melted with decomposition at 140°C.

ANAL. Calcd: C, 49.2%; H, 7.12%; Br, 41.7%. Found: C, 49.2%; H, 7.37%; Br, 42.5%.

In Decalin. Dry, purified decalin (20.0 ml) in a 200 × 15 mm glass tube was treated at −15°C with HBr gas until excess HBr fumes were noted. Titration of a 10.0-ml aliquot with 0.175*N* KOH in ethanol showed the presence of 3.7 mmole of HBr. The remaining 10.0 ml portion (3.7 mmole HBr), was immediately treated with 0.100 g (1.5 mmole) of isotactic polyvinylcyclopropane, sealed off, and rotated in the dark at 65°C for 100 hr. Workup, as described above, yielded 0.162 g (81%) of a tan powder as above.

ANAL. Calcd: C, 48.5%; H, 6.70%; Br, 42.8%. Found: C, 48.5%; H, 7.04%; Br, 45.0%.

Characterization by X-Ray, Infrared, and Nuclear Magnetic Resonance

The x-ray diffraction patterns were obtained on powdered samples. Both samples exhibited only amorphous halos, even after annealing at 130°C.

Infrared analysis on KBr disks (8 mg/400 mg KBr) showed complete absence of cyclopropyl absorptions at 3080 cm^{-1}, appearance of methyl absorption at 1380 cm^{-1}, and absorptions at 1020 and 970 cm^{-1} indicative of cyclohexyl ring (f), absorptions at 820 cm^{-1} for substituted vinylidene and at 797 cm^{-1} indicative of 2-bromobutane structure.

NMR analyses were carried out on a 3% solution of the product from the decalin experiment dissolved in tetrachloroethylene with a tetramethylsilane internal standard at 60 Mcps over the temperature range 25–120°C. Peak areas were measured with a planimeter. The τ values and areas were: 5.85 (12.5%), 8.25 (51.5%), 8.88 triplet (36%) for a ratio of 1:4:3. The same result was obtained on a 10% solution in chlorobenzene at 25–175°C.

Acetic Acid Addition to Isotactic Polyvinylcyclopropane

Acetic Acid Solvent. Isotactic polyvinylcyclopropane (0.110 g, 1.6 mmole) was reacted with 2.0 ml of glacial acetic acid and 1.8 mmole of concentrated H_2SO_4 in a tube at 70°C for 100 hr. The tube was then cooled in ice water and the contents quenched in ice water. The product was then washed with distilled water until acid-free. After drying to constant weight, there was recovered 0.106 g of hard black granules.

ANAL. Calcd: C, 73.4%; H, 10.0%; S, 2.65%. Found: C, 73.7%; H, 10.2%; S, 2.97%.

The product did not exhibit birefringence and was infusible up to 350°C. Its infrared spectrum was similar to that of the original polymer with additional absorptions at 1742 and 1242 cm^{-1} due to acetate group, a strong 1450 and 1380 cm^{-1} for CH_3–C and a strong 1640 cm^{-1} for >C=C<. The cyclopropyl group absorption at 3090 cm^{-1} was somewhat diminished. A medium absorption at 970 cm^{-1}, attributable to a cyclohexyl ring, also appeared.

Decalin as Solvent. Isotactic polyvinylcyclopropane (0.100 g, 1.5 mmole) was swollen in 10 ml of decalin for 1 hr at 180°C and cooled to 25°C. It was treated with 1 ml of glacial acetic acid and 1.8 mmole of concentrated H_2SO_4 and rotated in a sealed tube at 65°C for 112 hr. It was then cooled and poured into 200 ml of ice water. The decalin layer was washed further with water and the polymer was coagulated with 150 ml ethanol and was washed and soaked with three 150 ml portions of ethanol to remove the decalin. It was then extracted in a micro-Soxhlet apparatus for 24 hr and dried to yield 0.092 g of a fine, tan powder.

ANAL. Found: C, 76.8%; H, 10.8%; S, 1.82%; O, 10.6% (direct).

Melting behavior and infrared absorption were identical with the results listed above.

Hydrogen Sulfide Addition to Isotactic Polyvinylcyclopropane

Catalyzed by H_2SO_4. Decalin (15 ml) in a reaction tube was saturated at −10°C with 3.8 mmole of H_2S gas. A drop of concentrated H_2SO_4

and 0.100 g (1.5 mmole) of isotactic polyvinylcyclopropane were added and the sealed tube rotated at 65°C for 115 hr. The contents were washed in a separatory funnel with water and were coagulated and soaked four times in 50 ml of ethanol. Final drying at 60°C in a vacuum oven yielded 0.090 g (90%) of white polymer. Crystalline melting point and infrared spectra showed that it was unchanged isotactic polyvinylcyclopropane.

Catalyzed by BF_3 Dihydrate. Decalin (20 ml) in a reaction tube was saturated at −10°C with 5.0 mmole of H_2S gas and treated with 30 μl of BF_3 dihydrate and 0.100 g (1.5 mmole) of isotactic polyvinylcyclopropane. The sealed tube was rotated at 70°C for 90 hr. Workup, as described above, yielded 0.89 g (89%) of white polymer. It was shown to be unchanged isotactic polymer, crystalline mp 225–227°C; infrared spectrum identical with that of the original polymer.

ANAL. Found: C, 85.9, 86.2%; H, 11.7, 11.9%; S, nil.

Hydrogenation of Atactic Polyvinylcyclopropane

Atactic polyvinylcyclopropane (0.250 g, 3.7 mmole), mp 70°C, was placed in a 500-ml hydrogenation bomb along with 1.7 g Raney nickel in 170 ml *n*-heptane. The bomb was pressured with 180 atm of hydrogen and agitated at 170°C for 18 hr. Filtration of the resulting solution followed by vacuum distillation of the solvent yielded a 98.6% recovery of hydrogenated product. It now had a flow point under a microscope on a hot stage of 160–188°C.

Examination of a film cast from ether onto a salt window in the infrared and comparison with the unhydrogenated polymer showed complete absence of the cyclopropyl absorptions at 3080 and 1030 cm^{-1}. A strong isopropyl group doublet appeared at 1385 and 1365 cm^{-1} and also at 1175 cm^{-1}. Comparison with the spectrum of authentic amorphous poly-3-methylbutene-1 from hydrogenation of amorphous poly-3,4-isoprene showed that a quantitative conversion to atactic poly-3-methylbutene-1 had occurred.

This paper comprises a portion of the dissertation submitted by G. W. Halek in partial fulfillment of the requirements for the degree of Doctor of Philosophy in the Graduate School of the Polytechnic Institute of Brooklyn.

References

1. C. G. Overberger, A. E. Borchert, and A. Katchman, *J. Polym. Sci.*, **44**, 491 (1960).
2. F. Strauss, *Ber.* (1921).
3. T. Takahashi and I. Yamashita, *J. Polym. Sci. B*, **3**, 251 (1965).
4. P. Cossee, *J. Catal.*, **3**, 80 (1964).
5. E. Arlman, *J. Catal.*, **3**, 89 (1964).
6. E. Arlman and P. Cossee, *J. Catal.*, **3**, 99 (1964).
7. G. Natta, D. Sianisi, D. Morero, I. Bassi, and G. Caporiccio, *Atti Accad. Nazl. Lincei, Rend. Classe Sci. Fis. Mat. Natl.* **28**, 5 (1960).
8. H. D. Noether, C. G. Overberger, and G. W. Halek, *J. Polym. Sci.*, in press.
9. A. E. Borchert and C. G. Overberger, *J. Polym. Sci.*, **44**, 483 (1960).

10. J. Pople, W. Schneider, and H. Bernstein, *High Resolution Nuclear Magnetic Resonance*, McGraw-Hill, New York, 1959.

11. L. Jackman, *Nuclear Magnetic Resonance Spectroscopy*, Pergamon Press, New York, 1959, (a) p. 54; (b) p. 53.

12. D. McCall and W. Slichter, in *Newer Methods of Polymer Characterization*, Interscience, New York, 1964.

13. Sadtler Spectrum No. 4620.

14. W. Cooper, in *The Chemistry of Cationic Polymerization*, P. H. Plesch, Ed., Pergamon Press-Macmillan, New York, 1963, Chap. 8.

15. M. A. Golub and J. Heller, *J. Polym. Sci. B*, **2**, 523 (1964).

16. A. D. Ketley and R. J. Ehrig, *J. Polym. Sci. A*, **2**, 4461 (1964).

17. N. Gaylord, I. Kossler, M. Stolka, and J. Vodehnal, *J. Polym. Sci. A*, **2**, 3969 (1964).

18. M. Stolka, J. Vodehnal, and I. Kossler, *J. Polym. Sci. A*, **2**, 3987 (1964).

19. J. Goodrich and R. Porter, *J. Polym. Sci. B*, 2, 353 (1964).

20. J. Kennedy, L. Minckler, Jr., G. Wanless, and R. Thomas, *J. Polym. Sci. A*, **2**, 2093 (1964).

21. M. Gordon, *Ind. Eng. Chem.*, **43**, 386 (1951).

22. G. Bloomfield, *J. Chem. Soc.*, **1943**, 289.

23. L. Bellamy, *Infra-Red Spectra of Complex Molecules*, 2nd Ed., Methuen, London, 1958.

24. L. Marrison, *J. Chem. Soc.*, **1951**, 1614.

25. J. van Schooten and S. Mostert, *Polymer*, **4**, 135 (1963).

26. R. LaLonde and M. Tobias, *J. Amer. Chem. Soc.*, **85**, 3771 (1963).

27. W. A. Schulze and W. W. Crouch (Phillips Petroleum Co.), U. S. Pat. 2,426,648. (Sept. 1947).

28. R. LaLonde and L. Forney, *J. Amer. Chem. Soc.*, **85**, 3767 (1963).

29. Z. Knor, V. Ponec, Z. Herman, Z. Dolejsek, and S. Cerny, *J. Catal.*, **2**, 299 (1963)

Received July 1, 1969

JOURNAL OF POLYMER SCIENCE: PART A-1 VOL. 8, 377–386 (1970)

Stereospecific Polymerization of Methacrylonitrile. IV. Polymerization by Ate Complex-type Catalysts

YASUSHI JOH, SEIKI KURIHARA, TOSHIO SAKURAI, YOSHIKATSU IMAI, TOSHIO YOSHIHARA, and TATSUNORI TOMITA, *Research Laboratory, Mitsubishi Rayon Co., Ltd., Otake, Hiroshima, Japan*

Synopsis

Methacrylonitrile was polymerized by a number of ate-complex catalysts. The catalysts used were $NaAlR_4$, $LiAlR_4$, $LiZnR_3$, Li_2ZnR_4, $RMg[AlR_4]$, and $Mg[AlR_4]_2$. It was found that the ate-complex catalysts in which one of the alkyls is replaced by a diphenylamino group are capable of producing polymers with higher degrees of crystallinity than those of polymers obtained by unmodified catalysts. It was shown that the diphenylamide linkage in these catalytic systems must play an important role in the steric control in the propagation steps of this type of polymerization, although the mechanism is not clear at present. The crystallinity index used in this research gave a linear relation against I measured by NMR, and can be used as a measure of the stereoregularity of the polymer.

INTRODUCTION

Though a number of papers describe the stereospecific polymerization of polar monomers, very little has been reported on the stereospecific polymerization of monomers containing a nitrile group. In fact the only major study is one by us, which deals with the stereospecific polymerization of methacrylonitrile.[1] A novel crystalline polymer was recently reported by Sumitomo and Kobayashi,[2] who polymerized β-cyanopropionaldehyde to a crystalline poly(cyanoethyl)oxymethylene by using organometallic catalysts. Chang et al.[3] reported the polymerization of acrylonitrile by using organometallic catalysts and concluded from the high dissolution temperatures of their polymers that the polymers obtained with these catalysts are more stereoregular than a conventional radical-initiated polyacrylonitrile. Their claims were not fully documented, however, since their polymers showed the same x-ray diagrams as conventional polyacrylonitrile, and the steric structure of the polymers was not clarified.

In recent publications from this laboratory, we have presented a convincing picture of the success in the syntheses and characterization of the isotactic polymethacrylonitrile (PMAN).[4,5] We have also disclosed a number of new catalysts which are effective in the stereospecific polymerization of methacrylonitrile.[6] Among these catalysts, organometallic

compounds containing a metal-nitrogen bond are particularly interesting, since these catalysts show high catalytic activity for this type of polymerization.

In the course of studies on these stereospecific catalysts, we have found that some of the ate-complex type catalysts in which one of the alkyls is replaced by a diphenylamino group are capable of producing polymers with higher degrees of crystallinity than those of polymers obtained by unmodified catalysts. The purpose of this paper is to describe this interesting information on these catalysts.

EXPERIMENTAL

Monomer

Methacrylonitrile (Eastman Organic Chemicals Corp.) was purified by washing with 1% aqueous sodium hydroxide solution followed by washing with water. It was then dried over $CaCl_2$ and fractionally distilled immediately before use over CaH_2 under nitrogen; bp 90.3°C; $n_D^{30} = 1.3942$.

Catalysts

All the catalysts were prepared *in situ* by the same method described in the previous paper. Diethylmagnesium was prepared according to Schlenk's precedure from ethylmagnesium bromide. Butyllithium was supplied by Foote Mineral Co., and triethylaluminium and diethylzinc were supplied by Ethyl Corporation and Wako Chemical Drug Co., respectively. These were used without further purification.

Solvents

Toluene was treated with concentrated H_2SO_4 followed by successive washing with aqueous NaOH and water, dried over $CaCl_2$, and then distilled over metallic sodium under nitrogen. Acetone and methanol were used without purification.

Polymerizations

The polymerizations were run under a nitrogen atmosphere in a flask fitted with a stirrer, reflux condenser, and a nitrogen inlet. After the system was purged with nitrogen, solvent and catalyst were introduced, and then the system was warmed to a required temperature.

The polymerizations were started by injecting the monomer with a syringe through a self-sealing rubber cap. After the required time, the polymerizations were terminated by addition of acidic methanol. The products were filtered and dried. Details of the polymerization were given in a preceding paper.[6]

Index of Solubility

Crude polymers were extracted with acetone in a Soxhlet extractor for 24 hr. The index of solubility was determined as the per cent of the ace-

tone-insoluble fraction to total yield. This has been used as one measure of the stereospecificity of the polymer in this series.

Index of Crystallinity

For the acetone-insoluble crystalline fractions, a crystallinity index was determined. The determination of the index was as follows (see Fig. 1).

A base line is drawn between $2\theta = 8°$ and $2\theta = 24°$ in the radial intensity diffraction curve. The area enclosed by the diffraction curve and the base line is assumed to be a total coherent integrated intensity (A_{tot}) of all radiation scattered from $2\theta = 8°$ to $2\theta = 24°$. Two vertical lines to the abscissa at $2\theta = 14.5°$ and $2\theta = 13°$ are drawn and the height I from the baseline to the diffraction curve on the vertical line at $2\theta = 14.5°$ is measured. A straight line through the points P and Q on the vertical lines are drawn, where P and Q are situated at heights of $0.75 \times 0.9I$ and $0.9I$ from the baseline at $2\theta = 13°$ and $2\theta = 14.5°$, respectively. Another straight line is drawn through a point Q and a point on the diffraction curve at $2\theta = 18°$. The integrated amorphous intensity (A_{am}) is conveniently expressed as the area of the triangle QRS determined by the three straight lines (see Fig. 1).

The crystallinity index α is calculated by the equation:

$$\alpha = [(A_{tot} - A_{am})/A_{tot}] \times 100$$

This index was used as a measure of the crystallinity of the resulting polymer. This procedure is justified on the bases of the radial intensity diffraction curve for an amorphous PMAN which shows a pronounced halo with a peak at about 14.5°. Details of the crystallinity measurement will be reported in a separate paper in the near future.

Viscosity Measurements

Viscosities were determined in dichloroacetic acid solutions at 30°C. in an Ubbelohde viscometer which had a flow time of approximately 135 sec for pure solvent. No kinetic energy corrections were made.

NMR Measurements

The NMR spectra were measured in trifluoroacetic acid at 70°C with a Nippon Denshi JNM 4H-100 spectrometer and analyzed by the method of Segre et al.[7]

RESULTS

Li–Zn Complex Catalysts

When $LiZnEt_2N(C_6H_5)_2$ and $Li_2ZnEt_2BuN(C_6H_5)_2$ were used as catalysts instead of $LiZnEt_2Bu$ and $Li_2ZnEt_2Bu_2$, the crystallinity of the acetone-insoluble fractions of the resulting products increased, although the solubility index remained approximately constant. As to the polymeriza-

TABLE I
Polymerization of Methacrylonitrile with Organolithium–Zinc Complexes[a]

Catalyst	Polymerization temperature, °C	Conversion, %	Index of solubility, %[b]	Intrinsic viscosity, dl/g[c]	Crystallinity index, %
$LiZnEt_2Bu$	90	63.9	44.0	1.18	22.9
$LiZnEt_2N(C_6H_5)_2$	90	34.3	40.2	1.91	37.1
$Li_2ZnEt_2Bu_2$	90	76.3	43.0	1.73	30.8
$Li_2ZnEt_2BuN(C_6H_5)_2$	90	65.6	49.3	2.22	35.2

[a] Polymerization conditions: toluene, 270 ml; catalyst, 0.005 mole; monomer, 30 ml; polymerization time, 4 hr.

[b] Expressed as per cent of the acetone-insoluble part to total yield.

[c] Determined in $Cl_2CHCOOH$ at 30°C for the acetone-insoluble fractions.

tion activity in these catalytic systems, the amine-modified catalysts exhibit lower polymerization activities than the unmodified catalysts. These results are summarized in Table I.

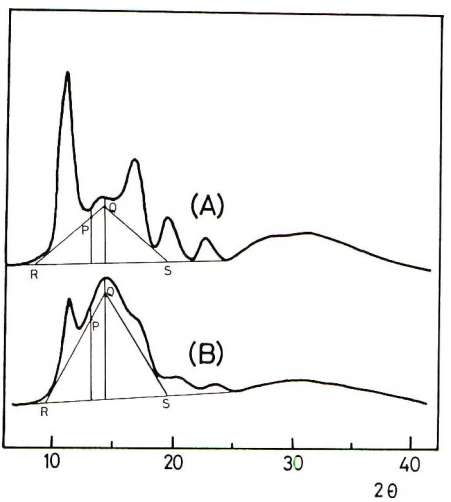

Fig. 1. X-Ray diagrams for the acetone-insoluble fraction obtained at 70°C: (*A*) $LiZnEt_2N(C_6H_5)_2$ catalyst; (*B*) $LiZnEt_2Bu$ catalyst.

Figure 1 also shows an example of this substituent effect on the crystallinity of the resulting polymer.

Li–Al and Na–Al Complex Catalysts

Table II shows the substituent effect of a diphenylamino group for an alkyl group in $LiAlR_4$ and $NaAlR_4$ catalytic systems. A trend similar to that for Li–Zn complex catalysts was observed in these catalytic systems, namely, when $LiAlEt_3N(C_6H_5)_2$ and $NaAlEt_3N(C_6H_5)_2$ were used as cata-

TABLE II
Polymerization of Methacrylonitrile with Organolithium–Aluminum Systems and Organosodium–Aluminum Systems[a]

Catalyst		Polymerization temperature, °C	Polymerization time, hr	Conversion, %	Index of solubility, %[b]	Intrinsic viscosity, dl/g[c]	Crystallinity index, %
Type	Amt, mole						
$NaAlEt_4$	0.006	90	4	5.0	49.6	2.15	30.9
$NaAlEt_3N(C_6H_5)_2$	0.006	70	4	3.5	34.6	1.05	44.8
$LiAlEt_3Bu$	0.005	90	7	28.7	54.4	3.29	33.3
$LiAlEt_3(C_6H_5)_2$	0.005	90	4	16.0	63.4	2.61	45.0

[a] Polymerization conditions: toluene, 270 ml; monomer, 30 ml.
[b] Expressed as per cent of the acetone-insoluble fraction to total yield.
[c] Determined at 30°C in $Cl_2CHCOOH$ for the acetone-insoluble fractions.

lysts instead of $LiAlEt_3Bu$ and $NaAlEt_4$, the crystallinity indices of the resulting polymers were increased, while the conversions were appreciably lowered.

Mg–Al Complex Catalysts

Table III shows the substituent effect of a diphenylamino group for an alkyl group in organoaluminum-magnesium ate-complexes. It was observed that the crystallinity indices increased with the amine-modified complex catalysts. However, the solubility indices were lower than for those of the polymers obtained by the unmodified catalysts.

TABLE III
Polymerization of Methacrylonitrile with Organoaluminum–Magnesium Systems[a]

Catalyst	Polymerization time, hr	Conversion, %	Index of solubility, %	Crystallinity index, %
$Mg[AlEt_4]_2$	2.0	45.6	70.0	36.3
$Mg[AlEt_4][AlEt_3N(C_6H_5)_2]$	0.5	27.9	55.3	51.9
$EtMg[AlEt_4]$	2.0	42.5	68.5	36.8
$EtMg[AlEt_3N(C_6H_5)_2]$	0.5	36.2	48.2	39.5

[a] Polymerization conditions: anisole, 100 ml; catalyst, 0.006 mole; polymerization temperature, 70°C.

Substituent Effect

The substituent effect of a diphenyl amino group for an alkyl group in the above-mentioned ate-complex catalysts on the crystallinity of the resulting polymer is obvious and in every case, the crystallinity index increased by using the amine-modified catalyst.

Another common tendency on the ate-complex catalysts containing one or more diphenylamide linkages is a decrease of the polymerization activities, that is, the conversions decreased by these catalysts compared with those by the unmodified catalysts. This tendency was observed in all the catalysts dealt with in the present study.

On the other hand as substituent effect, no general tendency was observed concerning solubility index; for example, with Mg–Al complex catalyst the solubility index was lowered by using the catalyst with a diphenylamide linkage, while in the case of Li_2–Zn or Li–Al catalytic systems containing a diphenylamide linkage, the solubility indices are higher than those obtained with catalysts with no amide linkage.

The increase in the crystallinity of the acetone-insoluble fractions by these catalysts with a diphenylamide linkage is an interesting problem, but the reason for this effect is not clear at present.

Effect of Number of Amide Linkages in the Catalysts

In view of the stereospecific polymerization, the decrease of conversion with the use of a diphenylamine-modified catalyst is an undesirable problem.

Thus, we studied the effect of number of the amide linkage in the ate complexes on the polymerization; some results are summarized in Tables IV–VII.

TABLE IV
Effect of Number of Amide Linkages in $NaAlR_4$ Catalytic Systems[a]

Catalyst		Conversion, %	Solubility index, %	Intrinsic viscosity, dl/g[b]
Type	Amt, mole			
$NaAlEt_4$[c]	0.006	3.8	37.0	0.87
$NaAlEt_3(N(C_6H_5)_2)$	0.006	3.5	34.6	1.05
$NaAlEt_2(N(C_6H_5)_2)_2$	0.006	3.0	30.2	0.97
$NaAlEt(N(C_6H_5)_2)_3$	0.006	3.3	32.6	0.95
$NaAl(N(C_6H_5)_2)_4$	0.006	3.3	4.2	0.91

[a] Polymerization conditions: solvent, toluene, 270 ml; monomer, 30 ml; polymerization temperature, 70°C, polymerization time, 4 hr.
[b] Determined at 30°C in dichloroacetic acid for acetone-insoluble fractions.
[c] Polymerization time, 7 hr.

TABLE V
Effect of Number of Amide Linkages in the $LiAlR_4$ Catalytic Systems[a]

Catalyst		Conversion, %	Solubility index, %	Intrinsic viscosity, dl/g[b]
Type	Amt, mole			
$LiAlEt_3Bu$[c]	0.005	20.7	38.3	1.59
$LiAlEt_2Bu(N(C_6H_5)_2)$	0.005	9.1	59.8	1.02
$LiAlEt_2(N(C_6H_5)_2)_2$	0.005	7.9	9.1	1.50
$LiAlEt(N(C_6H_5)_2)_3$	0.005	4.7	8.3	2.03
$LiAl(N(C_6H_5)_2)_4$	0.005	3.8	6.1	1.97

[a] Polymerization conditions: solvent, toluene, 270 ml; monomer, 30 ml; polymerization temperature, 70°C; polymerization time, 4 hr.
[b] Determined at 30°C in dichloroacetic acid for acetone-insoluble fractions.
[c] Polymerization time; 7 hr.

TABLE VI
Effect of Number of Amide Linkages in the $LiZnR_4$ Catalytic Systems[a]

Catalyst		Conversion, %	Solubility index, %	Intrinsic viscosity, dl/g[b]
Type	Amt, mole			
$LiZnEt_2Bu$[c]	0.005	48.1	36.7	1.03
$LiZnEt_2[N(C_6H_5)_2]$	0.005	44.5	41.8	1.32
$LiZnEt[N(C_6H_5)_2]_2$	0.005	41.3	41.8	1.50
$LiZn[N(C_6H_6)_2]_3$	0.005	15.8	67.3	1.56

[a] Polymerization conditions: solvent, toluene, 270 ml; monomer, 30 ml; polymerization temperature, 70°C; polymerization time, 4 hr.
[b] Determined at 30°C in dichloroacetic acid for acetone-insoluble fractions.
[c] Polymerization time, 7 hr.

TABLE VII
Effect of Number of Amide Linkages in the Li_2ZnR_4 Catalytic Systems[a]

Catalyst		Conversion, %	Solubility index, %	Intrinsic viscosity, dl/g[b]
Type	Amt, mole			
$Li_2ZnEt_2Bu_2$[c]	0.005	76.3	43.0	1.16
$Li_2ZnEt_2Bu[N(C_6H_5)_2]$	0.005	68.7	54.2	1.14
$Li_2ZnEt_2[N(C_6H_4)_2]_2$	0.005	47.1	41.6	1.57
$LiZnEt[N(C_6H_5)_2]_3$	0.005	24.2	66.4	1.44
$Li_2ZnEt[N(C_6H_5)_2]_4$	0.005	30.4	42.0	1.49

[a] Polymerization conditions: solvent, toluene, 270 ml; monomer, 30 ml; polymerization temperature, 70°C; polymerization time, 4 hr.
[b] Determined at 30°C in dichloroacetic acid for acetone-insoluble fractions.
[c] Polymerization time; 7 hr.

The crystallinity of the resulting polymers was carefully examined. All the polymers obtained by the catalysts with one or more amide linkages in the same series gave polymers with a comparable degree of the crystallinity, regardless of number of amide linkages in the catalysts.

However, quantitative examination of Tables IV–VII reveals a tendency for decreasing conversion with increasing number of amide linkages in the same series of the catalysts.

Almost comparable or slightly higher values of solubility index were obtained in the case of Li–Zn and Li_2Zn complex catalysts, but in $NaAlR_4$ and $LiAlR_4$ series the solubility indices decreased with increasing number of amide linkages in the catalysts, except for $LiAlEt_3N(C_6H_5)_2$ catalyst.

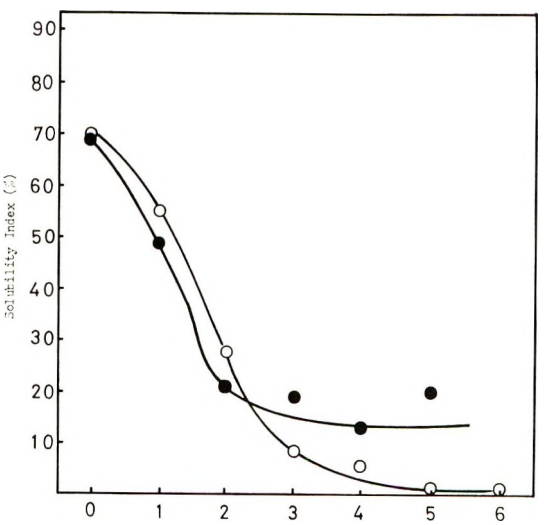

Fig. 2. Number of diphenylamide linkages: (○) $Mg[AlR_4]_2$ catalyst; (●) $RMg[AlR_4]$ catalyst. Polymerization conditions: catalyst, 0.006 mole; solvent, anisole, 100 ml.; 70°C; 0.5 hr.

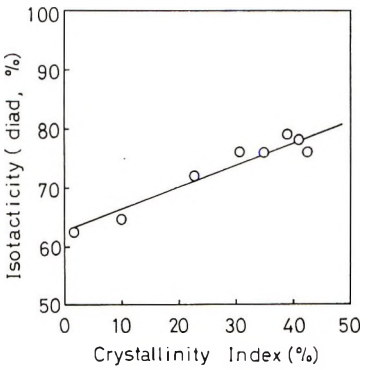

Fig. 3. Relation between stereoregularity and crystallinity of PMAN.

Figure 2 shows the effect of number of the amide linkages on solubility index in $Mg[AlR_4]_2$ and in $RMg[AlR_4]$ catalysts.

The solubility index decreased with increasing number of the amide linkages in both types of catalyst, although conversions increased gradually in both cases.

Correlation between Crystallinity Index and Stereoregularity

Figure 3 shows the correlation between the crystallinity index and stereoregularity I which was obtained by NMR examination of steric arrangement by the method of Segre et al.[7]

A linear relation between the crystallinity index and stereoregularity was obtained.

DISCUSSION

Effect of the Diphenylamine Linkage in the Catalysts

We found that some of the ate-complex type catalysts are effective in the stereospecific polymerization of methacrylonitrile. In the course of the experiments to find more effective catalysts, we found the diphenylamine-modified ate-complexes are more efficient in the formation of polymers with higher degrees of crystallinity.

The crystallinity of the acetone-insoluble fractions obtained by the same catalytic series containing one or more diphenylamide linkages are almost comparable, regardless of the number of amide linkages. This fact suggests that the diphenylamide linkage in the catalytic systems must play an important role in the steric control in the propagation steps.

This may involve an essential problem in the steric control mechanism of this type of polymerization. However, explanation of this effect is beyond the scope of our present study, and more detailed careful studies are necessary to elucidate the mechanism.

In the present series concerning the stereospecific polymerization of methacrylonitrile, we have used the solubility index as a measure of the

stereoregularity. As we carefully discussed in another paper,[1] the insolubility of crystalline polymethacrylonitrile in the usual solvents for amorphous PMAN is due to the crystallinity of the polymer. However, it becomes apparent that the solubility index does not strictly correspond to the degree of the crystallinity of the polymer. The solubility index is a measure of the content of insoluble material, which may have a certain degree of the crystallinity, probably more than 5%. In other words, even if the solubility index is extremely high, the degree of the crystallinity is not always very high.

In conclusion, it can be said that the solubility index is certainly related to the stereoregularity of the polymer but does not strictly represent a measure of stereoregularity which is better measured by NMR.

The crystallinity index used in this paper can be better used as one of the measure of the stereoregularity, since, as shown in Figure 3, there is a linear relation between the crystallinity index and isotactic content I measured by NMR examination of steric arrangement.

The above-mentioned fact does not mean that the solubility index is of no significance; however, we must note the true meaning of the solubility index.

The authors are grateful to Dr. T. Isoshima for his encouragement throughout this work and are also indebted to Mr. H. Kado for his experimental assistance and to Mr. H. Yoshiyama for the x-ray diffraction measurements.

References

1. Y. Joh, T. Yoshihara, Y. Kotake, F. Ide, and K. Nakatsuka, *J. Polym. Sci. B*, **3**, 933 (1965); *J. Polym. Sci. B*, **4**, 673 (1966); *J. Polym. Sci. A-1*, **5**, 593 (1967).
2. H. Sumitomo and K. Kobayashi, *J. Polym. Sci. A-1*, **4**, 907 (1966).
3. R. Chang, J. H. Rhodes, and V. F. Holland, *J. Polym. Sci. A-1*, **3**, 479 (1965).
4. Y. Kotake, T. Yoshihara, H. Sato, N. Yamada, and Y. Joh, *J. Polym. Sci., B* **5**, 163 (1967).
5. T. Yoshihara, Y. Kotake, and Y. Joh, *J. Polym. Sci. B*, **5**, 459 (1967).
6. Y. Joh, T. Yoshihara, Y. Kotake, Y. Imai, and S. Kurihara, *J. Polym. Sci. A-1*, **5**, 2503 (1967).
7. A. L. Segre, F. Ciampelli, and G. Dall'Asta, *J. Polym. Sci. B*, **4**, 633 (1966).

Received October 22, 1968
Revised July 3, 1969

JOURNAL OF POLYMER SCIENCE: PART A-1 VOL. 8, 387–397 (1970)

Polymerization Initiated by an Electron Donor–Acceptor Complex. Part IV. Kinetic Study of Polymerization of Methyl Methacrylate Initiated by the Charge-Transfer Complex Consisting of Poly-2-vinylpyridine and Liquid Sulfur Dioxide

MINORU MATSUDA and YASUHIRO ISHIOROSHI,
Chemical Research Institute of Non-aqueous Solutions, Tohoku University, Sendai, Japan

Synopsis

A kinetic study has been made of the polymerization of methyl methacrylate (MMA) initiated by a charge-transfer complex of poly-2-vinylpyridine (electron donor) and liquid sulfur dioxide (acceptor) in the presence of carbon tetrachloride. It is concluded that the polymerization proceeds through free-radical intermediates, as with the pyridine–liquid sulfur dioxide complex system. The association constants K of acceptor and polymer electron donors which range widely in their molecular weight were determined spectrophotometrically, and it has been found that both K and overall rate of polymerization R_p of MMA decrease with increasing molecular weight of polymer donor; contrary to this, molecular weight of PMMA formed increases with increasing molecular weight of the polymer donor. Other kinetic behaviors was essentially the same as in the pyridine–liquid sulfur dioxide system, i.e., R_p is proportional to the square root of the concentration of the complex and to the $^3/_2$-order of the monomer concentration; R_p is clearly sensitive to the carbon tetrachloride concentration at low concentration of carbon tetrachloride, but for a higher concentration it is practically independent of the carbon tetrachloride concentration. It has been deduced from a kinetic mechanism for the initiation that a primary radical may be produced from the reduction of carbon tetrachloride by an associated complex consisting of liquid sulfur dioxide–polymer donor and the monomer.

INTRODUCTION

It is well known that liquid sulfur dioxide behaves as an electron acceptor toward a large number of organic compounds and forms charge-transfer type complexes with donors such as amines, pyridines, aromatic hydrocarbons, and some olefins. It has been recently reported that a complex of liquid sulfur dioxide and pyridine can easily initiate the radical polymerization of vinyl monomers in the presence of an organic halide such as carbon tetrachloride, dichloroacetic acid, or bromoform.[1] That the organic halides play an important role in the polymerization of *N*-vinylcarbazole in the absence of any initiator has also been reported.[2–4]

It is the purpose of the present paper to examine the polymerization of methyl methacrylate (MMA) initiated by the complex formed between poly-2-vinylpyridine and liquid sulfur dioxide in the presence of carbon tetrachloride without any initiator.

EXPERIMENTAL

The purification of the reagents and the technique used in this polymerization were essentially the same as described in the preceding paper.[5] The association constants were determined spectrophotometrically in chloroform in a pressure-resistant quartz photocell.

Intrinsic viscosities were determined in toluene at 25°C; the Moore-Fort equation[6] was used for extrapolating specific viscosities to infinite dilution. The molecular weight $\bar{M}_n$ was calculated from the intrinsic viscosity by means of the relation,

$$[\eta] = 8.12 \times 10^{-5} \bar{M}_n^{0.71}$$

RESULTS

Association Constant for the Formation of a Charge-Transfer Complex of Poly-2-vinylpyridine and Sulfur Dioxide

The molar ratio of poly-2-vinylpyridine (P2VP) and sulfur dioxide which participated in the complex was found to be 1 : 1, since for all results in this measurement fairly good straight lines of optical density plots were

$$\text{P2VP (donor)} + SO_2 \text{ (acceptor)} \overset{K}{\rightleftharpoons} \text{Complex} \qquad (1)$$

obtained. The relationship between molecular weight of P2VP and K, calculated in terms of a polymerized monomer unit, is shown in Figure 1.

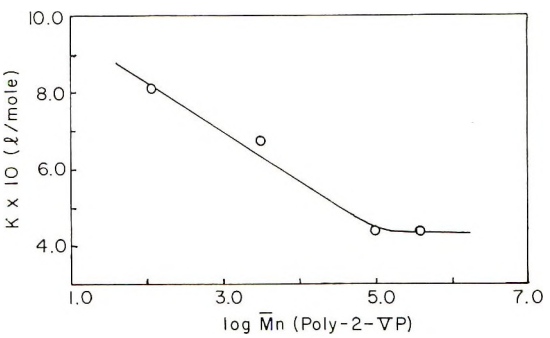

Fig. 1. Relationship between molecular weight $\bar{M}_n$ of P2VP and K at 20°C in chloroform.

Effect of the Complex Concentration on the Rate of Polymerization

The relationship between the overall rate of polymerization R_p and the square root of the complex concentration which was calculated by using Figure 1 is shown in Figure 2. R_p is proportional to the square root of the complex concentration, which indicates that the initiation of methyl methacrylate by a radical mechanism is probably involved in this polymerization.

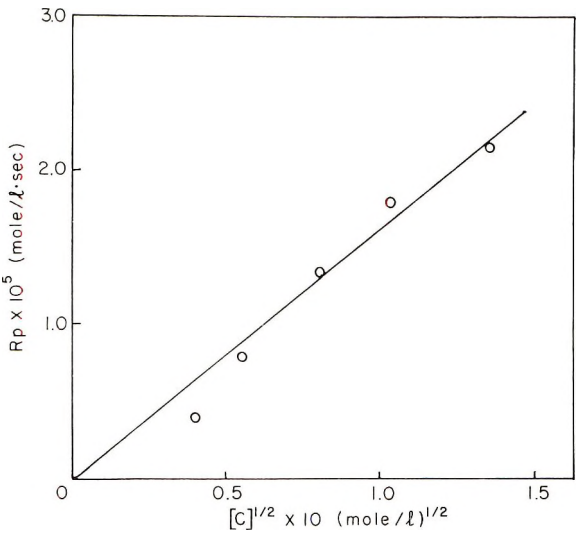

Fig. 2. Relationship between overall rate of polymerization R_p and the square root of the concentration of the complex. [MMA] = 3.36 mole/l.; [CCl_4] = 0.74 mole/l.; 50°C.

Effect of Methyl Methacrylate (MMA) Concentration on the Rate of Polymerization

Figure 3 shows that the overall rate of polymerization can be represented by eq. (2):

$$R_p \propto [C]^{0.5}[MMA]^{1.5} \tag{2}$$

where C represents the complex.

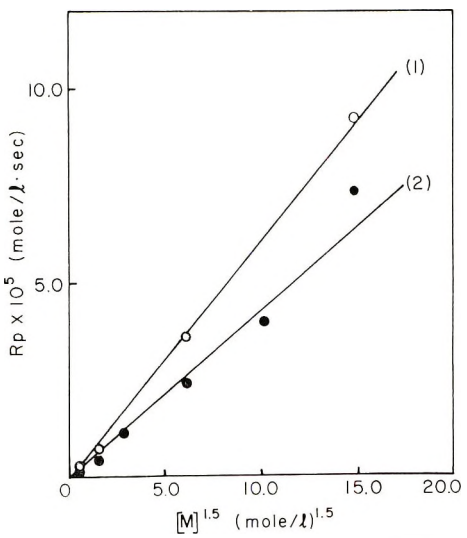

Fig. 3. Relationship between the overall rate of polymerization R_p and three-halves order of the monomer concentration: (*1*) P2VP $\bar{M}_n = 2.9 \times 10^3$, [C] = 0.046 mole/l; (*2*) P2VP $\bar{M}_n = 8.9 \times 10^4$, [C] = 0.039 mole/l. [$CCl_4$] = 0.74 mole/l.; 50°C.

Effect of Carbon Tetrachloride Concentration on the Rate of Polymerization of MMA

As shown in the preceding paper,[5] no polymer is obtained when carbon tetrachloride is not present in the polymerization systems. The relationship between R_p and the concentration of carbon tetrachloride is shown in Figure 4; it can be seen that the rate increases rapidly with carbon tetrachloride concentration up to a concentration of 0.2 and 0.4, depending on the concentrations of the complexes.

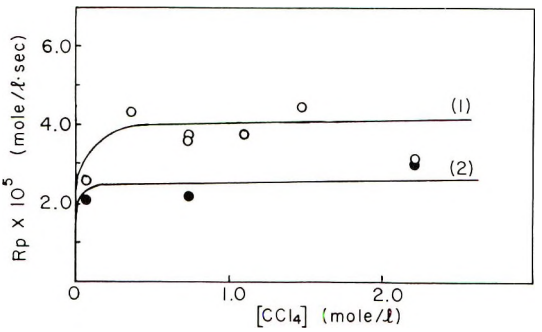

Fig. 4. Relationship between R_p and the concentration of carbon tetrachloride: (*1*) P2VP $\bar{M}_n = 2.9 \times 10^3$ [C] = 0.046 mole/l.; (*2*) P2VP $\bar{M}_n = 4.94 \times 10^5$. [MMA] = 3.36 mole/l.; [C] = 0.039 mole/l.; 50°C.

Overall Activation Energy of Polymerization

The Arrhenius plot is shown in Figure 5. The activation energy was evaluated as 6.7 kcal/mole.

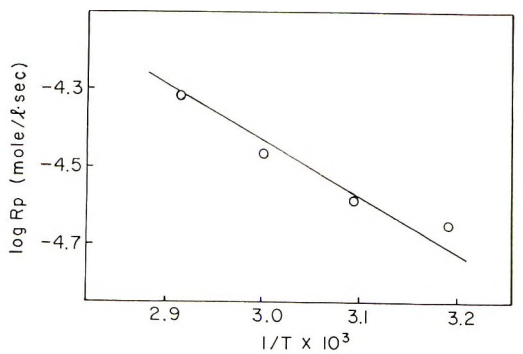

Fig. 5. Arrhenius plot for the overall rate of polymerization.

Activation Energy of the Initiation

The values of $k_p/k_t^{1/2}$ [in $(\text{l./mole-sec})^{1/2}$] were calculated by using the conventional relationship,

$$-\bar{P}_n d[\text{M}]/dt = (k_p^2/k_t)[\text{M}]^2$$

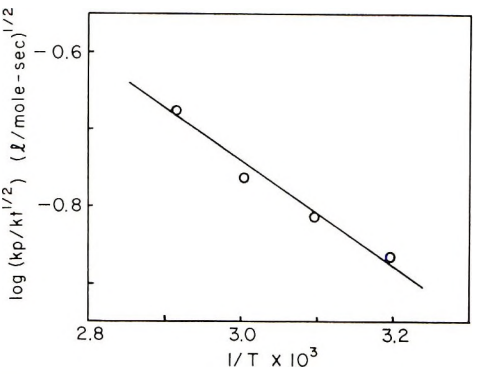

Fig. 6. Arrhenius plot for values of $k_p/k_t^{1/2}$.

where k_p and k_t represent the rate constants of propagation and termination, respectively. The Arrhenius plot of these values at temperatures between 40 and 70°C is shown in Figure 6. The activation energy, $E_p - {}^1/_2 E_t$, can be evaluated as 3.1 kcal/mole, E_p and E_t being the activation energy of propagation and termination, respectively. Therefore, it follows that the activation energy of the initiation is 7.2 kcal/mole.

Effect of the Complex Concentration on the Molecular Weight of PMMA

The molecular weight of PMMA formed is shown in Figure 7 as a function of the complex concentration; the molecular weight decreases with increasing concentration of the complex.

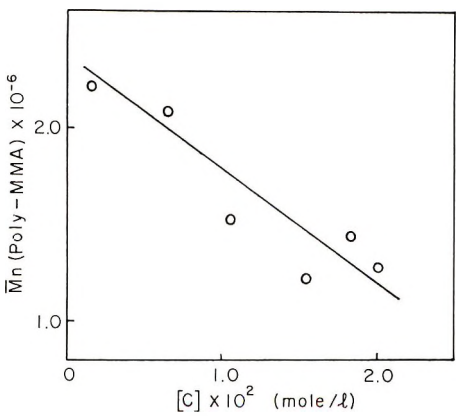

Fig. 7. Relationship between molecular weight of PMMA formed and the concentration of the complex.

Effect of Molecular Weight of the Polymer Donor on the Rate of Polymerization

Figure 8 shows the relationship between the molecular weight of P2VP and the rate of polymerization.

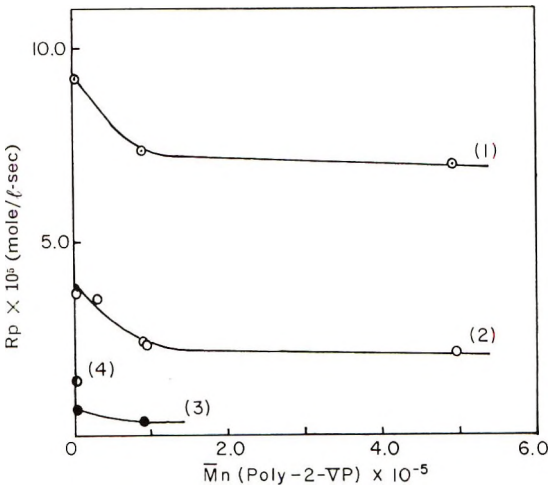

Fig. 8. Relationship between the overall rate of polymerization R_p and molecular weight of P2VP: (*1*) [M] = 6.04 mole/l.; (*2*) [*M*] = 3.36 mole/l.; (*3*) [*M*] = 1.34 mole/l.; (*4*) 2-ethylpyridine.

Effect of Molecular Weight of the Polymer Donor on the Molecular Weight of PMMA

Figure 9 shows the relationship between molecular weight of P2VP and that of PMMA.

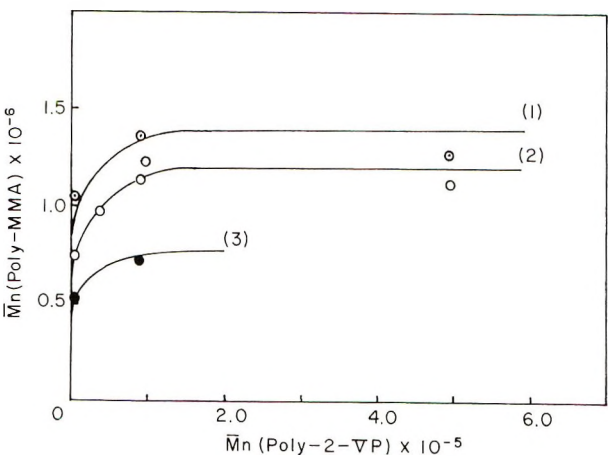

Fig. 9. Relationship between molecular weight of PMMA and molecular weight of P2VP: (*1*) [*M*] = 6.04 mole/l., (*2*) [*M*] = 3.36 mole/l.; (*3*) [*M*] = 1.34 mole/l.

Chain Transfer Constant to Methyl Methacrylate

The chain transfer constant to monomer was evaluated by using eq. (3):

$$1/\bar{P}_n = C_M + C_S([S]/[M]) + 1/2\,(1 + \lambda)\,(R_p/[M]^2)\,(k_t/k_p^2) \qquad (3)$$

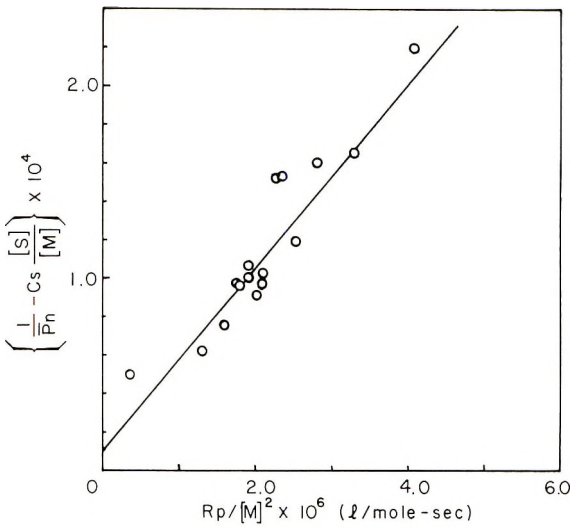

Fig. 10. Plot of eq. (3).

where C_M and C_S represent the chain-transfer constants to monomer and to solvent (benzene), respectively. Figure 10 was plotted according to the eq. (3), and a value of C_M of 1.0×10^{-5} was found from the intercept by using a literature value of C_S of 0.4×10^{-5} at 50°C.[7] The value of $k_p/k_t^{1/2}$ at 50°C can be evaluated as 0.130 (l./mole-sec)$^{1/2}$ from the square root of the reciprocal of the slope, where a literature value[8] of 0.6 for the fraction of disproportionation λ was used. The transfer constant to monomer obtained here is inconsistent with the literature value[9] and $k_p/k_t^{1/2}$ is also in agreement with a literature value,[10] indicating that the present polymerization proceeds through free-radical intermediates. In the above calculation the chain transfer reaction to carbon tetrachloride was ignored, since carbon tetrachloride had no influence on the molecular weight of PMMA as shown in a previous paper.[5] However, we do not have a satisfactory explanation for this phenomenon.

Incorporation of Fragments of Carbon Tetrachloride into Polymers

To evaluate the extent of incorporation of fragments of carbon tetrachloride into polymers, the complex-initiated polymer and a 2,2′-azobisisobutylonitrile (AIBN)-initiated polymer, were submitted to measurement of fluorescent x-rays, as shown in Figure 11. Both polymers were prepared under similar polymerization conditions, i.e., the concentrations of monomer, liquid sulfur dioxide, and carbon tetrachloride were kept constant for both polymerizations, and the concentrations of the complex and AIBN were 4.6×10^{-2} and 5.0×10^{-2} mole/l., respectively. Despite the fact that the molecular weight of PMMA formed from complex (11.05×10^5) is greater than that of AIBN-initiated polymer (2.58×10^5), the former polymer showed a higher intensity at 4.73 Å which is assigned to the

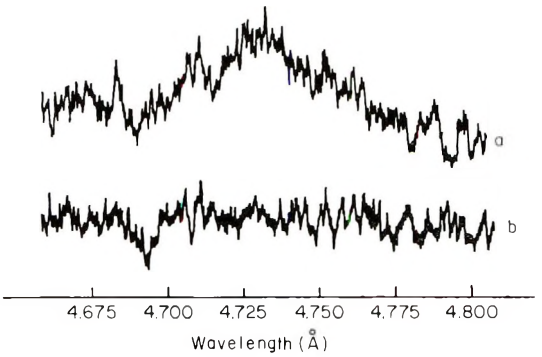

Fig. 11. Fluorescent x-rays for (*a*) complex-initiated and (*b*) AIBN-initiated polymers.

chlorine incorporated into polymer chains.[11] As polymer samples used for the measurement were in the form of tablets of the same thickness, it is possible to use the intensities as a rough measure of the CCl_4 fragments incorporated.

DISCUSSION

Most of vinyl polymerizations induced by free radicals in liquid sulfur dioxide give polysulfone,[12] but methyl methacrylate[13] and acrylonitrile,[14] which do not show charge-transfer interaction with liquid sulfur dioxide, polymerize to give the respective homopolymers. To confirm this fact, the polymers obtained were subjected to the measurement of the infrared absorption spectra and elementary analyses. In the present polymerization system, no free radical sources have ever been added; thus it is clear that the polymerization proceeds through free-radical intermediates as discussed in preceding paper.[5] The value of the chain-transfer constant to monomer and the kinetic behaviors described above also support the free-radical mechanism. Consequently, the polymerization kinetics could be treated according to the same kinetic technique as the free-radical polymerization of methyl methacrylate.

It has already been reported[5] that polymer cannot be obtained when either the complex [that is, the electron donor (P2VP) and liquid sulfur dioxide] or the organic halide is missing from the polymerization system. Poly-2-vinylpyridine acts as an electron donor for both liquid sulfur dioxide and carbon tetrachloride. The existence of the charge transfer complex with liquid sulfur dioxide was confirmed spectrophotometrically, and the molar ratio of donor and acceptor which participated in the complex was found to be 1:1. The association constants K decreased with increasing molecular weight of the polymer donor, probably as a result of the increase in the steric interference. On the other hand, the interaction of P2VP and carbon tetrachloride was not detected from the spectrophotometric study. Therefore, it is reasonable to consider that the active complex for the initiation is the P2VP–liquid sulfur dioxide complex, since the electron

affinity of liquid sulfur dioxide is much larger than that of carbon tetrachloride.

The overall rate of polymerization is clearly sensitive to the concentration of carbon tetrachloride at low concentration of carbon tetrachloride, but for a carbon tetrachloride concentration of more than 0.2 and 0.4 mole/l. (complex concentrations in these polymerizations were kept constant at 0.04 and 0.05 mole/l., respectively), it is practically independent of the carbon tetrachloride concentration. Bamford et al.[15] reported that radioactive fragments of carbon tetrachloride were incorporated into the polymer chains during the initiation, and we have also obtained similar evidence by using $CH^{77}BrBr_2$ as an organic halide.[16] As shown in Figure 11 more carbon tetrachloride fragments were incorporated than for polymer obtained from the AIBN-initiated polymer and it has become apparent that carbon tetrachloride participates in the polymerization in a different way from ordinary radical polymerization. The process of incorporation of carbon tetrachloride fragments during the radical polymerization is probably attributable to the reduction of carbon tetrachloride by an associated complex which consists of the P2VP–liquid sulfur dioxide complex and the monomer.

The facts that carbon tetrachloride fragments are incorporated into polymer chains and that the overall rate of polymerization (R_p) is proportional to the square root of the complex concentration and to $^3/_2$-order of the monomer concentration, which indicates that we should consider an equilibrium between monomer and complex, are strong evidence that the initiation mechanism is similar to that encountered in the complex of pyridine and liquid sulfur dioxide–carbon tetrachloride system.[1] These kinetic results can be explained by the reaction scheme shown in eqs. (4) and (5).

$$C + M \underset{k_2}{\overset{k_1}{\rightleftharpoons}} (I) \tag{4}$$

$$(I) + CCl_4 \xrightarrow{k_3} Cl_3CM\cdot + \overset{\ominus}{Cl} + \overset{\cdot\oplus}{(II)} \tag{5}$$

The formation of an associated complex (I) consisting of P2VP–liquid sulfur dioxide complex and monomer is presumed to be reversible, but it could not be confirmed experimentally. The associated complex (I) enters into a reaction with carbon tetrachloride forming (II), which is probably a radical cation. The activation energy for the initiation, 7.2 kcal/mole, is much less than that for initiation which was induced by homolysis of radical initiator such as peroxide and azocompound, supporting that the initiation is induced by a redox mechanism as shown in eq. (5). By assuming a stationary concentration of an associated complex (I) we may easily derive the expression (6) for the rate of initiation, R_i,

$$R_i = k_1 k_3[C][M][CCl_4]/(k_2 + k_3[CCl_4]) \tag{6}$$

The overall rate of polymerization R_p can be represented by eq. (7):

$$R_p = -(d[M]/dt) = k_p[M_n\cdot][M] \tag{7}$$

By assuming bimolecular termination and constant concentration of radicals, eq. (8) can be obtained:

$$R_p = k_p[\mathrm{M}](V_i/k_t)^{1/2} = \frac{k_p}{k_t^{1/2}}[\mathrm{M}]\left(\frac{k_1k_3[\mathrm{C}][\mathrm{M}][\mathrm{CCl_4}]}{k_2 + k_3[\mathrm{CCl_4}]}\right)^{1/2} \quad (8)$$

This type of expression is in qualitative agreement with the experimental results. The rate of polymerization is proportional to the square root of the concentration of the complex for constant concentration of monomer and carbon tetrachloride and to the monomer concentration to the three-halves order for constant concentration of the complex and carbon tetrachloride. The relationship between the rate of polymerization and the concentration of carbon tetrachloride given in eq. (8) is also consistent with the experimental result shown in Figure 4, i.e., the rate initially increases with increasing concentration of carbon tetrachloride and finally becomes constant when $k_3[\mathrm{CCl_4}] \gg k_2$.

From the experimental result shown in Figure 4, the kinetic constants at 50°C can be evaluated as follows: $k_1 = 2.17 \times 10^{-8}$ l./mole-sec, $k_2/k_3 = 3.91 \times 10^{-2}$ mole/l. By using these numerical values, the complete rate equation can be obtained:

$$R_p = 2.67 \times 10^{-5}\{[\mathrm{CCl_4}]/(3.91 \times 10^{-2} + [\mathrm{CCl_4}])\}^{1/2} \quad (9)$$

or

$$R_p = 2.23 \times 10^{-5}[\mathrm{M}]\{[\mathrm{M}][\mathrm{C}][\mathrm{CCl_4}]/(3.91 \times 10^{-2} + [\mathrm{CCl_4}])\}^{1/2} \quad (10)$$

For the rate of initiation, eq. (11) can be obtained:

$$V_i = 2.76 \times 10^{-9}[\mathrm{CCl_4}]/(3.91 \times 10^{-2} + [\mathrm{CCl_4}]) \quad (11)$$

Equation (12) represents the initiation step for the polymerization of

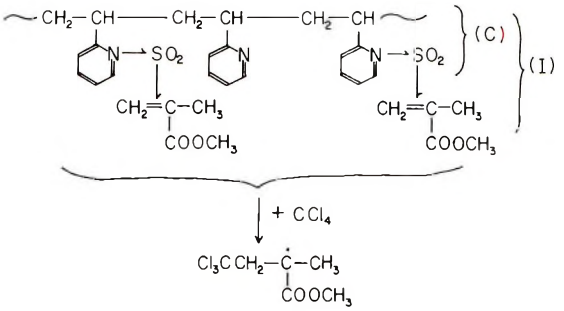

methyl methacrylate by an associated complex (I). The association complex reduces carbon tetrachloride to give a primary radical in which liquid sulfur dioxide may assist in the reduction, since the solvation power of liquid sulfur dioxide for the anion stabilizes chlorine anion.

The effects of the molecular weight of the donor polymer on the polymerization are shown in Figures 8 and 9; the rate and the molecular weight of PMMA formed are clearly sensitive to the molecular weight of donor at

relatively low molecular weight of donor, but for a molecular weight more than 10^5, it is practically independent of the molecular weight of donor. It is clear that these curves show the same trend as that of Figure 1. The effects expected due to an increment of the molecular weight of donor on the polymerization would be divided into three main classes: (1) effect which causes variation of the complex concentration; (2) effect which causes the increase of apparent viscosity of the polymerization system; (3) effect which causes localization of the active centers which induced the initiation. Of these effects the increase of viscosity can be easily disregarded since weight fraction of polymer donor is only 0.008 (0.100 g of polymer donor dissolved into 14.0 ml of total volume). The localization of active centers would have no effect on rate and molecular weight of PMMA. On the other hand, the localization of propagating species (monomer) leads to increase in both rate and molecular weight. We conclude, therefore, that the results shown in Figures 8 and 9 are directly attributable to the decrease of the complex concentration; this is supported by the parallel between Figure 1 and Figures 8 and 9. It is reasonable to postulate that a molecular weight greater than 10^5 interferes sterically with the interaction between polymer donor and liquid sulfur dioxide.

References

1. M. Matsuda and T. Hirayama, *J. Polymer Sci. A-1*, **5**, 2769 (1967).
2. L. P. Ellinger, *Polymer*, **5**, 559 (1964).
3. J. W. Breitenbach and O. F. Olaj, *J. Polym. Sci. B*, **2**, 685 (1964).
4. H. Scott, J. P. Konyon, and M. M. Labes, *J. Polym. Sci. B*, **2**, 689 (1964).
5. M. Matsuda and Y. Ishioroshi, *Makromol. Chem.*, **126**, 16 (1969).
6. W. R. Moore and R. J. Fort, *J. Polymer Sci. A*, **1**, 929 (1963).
7. G. V. Schulz, G. Henrici, and S. Olive, *Z. Elektrochem.*, **60**, 296 (1956).
8. J. Bevington, H. Melville, and R. Taylor, *J. Polym. Sci.*, **12**, 449 (1954); *ibid.*, **14**, 463 (1954).
9. G. Henrici-Olive, S. Olive, and G. V. Schulz, *Makromol. Chem.*, **23**, 207 (1957).
10. J. C. Bevington, *Radical Polymerization*, Academic Press, New York-London, 1961.
11. Shimazu Sheisakusho Ltd., *X-Ray Wavelengths for Crystal Change*, Japan, 1964.
12. M. Matsuda and M. Iino, *Macromolecules*, **2**, 216 (1969).
13. M. Matsuda, M. Iino, and N. Tokura, *Makromol. Chem.*, **65**, 232 (1963).
14. N. Tokura, M. Matsuda, and F. Yazaki, *Makromol. Chem.*, **42**, 108 (1960).
15. C. H. Bamford, R. J. W. Reynolds, and J. D. Seddon, *Makromol. Chem.*, **111**, 247 (1968).
16. M. Matsuda and T. Hirayama, *Kogyo Kagaku Zasshi*, to be published.

Received June 18, 1969
Revised July 9, 1969

JOURNAL OF POLYMER SCIENCE: PART A-1 VOL. 8, 399–405 (1970)

Polymerization of Vinyl Acetate in Aqueous Media. Part III. Distribution of Free Monomer and its Effect upon the Particle Size of Poly(vinyl acetate) Latices

A. NETSCHEY and A. E. ALEXANDER, *Department of Physical Chemistry, The University of Sydney, Sydney, N.S.W., Australia*

Synopsis

The distribution of the monomer vinyl acetate between an aqueous phase and its polymer (the latter in the form of a latex) has been measured at 20 and 40°C. The diameter of particles in a fine poly(vinyl acetate) latex has been measured in the presence of various concentrations of monomer in the aqueous phase, by means of the analytical ultracentrifuge. Comparison of the diameters so measured with those calculated from the distribution data show quite reasonable agreement (<3.7%).

INTRODUCTION

In heterogeneous polymerization of systems where monomer and polymer are intersoluble, the reaction is frequently assumed to occur exclusively in particles of polymer swollen by monomer and this is supported by the evidence presented in Part IV of this series.[1] The rate should then be given by the well known equation

$$-d[\mathrm{M}]/dt = k_p C_\mathrm{m} N \bar{n}$$

where k_p is the propagation constant, N the number of particles, $\bar{n}$ the average number of free radicals per particle, and C_m the concentration of monomer (M) in the particles. (C_m will be the concentration under the dynamic conditions of polymerization and thus is less than the equilibrium values presented in this paper.)

For the aqueous systems of vinyl acetate/poly(vinyl acetate) in which we are interested,[2,3] a knowledge of C_m and N was required at 40°C, the usual polymerization temperature. Measurement of C_m entailed studying the distribution of monomer between aqueous phase and polymer, the results being checked by measuring, in the ultracentrifuge, the particle size of "dead" polymer latices in the presence of various concentrations of monomer. N was measured directly, by means of the ultracentrifuge, at various stages of the conversion.

EXPERIMENTAL

Distribution of Monomer between Aqueous Phase and Polymer

Partition of vinyl acetate between poly(vinyl acetate) and the aqueous phase at 40°C was measured by Napper.[2] His method involved separation of the polymer particles by centrifugation of the latex and estimation of the vinyl acetate in the supernatant solution by bromometric titration. Subsequently Dunn and Taylor[4] used the same technique, at 20°C, for the same system.

In the present investigation a Zeiss laboratory interferometer was used to determine the concentration of the residual vinyl acetate in the aqueous phase, a 3.75*mM* solution of $K_2S_2O_8$ (thermally decomposed) being present in the reference solutions. A number of solutions containing 3 wt-% of vinyl acetate, initiated by 3.75*mM* $K_2S_2O_8$, were allowed to polymerize in 100-ml stoppered volumetric flasks for 7 days at 40°C. Tests showed that conversion was then complete. Known mixtures of the resulting latex and monomer were allowed to equilibrate in a thermostat for 24 hr at 20°C or 45 min at 40°C. Tests showed these times to be adequate. The latex was then coagulated by addition of 1/2 mg hexadecyltrimethylammonium bromide and the clear supernatant used for interferometric analysis at 20°C.

The uptake of monomer in grams per gram of polymer was then calculated.

Density and Viscosity Measurements

In order to calculate the PVA latex particle size in the presence of monomer from ultracentrifuge data it is necessary to know the density of the particles when swollen by monomer, as well as the density and viscosity of the medium. These were measured at 20°C, the usual temperature for the ultracentrifuge runs.

Densities of the polymer/monomer mixtures were measured by using 10-ml graduated stoppered flasks, calibrated by means of water and mercury. Known weights of polymer and monomer were equilibrated at 20°C and the empty space in the flasks then measured by filling with mercury to the calibration mark.

The densities of a series of solutions containing different amounts of monomer together with the appropriate amount of thermally decomposed initiator were measured at 20°C in the usual way. Viscosity of the same systems was measured by means of an Ostwald viscometer.

Measurement of Particle Size in Presence of Monomer

PVA latices were obtained by the complete polymerization of 3% vinyl acetate in the presence of 3.75*mM* $K_2S_2O_8$ and 0.5*mM* sodium hexadecyl sulfate. The latices so obtained were then subdivided into test samples, containing exactly 1 g of polymer, by dilution with water, and 0.1 g hydro-

quinone was added to each system. To the various samples different weights of monomer were added and equilibrated (not less than 24 hr) at 20°C. The corresponding diameters of the latex particles swollen with monomer were then calculated from the sedimentation velocity measured in a Spinco Model E centrifuge at 20°C by using the position of the maximum of the gradient curve at suitable times.

Measurement of Saturation Concentration of Monomer in Water

Known weights of water and of monomer (in excess) were mixed in 100-ml graduated flasks at 20 and 40°C. After 24 hr, which was found to be adequate, the volumes of the excess monomer were measured by means of a cathetometer. The true saturation value was found by a graphical plot of excess volume against molal concentration of monomer. Analysis by interferometer was used as a check method, the drum reading being plotted against the molal concentration of monomer.

RESULTS

Partition Coefficient of Monomer between Aqueous Phase and Polymer

Figures 1 and 2 show the monomer uptake by polymer versus the monomer concentration in the aqueous phase at equilibrium at 20 and 40°C,

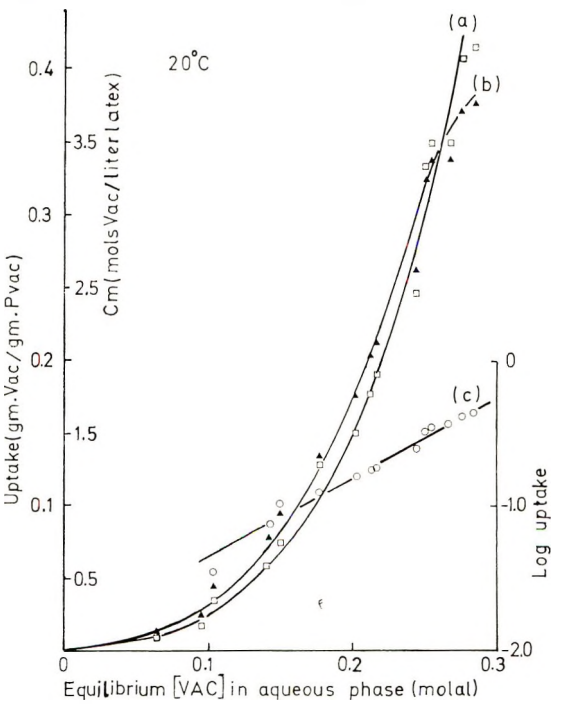

Fig. 1. (*a*) Monomer uptake by polymer as function of the equilibrium monomer concentration in aqueous phase at 20°C; (*b*) monomer concentration in the polymer latex C_m, calculated from data in (*a*); (*c*) logarithmic plot of the uptake.

respectively. These results differ substantially from those previously published, the discrepancy arising, we believe, from the ready loss of monomer during the centrifugation and titration operations used by earlier investigators.

As the monomer and polymer are completely miscible in this system the distribution studies were not extended beyond the saturation point, which

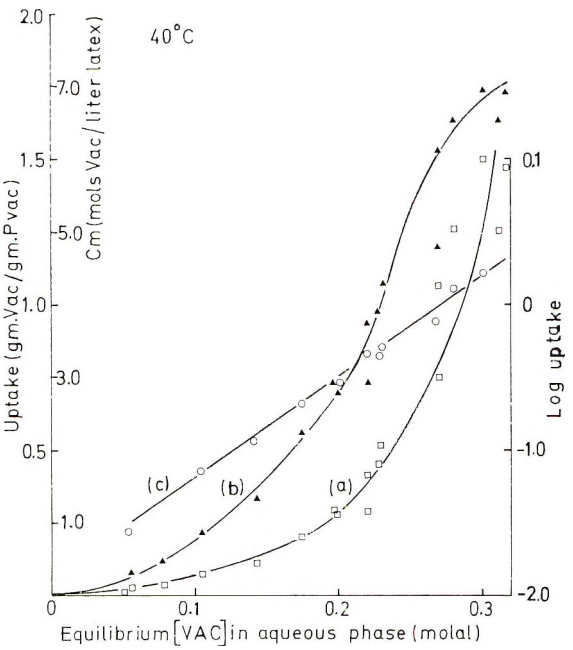

Fig. 2. (*a*) Monomer uptake by polymer as function of the equilibrium monomer concentration in aqueous phase at 40°C; (*b*) monomer concentration in polymer latex C_m calculated from data in (*a*); (*c*) logarithmic plot of the uptake.

was found to be 2.54 ± 0.03% (0.295*M*) and 2.94 ± 0.03% (0.342*M*) at 20 and 40°C, respectively. (Recently Casson and Dunn[5] obtained a value of 0.29*M* at 25°C.)

The experimental data of Figures 1 and 2 were used to calculate the partition coefficient K defined by the following expression:

$$K = \frac{\text{Vinyl acetate in polymer (g/g)}}{\text{Vinyl acetate in aqueous phase (g/g)}}$$

The results are plotted in Figure 3 as a function of the monomer concentration in the aqueous phase.

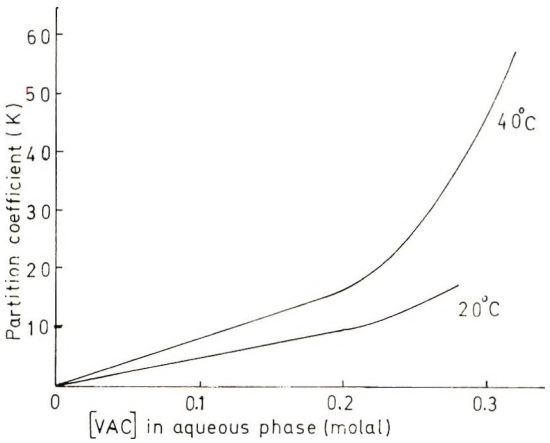

Fig. 3. Partition coefficient of monomer between polymer and aqueous phase as function of monomer concentration in aqueous phase at 20 and 40°C.

Particle Size of Polymer Particles in Presence of Monomer

The density (at 20°C) of the particles swollen by monomer at the various compositions were calculated from the experimentally determined relationship:

$$\text{Density} = 1.201 - 0.003(\text{wt-\% vinyl acetate in particle})$$

(The density of the polymer, 1.201 was separately determined.)

The density of the aqueous phase at 20°C, as a function of monomer concentration, was found to be given by:

$$\text{Density} = 0.99870 + 436 \times 10^{-6}$$
$$(\text{wt-\% vinyl acetate in aqueous phase})$$

From the partition data the diameter of the swollen particle can be calculated for the various systems prepared. These calculated diameters, together with the experimentally measured ones from ultracentrifugal data, are given as a function of monomer uptake in Figure 4.

Variation of Particle Number with Degree of Conversion

A knowledge of the number of particles at any stage of conversion is of very considerable importance in any study of heterogeneous polymerization. Polymerization of a mixture of vinyl acetate (3 wt-%) sodium hexadecyl sulfate ($0.5mM$) and $K_2S_2O_8$ ($3.75mM$), was carried out at 40°C and stopped at various conversions by cooling in ice and adding 0.1 g hydroquinone. Ultracentrifugal runs of the resulting latices were performed 12–20 hr after stopping the polymerization.

The percentage conversion was obtained by coagulating a known weight of the latex with $0.5M$ NaCl, washing the coagulated polymer, and then drying it to constant weight.

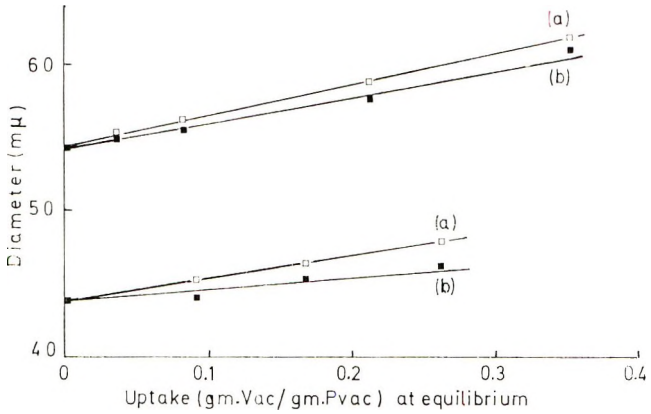

Fig. 4. Plots of (*a*) calculated and (*b*) observed diameters for two latices as a function of monomer uptake at equilibrium.

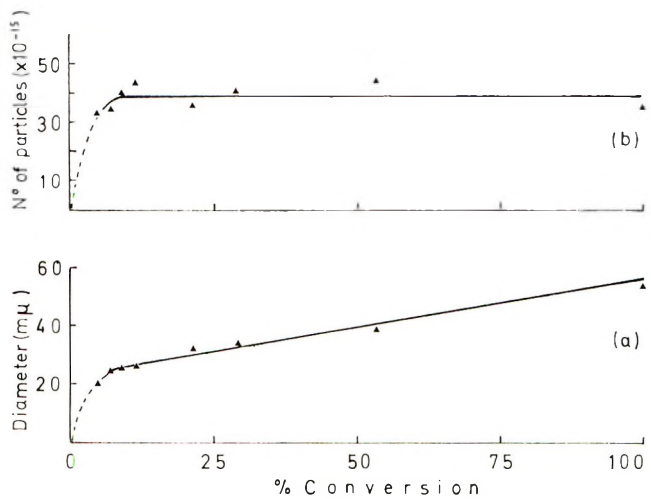

Fig. 5. Plots of (*a*) particle diameter and (*b*) number of particles in the system as functions of percentage conversion. System polymerized was 3% vinyl acetate, 3.75*mM* $K_2S_2O_8$, 0.5*mM* $C_{16}H_{33}SO_4Na$; total volume 100 ml; 40°C.

From this dry weight and a knowledge of the percentage conversion, the amount of monomer in the polymer when polymerization was stopped was calculated, and hence the diameter of the particles (swollen with monomer) at the various stages of the conversion.

The results for the number of particles and particle diameter, plotted as a function of percentage conversion, are given in Figures 5*a* and 5*b*, respectively.

DISCUSSION

The observed and calculated diameters of the monomer swollen polymer particles are seen from Figure 4 to be in very reasonable agreement

(<3.7%). This gives support to the essential validity of the partition data and enables us to calculate C_m at any stage in the polymerization, assuming, as is usually done, that monomer diffusion is sufficiently rapid to maintain equilibrium.

Further support for our partition data comes from the values of the interaction parameter (χ_1) for the monomer–polymer system, which can be calculated if the activity coefficient of vinyl acetate in water is assumed constant over the range studied. With this assumption the activity of the monomer in the polymer (a_M^P) will be given by

$$a_M^P = \frac{\text{Monomer concn in aqueous phase at equilibrium}}{\text{Monomer concn in aqueous phase at saturation}}$$

Application of Flory-Huggins theory[6] to the activity data thus obtained gives values for the interaction parameter (χ_1) in the range +0.45–0.85 at 20°C. These values seem rather large, probably because of the constant activity coefficient assumption. However the positive sign of χ_1 seems correct and contrasts with the negative values derived from previously published partition data.

The variation of number of particles with percentage conversion (Fig. 5*b*) shows that, within experimental error, the number of latex particles has stabilized by about 10% conversion. A similar conclusion was reached by Napper and Parts[2] in their study of vinyl acetate polymerization in surfactant-free solutions, using electron microscopy to measure N. The results from seeded systems presented in Part IV[1] are also consistent with the conclusion that, in these systems, N is stabilized at a very early stage of the polymerization process.

References

1. A. Netschey and A. E. Alexander, *J. Polym. Sci. A-1*, in press.
2. D. H. Napper and A. G. Parts, *J. Polym. Sci.*, **61**, 113 (1962).
3. D. H. Napper and A. E. Alexander, *J. Polym. Sci.*, **61**, 127 (1962).
4. A. S. Dunn and P. A. Taylor, *Makromol. Chem.*, **83**, 207 (1965).
5. D. Casson and A. S. Dunn, *J. Chem. Soc. A* **1967**, 201.
6. P. J. Flory, *Principles of Polymer Chemistry*, Cornell Univ. Press, Ithaca, N. Y., 1953, p. 514.

Received March 13, 1969
Revised July 14, 1969

JOURNAL OF POLYMER SCIENCE: PART A-1 VOL. 8, 407–413 (1970)

Polymerization of Vinyl Acetate in Aqueous Media. Part IV. Influence of Preformed("Seed") Latex upon Polymerization Kinetics and Particle Size

A. NETSCHEY and A. E. ALEXANDER, *Department of Physical Chemistry, The University of Sydney, Sydney, N.S.W., Australia*

Synopsis

The polymerization of aqueous solutions of vinyl acetate, initiated by $K_2S_2O_8$, has been studied in the presence of different concentrations of a fine "seed" latex, both in the absence and in the presence of a surfactant (sodium hexadecyl sulfate). Both kinetics and final latex size were measured, the latter showing whether fresh nucleation had occurred or not. The results suggest that surfactant adsorbed on the latex surface greatly influences the capture, by the latex surface, of oligomers formed in the aqueous phase and this, in turn, markedly affects both nucleation and kinetics. The number of free radicals per particle does not appear to be constant even with the finest particles used (ca. 50 mμ).

INTRODUCTION

The first two papers[1,2] of the present series discussed the polymerization kinetics and particle size of the resultant latex when solutions of vinyl acetate were polymerized with the use of potassium persulfate as initiator. The striking effects upon rates and particle sizes observed when very dilute solutions of surface active agents were added were interpreted in terms of the formation of embryos (subcritical nuclei) and of stable nuclei in the initial stages of the polymerization process.

This aspect has now been investigated more fully by carrying out the same polymerization reaction in the presence of different concentrations of fine "seed" latices (about 50 mμ diameter) both in the absence and in the presence of surfactant. (The initial seed contained no free radicals.) The kinetics of polymerization and the final particle size of the latex were measured, the latter showing very clearly whether fresh nucleation has occurred or not.

It appears that surfactant adsorbed on the latex surface greatly influences the capture, by the latex particle, of oligomers formed in the aqueous phase, and this in turn markedly affects both nucleation and kinetics.

The fact that, under all conditions studied, the kinetic curves are invariably sigmoidal, suggests that the number of free radicals per particle is never constant, even with the finest particles used (ca. 50 mμ).

EXPERIMENTAL

The kinetics of polymerization were measured dilatometrically and the latex particle sizes by ultracentrifugation as detailed in earlier papers.[1,2] With some of the coarse latices the electron microscope was used as well. The seed latices were prepared by polymerizing 3% monomer, 3.75*mM* potassium persulfate and 0.5*mM* sodium hexadecyl sulfate at 40°C. Unless otherwise stated they had been dialyzed to remove any free initiator and surfactant.

The possibility that free radicals were trapped in the seed latices was checked by adding monomer and observing no polymerization in 24 hr at 40°C.

RESULTS AND DISCUSSION

Effect of Added "Seed" Latex in Absence of Surfactant

Figure 1 shows the effect of added seed latex (from zero up to ca. 10^{14} particles/ml) upon the rate of polymerization of 3 wt-% vinyl acetate, initiated by 3.75*mM* potassium persulfate at 40°C.

Measurements of particle size were performed on latices polymerized to not less than 80% conversion at 40°C, followed by standing at room temperature for not less than 12 hr. The measured diameters as determined by the ultracentrifuge, and in some cases by electron microscopy, are shown in Table I. This table also gives the diameters calculated on the assumption that no fresh nucleation had occurred, i.e., that all polymer formed was incorporated into the seed particles.

Although the ultracentrifuge and electron microscope data differ somewhat, nevertheless it can be concluded that even with the lowest concentration of seed latex (ca. 7×10^{11} particles/ml) no new particles are formed. This conclusion is strengthened by the observations that in the ultracentrifuge runs and electron micrographs there was no sign of any fine particles and no turbidity in the ultracentrifuge cell at the end of a run.

TABLE I
Effect of Added Seed upon Diameter of Final Latex

d seed latex, mμ	Seed latex added, (particles/ml)	d final latex, mμ	
		Observed	Calculated
54.5	0	438	—
	2.95×10^{13}	138	122
	5.9×10^{13}	110	100
	9.8×10^{13}	93	88
47.6	0	438 (E.M. 383[a])	—
	7.37×10^{11}	422 (E.M. 380[a])	402
	7.37×10^{12}	272 (E.M. 230[a])	220
	4.42×10^{13}	137	106

[a] Based on Dow standard polystyrene latex of $d = 365 \pm 10$ mμ.

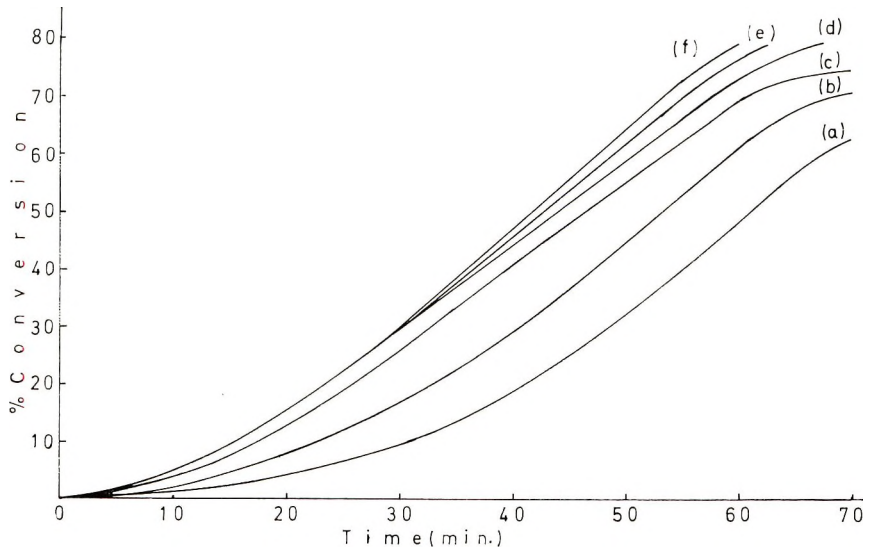

Fig. 1. Effect of concentration of added seed latex upon the polymerization of 3% vinyl acetate at 40°C: (*a*) nil; (*b*) 7.4 × 10^{11} particles/ml; (*c*) 7.4 × 10^{12} particles/ml; (*d*) 4.4 × 10^{13} particles/ml; (*e*) 5.9 × 10^{13} particles/ml; (*f*) 9.7 × 10^{13} particles/ml. $K_2S_2O_8$, 3.75 *mM*.

The kinetics are less easy to interpret than the particle size data.

If, as suggested by the above results, polymerization proceeds predominantly in the seed particles (swollen by monomer), then

$$-d[\mathrm{M}]/dt = k_p C_\mathrm{m} N \bar{n}$$

If k_p, C_m, and $\bar{n}$ were constant, then the initial rate should be proportional to N, i.e., to the concentration of added seed latex. The data in Table I show that the added seed has been varied by a factor of 130, whereas the initial rates of reaction are seen from Figure 1 to vary by a factor of about 2 at most, and for the three highest seed concentrations the initial rates are the same.

There would seem to be no obvious reason to invoke any variation in k_p, thus leaving C_m and $\bar{n}$ for consideration.

TABLE II
Calculated Diameter *d* and Calculated Volume *v* for the Seed Particle at the Start of Polymerization

d seed latex, mμ	Seed latex added, particles/ml	C_m, moles/l.	*d* latex (calcd), mμ	*v* (calcd), ml × 10^{16}
54.5	9.8 × 10^{13}	4.8	69	1.73
	5.9 × 10^{13}	7.3	80.3	2.7
	2.95 × 10^{13}	9.5	104.5	6.1
47.6	7.37 × 10^{12}	10	187	34
	7.38 × 10^{11}	10.5	a	a

[a] Estimation unreliable.

From the distribution data in Part III,[3] the values of C_m, and hence the diameter and volume of the monomer swollen seed particles at the start of polymerization, can be estimated. The results are shown in Table II.

Since the variation in C_m is only about 2, it would seem that $\bar{n}$ is the factor which is chiefly responsible for offsetting the effect of a reduction in N. As shown in Table II, a reduction in N increases the initial size of the swollen polymer particles, since a fixed amount of monomer is added in each case. It is believed that $\bar{n}$ increases with the volume of the particles, as deduced from earlier studies of these systems.[1,2]

On this basis an increase in $\bar{n}$ by a factor of 6 would be necessary as N changes from 9.8 to 0.74 $\times$ 10^{13}, i.e., as v changes from 1.7 $\times$ 10^{-16} to 34 $\times$ 10^{-16} ml.

Effect of Added Seed Latex in Presence of Surfactant

The polymerization mixture used was the same as for Figure 1, i.e., 3% monomer, 3.75mM $K_2S_2O_8$ (T = 40°C). The surfactant was 0.5mM sodium hexadecyl sulfate, and this was examined by using a high and a low concentration of seed (4.4 $\times$ 10^{13} and 7.4 $\times$ 10^{11} particles/ml, respectively).

The kinetics of polymerization of the various systems are shown in Figure 2.

The particle sizes of the final latices as measured in the ultracentrifuge and as calculated assuming no fresh nucleation are given in Table III.

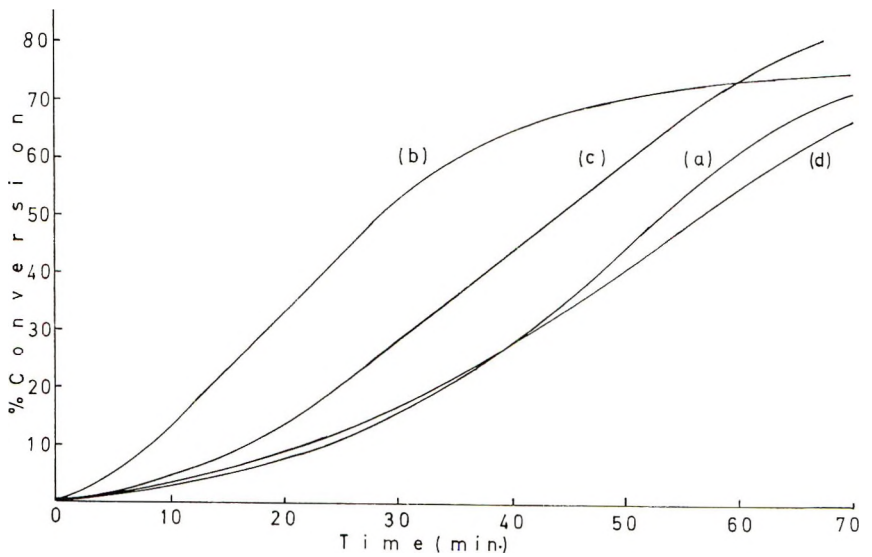

Fig. 2. Effect of surfactant and seed latex upon the polymerization of 3% vinyl acetate at 40°C: (*a*) seed latex 7.4 $\times$ 10^{11} particles/ml, no surfactant; (*b*) seed latex 7.4 $\times$ 10^{11} particles/ml, 0.5mM surfactant; (*c*) seed latex 4.4 $\times$ 10^{13} particles/ml, no surfactant; (*d*) seed latex 4.4 $\times$ 10^{13} particles/ml, 0.5 mM surfactant. Initiator $K_2S_2O_8$, 3.75 mM; surfactant, sodium hexadecyl sulfate.

There is clearly a dramatic difference between the high and low seed systems. With the high concentration of seed addition of surfactant reduces the rate considerably but no fresh nuclei are formed; with the low concentration of seed, addition of surfactant considerably increases the rate, and fresh nucleation must have occurred since the final particle size is the same as for the seed.

The calculations in Table III are oversimplified, since the experimental particle sizes quoted were all obtained from the maximum gradient in the ultracentrifuge sedimentation curve. This was done deliberately, since we do not know how $\bar{n}$ varies with particle size, which will determine the final distribution of particle sizes. A more refined treatment would not, however, affect the conclusions drawn from Table III.

In order to elucidate the possible reason for these phenomena, calculations of the likely coverage of the particles by surfactant molecules have been made on the assumption that all the surfactant ($0.5mM$) is adsorbed.

TABLE III
Effect of Added Seed in Presence of Surfactant upon Latex Diameter d

	Latex d, mμ
Seed latex d = 47.6 mμ	
4.4×10^{13} particles/ml of seed, no surfactant	137
4.4×10^{13} particles/ml of seed, plus surfactant	130
Calculated assuming no fresh nucleation	106
7.4×10^{11} particles/ml of seed, no surfactant	422
7.4×10^{11} particles/ml of seed, plus surfactant	48
Calculated assuming no fresh nucleation	402
Seed latex d = 44 mμ[a]	
5.6×10^{13} particles/ml of seed, no surfactant	130
5.6×10^{13} particles/ml of seed, plus surfactant	97
Calculated assuming no fresh nucleation	104

[a] In this experiment the seed latex was not dialyzed before use.

Thus for the high seed system (4.4×10^{13} particles/ml), with d initial = 47.6 mμ, the area per molecule is ca. 80 Å^2 at the start and ca. 330 Å^2 for the final latex. For the low seed system (7.4×10^{11} particles/ml), the corresponding figures are 1.8 Å^2 (at start) and ca. 105 Å^2 (for the final latex).

These data provide a very plausible explanation for the observed phenomena. With the high seed system the seed particle surface is clearly not saturated with surfactant, even at the commencement of polymerization, since the close-packed area for the surfactant is ca. 30 Å^2/molecule. In view of its chain length, sodium hexadecyl sulfate would be very strongly adsorbed, resulting in such depletion that any oligomer molecules forming in the aqueous phase cannot be stabilized by surfactant adsorption before they collide with, and are incorporated by, a seed particle. In other words no fresh nuclei are formed, and all polymer is deposited on the seed particles.

With the low seed system, the conditions are very different. At the start there is clearly a considerable excess of surfactant, only ca. 15% being required to saturate the surface of the seed particles, and polymerization can proceed to ca. 30% with the surfactant still adequate to maintain saturation of the surface of the growing particles. Under these conditions, oligomers forming in the aqueous phase are rapidly stabilized by adsorption of surfactant, leading to fresh nucleation and a consequent small particle size in the final latex.

In these calculations no allowance was made for the surface coverage by $-SO_4^-$ ions at the end of polymer chains, arising from incorporation of the initiating radical $\cdot SO_4^-$. However on the basis of a degree of polymerization of ca. 2000 (as found earlier) and assuming two SO_4^- groups per chain, the surface coverage is insufficient to substantially affect the above conclusions.

The reason for the surfactant reducing the rate under conditions where no fresh nuclei are formed (the high seed system) can also be explained on the above picture.

It would be expected that growing radicals in the aqueous phase would terminate more readily (by mutual termination) than those in a polymer particle, due, on the one hand, to the hydrophobic nature of the chain in water tending to make all collisions "inelastic" and on the other, to the high viscosity of the monomer/polymer particle. (At 10% conversion the particle contains ca. 50% by weight of monomer, at 20% conversion, ca. 35%.) Before a radical $\cdot M(M)_nSO_4^-$ generated in the aqueous phase can penetrate the surface of the seed latex, it will have to overcome a coulombic barrier (since its charge has the same sign as the surfactant), as well as a steric barrier, since it must necessarily displace some strongly adsorbed surfactant molecules. Relative to the system without surfactant a lower concentration of free radicals in the particles, and hence a lower rate of reaction, would then result.

Influence of Surfactant in Absence of Added Seed Latex

The influence of surfactant concentration upon the polymerization kinetics in the absence of seed latex is presented in Figure 3. It is seen that the rate is virtually unchanged above ca. $10^{-4}M$ surfactant, a concentration which corresponds quite closely to the critical micelle concentration of sodium hexadecyl sulfate under these conditions.

In a system containing $10^{-3}M$ surfactant and 3% monomer, about 90% of the surfactant must be in micellar form, the micelles being considerably swollen by solubilized monomer. The fact that the rate of polymerization is no higher under these conditions than at $10^{-4}M$ surfactant (where few if any micelles exist) shows that direct radical attack on monomer solubilized in micelles provides a quite negligible contribution to the overall rate.

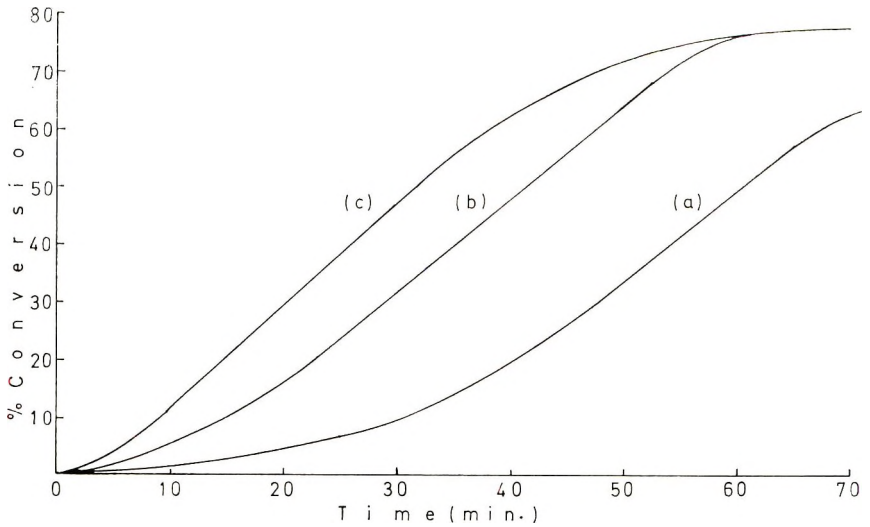

Fig. 3. Effect of surfactant (sodium hexadecyl sulfate) concentration in absence of seed latex upon the polymerization of 3% vinyl acetate at 40°C: (*a*) nil; (*b*) 2.3×10^{-5} *M*, (*c*) $10^{-4}M$, $10^{-3}M$. Initiator $K_2S_2O_8$, 3.75 *mM*.

It can thus be concluded that the role played by the micelles is merely that of a reservoir, supplying single surfactant molecules to the oligomers, embryos, and growing particles as suggested earlier.[4]

One further important conclusion is that the free radicals seem unlikely to be attacking the surfactant molecules appreciably, since, if this were the case, some change in kinetic behavior at the highest surfactant concentrations might have been expected.

The possible relevance of this work to "normal" high solids formulations can only be assessed after further work at higher monomer concentrations has been undertaken.

We would like to thank Dr. A. G. Parts and Dr. D. H. Napper for helpful discussions.

References

1. D. H. Napper and A. G. Parts, *J. Polym. Sci.*, **61**, 113 (1962).
2. D. H. Napper and A. E. Alexander, *J. Polym. Sci.*, **61**, 127 (1962).
3. A. Netschey and A. E. Alexander, *J. Polym. Sci. A-1*, this issue.
4. A. E. Alexander, *Proceeding 4th International Congress on Surface Active Substances, 1964*, Vol. III, Gordon and Breach, New York, p. 627.

Received March 13, 1969
Revised July 14, 1969

JOURNAL OF POLYMER SCIENCE: PART A-1 VOL. 8, 415–427 (1970)

Poly(ester-acetals) from Azelaaldehydic Acid-Glycerol Compounds

W. R. MILLER, R. A. AWL, E. H. PRYDE, and J. C. COWAN,
Northern Regional Research Laboratory,
Northern Utilization Research and Development Division,
Agricultural Research Service, United States Department of Agriculture,
Peoria, Illinois 61604

Synopsis

Poly(ester-acetals) have been prepared from isopropylideneglyceryl azelaaldehydate dimethyl acetal and from methyl azelaaldehydate glycerol acetal. Acid hydrolysis of isopropylideneglyceryl azelaaldehydate led to oligomeric poly(ester-acetals) with six to seven repeating units and carboxylic acid endgroups from which the sodium salt and the methyl ester could be prepared. The polymer sodium salt showed some surfactant properties. Methyl azelaaldehydate glycerol acetal, a mixture of geometric and structural isomers, was polymerized under typical polyesterification conditions. Lime was the best catalyst found. Molecular weights of 5000 to 12000 were obtained. Some of these polymers contained significant quantities of calcium as the carboxylate salt. A tough elastomer was prepared by heating a poly(ester-acetal) with *p*-toluenesulfonic acid and zinc oxide.

INTRODUCTION

Methyl azelaaldehydate is one product when methyl esters of fatty acids having unsaturation at the C_9 position are ozonized.[1] Selective modification of either the ester or the aldehyde function through suitable choice of reaction conditions was described earlier,[2] as well as use of this selectivity to prepare polymers.[3,4]

Four compounds are possible from 1 mole each of methyl azelaaldehydate and glycerol, two glycerol monoesters (I) and two glycerol acetals (II). Each compound is a bifunctional molecule theoretically capable of homopolymerization to give a poly(ester-acetal).

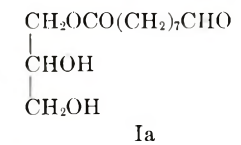

Ia

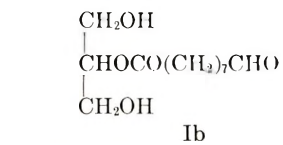

Ib

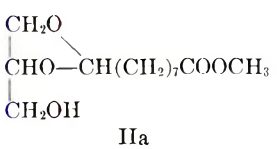

IIa

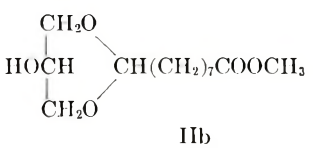

IIb

In a preliminary communication[5] we reported the preparation of isopropylideneglyceryl azelaaldehydate dimethyl acetal, a derivative of Ia, and its polymerization by a new technique to oligomeric poly(ester-acetals). We also discussed preparation of compound II[2] (a mixture of isomers) and its polymerization to similar but higher molecular weight polymers. This paper covers further investigations on these monomers and the polymers therefrom. The effects of isomeric structure on polymer properties are described in another paper.[6]

EXPERIMENTAL

Monomer Preparation

Isopropylideneglyceryl Azelaaldehydate Dimethyl Acetal. This compound (III) was prepared by two methods.

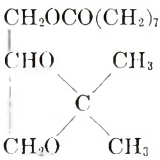

III

Ozonolysis of Monoolein. Monoolein (IV) was prepared from methyl

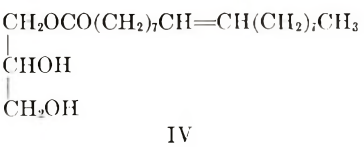

IV

oleate and glycerol essentially by the method of Mattil and Sims.[7] This monoolein, which contained 80% α-monoglyceride,[8] was ozonized in methanol, and glycerol monoazelaaldehydate (Ia) was recovered in 93% crude yield after reduction with zinc and acetic acid.[1] The crude product (30 g) was heated with 100 ml methanol and 100 ml dimethoxypropane at reflux, with 0.1 g potassium bisulfate as catalyst. Methanol and dimethoxypropane were removed on a steam bath under vacuum, the residue was dissolved in methylene chloride, and this solution was washed first with water and then with a saturated salt solution. After the washed solution was dried with sodium sulfate, solvent was removed and the volatile pelargonaldehyde acetal was distilled at ca. 0.1 mm. Distillation of the residue gave a 58% yield of III, bp 156–162°C/0.07 mm, n_D^{30} 1.4436. Analytical data are given in the following paragraph.

Alcoholysis of Methyl Azelaaldehydate Dimethyl Acetal with Isopropylideneglycerol. The procedure of Norris[9] was adapted for this synthesis. Isopropylideneglycerol[10] (13 g, 0.1 mole), methyl azelaaldehydate dimethyl acetal[4] (23 g, 0.1 mole), and litharge (0.2 g) were mixed and heated at 190–222°C for 1 hr until distillation of methanol (2.5 ml, 62% of theory) stopped. The reaction mixture was filtered and distilled. Unreacted iso-

propylideneglycerol (4.0 g) and methyl azelaaldehydate dimethyl acetal (8.6 g) were recovered. The desired product was obtained in 52.8% conversion and 83.8% yield based on unrecovered methyl azelaaldehydate dimethyl acetal. A sample, redistilled for analysis, boiled at 148–150°C/0.05 mm, n_D^{30} 1.4431. The infrared spectrum of this product was the same as that of the product obtained by ozonolysis of monoolein with absorption at 1053, 1076, 1126, 1150, and 1190 cm^{-1}, due to the acetal structure, and at 1370 and 1385 cm^{-1}, due to the *gem*-dimethyl group. The nuclear magnetic resonance spectrum with peaks at δ 1.28 (CCH_3), 1.35 (CH_2), 2.27 ($CH_2C{=}O$), and 3.20 ppm (OCH_3), and with the acetal and glyceryl protons unresolved at 5.5–6.5 ppm agreed with the assigned structure.

Use of sodium methoxide instead of litharge as catalyst gave essentially identical results.

ANAL. Calcd for $C_{17}H_{32}O_6$: C, 61.42%; H, 9.70%. Found: C, 61.74%; H, 9.64%.

Methyl Azelaaldehydate Glycerol Acetal (IIa,b). The glycerol acetal of methyl azelaaldehydate (MAzGA) was prepared by the transacetalation procedure reported previously.[2] This procedure leads to a mixture of four isomers as determined by gas–liquid chromatography.[6]

Polymerization

Isopropylideneglyceryl Azelaaldehydate Dimethyl Acetal (III), Hydrolysis Polymerization. Table I gives details on reaction conditions for a number of hydrolysis polymerizations or hydrolytic transacetalations.[11] In a typical procedure, compound III (34 g) was dissolved in 340 ml of benzene. This solution was stirred magnetically with 340 ml concentrated hydrochloric acid in a water bath at 7–9°C for 1 hr. The benzene layer was separated and washed with ten 250-ml portions of water. The final wash was neutral to universal pH paper. The benzene solution was dried over sodium sulfate. Solvent was removed to leave 17.7 g (77%) of colorless viscous liquid, n_D^{30} 1.4822, which set to a semisolid on standing (V, R=H). The molecular weight, determined in chloroform solution with a vapor-

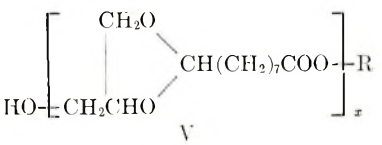

V

pressure osmometer, was 1530, equivalent to 6.7 repeating units.

To obtain the sodium salt of the polymer, the benzene solution from a smaller (5 g) run was washed with four 25-ml portions of water and with 25 ml of 5% sodium carbonate solution. This last wash caused formation of a thick emulsion, which could be broken only partially by addition of salt and ethanol. After drying over sodium sulfate, the benzene solution was still milky. The solvent was removed under vacuum on a steam bath. To remove residual water more benzene was added and this mixture was

TABLE I
Hydrolysis of Isopropylideneglyceryl Azelaaldehydate Dimethyl Acetal[a]

Monomer concentration, %	Temperature, °C	Time, hr	Washed with	Product		Yield, %
				n_D^{30}	Molecular wt[b]	
10	7–9	1	Water	1.4822	1530	77
10	24–30	1	Water	1.4736	—	60
5	23–31	1	Water	1.4717	550	69
5	5–6	1	Water	1.4806	720	71
5	5–7	2	Water	1.4785	820	71
5	5	6	Water	1.4760	750	68
5[c]	1–3	6	Water	1.4784	850	86
10	27–34	1	Na_2CO_3	[d]	—	77
10	Room	2	Na_2CO_3	1.4550	—	24
10	26–27	0.25	Na_2CO_3	[d]	—	72
5	25–32	1	Na_2CO_3	[d]	—	88
10	Room	1	NaOH	[d]	—	(35)[e]
10	Room	1	$NaHCO_3$	1.4756	—	59
10	Room	1	Piperidine in benzene	1.4875	—	44

[a] All hydrolyses were run in benzene, except as indicated, with concentrated hydrochloric acid. Wash solutions were 5% concentration.

[b] Molecular weights of the solid polymer salts have been omitted because of solubility problems in the determinations.

[c] Methylene chloride was the solvent.

[d] Solid polymer V, R=Na, was isolated.

[e] Gel formation probably lowered yield.

stripped. The final residue was 2.7 g (72%) of a white, coarse, foamlike, slightly tacky polymer (V, R=Na), which softened at 105–115°C. On resolidifying, the polymer gave diffraction patterns in polarized light. The molecular weight, determined as above, was 1560, equivalent to seven repeating units. Surface tension measurements of aqueous solutions of V (R=Na) were made with a Du Noüy tensiometer.

Further polymerization of V (R=H) was achieved by heating. After 18 hr at 270–280°C/0.1 mm, a light-yellow, insoluble, infusible gel had formed. Another sample heated at 220–230°C gave after 18 hr an extremely viscous liquid, after 24 hr a soft, tacky solid, and after 36 hr a gel.

For esterification of V (R=H), an ethereal solution of diazomethane[12] was added to a solution of 10.2 g of hydrolysis polymer (mol. wt. 1530, n_D^{30} 1.4822) in 50 ml of ether until the yellow persisted. A little chloroform was added to give a clear solution. Excess diazomethane was destroyed with acetic acid. The solvents were removed under vacuum. About 200 ml of benzene was added to the residue and then distilled to remove any water or acetic acid. The product was 9.9 g of hydrolysis polymer methyl ester (V, R=CH_3), n_D^{30} 1.4804. This esterified polymer (2.0 g) was placed

in a side-arm test tube together with about 20 mg of lime. The mixture was heated to 242–253°C/0.1–0.2 mm with nitrogen ebullition for 5 hr to give a light brown, fairly tough, resilient polymer, soluble in chloroform, melting at about 97–104°C.

Methyl Azelaaldehydate Glycerol Acetal (IIa,b), Polytransesterification. The isomeric mixture of MAzGA was polymerized in bulk with different catalysts in different proportions (Table II). A continuous stream of nitrogen was passed through the melt during polymerization to keep insoluble catalysts in suspension. Polymerizations were carried out under vacuum, which was slowly increased from 40 mm to 0.1–0.05 mm as the temperature was increased from 240 to 285°C over 4–6 hr. Evolved methanol was collected by a Dry Ice trap in better than 98% yield.

The crude poly(ester-acetal) was dissolved in benzene (1:25), and the solution was filtered through a medium porosity sintered glass filter, then evaporated in a rotary evaporator, up to 140–160°C (0.05 mm). Precipitated polymers listed in Table II were precipitated in methanol from concentrated benzene solution and dried at 150°C/1 mm. Solubilities (Table III) were determined by the procedure of Sorenson and Campbell.[13] Melting points (Table II) were determined with a hot-stage polarizing microscope. Other thermal data also given in Table II were recorded with a Du Pont 900 differential thermal analyzer and 950 thermogravimetric analyzer. Intrinsic viscosities were determined in chloroform at 30°C within a few hours after dissolution, and number-average molecular weights, by vapor-pressure osmometry in benzene at 37°C.

Endgroup analyses were carried out by conversion of hydroxyl endgroups to titratable carboxylic acid endgroups with succinic anhydride.[14] Because titrating dark (high-ash) polymers was difficult, a nonaqueous, potentiometric titration was developed. The polymer sample (ca. 0.2 meq) was dissolved in 75 ml of anhydrous ethyl acetate to which several millimoles of an aliphatic ammonium tosylate, such as tetraethylammonium tosylate, had been added.[15] Solutions of the polymer before (control)and after conversion were titrated under dry nitrogen at room temperature with 0.1*N* potassium hydroxide in methanol–ethylene glycol (1:10). The glass and calomel electrodes used were equilibrated for several days in solvent containing electrolyte.[15] A range of −70 to −330 mv was observed.

Infrared spectra were obtained from liquid films on KBr disks. Ash was determined by heating the sample at 600°C for several hours and repeatedly treating it with 35% nitric acid.

RESULTS AND DISCUSSION

Monomer Preparation

Two methods of preparation of glycerol monoazelaaldehydate (Ia) were studied: ozonolysis of monoolein and glycerolysis of a methyl azelaaldehydate acetal. By either method, simple derivatives of the monomeric

TABLE II
Poly(ester-acetals) from Methyl Azelaaldehydate Glycerol Acetal (MazGA)

Polymer[a]	Catalyst: Type	Catalyst: Amt, wt-%	Melting range, °C	Ash, %	[η]	$\bar{M}_n$: VPO[b]	$\bar{M}_n$: EGA[c]	Differential thermal analysis maxima, °C[d]: T_g (ΔT)	T_c (ΔT)	T_m (ΔT)	Remarks	TGA temperature, °C[e]: T_0	T_{10}
1	Lime	1	78–82	2.91		7,000						260	381
2	Pyrolyzed $CaCO_3$	1	50–62			5,580						231	381
3	Na_2CO_3	1	41–47	0.16	0.29	5,110						285	385
4	Na	1	45–70	0.60		6,890						291	383
5	Lime	1	49–135	3.64	0.29[f]	14,460		−22.5 (6.5)	−3 (24)	80·5? (29)	Cooled slowly, 1st cycle	261	378
								−21.5 (9)		31.5 (55)	Cooled fast, 2nd cycle		
6	Polymer from experiment 5	1	43–49	0.08		4,120						264	372
7	Lime	1	41–105	3.19	0.27[f]	10,500		−21 (18)		50 (21)		304	377
8	Lime	0.10	43–50	0.43		5,310						272	387
9	Lime	0.01	40–50	0.70	0.30	11,600		−25 (9.5)		50 (35.8)	Cooled slowly, 1st cycle	231	358
								−23.5 (5)	−10.3? (31)	37.5 (32.5)	Cooled fast, 2nd cycle		

10	Lime	0.01	45–48	0.04		3,850					272	387
11	Lime	0.01	42–45	0.0		4,690					306	372
12	Lime	0.01	45–52	0.01	0.33	8,640		−28 (12)	48 (33)		246	370
13	Li	0.05	42–114	0.37	0.34	6,650		−21 (11)	44 (33)		309	376
14	$LiOCH_3$	0.05	47–106	8.0	0.37	4,850		−24 (10)	44 (22)		182	360
14P				0.08	0.37	8,810	6,180	−20 (10)	51 (53)		256	357
14PA				0.05		10,000	6,280					
15	Lime	1	49–75	5.8	0.35	7,080		−22 (19.5)	51 (34)		246	374
15P				1.43	0.35	11,390	3,610	−23.5 (13)	52 (26)		222	376
						(5,890)[g]	(6,125)[h]					
15PA				0.35		7,143	3,710					
16	Lime	0.02	46–54	0.07	0.37	4,320		−23.1 (10.3)	52.2 (42.5)		244	370
16P				0.05	0.38	7,575	7,870	−23.5 (19.5)	49.4 (85)		229	357
							(7,400)[h]					
16PA				0.03	0.33	7,673	7,970		46			

[a] P = precipitated polymer; A = polymer had —OH endgroups converted to $—OCO(CH_2)_2COOH$.

[b] Vapor-pressure osmometry in C_6H_6 at 37°C.

[c] Endgroup analysis in ethyl acetate at room temperature.

[d] Heating rate, 10°C/min; range, ca. −100 to 300°C. (On two cycles, range extended slightly beyond T_m and T_g.) T_m = melting point; T_c = crystallization temperature; T_g = glass transition temperature; ΔT = recovery temperature minus onset temperature.

[e] Thermogravimetric analysis, heating rate 10°C/min; T_0 = temperature at start of weight loss; T_{10} = temperature at 10% weight loss.

[f] 43% of polymer 5 and 1.35% of polymer 7 did not dissolve.

[g] Determined in ethyl acetate.

[h] Determined by gel-permeation chromatography in tetrahydrofuran.

TABLE III

Solubility of a Poly(ester-acetal) of MAzGA[a]

Solvent	Solubility[b]	Time, min[c]
Methylene chloride	3	2
Chloroform	3	3
Ethyl acetate	3	4
Tetrahydrofuran	3	5
Benzene	3	5
Pyridine	3	6
1,2-Dichloroethane	3	6
Carbon tetrachloride	3	14
Dimethylformamide	3	15
Benzyl alcohol	3	29
Acetone	2	—
Cyclohexanol	2	—
Ethanol	1	—
Ethylene glycol	1	—

[a] Polymer 15P (Table II), 0.1 g in 2 ml solvent.

[b] 1 = Melted or sticky in hot solvent; 2 = soluble in hot solvent, precipitated cold; 3 = soluble in cold solvent.

[c] Time required for dissolution with intermittent stirring.

ester were made in which the aldehyde group was protected as the acetal. By neither method was the monomeric free aldehyde isolated.

Ozonolysis of α-monoolein (IV) proceeded smoothly with no apparent attack on the *vic*-glycol. Distillation of the crude product gave a viscous, cloudy, yellowish semisolid. Attempted preparation of a 2,4-dinitrophenylhydrazone gave a red oil and a minute quantity of solid with a wide melting range. No solid hydroxyl derivative could be formed.

Because of the apparent heterogeneity of the free aldehyde, isolation as the dimethyl acetal was attempted to minimize possible condensation reactions of the aldehyde function. In the preparation of the dimethyl acetal (VI), dimethoxypropane was used as a water scavenger.[16,17] Hydrolysis

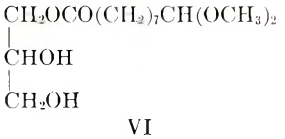

VI

of dimethoxypropane furnished acetone, and this liberated ketone reacted with the free hydroxyl groups of the glycerol monoester to form a ketal. The final reaction product was isopropylideneglyceryl azelaaldehydate dimethyl acetal (III). Infrared and nuclear magnetic resonance spectra were consistent with such a structure.

The alternate route to glycerol monoazelaaldehydate is ester glycerolysis, but to ensure a uniform product of known composition it is necessary to block two of the glycerol hydroxyls,[18] as well as to protect the aldehyde group. Consequently, isopropylideneglycerol was used in an alcoholysis

reaction with methyl azelaaldehydate dimethyl acetal. This reaction went smoothly to give compound III in good yield.

Hydrolysis of compound III did not give the expected monomer Ia, but III could be used directly in a particular polymerization. Other attempts to prepare compounds I or VI did not succeed, either by glycerolysis of methyl azelaaldehydate dimethyl acetal under conditions for monoglyceride synthesis or by reaction of III with $B(OCH_3)_3$.

MAzGA (II) was prepared by transacetalation of methyl azelaaldehydate dimethyl acetal with glycerol.[2] This procedure gave a mixture of structural and geometric isomers, the identification, characterization, and polymerization of which are described in another paper.[6]

Polymerization

Isopropylideneglyceryl Azelaaldehydate Dimethyl Acetal. Isopropylideneglyceryl esters of simple fatty acids readily hydrolyze under mild conditions to the corresponding α-monoglycerides.[9,18] Attempted hydrolysis of compound III with 5% sulfuric acid, however, resulted in recovery of starting material. Treatment with warm 1:1 hydrochloric acid appeared to effect hydrolysis, but the product, a viscous oil, contained only about 20% α-monoglyceride. Further attempts at hydrolysis under a variety of conditions gave similar results. The products were cloudy, viscous oils, many of which turned to gelatinous solids on standing. Refractive indices of the products varied with hydrolysis conditions. Chemical and infrared analyses showed that none of the products contained more than small amounts of α-monoglyceride. Even in reactions carried out at $-40°C$ the free glycerol azelaaldehydate was not isolated.

In acidic media acetals exist in labile equilibrium with their component aldehydes and alcohols.[19] Thus, the conditions for acetal hydrolysis are essentially those for acetal formation. When the ester-acetal was hydrolyzed, the free glycerol ester-aldehyde apparently reacted rapidly with other liberated molecules of glycerol ester-aldehyde, and the product isolated was a poly(ester-acetal) (V, R=H). The different properties obtained under different conditions can be ascribed to varying degrees of polymerization and to the presence of some monomer (I) or internal acetal (VII), or both, which might also be formed under some conditions.

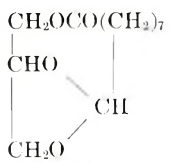

VII

In a typical hydrolysis-polymerization,[11] a solution of compound III in benzene or in methylene chloride was stirred vigorously with an equal volume of concentrated hydrochloric acid. Without vigorous stirring there was little apparent reaction. When the organic phase was washed

free of mineral acid with water, the recovered polymer was the viscous, water-insoluble oil described. This procedure represents a new polymerization technique for the preparation of poly(ester-acetals) in which the ketal of the glycerol monoesteracetal is converted to a polymer at an aqueous–organic interface. The new technique might be considered similar to interfacial polymerization,[20] because the initial hydrolysis and possibly the subsequent polymerization take place at an interface; however, this hydrolysis polymerization is a homopolymerization with the monomer precursor entirely in the organic phase. The aqueous phase contains only the catalyst for hydrolysis and polymerization. The polymer remains in the organic phase and is recovered from it.

The products were low molecular weight oligomers; the maximum molecular weight was 1530, representing 6.7 repeating units. That the polymerizing chain was terminated by hydrolysis of the ester group was indicated by the following observations.

When the polymer solution was washed with 5% sodium carbonate solution to remove the last traces of mineral acid, an exceedingly stable emulsion formed. The product isolated from this emulsion was a white, foamlike solid that did not melt sharply but only softened at about 110°C. It swelled in benzene, apparently dissolved in chloroform difficultly, but dissolved in water readily. These properties lead to the conclusion that the original polymer (V, R=H) had an acidic group that could be neutralized to form a salt (V, R=Na). The properties of the salt varied somewhat from experiment to experiment, perhaps corresponding to the variations in the acid polymer. Additional confirmation of the presence of the carboxyl end group was found in the esterification of V, R=H, with diazomethane to give a methyl ester V, R=CH_3.

Some effects of varied reaction conditions on properties and yields of polymer are shown in Table I. All the experiments shown were run with concentrated hydrochloric acid. Use of 1:1 concentrated hydrochloric acid:water gave reasonably satisfactory results; more dilute acid gave little hydrolysis, if any.

Optimum conditions consisted of a 10% solution of monomer in benzene stirred with an equal volume of concentrated hydrochloric acid for 1 hr at 7–9°C. Raising the temperature lowered both yield and molecular weight. Lower concentrations of monomer at the higher temperature increased yield. Conducting the reaction near the freezing point of benzene did not improve yields significantly even with longer reaction times. That the low molecular weight was not the result of the freezing solvent was demonstrated by substituting methylene chloride for benzene. Although the yield was higher, molecular weight was affected only slightly.

Experiments in which the salt of the polymer was isolated by washing with aqueous alkali, as outlined above, supplemented those in which acid polymer was isolated. Yields of polymer salt were generally higher than those of acid obtained under comparable conditions. The apparent high

yield was probably caused by inclusion of some inorganic salt with the polymer. Increased hydrolysis time at room temperature may have caused some degradation since the final product was not a solid and yield was low. Reducing the hydrolysis time lowered yield only slightly. Reducing monomer concentration increased yield as in the series with isolation of acid. When the polymer solution was washed with 5% sodium hydroxide, a stable gel formed that made isolation difficult and, accordingly, lowered the yield. Washing with sodium bicarbonate or piperidine, bases weaker than sodium carbonate, also did not give a solid product.

The stability of emulsions formed during isolation indicated that the polymer salt had surfactant properties. Surface tension measurements on aqueous solutions of the polymer sodium salt are summarized in Table IV.

Although the hydrolysis-polymerization technique did not produce high polymers directly, the oligomers could be used as prepolymers. When polymer acid V (R=H), was heated under vacuum (conditions for polymerization of hydroxyacids), the viscosity increased until gelation occurred.

TABLE IV

Concentration of solution, %	Surface tension at 23°C, dyne/cm
0	72.1
0.02	50.4
0.1	47.4
1.0	45.0

The gelation was the result of crosslinking brought about by the acidic nature of the polymer itself. The polymer ester V, R=CH_3, polymerized to an ungelled, essentially linear poly(ester-acetal) when it was heated under vacuum with lime as catalyst.

Methyl Azelaaldehydate Glycerol Acetal. In contrast to the low molecular weight poly(ester-acetals) obtained by the hydrolysis-polymerization method, molecular weights in the range of 5000–10000 were obtained by polycondensation of II. Of the catalysts tested (CaO, PbO, Sb_2O_3, $Zn(OAc)_2$, Li, Na, Na_2CO_3, $LiOCH_3$, and $CaCO_3$) (Table II), lime was best for the polycondensations at 240–285°C and was used in most of the polymerizations described below. The latent crosslinking activity of these poly(ester-acetals) was demonstrated when crosslinked polymers were obtained with use of zinc acetate or excessive heating during polymerization.

When present in amounts of about 1%, lime was bound to the polymer as carboxylate salt, as shown by the ash content of precipitated polymers, the occurrence of carboxylate absorption at 1550 cm^{-1} in their infrared spectra, and by anomalous molecular weight measurements. A dilute sulfuric acid wash of the polymer was partially successful in removing bound calcium and lowered the ash content by two-thirds.

Agreement was excellent for molecular weight measurements of polymers without bound calcium by vapor-pressure osmometry, gel-permeation chromatography (GPC), and endgroup analysis, but the intrinsic viscosities of these amorphous polymers did not have a simple relationship to molecular weight as in the Mark-Houwink equation. For polymers with bound calcium, the molecular weight by GPC and vapor-pressure osmometry in ethyl acetate was half that by vapor-pressure osmometry in benzene and double that by endgroup analysis. Dissociation of the calcium polymer dicarboxylate in polar solvents as opposed to lack of dissociation in nonpolar solvents would explain these anomalous results.

GPC was carried out and interpreted by a commercial laboratory for two precipitated polymers (15P and 16P, Table II) and for one unprecipitated polymer (16, Table II). Since an accurate value for the Q factor (molecular weight per unit Ångström) has not as yet been determined for these polymers, a nominal value of 25, characteristic of polyesters, was selected as most reasonable. The molecular weight ratios ($\bar{M}_w/\bar{M}_n$) for polymers 15P and 16P were 2.15 and 2.16, with $\bar{M}_n$ 6125 and 7400, respectively. Polymer 16, which contained material of lower molecular weight, had an $\bar{M}_n$ value of 5600 and a molecular weight ratio of 2.69. The molecular weight distributions for 16P and 16 were essentially identical for the upper 70% of the range. Agreement was excellent among $\bar{M}_n$ values for polymer 16P determined by GPC, vapor-pressure osmometry, and endgroup analysis.

In differential thermal analyses the polymers melted over a broad range, with endothermic maxima at 45–50°C and glass transitions at −20 to −25°C (Table II). High-ash polymers also had a series of broad and shallow endotherms at 50–145°C. High-ash polymers had a broader, higher melting range and seemed slightly more stable thermally (Table II).

A tough, tan elastomer was prepared from precipitated polymer 14P by heating it to 250–260°C at 0.3 mm for 0.5 hr with 0.05% *p*-toluenesulfonic acid and 3% zinc oxide filler. This elastomer was only partially soluble in ethyl acetate, benzene, chloroform, or dichloromethane. The swelling ratio[22] was 2295, with 14.9% solubility in chloroform. Corresponding values were 697 and 30.2% in ethyl acetate after 6 days at room temperature. The elastomer had a glass transition at −21°C and endothermic maximum at 47°C.

We thank B. R. Heaton, K. A. Horton, and C. E. McGrew for microanalyses and molecular weight determinations; D. J. Moore for thermal analyses; G. E. McManis for some of the infrared spectra; and R. B. Bates, Univerity of Arizona, for nuclear magnetic resonance spectra and advice. GPC was performed and interpreted at ARRO Laboratories, Inc., Joliet, Illinois.

The mention of firm names or trade products does not imply that they are endorsed or recommended by the Department of Agriculture over other firms or similar products not mentioned.

References

1. E. H. Pryde, D. E. Anders, H. M. Teeter, and J. C. Cowan, *J. Org. Chem.*, **25**, 618 (1960).

2. E. H. Pryde, D. J. Moore, H. M. Teeter, and J. C. Cowan, *J. Chem. Eng. Data*, **10**, 62 (1965).

3. E. H. Pryde, R. A. Awl, H. M. Teeter, and J. C. Cowan, *J. Polym. Sci.*, **59**, 1 (1962).

4. E. H. Pryde, D. J. Moore, H. M. Teeter, and J. C. Cowan, *J. Polym. Sci.*, **58**, 611 (1962).

5. W. R. Miller, E. H. Pryde, and J. C. Cowan, *J. Polym. Sci. B*, **3**, 131 (1965).

6. R. W. Lenz, R. A. Awl, W. R. Miller, and E. H. Pryde, *J. Polym. Sci. A-1*, in press.

7. K. F. Mattil and R. J. Sims, *J. Amer. Oil Chemists' Soc.*, **29**, 59 (1952).

8. W. D. Pohle and V. C. Mehlenbacher, *J. Amer. Oil Chemists' Soc.*, **27**, 54 (1950).

9. F. A. Norris, U. S. Pat. 2,619,493 (1952).

10. M. Renoll and M. S. Newman, in *Organic Syntheses* Coll. Vol. **3**, E. C. Horning, Ed., Wiley, New York, 1955, p. 502.

11. W. R. Miller, in *The Encyclopedia of Chemistry*, 2nd ed., G. L. Clark and G. G. Hawley, Eds., Reinhold, New York, 1966, p. 531.

12. J. A. Moore and D. E. Reed, in *Organic Syntheses*, Vol. 41, J. D. Roberts, Ed., Wiley, New York, 1961, p. 16.

13. W. R. Sorenson and T. W. Campbell, *Preparative Methods of Polymer Chemistry*, Interscience, New York, 1961, p. 54.

14. G. F. Price, in *Techniques of Polymer Characterization*, P. W. Allen, Ed., Butterworths, London, 1959, p. 226.

15. J. Kucharský and L. Šafařík, *Titrations in Non-aqueous Solvents*, Elsevier, New York, 1965, pp. 63–70.

16. J. H. Brown, Jr. and N. B. Lorette, U. S. Pat. 2,978,469 (1961).

17. E. H. Pryde, D. J. Moore, H. M. Teeter, and J. C. Cowan, *J. Org. Chem.*, **29**, 2083 (1964).

18. E. Baer and H. O. L. Fischer, *J. Amer. Chem. Soc.*, **67**, 2031 (1945).

19. L. F. Fieser and M. Fieser, *Advanced Organic Chemistry*, Reinhold, New York, 1961, pp. 441–442.

20. E. L. Wittbecker and P. W. Morgan, *J. Polym. Sci.*, **40**, 289 (1960).

21. L. J. B. Bellamy, *The Infra-red Spectra of Complex Molecules*, 2nd ed., Wiley, New York, 1959, p. 175.

22. L. W. Chen and J. Kumanotani, *J. Appl. Polym. Sci.*, **9**, 3649 (1965).

Received March 24, 1969
Revised July 14, 1969

JOURNAL OF POLYMER SCIENCE: PART A-1 VOL. 8, 429–441 (1970)

Poly(ester-acetals) from Geometric Isomers of Methyl Azelaaldehydate Glycerol Acetal*

ROBERT W. LENZ, *Polymer Science and Engineering Program, Chemical Engineering Department, University of Massachusetts, Amherst, Massachusetts 01003,*† R. A. AWL, W. R. MILLER, and E. H. PRYDE, *Northern Regional Research Laboratory, Northern Utilization Research and Development Division, Agricultural Research Service, U.S. Department of Agriculture, Peoria, Illinois 61604*

Synopsis

The glycerol acetal of methyl azelaaldehydate is an ω-hydroxy ester that exists as a mixture of dioxolanyl and dioxanyl isomers, each having two geometric isomers. Each of the four isomers was isolated by chromatographic (gas–liquid and column) and fractionating (crystallization and distillation) methods. Structural assignments were made on the basis of nuclear magnetic resonance and infrared spectral data. Linear poly(ester-acetals) were prepared from each of the *cis* and *trans* forms of the dioxanyl isomers and from a mixture of the dioxolanyl geometric isomers. Physical properties of these polymers were correlated with their structures. When prepared with basic condensation catalysts, the polymers retained the geometric configuration and structural identity of the monomer. When prepared with lead acetate, structural rearrangement as well as polycondensation occurred, resulting in an enrichment of the dioxolanyl isomer and simultaneous increase in polymer crystallinity. The enrichment took place at elevated temperatures and also, unexpectedly, at room temperature upon long standing of the polymer. Isomer redistribution at room temperature appears to be antithermodynamic in the reaction sense, yielding a polymer of unusually high dioxolanyl unit content. The driving force for this isomerization may be crystallization of these units by a phenomenon termed a "crystallization-induced reaction."

INTRODUCTION

The glycerol acetal of methyl azelaaldehydate (I) is an ω-hydroxy ester capable of self-condensation to a linear poly(ester-acetal). This monomer, as normally prepared in high yield by an acid-catalyzed acetal-interchange reaction between glycerol and methyl azelaaldehydate dimethyl acetal,[1,2] is a mixture of four isomers; namely the *cis* and *trans* isomers of both the dioxolane (Ia and Ib, respectively) and dioxane (Ic and Id, respectively) ring forms:

* Presented in part at the American Chemical Society Meeting, Division of Polymer Chemistry, Chicago, Illinois, September 1967.

† Work done in part at Fabric Research Laboratories, Dedham, Massachusetts.

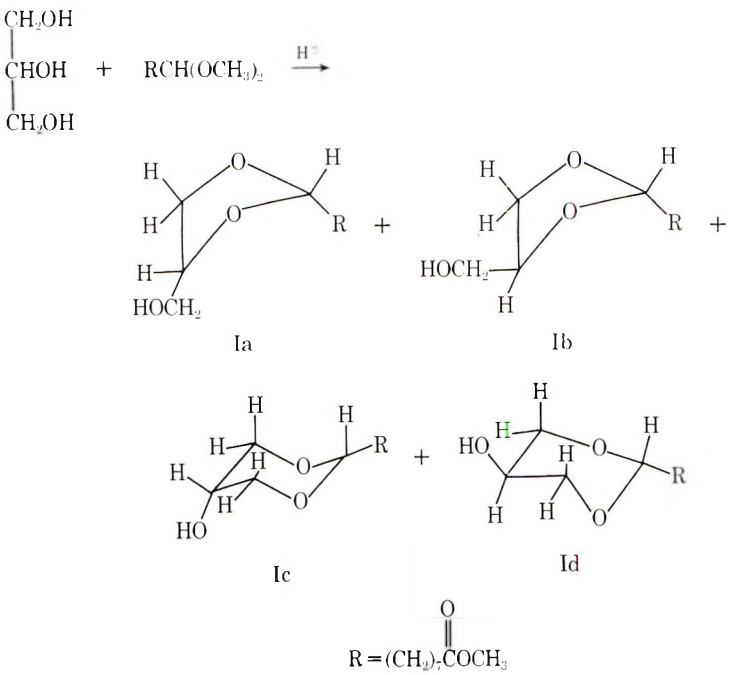

When a catalyst is used that promotes ester interchange but not acetal interchange, this monomer mixture can be converted to a high molecular-weight polyester containing a mixture of isomeric repeating units. The distribution of ring isomer structures in the polymer is not necessarily identical to that in the monomer mixture from which it is made. To the contrary, depending upon the catalyst and polymerization temperature, polymers of broadly different isomer compositions, and therefore different physical properties and chemical reactivities, can be prepared from the same monomer mixture.

EXPERIMENTAL

GLC Apparatus and Analyses

For analytical gas–liquid chromatography (GLC), an F&M Model 500 gas chromatograph (thermal conductivity detector) was used. Operating conditions were: block temperature, 290°C; bridge current, 150 ma; injection port temperature, 220°C; column temperature, 210°C with the 3% HI-EFF 8BP and 3% Versamid 900 packings (both from Applied Science Laboratories), and 260°C with the 20% Versamid 900 packing. Helium flow at exit, 40 ml/min with the HI-EFF 8BP packing, 50 ml/min with the 3% Versamid 900, and 75 ml/min with the 20% Versamid 900. Analytical columns were all 4 ft × $^1/_4$ in. aluminum tubing. Peak areas were determined by the method of triangulation.

For preparative GLC, an F&M Model 775 Prepmaster was used. Manual injection and collection were necessary under the circumstances because of restricted sample size (60 μl), high viscosity, and the variable peak heights and resolution. Operating conditions were: detector temperature, 280°C; buffer zone, 280°C; manifold, 290°C; injection port, 235°C; head pressure, ca. 16 psi; helium flow, 890 ml/min; column temperature, 205°C. The preparative column, packed with 208 g of 3% HI-EFF 8BP, was made from two sections of 8 ft $\times$ 1 in. (OD) aluminum pipe joined at the bottom to form a U shape with a $2^1/_2 \times {}^3/_8$ in. section of aluminum tubing.

GLC of glycerol acetals of methyl azelaaldehydate with any of the three packings listed will resolve and display four peaks (A, B, C, and D) in the order of their elution (Fig. 1). Total retention time with the analytical columns is about 25 min, and with the preparative column it is 1 hr, 21 min. When methyl oleate (97+%) serves as the internal standard, the recovery of isomer A has been estimated for the analytical column to be

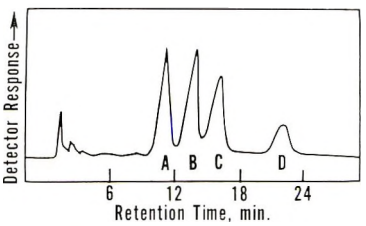

Fig. 1. Chromatogram of methyl azelaaldehydate glycerol acetal obtained with 3% HI-EFF 8BP on 60–80 mesh Gas Chrom Q (pretreated). Peaks A and D are the *cis* and *trans* isomers of the six-membered dioxane rings, respectively; peaks B and C are the isomers, as yet unidentified of the five-membered dioxolane rings.

ca. 85% with the HI-EFF 8BP packing, but only 62% with the 20% Versamid 900 packing. A rough estimate of the recovery of isomer D by this same procedure is ca. 63% on the HI-EFF 8BP packing. This packing is obviously quite superior to the 20% Versamid 900 packing with respect to the recovery of isomers Ib, Ic, and Id. Its superiority is especially evident when larger columns are employed as in preparative GLC.

To collect the effluent from our analytical column, solutions of pure isomer Ia (2–3 μl) were injected on an analytical column packed with 20% Versamid 900, and the effluent was collected by means of a modified Swinny hypodermic adaptor. Twelve injections provided enough collected sample for analysis by both GLC and IR (CCl_4 solution). Since neither analysis indicated that any alteration of the isomer had occurred, the same method was followed to separate and collect isomers Ib and Ic from a fraction rich in these two isomers. Approximately 15 injections of 2.5 μl size were required. GLC of the collected isomers indicated the following purities based on peak areas: for isomers Ib, 71.1% B, 21.3% C, and 7.6% A; for isomer Ic, 82.3% C and 17.3% B. Infrared spectra for each of these collected samples were determined with carbon tetrachloride solutions.

Monomer Synthesis

Methyl azelaaldehydate (II) was prepared by ozonization of methyl oleate in methanol followed by either catalytic hydrogenation of the ozonolysis products over palladium-on-charcoal catalyst or zinc–acid hydrogenation as previously described.[3] Immediately, II was converted to its dimethyl acetal, methyl 9,9-dimethoxynonate (III), for purification and storage; and the monomer mixture I was subsequently prepared by react- III with glycerol in the absence of solvent. A typical procedure for preparing I is as follows. A mixture of 5.56 g (0.024 mole) of III, 3.68 g (0.04 mole) of glycerol, and 0.1 g of potassium bisulfate was heated under nitrogen for 4 hr until the vapor temperature reached 92°C. The product was taken up in methylene chloride, washed three times with water, dried over anhydrous calcium sulfate, and filtered; then the solvent was evaporated to yield a total 5.38 g (86.2%) of crude I. Distillation at 158–165°C/0.4 mm yielded 55–60% of chromatographically pure monomer mixture I.

ANAL. Calcd for $C_{13}H_{24}O_5$: C, 59.97%; H, 9.29%; mol. wt. 260.3. Found: C, 60.0%; H, 9.6%; mol. wt. 265.

Isomer Separation

Monomer mixture I was separated into three fractions of good purity by three different procedures: (*1*) preparative GLC with an F&M Model 775 Prepmaster with 8 ft × 1 in. aluminum column packed with 208 g of 3% HI-EFF 8BP on 60–80 mesh Gas Chrom Q; (*2*) fractional distillation and low-temperature crystallization; and (*3*) dry-column chromatography.[4] The second and third methods were used to separate sufficiently large amounts of each fraction for polymerization studies, and typical procedures are described below.

Isolation of Isomers Ic and Id by Fractional Distillation and Crystallization. A vacuum fractional distillation was carried out on 195 g of I through a heated, vacuum-jacketed column (1 in. × 6 in.) packed with glass helices. The highest boiling fraction (bp 150–156°C/13 mm and bath temperature of 223–243°C; $n_D^{30} = 1.4594$) was a clear, colorless liquid, which weighed 8.2 g. Microanalyses were in accord with I. After storage in the refrigerator, the liquid solidified, and only partial liquefication resulted when the solid was warmed to room temperature. The residual solid portion was separated by rapid filtration on a chilled filter funnel, and the white filter cake was squeezed dry by means of rubber dam and applied vacuum. After the filter cake was air-dried, 1.08 g of a white, crystalline solid was obtained, and further crystallization from a 4:1 water–ethanol mixture gave 0.6 g of crystalline solid, which after drying in a vacuum oven at 40°C, melted at 43–45°C. In all, approximately 1.5 g of recrystallized product was isolated by repetition of this procedure, and this material was subjected to four recrystallizations from 10 ml of acetone at about −40°C to yield a first crop weighing 50 mg (mp 45.4–46.5°C) and a second crop weighing 86 mg (mp 44.5–45.5°C). GLC of both of these crops run on a

20% Versamid 900 analytical column indicated the presence of only one peak corresponding to isomer Id. From the combined filtrates of the third and fourth crystallizations, there was recovered 91 mg of crystalline solid (mp 41–45°C), which by GLC consisted of 94.9% Id, 3.3% Ia, and 1.7% Ib.

ANAL. Calcd for $C_{13}H_{24}O_5$: C, 59.97%; H, 9.29%. Found: C, 59.90%; H, 9.29%.

A 660-g sample of crude I was again subjected to a vacuum, fractional distillation with the previously described column of glass helices, and a low-boiling fraction was isolated, which weighed 59.0 g and was rich in isomer Ic. Partial crystallization of this fraction was observed after its storage in the refrigerator for several days. The solid portion was collected by several filtrations on a cold Buchner funnel, and the waxy, white solid so isolated was washed with cold heptane, scraped onto a porous plate, and dried in a vacuum desiccator to yield a white, crystalline solid which melted at 43–44°C. A total of 5.7 g. was collected in this manner and subjected to further purification by low-temperature crystallization. Three recrystallizations from acetone (1:5, 1:10, and 1:5 w/v) at −30 to −55°C afforded a white, crystalline solid. This solid was redissolved and filtered to remove foreign insoluble particles. The solvent was evaporated at reduced pressure to obtain a clear, colorless, and viscous liquid. Crystallization occurred on seeding to yield 2.1 g of white, crystalline solid (mp 44.0–45.0°C) which by GLC was pure Ic.

ANAL. Calcd for $C_{13}H_{24}O_5$: C, 59.97%; H, 9.29%; mol. wt. 260.3. Found: C, 60.28%; H, 9.37%; mol. wt. 252.

Isolation of Isomers by Dry-Column Chromatography.[4] A 30-in. section of nylon tubing (1.6 mm thickness, $2^1/_4$ in. flat diameter) was heat-sealed at one end so as to leave a 1 in. × $^1/_4$ in. sleeve through which was inserted a small glass tube containing a glass wool plug. This nylon tubing was packed with about 400 g of Florisil (Floridin Co., 60–100 mesh; activated at 275°C *in vacuo* and then deactivated with 6–7% water) to a height of 26–27 in. A 2-g sample of I was mixed with a little of the deactivated Florisil and placed on top of the column. The column was developed by adding anhydrous ether at such a rate as to maintain a 1–2 cm solvent head. The column was developed by passing 450 ml of ether through it over a 40-min period, and the glass tube was withdrawn and the sleeve and top of the column were clamped. The column was laid horizontally in the miter box and cut into sections with a razor according to the following R_f values: isomer Ic, 0.15–0.38; isomers Ia and Ib, 0.45–0.60; isomer Id, 0.69–0.85. Each section was extracted with three portions of methanol, totaling approximately 50 ml of solvent per gram of Florisil to a section. The filtered extract was evaporated; the residue, taken up in dichloromethane, was dried over anhydrous potassium carbonate, and filtered; and the solvent was removed. An overall recovery of 31–41% was obtained in three such runs. Significant overlap or tailing of isomer Id into isomers Ia and Ib

occurred between R_f values of 0.61 and 0.69 on the 26-in. column. Reasonably pure samples of isomer Ic were secured by this procedure. However, because of the low initial concentration of isomer Id (ca. 8%) in mixture I, as well as the tailing observed on the 25-in. column and the low overall recovery, this procedure was of limited usefulness for isolating isomer Id. Isomers Ia and Ib were not resolved in this manner; instead a fraction containing approximately 60% Ia and 40% Ib was used for polymerization studies.

Polymerization Reactions

Polymerization reactions were generally carried out either (1) with lead acetate trihydrate as catalyst at 190°C or (2) with calcium oxide as catalyst at 250–290°C. The reactions were conducted either under nitrogen or in vacuum with 0.5% by weight of the catalyst and 0.5% by weight of an antioxidant present. Often the polymeric products were characterized directly, without purification by reprecipitation, as described in the following example.

TABLE I
Polymerization of Methyl Azelaaldehydate Glycerol Acetal with $Pb(OAc)_2 \cdot 3H_2O$ at 190°C

Reaction time, hr	Final pressure, mm Hg	Intrinsic viscosity (benzene, 30°C)	Molecular weight[a]
6	9	0.12	—
6	9	0.17	3280
20	0.5	0.20	3260
67	0.5	0.29	5650

[a] Number-average molecular weight determined in benzene from vapor-pressure depression in a Mechrolab vapor-pressure osmometer.

TABLE II
Polymerization of the Isomers of Methyl Azelaaldehydate Glycerol Acetal (I)

	Catalyst		Reaction conditions			
Isomer	Type	Amt, wt-%	Temp, °C	Time, hr	Final pressure, mm Hg	Molecular weight[a]
Ia + Ib	None[b]		156–290	1.5	0.40	4140 (P)
Ic	CaO	0.1	240–281	13	0.05	5500
Ic	CaO	0.1	150–280	13.5	0.20	5910 (P)[c]
Id	CaO	0.1	240–281	13	0.05	6820 (P)

[a] Number-average molecular weight determined in benzene from vapor-pressure depression in a Mechrolab vapor-pressure osmometer. (P) Signifies polymer was dissolved, filtered, and precipitated before analysis.

[b] This sample apparently polymerized spontaneously upon an attempt to distill it.

[c] This polymer was insoluble in benzene; molecular weight was determined in a chloroform solution.

A mixture of 2.0027 g of monomer mixture I, 0.0107 g of lead acetate trihydrate, and 0.0103 g of *N*-phenyl-β-naphthylamine was heated at 190° in an oil bath at atmospheric pressure; nitrogen was bubbled through the mixture throughout the reaction. After 3 1/2 hr, the pressure was reduced gradually to 9 mm. While the nitrogen flow was maintained, and after an additional 1/2 hr, the pressure was reduced to about 0.5 mm with an oil pump. The nitrogen flow was stopped at this point. The reaction was continued for an additional 16 hr, after which the mixture was cooled at reduced pressure and then dissolved in benzene by stirring at room temperature. The benzene solution was filtered through a medium porosity, sintered glass funnel; the concentration was adjusted to approximately 4%; and the intrinsic viscosity and solids content of the solution were determined, as well as an elemental analysis of the solvent-free polymer.

ANAL. Calcd. for $(C_{12}H_{20}O_4)_n$: C, 63.13%; H, 8.83%. Found: C, 63.22%, 63.41%; H, 8.80%, 8.65%; ash, 0.46%, 0.48%.

Typical results for the products from both polymerization reactions are compiled in Tables I and II. Polymerization of the monomer mixture with lime catalyst has been described previously.[5]

RESULTS AND DISCUSSION

Monomer Structure

The preferred route for monomer preparation is the reaction of glycerol with the dimethyl acetal of methyl azelaaldehydate rather than with the free aldehyde.[1,2] Analysis of the purified monomer I by gas–liquid chromatography (GLC) shows the presence of four closely related components, now known to be the isomeric structures indicated above as isolated and identified by preparative GLC. Some success has also been realized in separating the isomers of I by column chromatography and by fractional crystallization.

In general, nuclear magnetic resonance (NMR) is a convenient method for qualitatively and quantitatively analyzing acetal mixtures of different ring sizes and, to a lesser extent of *cis–trans* isomeric structures. The chemical shift of the acetal proton signal depends strongly on ring size and, for six-membered acetal rings at least, on axial versus equatorial placement (for the *cis* and the *trans* structures) as previously demonstrated for carbohydrate derivatives.[6] For dioxolane rings in general, the acetal proton signal ranges from 285 to 295 cps downfield from tetramethylsilane, whereas the equivalent proton signal in dioxane rings resides at 260–275 cps with the axial proton signal generally shifted 10–20 cps upfield from the equatorial proton signal. Chemical shift data for a series of five-, six,- and seven-membered acetal monomers related to I will be presented in more detail in a subsequent publication.

Besides differing in ring size, which considerably influences the physical properties and chemical stabilities of their polyesters, the glyceryl acetal

monomers also differ in type of hydroxyl group, a distinction which considerably affects their relative rates of polymerization. The dioxolane forms Ia and Ib contain a primary hydroxyl group which is more reactive than the secondary group in the dioxane forms Ic and Id, and the reactivity of the secondary hydroxyl group, at least, is quite different when it resides in an axial instead of an equatorial position.[7,8] The difference in hydroxyl groups between the two ring forms also serves to characterize the isomers by both infrared (IR) and NMR. When NMR spectra are obtained for deuterodimethyl sulfoxide solutions,[9] the signal for the primary hydroxyl proton appears as a low-field triplet and that for the secondary at a higher field position as a doublet, with the signal for the axial OH in Ic again located upfield from that of the equatorial isomer in Id.

Polymer Structure and Properties

Polymerization of monomer I mixture by transesterification must be carried out under conditions that minimize or prevent intramolecular acetal interchange; otherwise, gelation can occur through conversion of the internal, cyclic acetal repeating units into acetal crosslinks. To ensure the absence of such crosslinking reactions, two model reactions were studied to

TABLE III
Catalyst Evaluation from Studies of Model Interchange Reactions

Catalyst	Ester interchange, ratio of butyl to methyl myristate[a]	Acetal interchange, amount of dibutyl acetal[b]
CaO	0.028	0
$CaTiO_3$	—	Trace
$CaTiF_6$	—	ca. 30%
K_2CO_3	—	0
$(MgCO_3)_4 \cdot Mg(OH)_2 \cdot H_2O$	0.015	0
$CaCO_3$	0.017	0
Li_2CO_3	0.012	0
Na_2CO_3	0.061	0
MgO	0.014	0
$Pb(OAc)_2 \cdot 3H_2O$	13.4	0
$PbCO_3$	0.17	0
KOAc	0.030	0
Na_2TiF_6	—	Trace
$Mg(OAc)_2 \cdot 4H_2O$	0.008	0
Ti(O-*i*-Pr)$_4$	11.1	Trace
Ti(O-*n*-Bu)$_4$	0.32	Trace
Sb_2O_3	0.0076	Trace
$Ca(OAc)_2 \cdot H_2O$	0.012	0
$NaSiO_3$	0.018	—
PbO	0.019	—

[a] Interchange reaction of methyl myristate in refluxing *n*-butanol for 4 hr.

[b] Interchange reaction of pelargonaldehyde ethylene acetal in refluxing *n*-butanol for 7 hr.

evaluate conditions and potential polymerization catalysts. The efficacy of certain catalysts for ester interchange was evaluated from the reaction of *n*-butanol with methyl myristate, whereas the inertness of these catalysts in affecting acetal interchange was judged from the extent of the exchange reaction between pelargonaldehyde ethylene acetal and *n*-butanol. Both reactions were carried out in refluxing *n*-butanol, the former for 4 hr and the latter for 7 hr, and the extent of interchange occurring in each was estimated by GLC analysis of the products (Table III).

Lead acetate trihydrate is an effective catalyst for the polymerization reaction at temperatures in the neighborhood of 120°C. This conclusion holds for reaction temperatures up to about 200°C, but this catalyst cannot be used at much higher temperatures since it was determined from other experiments that crosslinking occurs. Calcium oxide is also an effective catalyst but must be used at high temperatures. In general, it was observed that linear polymers of molecular weights in the range of 5000–10000 could be prepared in reasonable reaction times either with $Pb(OAc)_2 \cdot 3H_2O$ at 190°C or with calcium oxide at temperatures of 250–290°C. The generalized intrinsic viscosity–molecular weight relationship for these polymers in benzene at 30°C is $\log [\eta] = 3.5 \times 10^{-4} M^{0.78}$.

Polymerization of monomer mixture I at temperatures of 250°C and above with calcium oxide as catalyst yielded a remarkably different polymer from that obtained with the same monomer at 190°C or below with lead acetate trihydrate as catalyst. Although the former was a hard solid, the latter was an elastomer in the same molecular weight range. Observations with a polarizing microscope revealed the cause of this difference. The polymer prepared at the higher temperature with calcium oxide was crystalline, whereas the other process yielded an amorphous polymer. Identical samples of monomer were used in both polymerization reactions. This mixture of isomers, as purified by distillation at about 160–170°C and analyzed by NMR, had a ratio of five- to six-membered ring forms [(Ia + Ib)/(Ic + Id)] of approximately 3:1. The poly(ester-acetal) prepared with $Pb(OAc)_2 \cdot 3H_2O$ at 190°C contained essentially the same ratio of repeating units. In sharp contrast, polymers from distilled monomer with calcium oxide as catalyst at 250–290°C were markedly enriched in the dioxolane form up to ratios of the five-to six-membered ring repeating units of between 6:1 and 10:1. Apparently, therefore, isomerization towards a different equilibrium ratio of the two ring forms occurred either in the monomer or within the repeating units in the polymer or both during polymerization. The polymer was then sufficiently rich in the dioxolane ring forms to permit crystallization.

The change in isomer ratio in this reaction apparently indicates that some acidic impurities must have been present in the distilled monomer to catalyze the acetal isomerization reaction. Cyclic acetals are known to isomerize readily in the presence of an acid catalyst, and a number of studies have shown that equilibration of glyceryl acetal mixtures increasingly favors the five-membered ring with increasing temperature.[10–13]

If isomerization did occur during polymerization at temperatures of 250°C and above, it is not surprising that the ratio of dioxolane to dioxane units should increase as observed. What is surprising, however, is the subsequent contradictory behavior of the amorphous polymer on standing at room temperature for a long period of time after preparation.

Reexamination of the noncrystalline polymer prepared at 190°C or below after 2 months' storage at room temperature revealed that the original elastomeric material had slowly been converted to a hard solid. The cause of this transformation became apparent when the sample was observed under a polarizing microscope which showed the presence of spherulitic crystal growth in the previously amorphous material. Again, quantitative analysis of the cyclic acetal repeating unit by high-resolution NMR indicated that the polymer had become enriched in the five-membered ring units up to essentially the same level as produced in the higher temperature polycondensation, or to approximately twice the ratio of five- to six-membered ring repeating units as present in the original polymer. Both crystalline polymers also had essentially identical melting points within the range of 50–64°C.

Clearly, it would seem that if requilibration of the cyclic acetal units during polymerization at a temperature above that of monomer purification is in a direction toward a higher five-membered ring content, then requilibration considerably below the purification temperature should be in the opposite direction, toward a lower ratio of five- to six-membered ring units. Therefore, to verify the contrary conclusion based experimentally on NMR analysis, monomer mixture I was fractionated into the two ring forms, and each form was separately polymerized to its homopolymer for comparative characterization with the crystalline polymers described above.

Separation and Polymerization of Monomer Isomers

Monomer mixture I was separated into three fractions by preparative GLC. Analytical GLC had indicated the presence of four peaks (identified as A, B, C, and D in Fig. 1), as expected for four isomers, but the middle two peaks could not be resolved in the preparative-scale separations. Small amounts of peaks B and C, sufficient for infrared analyses, were resolved by analytical GLC. On subsequent infrared and NMR analysis, peaks B and C were found to be the *cis*- and *trans*-dioxolane derivatives, Ia and Ib. Similar analyses of the other two fractions revealed that the peak with the shortest retention time was the *cis*-dioxane isomer, Ic, and that with the longest retention time was the remaining *trans*-dioxane isomer, Id. Isomers Ic and Id were also isolated in high purity from monomer mixture I by a combination of fractional distillation and low-temperature crystallization and by dry-column chromatography.[4]

Two principal criteria used to assign specific structures to these fractions were as follows: (*1*) the NMR chemical shift of the acetal proton and splitting pattern of the hydroxyl proton and (*2*) the number and location of

TABLE IV
Characterization and Assignments of Isomers

GLC fraction[a]	Isomer assignment	Purity, wt.-%	δ of acetal proton, cps[b]	OH bands in infrared, cm^{-1} [c]		Melting point, °C
				Free	Associated	
A	Ic	100	265	Absent	3585 m	44.0–45.0
B	Ia + Ib	71 B + 21 C	285	3640 vw	3597 w	−38
C		82 C + 17 B		3640 vw	3600 w	
D	Id	100	257	3630 w	Absent	45.5–46.5

[a] According to increasing retention times.
[b] In deuterochloroform and deuterodimethyl sulfoxide.
[c] Concn, 50–60 mg/ml in carbon tetrachloride; vw = very weak, w = weak, m = medium.

hydroxyl absorption bands in the infrared spectra as summarized in Table IV.

As indicated in Table IV, the infrared spectrum of fraction A, in the nonpolar solvent used for these determinations, exhibited no free hydroxyl group absorption in the region of 3630–3640 cm^{-1}, fractions B and C contained both hydrogen-bonded and free OH bands, and fraction D had only a single band for a free hydroxyl group. This behavior and the relative retention times are consistent with the isomer assignments in Table IV based on NMR chemical shifts because of the following reasons: In a nonpolar solvent, the *cis*-dioxane isomer, Ic, will quite likely exist almost entirely in a chair conformation in which the hydroxyl group is locked in an axial position, intramolecularly hydrogen bonded to the ring oxygen atoms.[13,14] On the other hand, in a strong hydrogen-bonding solvent, such as dimethyl sulfoxide, the *cis*-isomer is expected to undergo a rapid chair–chair conformational inversion because there would be little or no steric preference for either the hydroxyl group or alkyl chain in the axial position:[15,16]

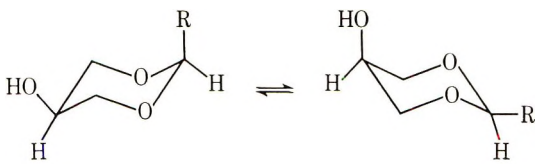

Ic

As observed, the NMR spectra of the *cis*-dioxane isomer contains a simple doublet peak for the four ring methylene protons because all four protons have identical environments as a result of the dynamic equilibration of conformations.[17,18] In contrast, the ring methylene protons of the *trans*-dioxane isomer show an extensive coupling pattern because this isomer will exist only in that chair conformation in which both substituents are equatorial. As a result, the ring protons will be locked into nonequivalent axial and equatorial positions.[6]

The particular monomer mixture I used for the preparative GLC separations was purified by distillation at a somewhat lower temperature (140°C) than that generally used for the polymerization reactions (170°C) and, apparently for this reason, had a lower ratio of five- to six-membered ring acetal isomers. That is, the ratios of dioxolane to dioxane isomers in these samples, as determined by analytical GLC, were generally in the range of 1.5:1 to 2:1 rather than the 3:1 mentioned earlier.

Polymerization reactions were carried out on individual samples of each fraction in Table IV, with calcium oxide as catalyst at temperatures of 240–280°C. Larger amounts of fractions A, B + C, and D were separated for this purpose by either fractional crystallization or dry-column chromatography.[4] Comparative analysis of the monomer fraction and the polymer obtained therefrom, by measurement of the peak area in the acetal

proton region of the NMR spectra of each, indicated that virtually no isomerization occurred during polymerization for any of the three monomer fractions. It may be concluded, therefore, that the isolation methods used completely freed the monomer fractions of acidic impurities and thereby prevented the occurrence of the acetal interchange reactions observed for the direct polymerization of samples of monomer mixture I purified by distillation only.

The polymeric products from each of the free fractions were hard solids, and all three polymers gave crystalline x-ray diffraction patterns. The thermal transition properties of each, reported in Table V, were determined by differential thermal analysis and differential scanning calorimetry. As expected, the melting points T_m and glass transition temperatures T_g of the dioxane-based polymers, Ic and Id, are much higher than those of the dioxolane-based polymers, Ia and Ib, because of the greater conformational rigidity of the six-membered ring compared to the five-membered ring.

TABLE V
Thermal Properties of Poly(ester-acetals) Obtained from Isomers of Methyl Azelaaldehydate Glycerol Acetal

Monomer isomer[a]	Molecular weight	T_g, °C[b]	T_m, °C[c]	T_{cr}, °C[d]
Ia + Ib (P)	4100	−35	54	−25
Ic	5500	6	122	40
Id (P)	6820	7	150	—
Ic (P)	5914	5	122	40

[a] (P) signifies polymer was dissolved, filtered, and precipitated.
[b] Median temperature of the endothermic baseline shift in DTA curve.
[c] Peak temperature of melting endotherm in DTA curve.
[d] Temperature of maximum rate of crystallization as determined by DTA.

Even with a wide variety of substituents, the dioxolane ring is known to be flexible and to undergo rapid conformational inversions.[13] Similarly, as expected, the *trans*-dioxane polymer, Id, had a much higher melting point than the *cis*-dioxane polymer, Ic, because of the greater symmetry and conformational stability of the *trans*-1,4-disubstituted ring compared to the *cis* ring. However, the glass temperatures of these two polymers were not as different as might be expected from ring inversion considerations.

The melting point temperature of 54°C for the dioxolane-based polymer from the Ia + Ib monomer mixture confirms the previous conclusion that both polymers obtained directly from monomer mixture I, as discussed in the previous section, owe their crystallinities entirely to the existence of blocks of ordered five-membered ring acetal repeating units. Interestingly, an all dioxolane-based poly(esteracetal) of identical structure to that from the Ia + Ib fraction, but of much lower molecular weight, has been prepared directly from isopropylidene-glycerol azelaaldehydate dimethyl acetal in this program.[5,19] However, while this polymer was found to have

an all-five-membered acetal ring repeating unit structure by NMR, it did now show a melting transition.

CONCLUSIONS

The observed identical, selective enrichment in dioxolane over dioxane repeating units in linear poly(ester-acetals) from a given mixture of geometric isomers of methyl azelaaldehydate glycerol acetal under two widely different sets of conditions (i.e., high-temperature polymerization on the one hand and prolonged room-temperature storage on the other) seems to present a thermodynamic paradox. The high-temperature reequilibration toward a higher five-membered ring acetal content is understandable from previous studies on closely related compounds which indicate that the equilibrium constant increasingly favors the dioxolane ring over the dioxane ring with increasing temperature. But while the former may still predominate to some extent, even at room temperature, it is difficult to rationalize on thermodynamic grounds the observed room temperature increase in the proportion of this isomer over that of either the original monomer or the very same sample of the polymer immediately after preparation.

TABLE VI
Isomerization of Peak A Isomer[a]

Reaction time, hr	Isomer composition, GLC peak area, %				(B + C)/(A + D)[b]
	A (Ic)	B	C	D (Id)	
0.0	96.8	2.5	0.7	0.0	0.03
2.0	24.8	37.8	32.2	5.2	2.33
4.0	22.0	41.4	32.2	4.4	2.79
6.5	16.8	44.7	34.1	4.4	3.72
31.5	16.6	42.7	33.9	6.8	3.27
77.0	15.3	43.1	34.4	7.2	3.44
168.0	15.6	42.3	34.5	7.6	3.31

[a] In benzene at room temperature, catalyzed with 1% of *p*-toluenesulfonic acid.
[b] (B + C)/(A + D) = (Ia + Ib)/(Ic + Id) is the ratio of five-membered (dioxolane) ring isomers to six-membered (dioxane) ring isomers.

An investigation was made in this study of the acid-catalyzed isomerization of monomer Ic in benzene at room temperature, and it was determined that the equilibrium ratio of dioxolane isomers, Ia and Ib, to dioxane isomers, Ic and Id, under these conditions was approximately 3.5:1 as shown by the data in Table VI. This ratio is higher than expected from NMR data on monomer mixture I (although comparable to that of related model compounds),[13,20] but it is still well below the 6:1 to 10:1 ratios observed for the polymer crystallized at room temperature. The *cis*-dioxane monomer, Ic, is thermodynamically preferred over the *trans* monomer, possibly because the former is stabilized by intramolecular hydrogen bonding, as discussed in the previous section.

One attractive rationale to explain the apparent thermodynamic paradox is that the isomer redistribution in the room temperature-crystallized polymer is not achieved by a homogeneous reequilibration of the geometric isomers but rather is caused by crystallization of the polymer itself. Possibly this polymer, which initially contained approximately 75–80% of five-membered ring acetal repeating units, was sufficiently regular to form metastable crystalline regions (which, however, were not large enough to be observed even at high magnification under a polarizing microscope). It is also possible that this copolymer may have had the structure of a block copolymer to begin with because of the higher expected reactivity of the primary hydroxyl groups in the dioxolane monomer, Ia and Ib. If these metastable crystallites of blocks of dioxolane units did exist, then isomerization of a dioxane to a dioxolane unit at the fringe of a crystallite might draw the latter unit into the crystallite; consequently, the reverse reaction of the dynamic equilibration would be prevented for that particular unit. By this mechanism, room temperature isomerization results from crystallization of the polymer and not *vice versa*. We have termed this proposed mechanism a *crystallization-induced reaction* of the polymer. Further investigations are in progress on this concept for this polymer and others.

This work was carried out in part at Fabric Research Laboratories, Inc., under contract to the U.S. Department of Agriculture as authorized by the Research and Marketing Act of 1946 and supervised by the Northern Regional Research Laboratory. Monomer and polymer synthesis and characterization studies at Fabric Research Laboratories, Inc. were performed by Mrs. Janet Nelson. Various analyses were done by Mrs. Clara McGrew, Mrs. Bonita Heaton, and Messrs. L. W. Tjarks, W. A. Boyd, and D. J. Moore of the Northern Laboratory.

The mention of firm names or trade products does not imply that they are endorsed or recommended by the Department of Agriculture over other firms or similar products not mentioned.

References

1. E. H. Pryde, D. J. Moore, H. M. Teeter, and J. C. Cowan, *J. Chem. Eng. Data* **10**, 62 (1965).
2. A. J. Showler and P. A. Darley, *Chem. Rev.*, **67**, 427 (1967).
3. E. H. Pryde, D. E. Anders, H. M. Teeter, and J. C. Cowan, *J. Org. Chem.*, **27**, 3055 (1962).
4. B. Loev and M. M. Goodman, *Chem. Ind.* (London), **1967**, 2026.
5. W. R. Miller, R. A. Awl, E. H. Pryde, and J. C. Cowan, *J. Polym. Sci., A-1*, this issue.
6. R. W. Lenz and J. P. Heeschen, *J. Polym. Sci.*, **51**, 247 (1961).
7. K. W. Buck, A. B. Foster, A. R. Perry, and J. M. Webber, *J. Chem. Soc.*, **1963**, 4171.
8. E. H. Eliel and C. A. Lukach, *J. Amer. Chem. Soc.*, **79**, 5986 (1957).
9. C. P. Rader, *J. Amer. Chem. Soc.*, **88**, 1713 (1966).
10. J. D. van Roon, *Rec. Trav. Chim.*, **48**, 173 (1929).
11. M. Trister and H. Hibbert, *Can. J. Res.*, **14B**, 415 (1937).
12. P. A. Levine and A. L. Raymond, *Ber.*, **66**, 384 (1933).
13. G. Aksnes, P. Albriktsen, and P. Juvvik, *Acta Chem. Scand.*, **19**, 920 (1965).
14. N. Baggett, M. A. Bukhari, A. B. Foster, J. Lehmann, and J. W. Webber, *J. Chem. Soc.*, **1963**, 4157.

15. J. S. Brimacombe, A. B. Foster, and A. H. Haines, *J. Chem. Soc.*, **1960**, 2582.

16. E. L. Eliel and Sr. M. C. Knoeber, *J. Amer. Chem. Soc.*, **90**, 3444 (1968).

17. N. Baggett, B. Dobinson, A. B. Foster, J. Homer, and L. F. Thomas, *Chem. Ind.* (London), **1961**, 106.

18. N. Baggett, J. S. Brimacombe, A. B. Foster, M. Stacey, and D. H. Whiffen, *J. Chem. Soc.*, **1960**, 2574.

19. W. R. Miller, E. H. Pryde, and J. C. Cowan, *J. Polym. Sci. B*, **3**, 131 (1965).

20. C. Piantadosi, C. E. Anderson, E. A. Brecht, and C. L. Yarbso, *J. Amer. Chem. Soc.*, **80**, 6613 (1958).

Received March 28, 1969
Revised July 14, 1969

JOURNAL OF POLYMER SCIENCE: PART A-1 VOL. 8, 445–450 (1970)

Vinyl Polymerization Initiated by System of Organic Halides and Tertiary Amines

TAKAYUKI OTSU, SHUZO AOKI, and KEISUKE ITAKURA
Department of Applied Chemistry, Faculty of Engineering, Osaka City University, Sumiyoshi-ku, Osaka, Japan

Synopsis

A study of the polymerization of vinyl monomers with binary systems of tertiary amines and various organic halides containing chemical bonds such as C—Cl, N—Cl, O—Cl, S—Cl, and Si—Cl has been made at 60°C. Some of the binary systems were found to be effective as radical initiator in the polymerization of methyl methacrylate. The relative initiating activities of the halides in the presence of dimethylaniline were found to be in the following order: *tert*-C_4H_9OCl > *n*-$C_4H_9NCl_2$ > $(n\text{-}C_4H_9)_2NCl \gg CH_3SiCl_3 \simeq C_6H_5SiCl_3 > C_6H_5SO_2Cl > C_6H_5CH_2Cl > C_6H_5SCl > C_6H_5PCl_2$. Styrene and vinyl acetate polymerized only with the initiator system of dimethylaniline and benzyl chloride. Tri-*n*-butylamine was less active than dimethylaniline. Pyridine and 4-vinylpyridine, in combination with some organic halides, also initiated the polymerization of methyl methacrylate. The *N*-vinylcarbazole–benzenesulfonyl chloride system, in the presence of methyl methacrylate, gave only the homopolymer of *N*-vinylcarbazole.

INTRODUCTION

In 1959, Fueno et al.[1] found that the binary systems of tertiary amines such as dimethylaniline and organic halides such as benzyl chloride initiates the radical polymerization of methyl methacrylate. In that system, a quarternary ammonium salt formed and then decomposed homolytically at the N^+—C bond to give the alkyl radical which reacted with the monomer to initiate the radical polymeriation.

In a previous study[2] the polymerization of methyl methacrylate with dimethylbenzylphenylammonium chloride was investigated by using kinetic and tracer techniques, and it was proposed that the initiating radical is produced through a redox interaction between dimethylbenzylphenylammonium chloride and dimethylaniline in which dimethylaniline produced from the dissociation of dimethylbenzylphenylammonium chloride.

Since a one electron transfer is thought to occur from the amine to the halide, the initiation mechanism may be closely related to the initiator system of metals and organic halides.[3] Recently, it was found that various organic halides containing weak chemical bonds such as C-X, O-X, N-X, S-X, and Si-X (where X represents halogen) could also serve as effective initiators of vinyl polymerization in the presence of reduced nickel.[4]

The present paper describes the results of the polymerization of vinyl monomers, especially methyl methacrylate, with the binary initiator system of the organic halides and some tertiary amines including pyridine and carbazole derivatives.

EXPERIMENTAL

Materials

Organic halides used in this study were the same reagents used in a previous work.[4] Tertiary amines and vinyl monomers were purified in the usual manners from the reagent grade materials.

Polymerization

Polymerizations were carried out in a sealed glass tube in the absence of light with shaking in a thermostat maintained at 60°C. After a given period of time, the contents of the tube were poured into a large excess of methanol to precipitate the polymer. The resulting polymer was filtered, washed with methanol, and then dried under vacuum.

Analysis of Polymer

The intrinsic viscosities $[\eta]$ of the poly(methyl methacrylates) obtained were determined in benzene at 30°C and the number-average molecular weights ($\bar{M}_n$) were calculated from the equation:[5]

$$[\eta] = 8.69 \times 10^{-5\ 0.76}\bar{M}_n$$

RESULTS AND DISCUSSION

Polymerization of Vinyl Monomers with the Initiator System of Dimethylaniline and Various Organic Halides

Table I shows the results of the polymerization of methyl methacrylate with the initiator system of dimethylaniline and various organic halides at 60°C.

Since dimethylaniline or organic halides alone did not induce the polymerization of methyl methacrylate, it is clear that an interaction of the amine and the halide in the binary system is necessary to initiate the polymerization. The relative initiating activity of the initiator system varied greatly with the nature of the halide used in the following order: *tert*-C_4H_9OCl > *n*-$C_4H_9NCl_2$ > $(n\text{-}C_4H_9)_2NCl$ ≫ CH_3SiCl_3 ≃ $C_6H_5SiCl_3$ > $C_6H_5SO_2Cl$ > $C_6H_5CH_2Cl$ > C_6H_5SCl > $C_6H_5PCl_2$.

The observed order for initiating activity of the halides does not always coincide with that obtained in the presence of reduced nickel.[4] The difference is assumed to be based on the ease of the formation of the intermediate complex and on its stability.

TABLE I
Polymerization of Methyl Methacrylate with the Binary Systems of Dimethylaniline and Various Organic Halides in Benzene at 60°C[a]

Organic halide[b]	Polymerization time, hr	Conversion, %	$\bar{M}_n \times 10^{-5}$
$C_6H_5CH_2Cl$	20	4.1	15.0
n-$C_4H_9NCl_2$	20	23.4	2.2
$(n$-$C_4H_9)_2NCl$	20	13.8	0.5
C_6H_5SCl	20	2.2	—
$C_6H_5SO_2Cl$	20	4.9	10.4
$tert$-C_4H_9OCl	9	15.7	5.7
CH_3SiCl_3	20	6.8	—
$C_6H_5SiCl_3$	20	6.8	9.1
$C_6H_5PCl_2$	20	1.6	—

[a] [Monomer] = 4.7 mole/l.; [dimethylaniline] = 0.1 mole/l.
[b] Ratio [dimethylaniline]/[halide] = 1.0.

Table II shows the results of polymerizations of styrene and vinyl acetate. The initiator systems studied showed rather weak activity for the initiation of the polymerizations of these monomers, except for the system containing benzyl chloride, which readily induced the polymerization of vinyl acetate. Similar results were observed for the initiator systems of reduced nickel and organic halides.[4]

TABLE II
Polymerizations of Styrene and Vinyl Acetate with the Binary System of Dimethylaniline and Organic Halides in Benzene at 60°C[a]

Halide	Yield of polystyrene, %	Yield of poly(vinyl acetate), %
$C_6H_5CH_2Cl$	5.5	34.0
n-$C_4H_9NCl_2$	0.6	0
$C_6H_5SO_2Cl$	Trace	Trace
$tert$-C_4H_9OCl	1.7	0
$C_6H_5SiCl_3$	0	0

[a] Polymerization conditions: [styrene] = 3.5 mole/l., [vinyl acetate] = 4.4 mole/l., [dimethylaniline] = 1.0 mole/l.; [dimethylaniline]/[halide] = 1.0; polymerization time, 40 hr.

Polymerization of Methyl Methacrylate with the Initiator System of Tri-n-butylamine, Pyridine, or Carbazole and Organic Halides

The results are shown in Table III. From Tables I and III, the system of benzyl chloride–tri-n-butylamine was found to be less effective for initiation than the benzyl chloride–dimethylaniline system. This coincides with the results reported by Fueno et al.[1] The initiator systems containing n-butylamine dichloride or benzenesulfonyl chloride, however, showed quite high activity.

TABLE III
Polymerization of Methyl Methacrylate with the Binary System of Tri-*n*-butylamine, Pyridine, or Carbazole and Organic Halides in Benzene at 60°C[a]

Halide	Polymer yield, %		
	$(n\text{-}C_4H_9)_3N$	Pyridine	Carbazole
$C_6H_5CH_2Cl$	1.4	2.9	0
$n\text{-}C_4H_9NCl_2$	10.7	6.7	1.0
$C_6H_5SO_2Cl$	12.1	2.9	1.6
$tert\text{-}C_4H_9OCl$	3.0	—	—
$C_6H_5SiCl_3$	1.6	—	—

[a] Polymerization conditions: [monomer] = 3.7 mole/l.; [amine] = 1.0 mole/l; [amine]/[halide] = 1.0; polymerization time, 20 hr.

It was also found that pyridine and carbazole in the presence of organic halides formed very weak initiator systems for the methyl methacrylate polymerization.

Fueno et al.[1] reported that the polymerization of methyl methacrylate in the presence of dimethylaniline and benzyl chloride proceeded via a radical mechanism. A similar conclusion was also obtained by the present authors[2] through kinetic and tracer studies and from product analyses.

The formation of quarternary ammonium salts from the reaction of tertiary amines with alkyl halides is known as the Menschutkin reaction. Accordingly, in an initiator system such as dimethylaniline–benzyl chloride, the formation of a quarternary anilinum salt seems to be significant for the initiation mechanism, as stated by Fueno et al.[1]

Recently Davis and Farmer[6] proposed that a charge-transfer complex is formed as an unstable intermediate through the reaction of dimethylaniline with organic halides. Since the stable quarternary anilinum salt has not been isolated from organic halides other than benzyl chloride, it might be better to consider the formation of a charge-transfer complex in the present initiator system, except for the dimethylaniline–benzyl chloride system.

Polymerizations with the Initiator Systems of 4-Vinylpyridine or N-Vinylcarbazole and Organic Halides

The results of the polymerization of methyl methacrylate with the initiator system of 4-vinylpyridine or *N*-vinylcarbazole and some organic halides are shown in Table IV.

From Table IV, it can be seen that some of these systems initiate polymerization. The polymer obtained with the 4-vinylpyridine–n-butylamine dichloride initiator system contained a considerable amount of nitrogen, which corresponds to 61 mole-% of vinylpyridine units in the polymer.

The monomer reactivity ratios in the radical copolymerization of 4-vinylpyridine (M_1) with methyl methacrylate (M_2) were reported by Tamikado[7] to be $r_1 = 0.79$, $r_2 = 0.574$ at 60°C. The composition of the present copolymer was found to agree approximately with that calculated from these

TABLE IV
Polymerization of Methyl Methacrylate with the Binary System of 4-Vinylpyridine or *N*-Vinylcarbazole and Organic Halides in Benzene at 60°C[a]

Amine	Halide	Polymer		
		Yield, %[b]	Nitrogen, %[c]	η_{sp}/c[d]
4-Vinylpyridine	$C_6H_5CH_2Cl$	0	—	—
"	n-$C_4H_9NCl_2$	35.3	8.31	—
"	$C_6H_5SO_2Cl$	0	—	—
N-Vinylcarbazole	$C_6H_5CH_2Cl$	2.1	—	—
"	n-$C_4H_9NCl_2$	7.1	0	0.263
"	$C_6H_5SO_2Cl$	29.9	7.12	0.082

[a] Polymerization conditions: [methyl methacrylate] = 3.7 mole/l, [amine] = 1.0 mole/l; [amine]/[halide] = 1.0; polymerization time, 20 hr.

[b] Calculated on the basis of total vinyl monomers used.

[c] Theoretical values of nitrogen content for poly-4-vinylpyridine and poly-*N*-vinylcarbazole were 13.33 and 7.25%, respectively.

[d] Determined in 0.5% benzene solution at 30°C.

reported values. Accordingly, it is concluded that this polymerization proceeds via a radical intermediate.

The polymerization behavior of methyl methacrylate with *N*-vinylcarbazole–halide systems was noted to be characteristic. When *n*-butylamine dichloride was used as the halide component, the resulting polymer was confirmed by nitrogen analysis and from the infrared spectrum to be the homopolymer of methyl methacrylate. Since methyl methacrylate is known to have a higher reactivity than *N*-vinylcarbazole in the radical copolymerizations,[8,9] the polymerization probably proceeds via a radical mechanism. When benzenesulfonyl chloride was used as the halide component, the homopolymer of *N*-vinylcarbazole was obtained (see Table IV). This observation is understandable if the polymerization proceeds through a cationic mechanism, because methyl methacrylate does not polymerize through a cationic mechanism. Similar conclusions were obtained in the polymerization of *N*-vinylcarbazole with various organic halides.[10]

Recently, Ellinger[11] stated that *N*-vinylcarbazole could homopolymerize in the presence of weak electron acceptors such as methyl methacrylate, and that the polymerization occurs through a charge-transfer complex intermediate.

Chapiro and Hardy[12] reported that carbon tetrachloride initiates the polymerization of *N*-vinylcarbazole according to the reaction scheme:

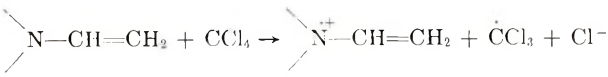

$$\text{N—CH=CH}_2 + \text{CCl}_4 \rightarrow \text{N}^{\cdot+}\text{—CH=CH}_2 + \dot{\text{C}}\text{Cl}_3 + \text{Cl}^-$$

It was assumed that the trichloromethyl radical produced might be effective in initiating the radical polymerization of *N*-vinylcarbazole.

However, Breitenbach et al.[13] suggested that the *N*-vinylcarbazole cation radical produced could initiate the cationic polymerization of *N*-vinyl-

carbazole. A similar conclusion was proposed by Okamura and his co-workers[14,15] for the cationic polymerization of *N*-vinylcarbazole with various organic electron acceptors and with cupric salts. Recently, it has been proved that some organic halides including benzenesulfonyl chloride can induce the cationic polymerization of *N*-vinylcarbazole with coloration, but *n*-butylamine dichloride is not effective.[10]

As is also shown in Table I, *n*-butylamine dichloride was more effective than benzenesulfonyl chloride for radical polymerization of methyl methacrylate in the presence of dimethylaniline. From the results mentioned above, it is assumed that the initiating species were produced through the reaction between *N*-vinylcarbazole and the halides in a manner almost similar to Chapiro's mechanism,[12] and the resulting radical cation and the heteroatom radical induce both the cationic polymerization of *N*-vinylcarbazole and the radical polymerization of methyl methacrylate. More detailed results will be described in a future publication.

References

1. T. Fueno, H. Okamoto, T. Tsuruta, and J. Furukawa, *J. Polym. Sci.*, **36**, 407 (1959).
2. T. Otsu, T. Sato, and M. Ko, *J. Polym. Sci. A-1*, in press.
3. T. Otsu and M. Yamaguchi, *J. Polym. Sci. A-1*, **6**, 3075 (1968).
4. T. Otsu, S. Aoki, M. Nishimura, M. Yamaguchi, and Y. Kusuki, *J. Polym. Sci. B*, **5**, 835 (1967).
5. T. G. Fox, J. B. Kinsinger, H. F. Mason, and E. M. Schnele, *Polymer*, **3**, 71 (1962).
6. K. M. C. Davis and M. F. Farmer, *J. Chem. Soc. B*, **1967**, 28.
7. T. Tamikado, *J. Polym. Sci.*, **43**, 489 (1960).
8. T. Alfrey, Jr., and S. L. Kapur, *J. Polym. Sci.*, **4**, 215 (1949).
9. R. Hart, *Makromol. Chem.*, **47**, 143 (1961).
10. T. Otsu, M. Ko, and T. Sato, *J. Polym. Sci.*, in press.
11. L. P. Ellinger, *Polymer*, **5**, 559 (1964).
12. A. Chapiro and G. Hardy, *J. Chim. Phys.*, **59**, 994 (1962).
13. J. W. Breitenbach and Ch. Srna, *J. Polym. Sci. B*, **1**, 263 (1963).
14. K. Tsuji, K. Takakura, M. Nishii, K. Hayashi, and S. Okamura, *Ann. Rept. Japan Assoc. Radiation Res. Polymers*, **6**, 176, 205 (1964–1965).
15. S. Tazuke, K. Nakagawa, and S. Okamura, *J. Polym. Sci. B*, **3**, 923 (1965).

Received March 13, 1969
Revised July 18, 1969

JOURNAL OF POLYMER SCIENCE: PART A-1 VOL. 8, 451–461 (1970)

Effect of Hydrogen on the γ-Radiation-Induced Polymerization of Ethylene

HIROSHI MITSUI, FUMIO HOSOI, and TSUTOMU KAGIYA,
Japan Atomic Energy Research Institute,
Takasaki Radiation Chemistry Research Establishment,
Takasaki, Gunma, Japan

Synopsis

The effects of hydrogen on the γ-radiation-induced polymerization of ethylene were studied from the viewpoint of polymer structure and kinetics. All experiments were carried out at 30°C. In the polymerization of ethylene containing 21.6% hydrogen, the solid polymer was obtained as a main product, while no liquid product was found. There was no difference in hydrogen contents before and after the irradiation; and acetylene, ethane, butane, and butene-1 were found as gaseous products. The polymer yield increased almost proportionally with dose rate in the presence of 8.0% hydrogen; on the other hand the molecular weight was independent of dose rate. At hydrogen contents of 0–8%, the polymerization rate increased with reaction time and decreased with hydrogen content. The molecular weight also increased with the time, and the extent of the increment decreased with the time and hydrogen content. The number of moles of polymer chain increased proportionally with the reaction time and increased linearly with hydrogen concentration. These results were analyzed by using a graphical evaluation method for kinetics, and the effects of hydrogen on the each elementary step in the polymerization were discussed.

INTRODUCTION

It has been reported that hydrogen and acetylene are the main gaseous products in the γ-radiation-induced polymerization of ethylene under high pressure.[1,2] In the previous papers,[3,4] we reported on the roles of acetylene in the polymerization from the viewpoint of the gaseous products, the polymer structure, and the kinetics. There is a paucity of data on the effects of hydrogen on the polymerization.

The purpose of this paper is to determine the effects of hydrogen on the γ-radiation-induced polymerization of ethylene from the viewpoint of gaseous products and kinetics.

EXPERIMENTAL

The reaction apparatus, ethylene, irradiation facilities, and experimental procedure, except that the premixed ethylene–hydrogen mixture was used, were the same as described in previous paper.[3] Commercially available hydrogen (99.99% pure) was used. The experiments, except for one ex-

periment, were carried out under a pressure of 400 kg/cm², the temperature was 30°C, the dose rates were 2.7×10^4 and 1.1×10^5 rad/hr, and the hydrogen content was 0–8.0%.

RESULTS AND DISCUSSION

Polymer Structure and Gaseous Products

In order to elucidate the effects of hydrogen on the polymer structure and gaseous products, the polymerization was carried out with ethylene containing 26.1% hydrogen under an initial pressure of 330 kg/cm² at 30°C with a dose rate of 1.1×10^5 rad/hr. A solid polymer (6.99 g) with a molecular weight of 6600 was formed in the 100-ml reactor as the main product after 40 hr; no liquid product was obtained. The structural changes in the polymer were not observed in the infrared spectrum, unlike the polymer formed by the polymerization of pure ethylene.

TABLE I
Gaseous Products in the γ-Radiation-Induced Polymerization of Ethylene Containing Hydrogen[a]

	Feed gas		Residual gas	
	ppm, $\times 10^4$	mole/l., $\times 10^{-5}$	ppm, $\times 10^4$	mole/l., $\times 10^5$
H_2	26.1	4.37	30.3	4.32
CH_4	11	19	15	22
C_2H_2	0	0	316	450
C_2H_6	46	76	124	176
C_4H_{10}	0	0	289	467
C_4H_8-1	0	0	328	412

[a] Reaction conditions: initial pressure, 330 kg/cm²; final pressure, 290 kg/cm²; temperature, 30°C; time, 40 hr; dose rate, 1.1×10^5 rad/hr; reactor volume, 100 ml.

As can be seen in Table I, there is no marked difference in hydrogen and methane contents before and after the irradiation. The rate of acetylene formation in this polymerization is about 11×10^{-5} mole/l./hr and that in the polymerization of pure ethylene under the same conditions can be calculated to be about 8.5×10^{-5} mole/l./hr by using the empirical equation given in a previous paper.[2] The fact that the two values are almost equal indicates the reaction of formation of acetylene proposed in previous paper[2] is not affected by addition of hydrogen. In addition, ethane, butane, and butene-1 are also formed, and these are considered to be produced by the reaction between the radicals and/or intermediates formed from hydrogen and ethylene under γ-irradiation.

Effects of Dose Rate and Reaction Time

Table II shows the results of the experiments at 2.7×10^4 and 1.1×10^5 rad/hr. The polymer yield increases almost proportionally with dose rate;

TABLE II
Effect of Dose Rate on Polymer Yield and Molecular Weight[a]

Dose rate $\times 10^{-4}$, rad/hr	Reaction time, hr	Polymer yield, g/l.	Molecular weight $\times 10^{-4}$
2.7	2	2.66	1.64
2.7	3	4.99	2.04
11.0	2	12.20	1.65
11.0	3	19.65	1.80

[a] Reaction conditions: pressure, 400 kg/cm²; temperature, 30°C; hydrogen content, 8.0%; reactor volume, 100 ml.

on the other hand the molecular weight is almost independent of dose rate. This indicates that the polymerization of ethylene containing hydrogen does not follow a square-root law for a stationary-state polymerization with bimolecular termination.

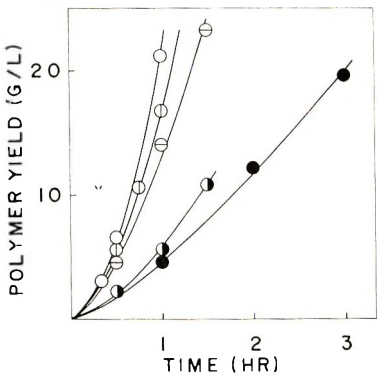

Fig. 1. Polymer yield vs. reaction time at various hydrogen contents: (○) 0.00; (◐) 0.18%; (⊖) 1.00%; (◑) 5.52%; and (●) 8.00%. Reaction pressure, 400 kg/cm²; temperature, 30°C; dose rate, 1.1 × 10⁵ rad/hr; reactor volume, 100 ml.

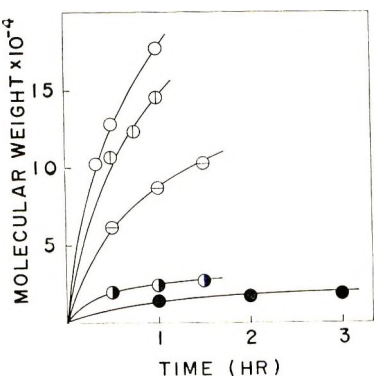

Fig. 2. Molecular weight vs. reaction time. Reaction conditions same as given for Fig. 1.

TABLE III
Effect of Reaction Time on Polymer Yield and Molecular Weight[a]

Hydrogen content, %	Reaction time, hr	Polymer yield, g/l.	Molecular weight $\times 10^{-4}$	Polymer chains $\times 10^4$, mole/l.
0.00	0.33	3.08	10.3	0.30
	0.5	6.55	12.8	0.51
	1.0	21.17	17.7	1.20
0.18	0.5	5.65	10.7	0.53
	0.75	10.57	12.3	0.86
	1.0	16.78	14.5	1.16
1.00	0.5	4.58	6.2	0.74
	1.0	14.01	8.7	1.61
	1.5	23.31	10.3	2.26
5.52	0.5	2.23	1.95	1.14
	1.0	5.64	2.4	2.33
	1.5	10.86	2.7	4.05
8.00	1.0	4.67	1.4	3.38
	2.0	12.20	1.65	7.39
	3.0	19.65	1.8	10.92

[a] Reaction conditions: pressure, 400 kg/cm^2; temperature, 30°C; dose rate, 1.1 $\times$ 10^5 rad/hr; reactor volume, 100 ml.

The results of the experiments which were carried out at various reaction times are summarized in Table III. Figure 1 shows that the rate of polymerization is accelerated, since the plot of polymer yield versus reaction time is a concave, upward curve in all experiments, and that the rate decreases with increasing hydrogen content in whole period of the reaction. As may be seen in Figure 2, the molecular weight increases with time and decreases with increasing hydrogen content.

Figure 3 shows the number of moles of polymer chain N_p (defined as the ratio of the polymer yield to the molecular weight) increases proportionally with the reaction time, which is considered to mean the rate of transfer is

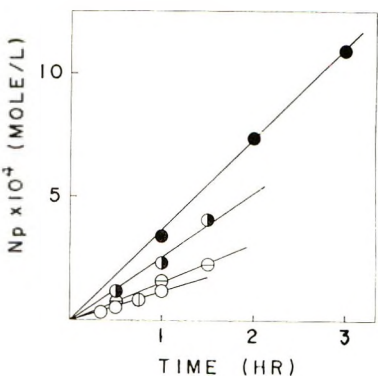

Fig. 3. Number of moles of polymer chain N_p vs. reaction time. Reaction conditions same as given for Fig. 1.

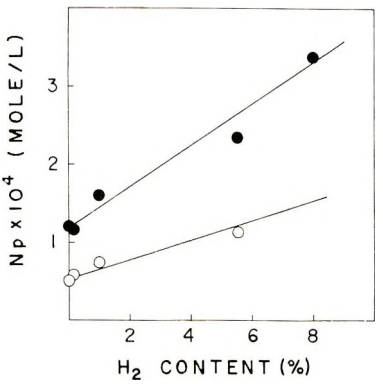

Fig. 4. Number of moles of polymer chain N_p vs. hydrogen concentration at various reaction times: (○) 0.5 hr; (●) 1.0 hr. Reaction pressure, 400 kg/cm²; temperature, 30°C; dose rate, 1.1×10^5 rad/hr; reactor volume, 100 ml.

negligible (small or considerably smaller than that of initiation). The same result has been already reported in the polymerization of pure ethylene.[5] Accordingly, since the number of moles of polymer chain increases linearly with hydrogen concentration (Fig. 4), the rate of initiation is considered to increase linearly with hydrogen concentration.

The effects of the reaction conditions, such as dose rate and reaction time, on the polymer yield, the molecular weight, and the number of moles of polymer chain are very similar to those in the polymerization of pure ethylene at room temperature.[5,6] Furthermore, the effects of the addition of hydrogen on the polymer yield and the molecular weight are similar to those observed in the polymerization of ethylene containing acetylene.[4]

Kinetics

Since the polymerization in all series was carried out under continuous γ-irradiation, the initiation reaction occurs continuously. In addition, both the rate of polymerization and the molecular weight increase with the reaction time. According to the classification from a kinetic point of view proposed by Kagiya et al.,[7] the polymerization of ethylene containing hydrogen is classified as a non-stationary, successive polymerization with a slow initiation. Accordingly, the kinetic constants of this system can be obtained by using the graphical evaluation method for kinetics proposed by Kagiya et al.[8]

Rate of Polymerization and Degree of Polymerization. As described above, since the similar kinetical features to the polymerization of pure ethylene and of ethylene containing acetylene were observed in the polymerization of ethylene containing hydrogen, the reaction mechanism given in eqs. (1)–(7) is assumed for this polymerization.

Initiation:

$$E \overset{k_{iE}}{\rightsquigarrow} R_1\cdot$$

with

$$R_{iE} = k_{iE} I \rho_E \tag{1}$$

and

$$H_y \overset{k_{iH}}{\underset{E}{\rightsquigarrow}} R_i\cdot$$

with

$$R_{iH} = k_{iH} I \rho_H \tag{2}$$

Ethylene excitation:

$$E \rightleftharpoons E^*$$

$$E + E^* \overset{K_e}{\rightleftharpoons} E_2^*$$

with

$$f_{E_2}^* = K_e f_E^2 \tag{3}$$

Propagation:

$$R_n\cdot + E_2^* \xrightarrow{k_p} R\cdot_{n+1} + E^*$$

with

$$R_p = k_p f_{E_2}^* [R\cdot] = k_p K_e f_E^2 [R\cdot] \tag{4}$$

Coordination:

$$R_n\cdot + H_y \overset{K_H}{\rightleftharpoons} R_n\ldots H_y$$

with

$$[R_n\ldots H_y] = K_H f_H [R\cdot] \tag{5}$$

Termination:

$$R_n\cdot + Z \xrightarrow{k_t} P_n$$

with

$$R_t = k_t [Z][R\cdot] \tag{6}$$

Transfer:

$$R_n\cdot + Y \xrightarrow{k_{tr}} P_n + Y\cdot$$

with

$$R_{tr} = k_{tr} [Y][R\cdot] \tag{7}$$

In this scheme, E is ethylene; H_y is hydrogen; $R_i\cdot$ is the initiating species; E^* is the excited ethylene; E_2^* is the excited ethylene dimer; $R_n\cdot$ is the active polymer chain composed of n monomers; $R_n\ldots H_y$ is the coordination product of hydrogen to $R_n\cdot$; Z is the substance by which $R_n\cdot$ is deactivated in the polymerization; P_n is the dead polymer composed of n

monomers; Y is the substance to which the activity of $R_n\cdot$ is transferred; $R_{i\mathrm{E}}$, $R_{i\mathrm{H}}$, R_p, R_t, and R_{tr} are the rates of initiation from ethylene, initiation from hydrogen, propagation, termination, and transfer, respectively, and $k_{i\mathrm{E}}$, $k_{i\mathrm{H}}$, k_p, k_t, and k_{tr} are the rate constants of these reactions, respectively; I is dose rate; ρ_{E} and ρ_{H} are the densities of ethylene and hydrogen, respectively; $f_{\mathrm{E}_2}{}^*$, f_{E}, and f_{H} are the fugacities of excited ethylene dimer, ethylene, and hydrogen, respectively; K_e is the equilibrium constant of the reaction between ethylene and excited ethylene to form the excited ethylene dimer; $[\mathrm{R}\cdot]$ is the total concentration of all the active polymer chains, irrespective of size (i.e., $\sum_{n=1}^{\infty} {}_2[\mathrm{R}_n]\cdot$); K_{H} is the equilibrium constant of the reaction between $\mathrm{R}_n\cdot$ and hydrogen to form the coordination product; $[\mathrm{R}_n\ldots\mathrm{H}_y]$, $[\mathrm{Z}]$, and $[\mathrm{Y}]$ are the concentrations of these substances, respectively.

Since a linear relation was observed between the number of moles of polymer chain and the hydrogen content, the polymer-linking reaction which was proposed in the polymerization of ethylene containing actylene[4] is not assumed. If the additivity of the rates of initiation from ethylene and from hydrogen is realized, the overall rate of initiation R_i is represented by eq. (8).

$$R_i = R_{i\mathrm{E}} + R_{i\mathrm{H}} = k_{i\mathrm{E}} I \rho_{\mathrm{E}} (1 + k_{i\mathrm{H}}\rho_{\mathrm{H}}/k_{i\mathrm{E}}\rho_{\mathrm{E}}) \tag{8}$$

The reaction pressure in the experiments listed in Table III remained essentially constant throughout the polymerization because of the low conversion (below 5%) of monomers, and no marked difference in hydrogen contents before and after the irradiation was observed. Accordingly, it seems reasonable to assume that the density and fugacity of ethylene and those of hydrogen are constant during the course of the polymerization.

On the basis of these considerations, eqs. (9) and (10) are derived from eqs. (4)–(8) by the same manner as previously.[4]

$$R/M_p \simeq R_p/M_p = [R_i k_p K_e f_{\mathrm{E}}{}^2/(1 + K_{\mathrm{H}} f_{\mathrm{H}})](t/M_p) - k_t[\mathrm{Z}]/(1 + K_{\mathrm{H}} f_{\mathrm{H}}) \tag{9}$$

$$1/\bar{P}_n = R_i(t/M_p) + k_{tr}[\mathrm{Y}]/k_p K_e f_{\mathrm{E}}{}^2 \tag{10}$$

In eqs. (9) and (10), R represents the overall rate of polymerization; M_p, the polymer yield at time t; and $\bar{P}_n$, the degree of polymerization.

Distinct linear relations exist between R_p/M_p and t/M_p and between $1/\bar{P}_n$ and t/M_p at every level of hydrogen content, as indicated in Figures 5 and 6. The slope of the line s and the intercept on the ordinate y in Figure 4 may be represented by

$$s = R_i k_p K_e f_{\mathrm{E}}{}^2/(1 + K_{\mathrm{H}} f_{\mathrm{H}}) \tag{11}$$

$$y = -k_t[\mathrm{Z}]/(1 + K_{\mathrm{H}} f_{\mathrm{H}}) \tag{12}$$

In Figure 6, the slope of the line represents the value of the overall rate of initiation. The result that the intercepts on the ordinate in Figure 6, which

is the value of $k_{tr}[Y]/k_pK_ef_E^2$, is equal in all series of experiments indicates that the transfer is not affected by adding hydrogen, because the ethylene fugacity is considered to be almost constant in the range of 0–8% hydrogen content.

Effects of Hydrogen on the Initiation. As can be seen in Figure 7, a linear relation is obtained between the rate of initiation and the ratio of the density of hydrogen to that of ethylene. This result is consistent with the result obtained from Figure 4, because the density of ethylene is considered

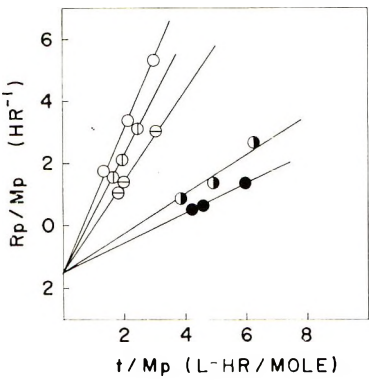

Fig. 5. R_p/M_p vs. t/M_p. Reaction conditions same as given for Fig. 1.

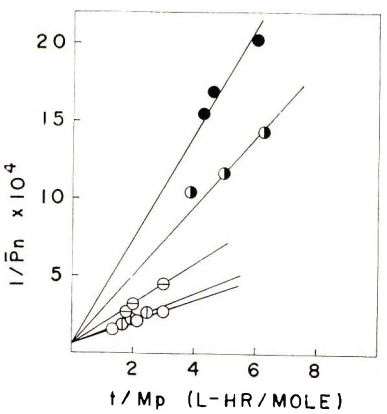

Fig. 6. $1/\bar{P}_n$ vs. t/M_p. Reaction conditions same as given for Fig. 1.

to be almost constant in the range of 0–8% hydrogen content. The value of k_{iH}/k_{iE} calculated from the slope of the line by using eq. (8) is about 43, which means the rate of initiation from hydrogen is about 43 times that from ethylene.

The fact that the formation of acetylene is not affected by adding hydrogen leads to the conclusion that the initiation from ethylene proposed before[2] is not influenced by hydrogen. Accordingly, although the mechanism of extremely rapid initiation from hydrogen is not clear in detail, the

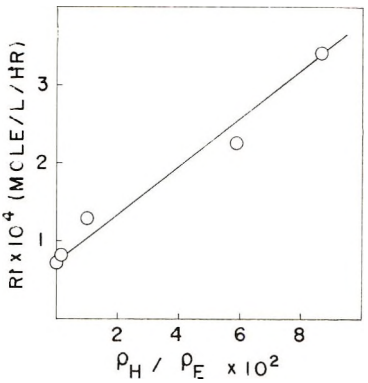

Fig. 7. Overall rate of initiation R_i vs. ratio of the density of hydrogen to that of ethylene ρ_H/ρ_E. Reaction pressure, 400 kg/cm²; temperature, 30°C; dose rate, 1.1 × 10^5 rad/hr; reactor volume, 100 ml.

initiation can be considered to be brought about by following mechanism in connection with the mechanism of catalytic hydrogenation of ethylene.

$$S \rightsquigarrow S^* \tag{13}$$

$$H_2 + S^* \rightleftharpoons (H_2 \ldots S)^* \tag{14}$$

$$(H_2 \ldots S)^* \rightarrow 2H\cdot + S \tag{15}$$

$$H\cdot + C_2H_4 \rightarrow C_2H_5\cdot \tag{16}$$

Here S represents the substance which acts as a catalyst. Hydrogen is adsorbed by the excited substance S* having sufficient energy to dissociate the H–H bond [eqs. (13) and (14)], and is released as a hydrogen radical [eq. (15)]. The initiating species $R_1\cdot$ ($C_2H_5\cdot$ in this scheme) is formed by the addition of ethylene to the radical [eq. (16)]. The initiating species may be directly formed by another mechanism in which ethylene is adsorbed by the excited substance adsorbed hydrogen by reaction (14) and is released as ethyl radicals.

$$(H_2 \ldots S)^* + 2C_2H_4 \rightarrow (H_2 \ldots S \ldots 2C_2H_4)^* \tag{17}$$

$$(H_2 \ldots S \ldots 2C_2H_4)^* \rightarrow 2C_2H_5\cdot + S \tag{18}$$

Effects of Hydrogen on the Propagation. When the ratio of the value of the slope of the line in Figure 5 to that in Figure 6 is given as s', s' is represented by eq. (19):

$$s' = s/R_i = k_p K_e f_E^2/(1 + K_H f_H) \tag{19}$$

Hence:

$$f_E^2/s' = 1/k_p K_e + K_H f_H/k_p K_e \tag{20}$$

As shown in Figure 8, a linear relation is obtained between the values of f_E^2/s' and hydrogen fugacity.

From this result, it seems reasonable that the rate of addition reaction of ethylene to $R_n\cdot$ [eq. (4)], that is, the absolute rate of propagation, is not

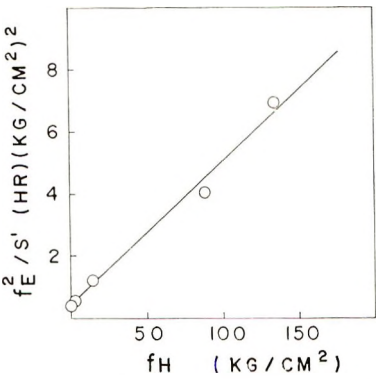

Fig. 8. f_E^2/s' vs. hydrogen fugacity f_H. Reaction conditions same as given for Fig. 7.

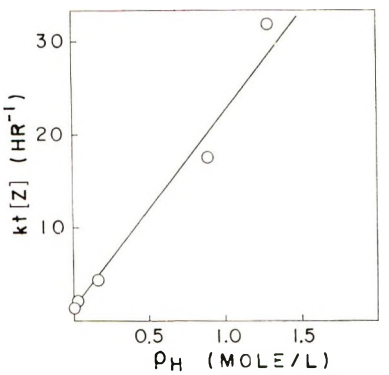

Fig. 9. $k_t[Z]$ vs. hydrogen density ρ_H. Reaction conditions same as given for Fig. 7.

affected by adding hydrogen, because the value of k_pK_e is considered to remain unchanged; apparent rate of propagation thus is decreased by the decrease of concentration of $R_n\cdot$ caused by the coordination of hydrogen itself and/or of the radiolysis intermediate or product (produced proportionally to hydrogen fugacity in the system) to the active polymer chain end.

Effects of Hydrogen on the Termination. From eqs. (11) and (12), the value of $k_t[Z]$ is given as:

$$k_t[\mathrm{Z}] = -R_i k_p K_e f_E^2 y/s \tag{21}$$

where R_i is obtained from the slope of the line in Figure 6 and the value of k_pK_e is also obtained from the intercept on the ordinate of the line in Figure 8. Figure 9 shows that a linear relation exists between the value of $k_t[\mathrm{Z}]$ obtained from eq. (21) and hydrogen density. This indicates that the termination is independently caused by terminator Z, which is observed in the polymerization of pure ethylene, and by hydrogen, and that the termination by Z is not affected by adding hydrogen. The overall rate of termination R_t, therefore, can be represented as:

$$R_t = R_{tZ} + R_{tH} \tag{22}$$

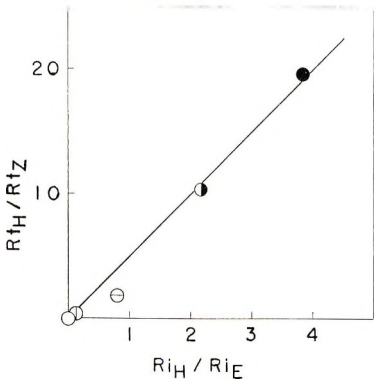

Fig. 10. R_{tH}/R_{tZ} vs. R_{iH}/R_{iE} at various hydrogen contents: (○) 0.00; (◔) 0.18%; (⊖) 1.00%; (◑) 5.52%; (●) 8.00%. Reaction pressure, 400 kg/cm²; temperature, 30°C; dose rate, 1.1×10^5; reactor volume, 100 ml.

where R_{tZ} and R_{tH} represent the rates of termination by Z and by hydrogen, respectively. In order to compare the contribution of hydrogen to the initiation and termination, the relation between R_{tH}/R_{tZ} and R_{iH}/R_{iE} at various hydrogen contents was obtained and is shown in Figure 10. The fact that the slope of the line is about 5 means the contribution of hydrogen to termination is much greater than that to initiation.

From the fact that the rate of termination by hydrogen is proportional to the hydrogen density and the low molecular weight hydrocarbons are observed in the polymerization of ethylene containing 26.1% hydrogen, the termination by hydrogen can be considered to be brought about by the primary species such as H· and C_2H_5· produced by reactions (13)–(18).

References

1. H. Mitsui, S. Machi, M. Hagiwara, and T. Kagiya, *J. Polym. Sci. B*, **4**, 881 (1966).
2. H. Mitsui, S. Machi, M. Hagiwara, and T. Kagiya, *J. Polym. Sci. A-1*, **5**, 1073 (1967).
3. H. Mitsui, F. Hosoi, M. Hagiwara, and T. Kagiya, *J. Polym. Sci. A-1*, **6**, 2881 (1968).
4. H. Mitsui, F. Hosoi, and T. Kagiya, *J. Polym. Sci. A-1*, in press.
5. S. Machi, M. Hagiwara, M. Gotoda, and T. Kagiya, *J. Polym. Sci. A-1*, **4**, 1517 (1966).
6. S. Machi, M. Hagiwara, M. Gotoda, and T. Kagiya, *Bull. Chem. Soc. Japan*, **39**, 675 (1966).
7. T. Kagiya, M. Izu, and K. Fukui, *Bull. Chem. Soc. Japan*, **40**, 1045 (1967).
8. T. Kagiya, M. Izu, S. Machi, and K. Fukui, *Bull. Chem. Soc. Japan*, **40**, 1049 (1967).

Received March 21, 1969
Revised July 22, 1969

JOURNAL OF POLYMER SCIENCE: PART A-1 VOL. 8, 463–482 (1970)

Polymerization of Coordinated Monomers. IV. Copolymerization of Methyl Methacrylate– and Methacrylonitrile–Lewis Acid Complexes with Styrene

TADASHI IKEGAMI and HIDEFUMI HIRAI,
Department of Industrial Chemistry, Faculty of Engineering, University of Tokyo, Hongo, Bunkyo-ku, Tokyo, Japan

Synopsis

Complexes of methyl methacrylate and methacrylonitrile with Lewis acids ($SnCl_4$, $AlCl_3$, and BF_3) were copolymerized with styrene at $-75°C$ under irradiation with a high-pressure mercury lamp in toluene solution. The resulting copolymers consisted of equimolar amount of methyl methacrylate or methacrylonitrile and styrene, regardless of the molar ratio of monomers in the feed. NMR spectroscopy showed the copolymers to have an alternate sequence. The tacticities of the copolymers varied with the complex species: the copolymer from the $SnCl_4$ complex system had a higher cosyndiotacticity, while those from the $AlCl_3$ and the BF_3 complex systems showed coisotacticity to predominate over cosyndiotacticity. NMR spectroscopic investigation of the copolymerization system indicated the presence of a charge-transfer complex between the styrene and the methyl methacrylate coordinated to $SnCl_4$. The concentration of the charge-transfer complex was estimated to be about 30% of monomer pairs at $-78°C$ at a 1:1 molar ratio of feed. The growing end radicals were identified as a methyl methacrylate radical for the $AlCl_3$ complex–styrene system and a styrene radical for the $SnCl_4$ complex–styrene system by the measurement of the ESR spectra of the copolymerization systems under or after irradiation with a high-pressure mercury lamp. The tacticity of the resulting polymer appears to be controlled by the structure of the charge transfer complex. In the case of the $SnCl_4$ complex a certain interaction of $SnCl_4$ with the growing end radical seems to be a factor controlling the polymer structure. These copolymerizations can be explained by an alternating charge-transfer complex copolymerization scheme.

INTRODUCTION

Many alternate copolymerization systems have been reported for such systems as maleic anhydride–styrene and its derivatives.[1,2] In these copolymerization systems the formation of a charge-transfer complex between the monomers was detected by ultraviolet spectroscopy.[3,4] It has been proposed that regulation of the alternation in the copolymerization was due to the polymerization of the charge-transfer complex.[5,6]

Acrylic monomers do not copolymerize alternately with styrene, whereas the complexes of acrylic monomers with $ZnCl_2$ or alkyl aluminum halide copolymerized to give alternating copolymers.[7–9] In our previous paper,[9] the presence of a charge-transfer complex of styrene with the vinyl mono-

mer (acrylonitrile, methacrylonitrile, or methyl methacrylate) coordinated to $ZnCl_2$ was established by ultraviolet spectroscopy in the alternating copolymerization of styrene with the complexes of vinyl monomers with $ZnCl_2$. Although the constant for formation of the charge-transfer complex was small as in the ordinary alternate copolymerization system, we concluded that the alternation of the copolymerization was controlled by the charge-transfer complex. It seems plausible that the coordination of the lone-pair electrons on the carbonyl or cyano group makes the double bond more electron-deficient and enables it to form the charge-transfer complex with styrene. Other complexes having a similar type of coordination bond will also form a charge-transfer complex with styrene. The bond strength of this charge-transfer complex will depend on the Lewis acid used. These complexes will copolymerize alternately with styrene if appropriately initiated.

In the present study, the complexes of various Lewis acids with acrylic monomers (methyl methacrylate and methacrylonitrile) were copolymerized with styrene. The copolymerizations were carried out at $-75°C$ in toluene solution by irradiation with a high-pressure mercury lamp. The structure and tacticity of the copolymer were determined by NMR for the methyl methacrylate–styrene copolymer. The NMR spectra of the polymerization system were recorded to detect the charge-transfer complex. The species and the structure of growing end were studied by ESR spectroscopy. It was found that any complex gave an alternating copolymer with the appropriate initiation and that the tacticities of the resulting copolymers and the species of the growing end were characteristic of the species of Lewis acid. On the basis of these findings, the participation of the Lewis acid in the propagation step of copolymerization was discussed.

EXPERIMENTAL

Materials

Monomers were purified by the usual procedures. Aluminum trichloride and stannic chloride were purified by sublimation and distillation, respectively. Boron trifluride was prepared from sodium fluoroborate and boron oxide.

Complex

A Lewis acid was added to an excess of monomer. The resulting clear solution was cooled. The complex was obtained upon the removal of the excess monomer by evaporation. The complex solution for copolymerization was made by mixing monomer and Lewis acid in toluene.

Copolymerization

A solution of styrene (St) in toluene was added to a solution of the complex in toluene in an ampoule cooled to $-78°C$ in a nitrogen atmosphere.

The mixture was then frozen and evacuated. After repeated freezing and evacuating (three times), the ampoule was sealed. The ampoule was placed in a Dewar flask at −75°C. The polymerization was effected by ultraviolet irradiation from a Ushio Denki HB500/B and a Ricoh Ltd., PHI-TC high-pressure mercury lamp. Light of wavelength shorter than 300 mμ, which is known to accelerate the homopolymerization of the methyl methacrylate (MMA) complexes, was cut off by using a Pyrex glass ampoule.

Spectral Measurement of Copolymerization System

The copolymerization system was studied by both NMR and ESR spectroscopy. The NMR spectra were recorded at −70 to 25°C on a Japan Electron Optics Laboratory Model C-60 spectrometer at 60 Mcps. The ESR spectra were measured on the copolymerization system irradiated with ultraviolet rays at −196°C and at higher temperatures in order to examine the initiation process, and on the system under the irradiation at −100°C, just below the melting point of the system for the purpose of studying the propagation step. A Japan Electron Optics Laboratory Model JES-3BSX and a Varian Associates Model 4502 spectrometer were used. The ultraviolet rays were filtered so as to pass only rays of wavelengths longer than 300 mμ.

Composition and Tacticity of Copolymer

The composition of the copolymer was determined by NMR spectroscopy for MMA–St copolymers and by elemental analysis for MAN-St copolymers. The structure and the tacticity of copolymers were determined on the copolymer of MMA with St as follows. A 10% solution of the copolymer in carbon tetrachloride was subjected to the NMR spectroscopy. The proportion of three methoxy proton chemical shifts (coisotacticity, heterotacticity, and cosyndiotacticity) were estimated from the peak intensities.

RESULTS AND DISCUSSION

Properties of Complexes

All the complexes are hygroscopic and soluble in toluene at −78°C. The infrared spectra of the complexes showed that the absorption band of the cyano group was shifted to a higher frequency and that of the carbonyl group to a lower frequency (Table I). As reported previously,[10,11] these complexes are formed by coordination of the lone electron pair to the metal atom. In the NMR spectra of the complexes (Table II), the chemical shifts of the protons in the monomer moved to lower magnetic fields. This suggests a decrease in the electron density of the C=C double bond, which may be ascribed to the withdrawal of electrons by the Lewis acid. The complexes of AN showed poorer solubility in toluene.

TABLE I
Changes in the Infrared Frequency of Monomers on Complex Formation

Complex composition[a]	Infrared shift[b] $\Delta\nu$(C≡N), cm^{-1}	$\Delta\nu$(C=O), cm^{-1}	$\Delta\nu$(C=C), cm^{-1}
MMA–$SnCl_4$, 1.06		−20, −65, −98	−3
MMA_2–$SnCl_4$, 2.09		−20, −66, −100	−3
MMA–$AlCl_3$, 1.10		−75	−3
MMA–BF_3, 1.03		−45, −75	−3
MAN_2–$SnCl_4$, 2.01	+35		−5

[a] Molar ratio of monomer to Lewis acid.

[b] MMA: ν(C=O at 1723 cm^{-1}, ν(C=C) at 1635 cm^{-1}; MAN: ν(C≡N) at 2230 cm^{-1}, ν(C=C) at 1623 cm^{-1}.

TABLE II
Charges in Proton Chemical Shift of Monomer on Complex Formation

Complex	Chemical shift, ppm[a] $\Delta\tau(\alpha\text{-}CH_3)$	$\Delta\tau(OCH_3)$	$\Delta\tau(H_c)$[b]	$\Delta\tau(H_t)$[b]
$SnCl_4$ (MMA)	−0.21	−0.43	−0.35	−0.26
$SnCl_4(MMA)_2$	−0.05	−0.28	−0.12	−0.05
$AlCl_3$(MMA)	−0.02	−0.42	−0.50	−0.60
BF_3(MMA)	−0.14	−0.47	−0.43	−0.15
$SnCl_4(MAN)_2$	−0.05		−0.30	−0.30

[a] Chemical shift τ referred to tetramethylsilane (τ = 10.00 ppm) at 60 Mcps. For pure monomers, MMA, $\tau(\alpha\text{-}CH_3)$ at 8.13 ppm, $\tau(OCH_3)$ at 6.30 ppm, $\tau(H_c)$ at 4.45 ppm, and $\tau(H_t)$ at 3.96 ppm; MAN, $\tau(\alpha\text{-}CH_3)$ at 8.00 ppm, $\tau(H_c)$ at 4.18 ppm and $\tau(H_t)$ at 4.29 ppm.

[b] H_c and H_t, are vinyl protons *cis* and *trans* to the cyano or ester group, respectively.

Copolymerization of Complexes

The results of the copolymerization are summarized in Tables III and IV and Figures 1 and 2.

The complexes with $SnCl_4$ gave copolymer only at −75°C. No cationic polymerization was observed. Figure 1 shows the copolymerization diagram for the MMA–$SnCl_4$ and the MAN–$SnCl_4$ complexes. Every complex affords the 1:1 copolymer of St and the comonomer over a wide range of monomer feed ratios. The 1:1:1 MMA–propionitrile(PN)–$SnCl_4$ complex gave a higher conversion than other complexes. The coordination bond between MMA and $SnCl_4$ would be affected by the coordination of PN so that the interaction between St and MMA coordinated to $SnCl_4$ might be easier.

In the case of $AlCl_3$–MMA complex, a cationic polymerization of St was found to occur in addition to the copolymerization. Upon removing the St homopolymer by washing with cyclohexane, a copolymer consisting of St and MMA in a molar ratio of 1:1 was obtained. Figure 2 shows the copolymerization diagram for the $AlCl_3$–MMA complex. A 1:1 copolymer

TABLE III
Copolymerization of the $SnCl_4$ Complexes with Styrene[a]

Complex	Styrene in monomer feed $[m_1]$, mole-%	Time, hr	Conversion, %	St in copolymer, mole-%	Tacticity[b]		
					X, %	*Y*, %	*Z*, %
1:1 MMA–$SnCl_4$ complex	10	3.0	2.5	43.3	35	58	7
	33	5.0	1.5	41.4	35	46	19
	50	4.0	3.5	59.0	31	51	18
	50[c]	3.0	16.6	50.0	19	46	35
2:1 MMA–$SnCl_4$ complex	10	2.5	4.5	48.0	45	55	0
	20	2.5	7.0	44.5	34	57	9
	50	2.5	2.4	47.5	39	61	0
	80	2.5	3.2	53.6	38	62	0
	90	2.5	2.0	49.0	40	54	6
2:1 MAN–$SnCl_4$ complex	20	3.0	3.3	45.8			
	80	3.0	8.7	44.3			

[a] The concentration of monomers in polymerization solution was 25 mole-%. The reaction temperature was −75°C.

[b] Tacticity was determined by NMR spectroscopy according to the method of Itoh and Yamashita.[12] *X*, cosyndiotacticity at 6.5 ppm; *Y*, heterotacticity at 7.0 ppm; *Z*, coisotacticity at 7.6 ppm.

[c] The 1:1:1 MMA–PN–$SnCl_4$ complex was used.

TABLE IV
Copolymerization of the MMA–$AlCl_3$ and MMA–BF_3 Complexes with Styrene[a]

Complex	$[m_1]$, mole-%	Time, min	Conversion, %	St in copolymer, mole-%	Tacticity[b] X, %	Y, %	Z, %
MMA–$AlCl_3$ complex	10	90	22.0	45.8	18	40	42
	20	90	38.0	53.9	19	45	36
	50	90	35.6	52.2	20	44	36
	80	90	7.4	51.8	21	45	34
	90	90	19.0	50.0	21	45	32
MMA–BF_3 complex	70	120	1.9	54.5	26	40	34

[a] The concentration of monomer was 25 mole-% in toluene. The reaction temperature was −75°C.

[b] Tacticity was determined by NMR spectroscopy. *X*, cosyndiotacticity at 6.5 ppm; *Y*, heterotacticity at 7.0 ppm; *Z*, coisotacticity at 7.6 ppm.

was also obtained from the complex of MMA with BF_3, in admixture with a large amount of polystyrene.

The MMA–$TiCl_4$ complex changed its color from yellow to brownish violet upon irradiation with ultraviolet rays at −75°C and gave only a trace of polymer. It is supposed that the reduction of Ti atom from the IV to III valence state is accelerated by the ultraviolet irradiation and the resulting Cl· radical inhibits the polymerization. The $AlEt_3$ and $B(n\text{-}Bu)_3$ complexes did not polymerize under the condition of this experiment. The intrinsic viscosities of MMA–St copolymers measured in chloroform were in the range of 1.0–2.0 for the $SnCl_4$ complex–St system and in the range of 2.0–3.0 for the $AlCl_3$ complex–St system.

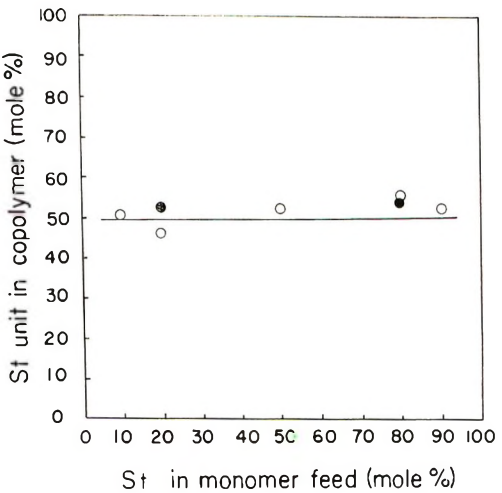

Fig. 1. Composition diagram for the copolymerization of the MMA–$SnCl_4$ and MAN–$SnCl_4$ complexes with styrene: (○) $SnCl_4(MMA)_2$–St; (●) $SnCl_4(MAN)_2$–St.

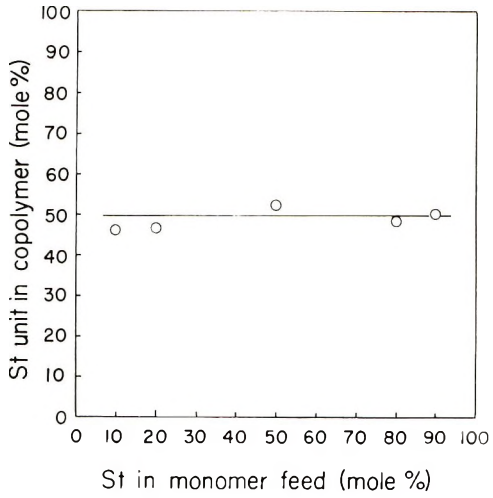

Fig. 2. Composition diagram for the copolymerization of the MMA–$AlCl_3$ complex with styrene.

Effect of Concentration of $SnCl_4$ and St

Figure 3 shows the effect of the concentration of $SnCl_4$ and St on the conversion of copolymer. The conversion increased with an increasing concentration of $SnCl_4$, but the conversion was kept constant at a molar ratio of $SnCl_4$/MMA 0.5–1.0, at higher molar ratios the conversion decreased because of a cationic polymerization of St. The broken line in

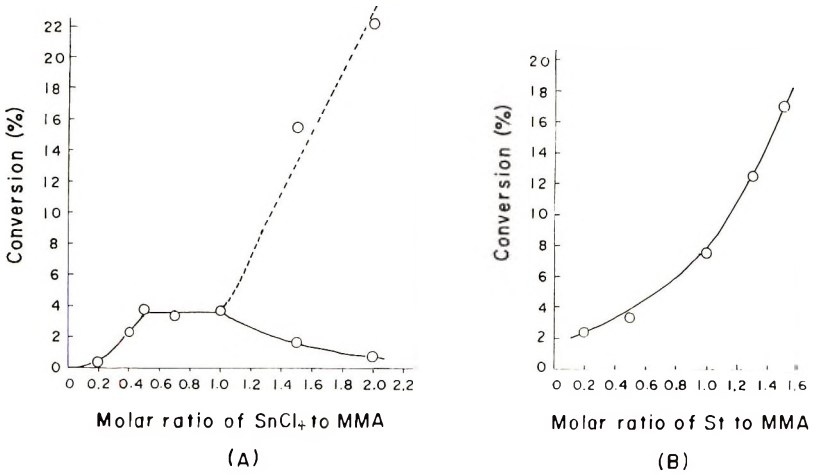

Fig. 3. Change in the conversion for the copolymerization of the MMA–$SnCl_4$ complex–St system in toluene solution irradiated with ultraviolet rays for 2 hr at −75°C: (*A*) effect of the concentration of $SnCl_4$ (concentration of St and MMA was 1.42 mole/l. and the conversion was based on the total weight of MMA and St); (*B*) effect of the concentration of St (2:1 MMA–$SnCl_4$ complex was used at constant concentration of 0.71 mole/l. and the conversion was based on the weight of MMA).

Figure 3 indicates the conversion including polystyrene. The constant conversion represents the condition where MMA monomer is in the form of complex. The conversion was found to be of higher order than first order in the concentration of St.

Structure and Tacticity of Copolymer

The NMR spectra of MMA–St copolymers are shown in Figure 4. All the copolymers have three split peaks for the α-methyl proton at about 9.0–9.5 ppm. This indicates the formation of an alternating copolymer, since the random copolymers obtained from the pure monomers by free-radical polymerization shown only one broad singlet in their NMR spectra.[12]

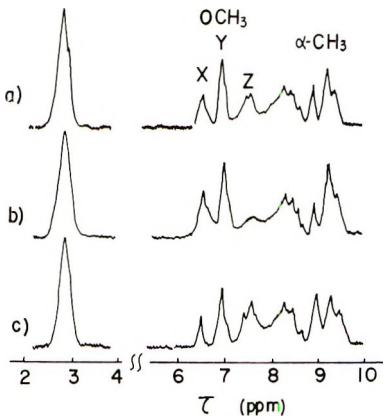

Fig. 4. NMR spectra of copolymers: (*a*) 2:1 MMA–$ZnCl_2$ complex–St; (*b*) 2:1 MMA–$SnCl_4$ complex–St; and (*c*) 1:1 MMA–$AlCl_3$ complex–St; where X = cosyndiotacticity, Y = heterotacticity, and Z = coisotacticity.

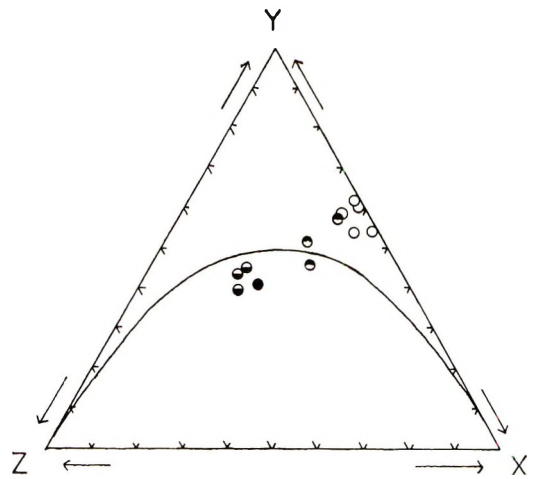

Fig. 5. Tacticity of MMA–St copolymers (X = cosyndiotacticity, Y = heterotacticity, and Z = coisotacticity): (○) 2:1 MMA–$SnCl_4$ complex–St; (◓) 1:1 MMA–$SnCl_4$ complex–St; (◒) MMA–$AlCl_3$ complex—St; (●) MMA–BF_3 complex–St.

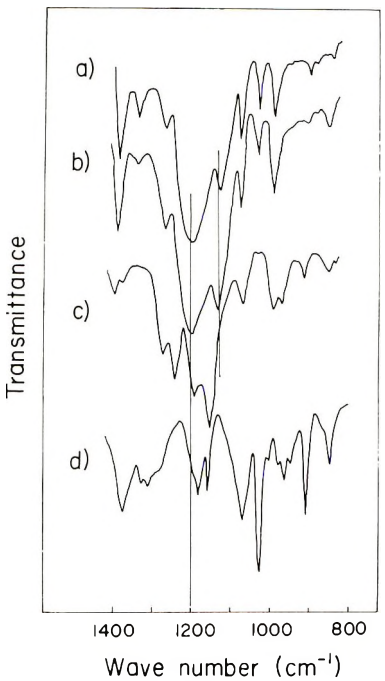

Fig. 6. Infrared spectra of MMA–St copolymers: (*a*) MMA–$AlCl_3$ complex–St (20/80); (*b*) 2:1 MMA–$SnCl_4$ complex–St (80/20); (*c*) PMMA; (*d*) PSt.

The proportion of the three peaks of the methoxy proton at about 6.5–7.5 ppm, which is the index of the tacticity of the resulting polymer, however, varies, depending on the complex species. It is noted from Tables III and IV that the sum of cosyndiotacticity and heterotacticity is approximately 100% in the case of the 2:1 MMA–$SnCl_4$ complex. The coisotacticity is increased for the 1:1 MMA–$SnCl_4$ complex, and is higher than the cosyndiotacticity for the 1:1:1 MMA-propionitrile–$SnCl_4$ complex where the more strong base is coordinated to stannic chloride. The copolymer from the $AlCl_3$ or BF_3 complexes, however, contains the more isotactic part. The tacticities can not be expressed by one parameter as shown in Figure 5.

Figure 6 shows the infrared spectra of MMA–St copolymers. The absorption bands in the range of 1100–1300 cm^{-1} are very different from those for PMMA or PSt. The bands in this range are characteristic of the tacticity of the MMA unit. The absorption bands of PMMA at 1240 and 1150 cm^{-1} disappear, and new bands are observed at 1200 and 1130 cm^{-1}.

NMR Spectra of Copolymerization System

The measurement of NMR spectra of the complex of MMA with the $SnCl_4$–St system can be measured at temperatures lower than 25°C since noticeable cationic polymerization did not occur in this system during the measurement. The change in chemical shift of MMA protons is summarized in Table V for free MMA, i.e., the uncoordinated MMA, and in

TABLE V
Change in Chemical Shift of the Uncoordinated MMA[a]

C_m[b] / C_s	Chemical shift, ppm[c]							
	α-CH_3		OCH_3		H_c[d]		H_t[d]	
	τ	$\Delta\tau_f$	τ	$\Delta\tau_f$	τ	$\Delta\tau_f$	τ	$\Delta\tau_f$
0.835	8.03	0.03	6.25	0.09	4.39	0.11	3.86	0.11
0.417	8.06	0.06	6.27	0.11	4.42	0.14	3.84	0.09
0.208	8.08	0.08	6.33	0.17	4.51	0.23	3.85	0.10
0.139	8.12	0.12	6.46	0.30	4.68	0.40	3.89	0.14
0.104	8.15	0.15	6.49	0.33	4.75	0.47	3.87	0.12

[a] Measurements were carried out at −28°C in chloroform solution.

[b] C_m, concentration of MMA = 0.91 mole/l.; C_s, concentration of St = 1.09–8.75 mole/l.

[c] $\Delta\tau_f = \tau - \tau_0$; τ_0 is the chemical shift of MMA proton in chloroform at −28°C, τ_0 (α-CH_3) at 8.00 ppm, τ_0 (OCH_3) at 6.16 ppm, $\tau_0(H_c)$ at 4.28 ppm and τ_0 (H_t) at 3.75 ppm.

[d] H_c and H_t are the vinyl protons *cis* and *trans* to the ester group.

TABLE VI
Change in Chemical Shift of the 2:1 MMA–$SnCl_4$ Complex[a]

C_m[b] / C_s	Chemical shift, ppm[c]							
	α-CH_3		OCH_3		H_c[d]		H_t[d]	
	τ	$\Delta\tau_c$	τ	$\Delta\tau_c$	τ	$\Delta\tau_c$	τ	$\Delta\tau_c$
0.835	8.03	0.09	6.10	0.26	4.24	0.29	3.66	0.29
0.417	8.10	0.16	6.17	0.33	4.30	0.35	3.65	0.28
0.208	8.20	0.26	6.34	0.50	4.41	0.46	3.70	0.33
0.139	8.32	0.38	6.50	0.66	4.58	0.63	3.74	0.37
0.104	8.37	0.43	6.54	0.70	4.65	0.70	3.72	0.35

[a] Measurements were carried out at −28°C in chloroform solution.

[b] C_m, the concentration of MMA = 0.91 mole/l.; C_s, concentration of St, (1.09–8.75 mole/l.).

[c] $\Delta\tau_c = \tau - \tau_0$; τ_0 is the chemical shiftof the 2:1 MMA–$SnCl_4$ complex in chloroform at −28°C. $\tau_0(\alpha$-$CH_3)$ at 7.94, $\tau_0(OCH_3)$ at 5.84, $\tau_0(H_c)$ at 3.95 and $\tau_0(H_t)$ at 3.37 ppm.

[d] H_c and H_t, vinyl protons *cis* and *trans* to ester group.

Table VI for the coordinated MMA. Both the free MMA and the coordinated MMA are affected similarly as a result of an interaction with St.

The specific effect of the complex formation on the interaction of MMA with St may be discussed from the change in chemical shift between the coordinated MMA and the free MMA, i.e., specific interaction is given by $\Delta\tau_s = \Delta\tau_c - \Delta\tau_f$. The values of $\Delta\tau_s$ are plotted against the molar ratio of the coordinated MMA to St in Figure 7. The effect of the concentration of St on $\Delta\tau_s$ was found to be larger for α-methyl and methoxy protons than for vinyl protons. The continuous variation curves of the change in the chemical shift are shown in Figure 8 and the data are summarized in Table

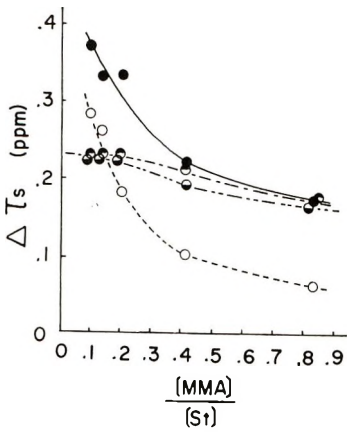

Fig. 7. Change in the chemical shifts of the 2:1 MMA–$SnCl_4$ complex–St system: (○) α-CH_3; (●) OCH_3; (◓) H_c; (◒) H_t.

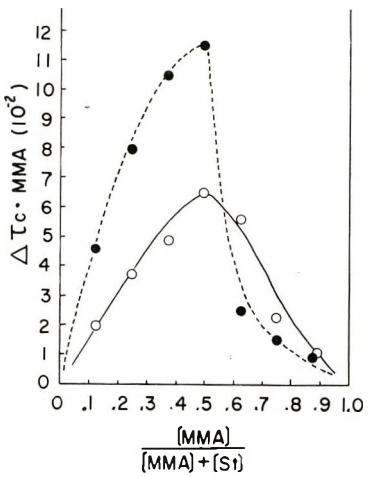

Fig. 8. Continuous variation curve of the chemical shift of the 2:1 MMA–$SnCl_4$–St system: (○) α-CH_3; (●) OCH_3.

VII. The concentration x of the charge-transfer complex of the MMA coordinated with St, if it were to exist, is expressed by eq. (1), since a rapid exchange occurs in this system:[13]

$$x = \Delta\tau_c \, C_m / \Delta\tau_{CT} \tag{1}$$

where C_m represents the concentration of the coordinated MMA and $\Delta\tau_{CT}$ represents the change in chemical shift of MMA protons upon formation of the charge-transfer complex. In Figure 8 the value of $\Delta\tau_c C_m$ is plotted instead of x. A maximum appeared at a 1:1 molar ratio of the coordinated MMA to St, that is, a charge-transfer complex with the molar ratio of MMA to St of 1:1 exists in the polymerization solution.

TABLE VII
Data for Continuous Variation[a]

MMA mole fraction[b]	Chemical shift, ppm[c]					
	α-CH_3		OCH_3		$\Delta\tau_c$ MMA $\times 10^{-2}$	
	τ	$\Delta\tau_c$[b]	τ	$\Delta\tau_c$	α-CH_3	OCH_3
0.125	8.10	0.16	6.21	0.37	2.00	4.63
0.250	8.09	0.15	6.16	0.32	3.75	8.00
0.375	8.07	0.13	6.12	0.28	4.78	10.5
0.500	8.07	0.13	6.07	0.23	6.50	11.5
0.625	8.03	0.09	5.88	0.04	5.60	2.50
0.750	7.97	0.03	5.86	0.02	2.25	1.50
0.875	7.95	0.01	5.85	0.01	0.88	0.88

[a] Measurements were carried out at $-28°C$ in chloroform solution of the 2:1 MMA–$SnCl_4$ complex.

[b] The total concentration of MMA and St was 3.63 mole/l.

[c] $\Delta\tau_c = \tau - \tau_0$; τ_0, chemical shift of the 2:1 MMA–$SnCl_4$ complex in chloroform at $-28°C$.

Consequently the following equations (2) and (3) hold:

$$\underset{C_s - x}{\text{St}} + \underset{C_m - x}{\text{MMA}} \quad \text{complex} \overset{K}{\rightleftharpoons} \underset{x}{\text{St----MMA}} \text{ complex} \tag{2}$$

$$K = x/[(C_m - x)\ (C_s - x)] \tag{3}$$

where C_m and C_s are initial concentrations of MMA and St, respectively, and x is as defined above. $\Delta\tau_{CT}$ can be estimated by plotting $1/\Delta\tau_c$ against $1/C_s$ and extrapolating $1/\Delta\tau_c$ to zero value of $1/C_s$. The values of $\Delta\tau_{CT}$ obtained by this method are 0.95 for α-CH_3, 1.45 for OCH_3, 1.43 for H_c and 0.39 for H_t. The heat of formation ΔH of the charge transfer complex was determined from the temperature dependence of the change in chemical

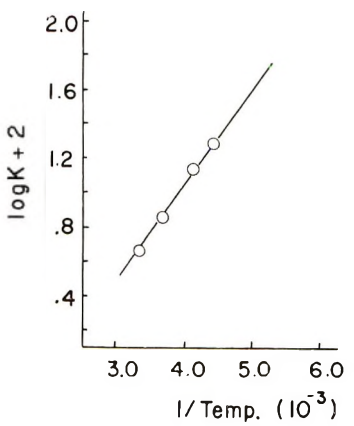

Fig. 9. Plot of log K vs. $1/T$ for the 2:1 MMA–$SnCl_4$ complex–St system.

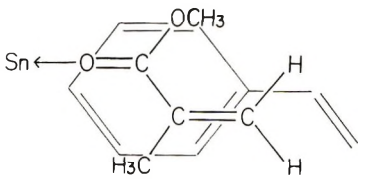

Fig. 10. Structure of the charge-transfer complex between the MMA–$SnCl_4$ complex and styrene.

shift as shown in Table VIII and Figure 9. ΔH is calculated by the equation:

$$4.57 \log K = \Delta S - (\Delta H/\mathrm{T})$$

$$-\Delta H = 4.57 \left[d\log K/d(1/\mathrm{T})\right]$$

$$\Delta H = -2.7 \text{ kcal/mol.}$$

The values of the entropy change (ΔS) and the free energy change (ΔG) are also shown in Table VIII. The formation constant K was calculated to be 0.56 at $-75°C$, which implies that 30% of monomer pairs forms the charge transfer complex at a feed molar ratio of 50/50 (concentration of monomer = 1.25 mole/l.). The heat of formation for the complex of aromatic molecules (e.g., toluene–anisole or toluene–*p*-nitroanisole) is in the range of 0.5–1 kcal/mole.[13] The higher heat of formation of the $SnCl_4$ complex–St system indicates that the interaction between MMA and St is strengthened on complex formation; this is also supported by the change in the chemical shift of MMA protons to lower fields on complex formation. A different orientation of MMA to St is inferred from the change in $\Delta\tau_s$ (Fig. 7). The structure shown in Figure 10 is suggested for the $SnCl_4$ complex–St system.

Stronger interaction can be expected for the $AlCl_3$ complex–St system, in consideration of the higher conversion of copolymerization. This system could not be investigated by NMR spectroscopy because of the case of cationic polymerization of St.

ESR Spectra of Copolymerization System

The ESR spectra of copolymerization systems subjected to irradiation with a high-pressure mercury lamp are shown in Figures 11 and 12. After irradiation at $-196°C$, a five-line spectrum with splitting width of 22.0 gauss and a doublet were observed at $-196°C$ in the 2:1 MMA–$SnCl_4$ complex–St system. The doublet was identified with a signal of hydrogen atom. The five-line spectrum consisted of a quintet and a triplet in view of the intensity of each peak. The quintet become weaker with increasing temperature and at $-100°C$ only the triplet remained. A seven-line spectrum appeared for the 1:1 MMA–$SnCl_4$ complex–St system at $-196°C$. A quintet was observed in the spectra of both the $AlCl_3$ complex–St and the $ZnCl_2$ complex–St systems at $-196°C$.

TABLE VIII
Estimation of ΔH of the Formation of C–T Complex[a]

Temp, °K	$\tau(\alpha\text{-}CH_3)$			$K \times 10^2$	log K	$1/T \times 10^3$	Entropy change ΔS, eu/mole	Free energy change ΔG, kcal/mole
	τ, ppm	τ_0, ppm	$\Delta\tau$, ppm					
298	8.16	8.05	0.11	4.14	$\bar{2}.617$	3.53	−15.5	+1.88
272	8.20	8.03	0.17	7.04	$\bar{2}.847$	3.68	−15.4	+1.46
243	8.22	7.94	0.28	13.9	$\bar{1}.143$	4.11	−15.2	+0.95
228	8.25	7.91	0.34	19.1	$\bar{1}.281$	4.39	−15.3	+0.75
195				55.6[b]	$\bar{1}.745$	5.13		

[a] Measurements were effected in n-hexane solution. The concentrations of MMA and St were 0.833 and 3.24 mol/l.
[b] Estimated value.

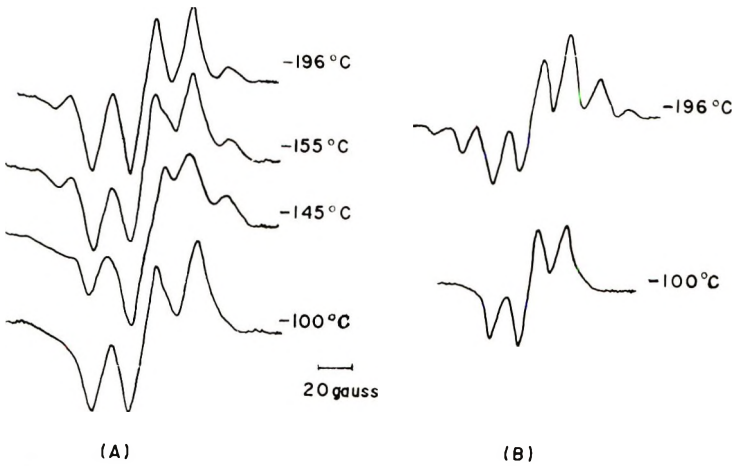

Fig. 11. ESR spectra of copolymerization systems irradiated with ultraviolet rays: (*A*) 2:1 MMA–$SnCl_4$ complex–St; (*B*) 1:1 MMA–$SnCl_4$ complex–St.

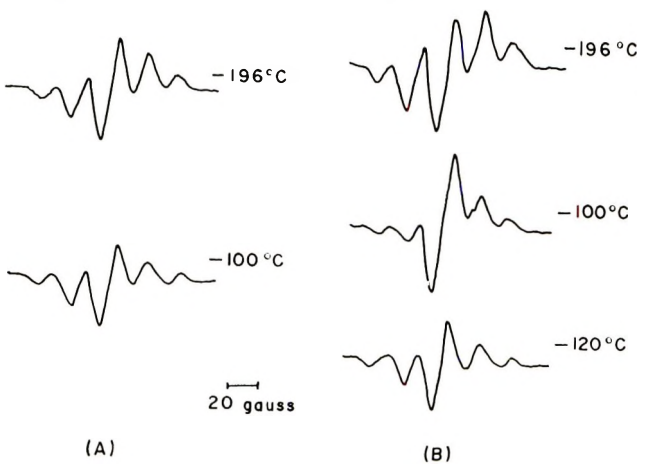

Fig. 12. ESR spectra of copolymerization system irradiated with ultraviolet rays; (*A*) 2:1 MMA–$ZnCl_2$ complex–St system; (*B*) MMA–$AlCl_3$ complex–St system.

Under or after the ultraviolet irradiation at −100°C only a triplet was observed for both the 2:1 and 1:1 MMA–$SnCl_4$ complex–St system. A quintet and an intense singlet appeared in the case of the MMA–$AlCl_3$ complex–St system at −100°C, while the singlet weakened under the irradiation at −120°C. The $ZnCl_2$ complex–St system gave a quintet. These complexes themselves gave no signal in the absence of St at −100°C after ultraviolet irradiation at wavelengths longer than 300 mμ. A mixture of St and the $ZnCl_2$–propionitrile complex also gave no signal under these conditions.

Figure 13 shows the proposed structure of the radicals observed in the ESR spectra of this copolymerization system. The triplet is characteristic of monomers having one α-hydrogen atom such as acrylonitrile or methyl

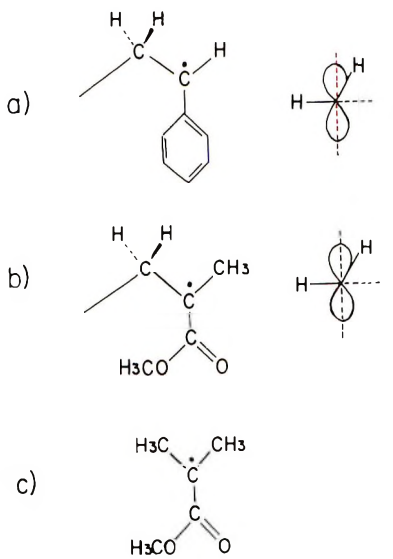

Fig. 13. Radical species and conformation of β-methylene protons: (*a*) triplet; (*b*) quintet; (*c*) septet.

acrylate.[14] The triplet may be reasonably ascribed to a styrene radical as shown in Figure 13*a*. A triplet with a splitting width of 47.5 gauss was observed in polystyrene irradiated with γ-rays from a ^{60}Co source. This triplet, however, was ascribed to the cyclohexadienyl radical owing to its large splitting value.[16] The quintet is due to the MMA radical as shown in Figure 13*b*, in which one of the two β-methylene protons and the protons of the α-methyl group interact with the unpaired electron. The septet can be ascribed to the radical shown in Figure 13*c* formed from MMA by the addition of a hydrogen to the double bond of MMA. The intense singlet may correspond to a benzyl radical, which is formed by the abstraction of hydrogen from toluene. The irradiation of toluene with γ-rays gives a singlet which is due to a benzyl radical.[17] The presence of a hydrogen-abstracting substance seems to be indispensable for the formation of singlet, since the singlet did not appear in the absence of styrene or MMA at −100°C.

Mechanism for Copolymerization

Initiation. ESR spectra of the polymerization system irradiated with ultraviolet rays at −196°C shows a triplet, a quintet, and a septet. Con-

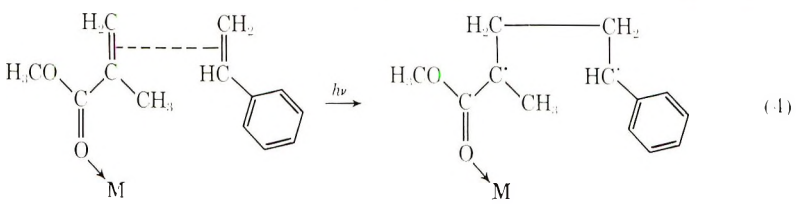

(4)

sidering the change of the spectra with temperature, the spectra obtained at −196°C may be assigned to the initiation radicals. The coexistence of a triplet with a quintet suggests the reaction (4).

The radical showing the seven-line spectrum is also one involved in initiation. In the case of the $AlCl_3$ complex–St system, an abstraction of a hydrogen atom from toluene molecule is suggested by the appearance of a benzyl radical. No signal attributable to the benzyl radical was observed in the polymerization system when St was absent. It is quite reasonable that the activated charge-transfer complex might abstract a hydrogen from toluene. This reaction [eq. (5)] would be predominant under irradiation at −100°C.

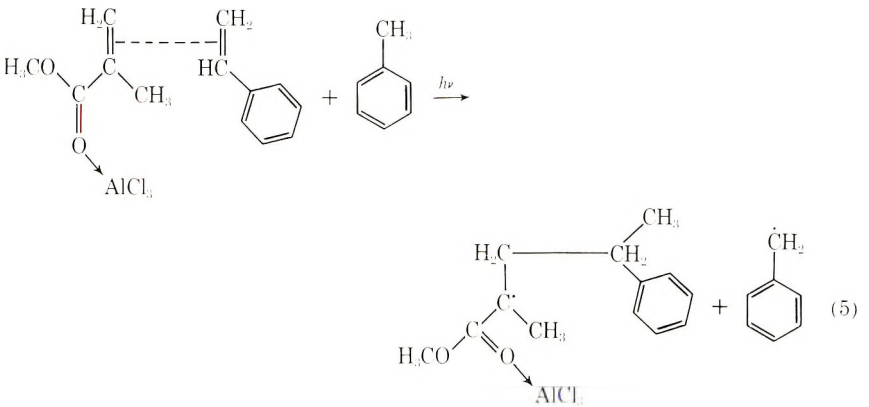

(5)

Matsuda and Abe[18] reported that polymerization was initiated by the addition of cumene, etc., in maleic anhydride–St system and that the initiation reaction was an abstraction of a hydrogen atom from the additive. The other initiation reaction in the copolymerization system of the charge transfer complex includes the formation of a biradical.[19] The two initiation reactions mentioned above may occur in the present copolymerization system.

Propagation. In the present copolymerization system, sufficient charge-transfer complex exists that the copolymerization may proceed through the reaction of the charge-transfer complex alone. Moreover, the charge-transfer complex will be more highly activated by the absorption of light, since the copolymerization was effected under ultraviolet irradiation.

The species of the growing end of the polymerization depends on the species of complex. The ESR spectra of the copolymerization system irradiated with ultraviolet rays at −100°C may reveal the species of the growing radical, since this temperature is just below the freezing point of polymerization mixture.[20] The growing end is an St unit for the $SnCl_4$ complex–St system, while it is a MMA unit for the $AlCl_3$ and the $ZnCl_2$ complexes–St systems. The species of growing end is supposed to depend on the stability of the radical. The extension of conjugation of monomer

on complex formation could lead to the stabilization of the coordinated monomer radical as compared with a St radical. In the case of the $SnCl_4$ complex–St system, the St radical might be more stabilized by interaction with stannic chloride.

The propagation step through the polymerization of the charge-transfer complex can be analyzed by two parameters, namely, those for the intercomplex reaction and intracomplex one. If the probability of syndiotactic diad addition in the intercomplex reaction and that in the intracomplex reaction one are designated by σ_r and σ_a, respectively, for the reaction scheme (6),

$$\mathrm{BA} + \underset{\text{C-T complex}}{\mathrm{B{-}{-}{-}{-}{-}A}} \xrightarrow{\sigma_r} \mathrm{BAB{-}{-}{-}{-}{-}A} \xrightarrow{\sigma_a} \mathrm{BABA} \qquad (6)$$

the triad tacticities of the resulting copolymers are expressed by eqs. (7)–(9).

$$I = (1 - \sigma_a)(1 - \sigma_r) \qquad (7)$$

$$H = \sigma_a(1 - \sigma_r) + \sigma_r(1 - \sigma_a) \qquad (8)$$

$$S = \sigma_a\sigma_r \qquad (9)$$

Tacticity Control in Propagation Step. The tacticities of the copolymer can not be analyzed by one parameter as depicted in Figure 5. The 2:1 MMA–$ZnCl_2$ complex gave a copolymer of random character, which indicated that both σ_a and σ_r were about 0.5.[9] The factors which contribute to the specific tacticity are considered to be (a) reaction temperature, (b) strength of the Lewis acid, and (c) coordination number. The effect of the reaction temperature on the tacticity would not be great. At 30°C the 2:1 MMA–$ZnCl_2$ complex gave an alternating copolymer with no specific tacticity, and even at a temperature as low as −78°C the tacticity of copolymer resulting from the $AlCl_3$ complex or the BF_3 complex and St was not much different from that from the $ZnCl_2$ complex at 30°C. The value of σ_r would be independent of temperature, so that the value would be also approximately 0.5 in the polymerization at −78°C. The value of σ_a can be calculated by eq. (10):

$$\sigma_a = 2S + H - \sigma_r \qquad (10)$$

The results are summarized in Table IX.

The value of σ_a is smaller than 0.5 in the polymerization system with $AlCl_3$ complex but is very near unity in the $SnCl_4$ complex–St system. These characteristic values of σ_a may reflect the specific structure of the charge transfer complexes. The high value of σ_a for the $SnCl_4$ complex–St system would be due to the participation of tin atom in the propagating radical. Stannic chloride can interact with the π electron system as reported in the several studies.[21,22] Figure 14 shows the probable growing end, in which stannic chloride interacts with both the carbonyl group of MMA and the π-electron system of St. In this scheme

TABLE IX
Estimation of the Probability of Syndiotactic Diad Addition of Intracomplex Reaction (σ_a) in Copolymerization of Methyl Methacrylate–Metal Salt Complexes with Styrene

Complex	$[m_1]$, mole-%	Temp, °C	St in copolymer, mole-%	σ_a
1:1 MMA–$ZnCl_2$ complex[a]	90	30	48.5	0.29
2:1 MMA–$ZnCl_2$ complex[a]	80	30	51.0	0.50
	90	30	48.5	0.50
1:1 MMA–$SnCl_4$ complex	10	−75	43.3	0.78
	33	−75	41.4	0.66
	50	−75	59.0	0.63
1:1:1 MMA–PN–$SnCl_4$ complex	50	−75	50.0	0.34
2:1 MMA–$SnCl_4$ complex	10	−75	48.0	1.00
	20	−75	44.5	0.75
	50	−75	47.5	0.89
	80	−75	53.6	0.88
	90	−75	49.0	0.84
MMA–$AlCl_3$ complex	10	−75	45.8	0.26
	20	−75	53.9	0.33
	50	−75	52.2	0.34
	80	−75	51.8	0.37
	90	−75	50.0	0.41
MMA–BF_3 complex	30	−75	54.5	0.42

[a] Data of Ikegami and Hirai.[9]

the monomer would come from the same side as that on which the stannic chloride is coordinated, because the unpaired electron density is higher in this side as a result of π interaction. Similar interaction of a growing radical with a Lewis acid was suggested in the case of the polymerization of MMA with the alkyl borons–O_2 or peroxide system.[23] The value of σ_a decreases in the order: 2:1 MMA–$SnCl_4$ > 1:1 MMA–$SnCl_4$ > 1:1:1 MMA–PN–$SnCl_4$. The value of σ_a is larger in the case of the 2:1 MMA–$SnCl_4$ complex. The 1:1 complex gives a smaller value than the 2:1 complex, and when a stronger base coordinates to $SnCl_4$ the smallest value is

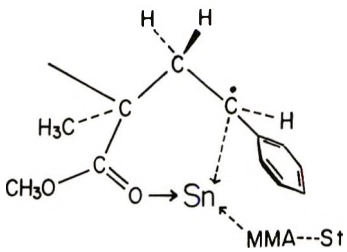

Fig. 14. Growing end for the 2:1 MMA–$SnCl_4$ complex–St system.

obtained. It is reasonable to consider that in the case of the 1:1:1 MMA–PN–$SnCl_4$ complex, interaction with the π-electron system of St is impossible and in the case of the 1:1 MMA-$SnCl_4$ complex the interaction with an incoming monomer will be hindered. Two requirements, that is, the interaction with the π-electron system and that with an incoming monomer, are believed be satisfied by the 2:1 complex because of its labile coordination bond as indicated by the weaker withdrawal of electron by stannic chloride shown by the smaller change in chemical shift compared with the 1:1 complex.

In the case of a strong acid, such as aluminum trichloride or boron trifluoride, the higher polarization of the complex might determine the orientation of the molecules in the charge-transfer complex. In these cases, interaction of the acid with the π-electron system of St does not occur, because of the impossibility of formation of a complex of these acids with an unsaturated compound through interaction between the π-electron in the C=C double bond and vacant orbitals of the acids and because of their capability of coordination with only one monomer. The tacticity would then be determined by the structure of the charge-transfer complex.

References

1. P. D. Bartlett and K. Nozaki, *J. Amer. Chem. Soc.*, **68**, 1495 (1946).
2. C. Walling, E. R. Briggs, K. B. Waltsirn, and F. R. Mayo, *J. Amer. Chem. Soc.*, **70**, 1537, 1544 (1948).
3. W. G. Barb, *Trans. Faraday Soc.*, **49**, 143 (1953).
4. E. R. Garret and R. L. Guile, *J. Amer. Chem. Soc.*, **75**, 3958 (1953).
5. S. Iwatsuki and Y. Yamashita, *J. Polym. Sci. A-1*, **5**, 1753 (1967).
6. S. Iwatsuki and Y. Yamashita, *Makromol. Chem.*, **89**, 205 (1965); *ibid.*, **104**, 263 (1967).
7. M. Hirooka, H. Yabuuchi, J. Iseki, and Y. Nakai, *J. Polym. Sci. A-1*, **6**, 1381 (1968).
8. N. G. Gaylord and A. Takahashi, *J. Polym. Sci. B*, **6**, 749 (1968).
9. T. Ikegami and H. Hirai, *J. Polym. Sci. A-1*, in press.
10. S. Okuzawa, H. Hirai, and S. Makishima, *J. Polym. Sci., A-1*, in press.
11. H. Hirai, T. Ikegami, and S. Makishima, *J. Polymer Sci. A-1*, in press.
12. K. Itoh and Y. Yamashita, *J. Polym. Sci. B*, **3**, 625 (1965).
13. J. H. Bowie, J. Ronayne, and D. H. Williams, *J. Chem. Soc.*, **1966**, 785.
14. R. Marx and M. R. Bensasson, *J. Chim. Phys.*, **57**, 674 (1960).
15. R. T. Abraham and D. H. Whiffen, *Trans. Faraday Soc.*, **54**, 291 (1958).
16. R. E. Florin, L. A. Wall, and D. W. Brown, *Trans. Faraday Soc.*, **56**, 1304 (1960).
17. S. Ohnishi, J. Tanei, and I. Nitta, *J. Chem. Phys.*, **37**, 2402 (1962).
18. M. Matsuda and K. Abe, *J. Polym. Sci., A-1*, **6**, 1441 (1968).
19. N. L. Zutty, C. W. Wuksib III, G. H. Porter, and D. C. Priest, *J. Polym. Sci. A*, **3**, 2781 (1965).
20. H. Sobue and Y. Tabata, *J. Polym. Sci.*, **43**, 459 (1960).
21. S. C. Jand and R. Rivest, *Inorg. Chem.*, **6**, 467 (1967).
22. E. B. Ludwig, A. R. Gantmacher and S. S. Medveder, paper presented at IUPAC Symposium on Macromolecules, Wiesbaden, 1959; Section III, IIIA 12 (1959).
23. F. S. Arimoto, *J. Polym. Sci., A-1*, **4**, 275 (1966)

Received April 21, 1969
Revised July 23, 1969

JOURNAL OF POLYMER SCIENCE: PART A-1 VOL. 8, 483–493 (1970)

Molecular Weight Distribution of Poly-*N*-vinylcarbazole Obtained in Catalytic Solid-State Polymerization

T. HIGASHIMURA,* T. MATSUDA, and S. OKAMURA,
Department of Polymer Chemistry, Kyoto University, Kyoto, Japan

Synopsis

The molecular weight distribution of poly-*N*-vinylcarbazole (PVCar) obtained in solid-state polymerization with various catalysts or γ-rays was measured by gel-permeation chromatography, in order to determine the mechanism of the solid-state polymerization. In addition, the molecular weight distribution of PVCar obtained in the solution polymerization by the cationic catalyst was also measured. The molecular weight distribution of PVCar obtained in the catalytic solid-state polymerization was broad and had three peaks, independent of the nature of catalysts, radical and cationic. A large amount of low molecular weight oligomer (probably dimer or trimer) was formed in the catalytic solid-state polymerization of VCar. The molecular weight distribution of PVCar obtained in the cationic solution polymerization showed only one sharp peak. On the other hand, the molecular weight of PVCar obtained in the radiation-induced solid-state polymerization was larger than that obtained in the catalytic solid-state polymerization, and dimer or trimer was not formed. The molecular weight distribution of PVCar obtained was composed of one sharp peak in the high molecular weight region, and a broad peak in the low molecular weight region, and was extremely different from that of PVCar obtained in the catalytic solid-state polymerization.

INTRODUCTION

It has been found in previous papers[1–5] as a characteristic of the solid-state polymerization that *N*-vinylcarbazole (VCar) produces low molecular weight polymer in solid-state polymerization with various catalysts, regardless of polymerization conditions. The mechanism of the solid-state polymerization has often been discussed on the basis of the molecular weight of polymer. For example, Enikolopyan et al.[6,7] investigated the relationship between the polymerization rate and the molecular weight of polymer in the radiation-induced solid-state polymerization of trioxane, Papissov and Kabanov[8] studied thermodynamically the relationship between the polymerization mechanism and the molecular weight of polymer. These investigations, however, are based on the average molecular weight of

* Present address: Research Laboratory, Sekisui Chemical Co., Hirose, Mishima-gun, Osaka, Japan.

polymer obtained. The catalytic solid-state polymerization of trioxane was previously discussed on the basis of the molecular weight distribution of polymer.[9]

In present work, the molecular weight distribution of poly-*N*-vinylcarbazole (PVCar) obtained in the solid state polymerization with various catalysts or γ-rays was measured by gel-permeation chromatography (GPC) in order to determine the reaction mechanism of the solid-state polymerization of VCar. It was found that the molecular weight distribution of PVCar was markedly dependent on the method of polymerization. The mechanism of the solid-state polymerization was discussed on the basis of the molecular weight distribution of PVCar obtained.

EXPERIMENTAL

Procedure

Solid-State Polymerization. PVCar was obtained by adding gaseous boron halides to crystalline VCar in a flask[1,4] or by adding a redox catalyst solution to VCar suspended in water[5] below the melting point as described in the previous papers.

Solution Polymerization. The solution polymerization was carried out by adding the catalyst solution to the VCar solution.[1] *n*-Hexane or ethylene chloride was used as solvent, and $BF_3 \cdot O(C_2H_5)_2$ as catalyst.

Suspension Polymerization. PVCar was obtained by adding *n*-hexane solution of $BF_3 \cdot O(C_2H_5)_2$ to crystalline VCar suspended in *n*-hexane;[1] *n*-hexane is a poor solvent for VCar and a nonsolvent for PVCar, and the VCar crystals did not dissolve in *n*-hexane during the polymerization.

Radiation-Induced Polymerization. The radiation-induced solid state polymerizarion was carried out by ^{60}Co γ-rays in the air.

Molecular Weight Distribution of PVCar

The molecular weight distribution was measured by GPC, with the use of a 0.5 wt-% polymer solution in tetrahydrofuran (column temperature, 25° ± 2°C; flow rate, 1 ml/min; injection time, 60 sec). Four columns of 10^1, 10^2, 10^3, and 10^4 Å pore size were connected in series.

The molecular weight of PVCar was estimated through the calibration curve. When the molecular weight was smaller than 10^4, two parallel straight lines could be obtained as calibration curve (the relationship between the logarithmic molecular weight and the elution volume) for polystyrene (PSt) and poly(ethylene glycol) (PEG). Therefore, the elution volume in GPC of VCar monomer was measured, and a straight line parallel with the calibration curve of PSt or PEG through the point measured for VCar was assumed as the calibration curve for PVCar. The error may be not so large in the estimation of molecular weight of an oligomer, and a comparison of the shape of the molecular weight distribution may deserve discussion, although the absolute molecular weight of a high polymer cannot be determined.

η_{sp}/c of PVCar was measured in benzene solution at a polymer concentration of 1 g/100 ml at 30°C.

RESULTS

The polymerization conditions and η_{sp}/c of PVCar whose molecular weight distribution was measured in this work are summarized in Table I.

Molecular Weight Distribution of PVCar Obtained in the Catalytic Solid-State Polymerization

The molecular weight distribution of PVCar obtained in the solid-state polymerization with boron halides is shown in Figure 1. The molecular weight distributions of all the PVCar samples obtained by these catalysts were similar. The molecular weight distribution was found to be broad and to have three peaks, the amount of the fraction at the highest molecular weight peak being larger than the others. The estimated values of the molecular weight corresponding to each peak from high to low molecular weight were 63000, 3200, and 390 with BF_3 catalysis (Fig. 1*a*). The molecular weight of 63000 seems to be too large in view of the value of η_{sp}/c of the polymer. This might be due to method of approximation used in the calibration as described in the experimental section. The

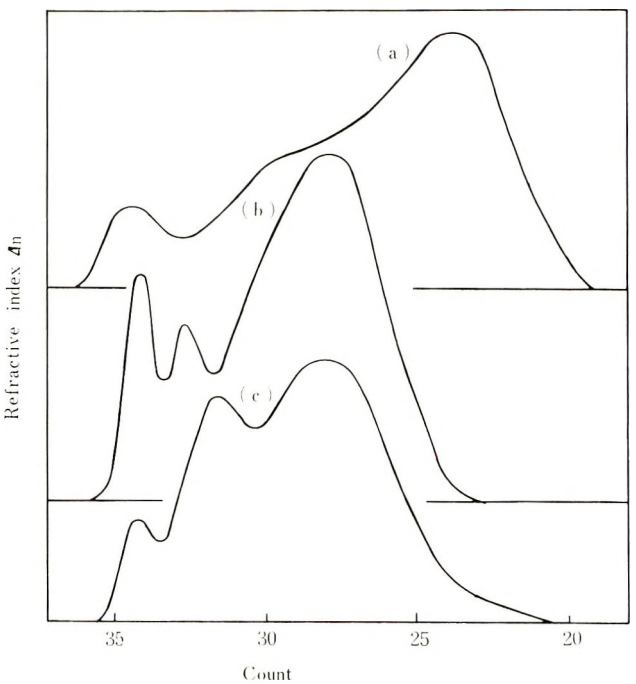

Fig. 1. Molecular weight distribution of the polymer obtained in the solid-state polymerization by various boron halides: (*a*) BF_3 (45°C, conversion 8.7%); (*b*) BCl_3 (40°C, conversion 13.4%); (*c*) BBr_3 (45°C, conversion 7.5%).

TABLE I
Conditions of Polymerization of Vinylcarbazole

Figure no.[a]	Catalyst	Method of polymerization	Temperature, °C	Polymerization time, min	Conversion, %	η_{sp}/c
1*a* (7*a*)	BF_3[b]	Solid state	45	21	8.7	0.053
1*b*	BCl_3[b]	"	40	360	13.4	0.048
1*c*	BBr_3[b]	"	45	300	7.5	0.046
2	I_2[c]	"	40	420	14.0	0.048
3	Redox[d]	"	50	60	53.8	0.042
4*a*	$BF_3 \cdot O(C_2H_5)_2$[e]	Solution (in ethylene chloride)	30	0.5	ca. 100	0.26
4*b*	"	Solution (in *n*-hexane)	30	20	86.9	0.17
5	"	Suspension	30	10	37.4	0.12
7*b*	BF_3[b]	Solid state	50	5	7.1	0.066
7*c*	"	"	50	120	33.6	0.063

[a] The number corresponds to that of curves in figures.
[b] [C] = 11 mmole/l. vessel; [M] = 2.0 g/90 ml vessel.
[c] [C] = saturated vapor pressure at 40°C; [M]: 2.0 g/90 ml vessel.
[d] [APS] = 0.66 mole/l. H_2O; [SBS] = 0.22 mole/l. H_2O; [M] = 1.0 g/20 ml vessel.
[e] [C] = 1.0 mmole/l.; [M] = 0.17 mole/l.

molecular weight of PVCar obtained by BF_3 was large compared with that obtained by BCl_3 or BBr_3, and the amount of oligomers (molecular weight about 390) was about 10%.

Figure 2 shows the molecular weight distribution of PVCar obtained with iodine catalyst in the solid-state polymerization. The molecular

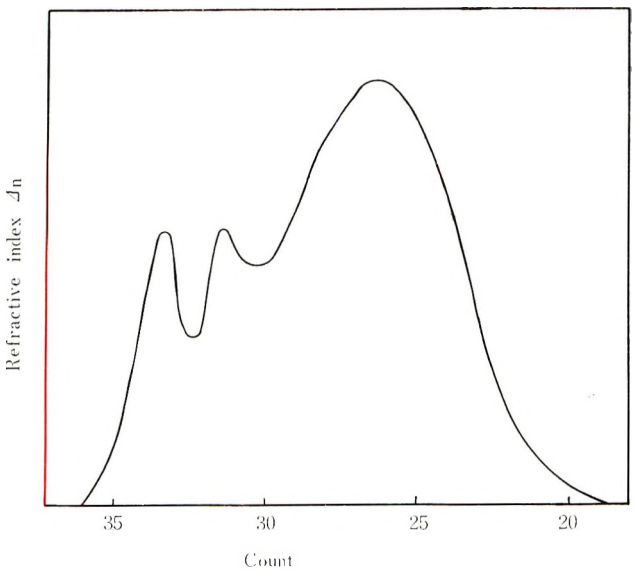

Fig. 2. Molecular weight distribution of the polymer obtained in the solid state polymerization by I_2 at 40°C (conversion 14.0%).

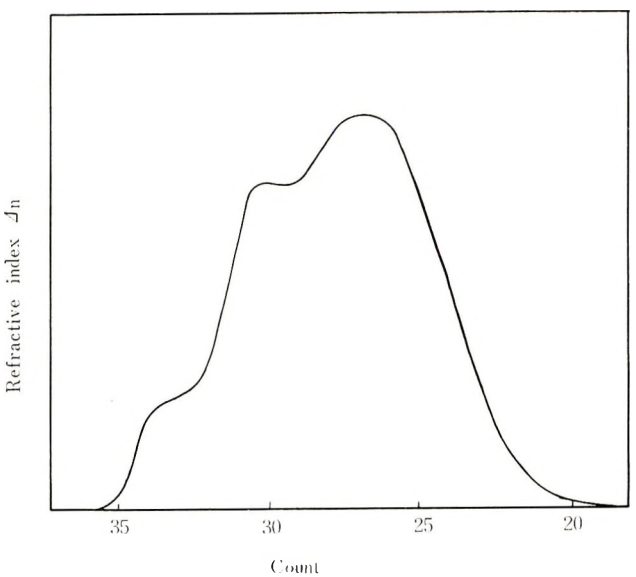

Fig. 3. Molecular weight distribution of the polymer obtained in the solid-state polymerization by redox catalyst at 50°C (conversion 53.8%).

weight distribution of PVCar formed was also broad, and three peaks appeared, similar to the case of boron halide catalysrs. As is seen from Figure 2, each peak was relatively sharp, and the fraction of the third peak at molecular weight of 560 was larger than that of the second peak at molecular weight of 1070.

In Figure 3 is shown the molecular weight distribution of PVCar polymerized by redox catalyst (ammonium persulfate–sodium bisulfite, 3:1 mole ratio) in the solid state. This was quite similar to the molecular weight distribution of PVCar obtained in the solid state by boron bromide in which the shape was broad and had three peaks. The amount of fraction of the peaks area at the lowest molecular weight was small compared with that of the solid-state polymerization by boron halides or idine.

Molecular Weight Distribution of PVCar Obtained in Solution and Suspension Polymerization

The molecular weight distributions of PVCar obtained in solution and suspension polymerization were measured and compared with that of the solid-state polymerization. As is shown in Figure 4, the molecular weight distribution of PVCar obtained in the solution polymerization of VCar was completely different from those of solid-state polymerization; there was

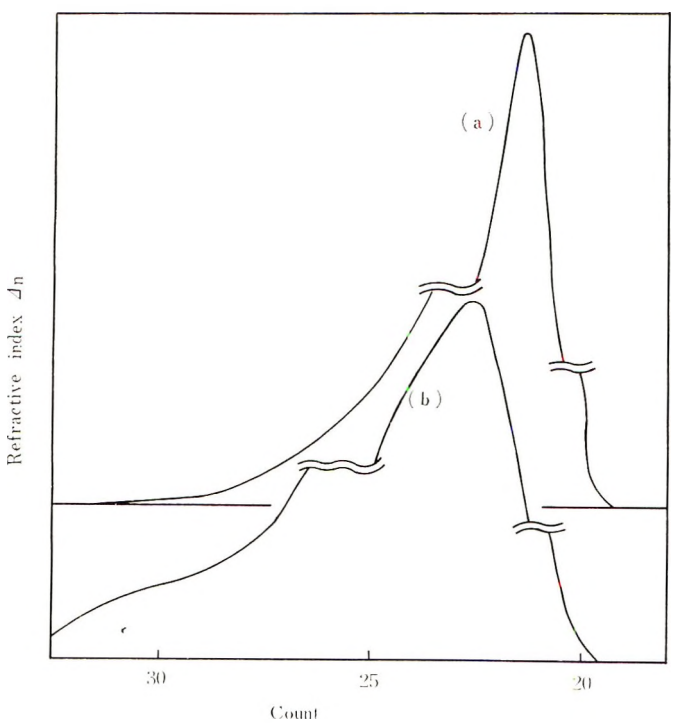

Fig. 4. Molecular weight distribution of the polymer obtained in solution polymerization by $BF_3 \cdot O(C_2H_5)_2$ at 30°C: (*a*) in ethylene chloride; (*b*) in *n*-hexane.

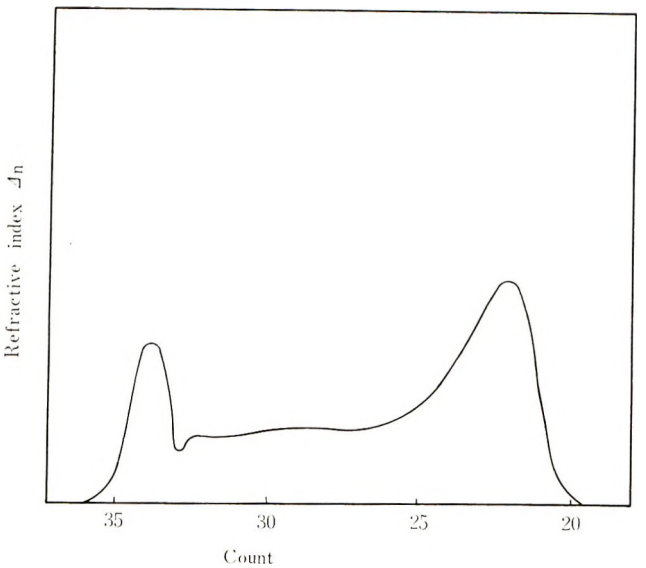

Fig. 5. Molecular weight distribution of the polymer obtained in suspension polymerization by $BF_3 \cdot O(C_2H_5)_2$ at 30°C.

only one relatively sharp peak. The molecular weight distribution of PVCar obtained in ethylene chloride (polar solvent) was found to be sharper than that obtained in *n*-hexane (nonpolar solvent), as is seen in Figure 4. The broad distribution in the latter case may be partly due to the precipitation of the resultant PVCar during the polymerization.

Figure 5 shows the molecular weight distribution of PVCar obtained in the suspension polymerization, in which the polymerization proceeded apparently in the solid-state although VCar was partially soluble in *n*-hexane.[1] The molecular weight distribution has a peak in the high molecular weight region followed by broad peak at a molecular weight of several thousand and a peak at a low molecular weight. The fact that the molecular weight distribution of PVCar obtained has several peaks in the low molecular weight region coincides with the results obtained in the solid-state polymerization.

Molecular Weight Distribution of PVCar Obtained in the Radiation-Induced Solid-State Polymerization

The molecular weight distribution of PVCar obtained at low and high conversions in the γ-ray-induced solid-state polymerization is shown in Figure 6. The polymerization conditions and η_{sp}/c of PVCar used for the molecular weight measurement were shown in Table II. The value of η_{sp}/c of PVCar obained in the radiation-induced solid-state polymerization was larger than that in the catalytic solid-state polymerization. The molecular weight distribution showed two peaks; the peak in the high molecular weight region was sharp, while the peak at a low molecular

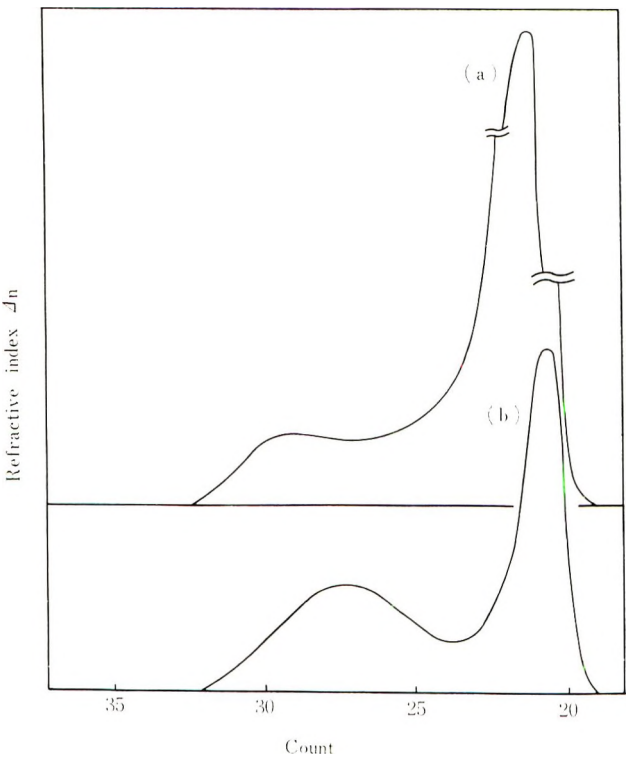

Fig. 6. Molecular weight distribution of the polymer obtained in the radiation-induced solid-state polymerization: (*a*) 4.4% conversion; (*b*) 56.0% conversion. (Polymerization conditions are shown in Table II.)

weight region was broad. The ratio of the peak area at the high molecular weight to that at the low molecular weight was dependent on the conversion being about 9:1 at low polymer yield (4.4% conversion) and about 1:1 at high polymer yield (56.0% conversion), as is seen in Figure 6.

TABLE II
Conditions of Polymerization of Vinylcarbazole Obtained in the Solid State by ^{60}Co γ-Rays[a]

Figure no.	Total dose, Mrad	Conversion, %	$[\eta]$
6*a*	2.2	4.4	—
6*b*	9.1	56.0	0.284

[a] Temperature, 35°C; dose rate, 1.4×10^5 rad/hr.

Thus, a large difference was observed between the radiation-induced and the catalytic solid-state polymerization, not only in the molecular weight of PVCar but also in the molecular weight distribution.

Effect of Polymerization Temperature and Conversion on the Molecular Weight Distribution

The effect of polymerization temperature on the molecular weight distribution was studied in the solid-state polymerization catalyzed by BF_3. As shown in Figure 7, a large difference in the molecular weight distribution was not observed, probably due to the small difference in polymerization temperature.

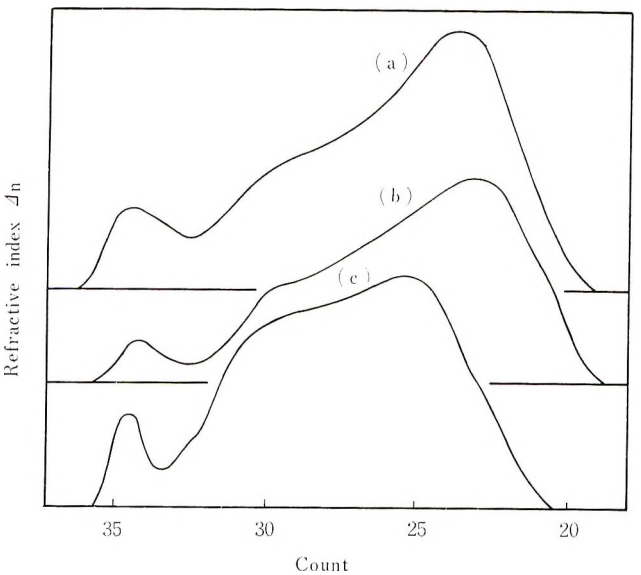

Fig. 7. Effect of temperature and conversion on molecular weight distribution of the polymer obtained in solid-state polymerization by BF_3; (*a*) 45°C, 8.7% conversion; (*b*) 50°C, 7.1% conversion; (c) 50°C, 33.6% conversion.

Also from Figure 7, it was observed that the amount of fraction of the low molecular weight polymer increased as the polymerization proceeded. This fact was also observed in the radiation-induced solid-state polymerization (Fig. 6).

DISCUSSION

The salient points which are concluded from the results can be summarized qualitatively as follows.

The molecular weight distribution of PVCar obtained by the cationic or radical mechanism in the catalytic solid state polymerization was broad and had three peaks. On the other hand, the molecular weight distribution of PVCar obtained in the solution polymerization had only one peak and was sharp compared with that of the solid-state polymerization.

A large amount of PVCar of low molecular weight was formed at higher polymer yield in the catalytic solid-state polymerization.

PVCar obtained in the radiation-induced solid-state polymerization had a higher molecular weight than that obtained by catalytic solid-state polymerization, and its molecular weight distribution had two peaks and was rather sharp.

A large amount of low molecular weight PVCar was formed in the catalytic solid-state polymerization, independent of the nature of catalyst, cationic or radical. PVCar obtained with BF_3 in the solid-state polymerization contained oligomer (the estimated molecular weight-390) which corresponds to the dimer of VCar. The amount of the dimer was 5–9 wt-% of the polymer obtained, as shown in Figure 7. The molecular weight distribution of PVCar obtained in the solid-state polymerization catalyzed by BBr_3, BCl_3, and I_2 showed a peak at molecular weights of 530, 530, and 560, respectively; these values correspond to the trimer of VCar, and the amount of the trimer formed was about 10%, independently of the nature of these catalysts as shown in Figure 1.

The formation of a low molecular weight PVCar such as dimer or trimer of VCar in the catalytic solid-state polymerization, regardless of cationic or radical catalyst, might be due to the ease of occurrence of side reactions other than propagation because of the limited movement of monomer molecule when the polymerization of crystalline monomer proceeds from its surface into the inside of crystal. The large difference between the molecular weight distribution of PVCar obtained in solution and in solid-state polymerization supports strongly the occurrence of reaction mainly in the solid phase in the so-called solid-state polymerization.

The molecular weight distribution of PVCar obtained in the suspension polymerization shows one peak at high molecular weight and several peaks at low molecular weight. The first peak in the high molecular weight region was similar to that of the solution polymerization, and several peaks at low molecular weight region were similar to those of the solid-state polymerization. These facts might be explained in the following terms. In the suspension polymerization of VCar, the polymerization proceeds not only along the interface between the monomer crystal and the dispersing medium but also within the monomer crystal. The propagation in the former case is close to that in the solution polymerization and the propagation in the latter case is similar to that in the solid-state polymerization.

On the other hand, the molecular weight distribution of PVCar obtained in the radiation-induced solid-state polymerization showed a sharp peak at high molecular weight and a broad peak in the low molecular weight region. This is quite different from the molecular weight distribution of PVCar obtained in the catalytic solid-state polymerization.

It has been reported that in the radiation-induced solid-state polymerization the initiation takes place not only on the surface of monomer crystal but also within the crystal and that the orientation of monomer is disordered around the growing chain end due to the reaction heat.[10] In view of this, the circumstance around the growing chain end in the radia-

tion-induced solid-state polymerization might be thought to be close to that in solution polymerization.

On the other hand, although low molecular weight polymer was produced, dimer or trimer was not formed in the radiation-induced solid state polymerization. The ratio of the amount of the low molecular weight polymer to the total amount of polymer increased with increasing polymer yield. This might be due to the possibility that the concentration of monomer around the growing chain end decreases as the polymerization proceeds and consequently the termination reaction takes place easily at the latter stages of the polymerization; alternatively, it may be that the polymer formed is decomposed during the polymerization as was reported by Papissov and Kabanov.[8] However, it is difficult to determine which of them serves predominantly in the formation of the low molecular weight polymer at the present.

Present paper indicates that the molecular weight distributions of PVCar obtained in the catalytic solid-state polymerization, the cationic solution polymerization and the radiation-induced solid-state polymerization are all quite different. This fact gives additional strong support to conclusions drawn in the previous papers[1–5] that the propagation reaction in the catalytic solid-state polymerization proceeds mainly in the solid phase.

References

1. T. Matsuda, T. Higashimura, and S. Okamura, *Kobunshi Kagaku*, **22**, 180 (1965).
2. T. Matsuda, T. Higashimura, and S. Okamura, *Kobunshi Kagaku*, **23**, 269 (1966).
3. T. Matsuda, T. Higashimura, and S. Okamura, *Kobunshi Kagaku*, **23**, 273 (1966).
4. T. Matsuda, T. Higashimura, and S. Okamura, *Kobunshi Kagaku*, **24**, 165 (1967).
5. T. Matsuda, T. Higashimura, and S. Okamura, *J. Macromol. Sci. Chem.*, **A2**, 43 (1968).
6. A. A. Berlin, G. M. Trofinova, L. K. Pakhomova, E. V. Prut, J. M. Barkalov, S. S. Kugmina, N. S. Enikolopyan, and V. I. Goldanskii; *J. Polymer Sci., Part C, No. 16*, 2323 (1967).
7. A. A. Berlin, and N. S. Enikolopyan; *Vysokomol. Soedin.*, **8**, 451 (1966).
8. I. M. Papissov and V. A. Kabanov, in *Macromolecular Chemistry Prague 1965*, *J. Polym. Sci. C*, O. Wichterle and B. Sedláček, Eds., Interscience, New York, 1967, p. 911.
9. E. Kobayashi, T. Higashimura, and S. Okamura, *J. Macromol. Sci. Chem.*, **A1**, 1519 (1967).
10. H. Morawetz, in *First Biannual American Chemical Society Polymer Symposium* (*J. Polym. Sci. C*, **1**), H. W. Starkweather, Jr., Ed., Interscience, New York, 1963, p. 65.

Received June 11, 1969
Revised July 29, 1969

JOURNAL OF POLYMER SCIENCE: PART A-1 VOL. 8, 495–503 (1970)

Radiation-Induced Postpolymerization of Nitroethylene

HITOSHI YAMAOKA, ISAMU OBAMA, KOICHIRO HAYASHI, and SEIZO OKAMURA, *Department of Polymer Chemistry, Kyoto University, Kyoto, Japan*

Synopsis

Radiation-induced postpolymerization of nitroethylene in 2-methyltetrahydrofuran glass has been studied and discussed in reference to the results obtained from ESR measurements. No postpolymerization occurred at the temperature below −150°C. In the temperature range between −135°C and −78°C, the polymer yield decreased with increasing postpolymerization temperature. The polymer yield increased linearly with the increase of the preirradiation dose in the range below 0.9×10^6 r. The mean value for chain initiation was estimated to be about 1.3. The following correlations were observed between the results of the postpolymerization and ESR measurements. The postpolymerization started in the temperature range between −140°C and −135°C, where the ESR spectrum due to the anion radicals of nitroethylene disappeared. The polymer yield of the postpolymerization decreased with the photoirradiation at −196°C before warming the samples in parallel with the photobleachability of the anion radicals observed in the glassy mixture by the ESR method. It was concluded from these results that the radiation-induced postpolymerization was initiated by the anion radicals of nitroethylene formed by the capture of electrons.

INTRODUCTION

Glassy systems containing monomers seems to be suitable for studying the initial processes of radiation-induced polymerizations, since active species involved in reactions are easily trapped in the glasses and can be observed by various spectroscopic techniques. Radiation-induced polymerizations in glasses at low temperatures have been reported in the last few years. The polymerizations of several derivatives of acrylic monomers,[1–6] vinyl acetate,[2,7] vinyl chloride,[5] styrene[2,5] and acrylonitrile[5] in oils or other glass-forming systems were found to proceed by a free-radical mechanism. Bodard and Marx[8] reported that the polymerization of acrylonitrile in 2-methyltetrahydrofuran glass at low temperature proceeded by an anionic mechanism. Kamiyama et al.[9] observed in-source polymerization of isobutene in 3-methylpentane glass at −196°C by measurements of near-infrared spectra. Recently, Chapiro et al.[10] studied the polymerizations of acrylonitrile and styrene in various glasses and found a marked post-effect of the polymerizations in both anionic and cationic propagation.

In the course of investigations of the radiation-induced polymerization of nitroethylene, the effect of additives and the copolymerization with acrylonitrile confirmed anionic propagation;[11] also the propagation by free anions was assumed from the results of kinetical experiments.[12] Further, electron spin resonance (ESR),[13,14] optical,[15] and mass spectrometric investigations[16,17] of nitroethylene suggested that the polymerization was initiated by anion radicals of nitroethylene formed by the capture of electrons.

The present study is concerned with the radiation-induced postpolymerization of nitroethylene. The glassy mixture of nitroethylene in 2-methyltetrahydrofuran (MTHF) at low temperature is chosen as a polymerization system, and the postpolymerizations and ESR measurements are carried out at the same conditions. The initiating species of the postpolymerization are discussed in relation to the results obtained from the ESR measurements.

EXPERIMENTAL

Materials

Nitroethylene was prepared from the dehydration of 2-nitroethanol by the procedure of Buckly and Scaife.[18] For the purification of the monomer, special attention was paid to eliminate traces of water as described in the previous paper.[12] Commercial MTHF was distilled twice and dried over a sodium mirror. The monomer and MTHF were transferred to measuring ampoules by trap-to-trap distillation in vacuum and finally condensed into quartz ampoules.

Polymerization

Preirradiations were done at $-196°C$ in the dark by γ-rays from a 1000 Ci ^{60}Co irradiation source at Osaka Laboratory, Japan Atomic Energy Research Institute. The postpolymerizations were carried out in the temperature range between $-150°C$ and $-78°C$. After the irradiation, the ampoules were removed to a Dewar vessel kept at the postpolymerization temperature by blowing nitrogen gas, which was previously cooled by passing through a spiral tube in liquid nitrogen, into the Dewar vessel. The regulation of the temperature between $-150°C$ and $-78°C$ was performed by changing the rate of flow of the cooled nitrogen gas. The precision of the temperature control was $\pm 2°C$. A polymerization temperature of $-78°C$ was attained in the Dewar vessel with a Dry Ice–methanol mixture.

Polymer

In order to avoid the effect of melting technique on the polymer yield, the reaction mixture after the polymerization was again cooled down to $-196°C$ and crushed to a powder. Then, the mixture was poured at room

temperature into a vigorously stirred 1:1 water + methanol mixture, previously acidified with concentrated hydrogen chloride to prevent further polymerization. The polymer was isolated by filtering and then washed successively with water, ethyl alcohol, and ether. The polymer yield was determined gravimetrically. The molecular weight of the polymer was estimated from viscosity measurements as already reported.[12] The degree of polymerization, $\overline{DP}_n$, was calculated on the assumption that $\overline{M}_w/\overline{M}_n$ is equal to 2.0 for a most probable distribution.

Other Procedures

Photo-bleaching of the irradiated samples was done at −196°C for 1 hr by a 150-W tungsten lamp before warming of the samples. ESR measurements were carried out with an X-band conventional type spectrometer (Varian model V-4500).

RESULTS

ESR Measurements

A transparent glassy sample was obtained by cooling MTHF rapidly in liquid nitrogen. When the MTHF glass was irradiated at −196°C in the dark, the sample became blue in color and gave an ESR signal composed of a septet and a sharp singlet as shown in Figure 1*a*. The former is due to free radicals formed from MTHF molecules and the latter is due to trapped electrons in the glass as reported by Smith and Pieroni.[19] On the other hand, MTHF glass containing 1.5 mole-% nitroethylene did not give the spectrum due to the trapped electrons, but showed a new complex spectrum superposed on the spectrum of the MTHF radicals (Fig. 1b). On exposure of the irradiated glassy mixture to visible light, the new complex spectrum disappeared, and the shape of the spectrum changed from that in Figure 1*b* to that of MTHF radicals (Fig. 1*c*). Further, with an increase in the temperature of the irradiated mixture from −196°C, the new spectrum disappeared in the temperature range between −140°C and −135°C.

The new complex spectrum in Figure 1*b* is thought to be due to anion radicals formed through electron capture by added nitroethylene. The observed spectrum showed good agreement with that expected from the Hückel LCAO-MO calculation as an anion radical of nitroethylene.[14] The MTHF glass containing 0.15 mole-% nitroethylene showed spectra of both trapped electrons and the nitroethylene anion radicals after the irradiation. When the irradiated glassy mixture was kept at −196°C in the dark, the intensity of the signal from the trapped electrons gradually decreased and that of the nitroethylene anion radicals increased with time. This indicates that the nitroethylene molecule has the ability to act as a strong electron acceptor in accordance with the results obtained from the optical[15] and the mass spectrometric investigations.[16,17] The new spectrum is readily bleached out with visible light. The sensitivity of the spectrum

to visible light seems not to result from the nature of ordinary neutral free radicals. From these results it is suggested that the new spectrum in Figure 1*b* is due to anion radicals of nitroethylene formed by the following mechanism:

$$\text{MTHF} \rightsquigarrow (\text{MTHF})^{+} + e$$

$$e + \text{nitroethylene} \rightarrow (\text{nitroethylene})^{-}$$

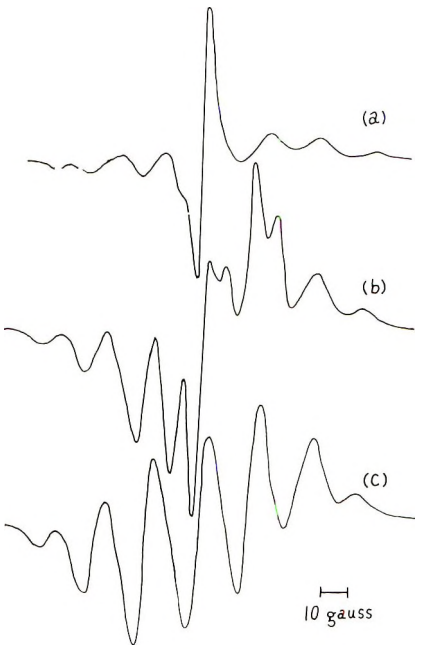

Fig. 1. ESR spectra of irradiated 2-methyltetrahydrofuran glass irradiated up to a dose of 1.0×10^5 r at -196°C: (*a*) pure 2-methyltetrahydrofuran glass (signal amplifier gain = 50); (*b*) glassy mixture of 2-methyltetrahydrofuran containing 1.5 mole-% nitroethylene (gain = 160), (*c*) pure 2-methyltetrahydrofuran glass and glassy mixture of 2-methyltetrahydrofuran containing nitroethylene bleached with visible light after γ-irradiation (gain: 160).

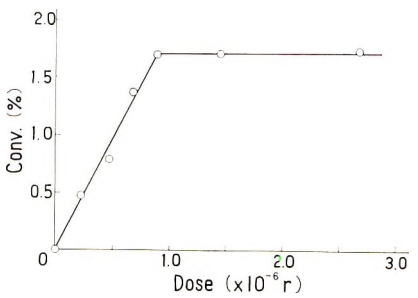

Fig. 2. Effect of preirradiation dose on polymer conversion. Experimental conditions are same as those of Table III.

Polymerization

In order to examine the in-source polymerization of nitroethylene, the samples were irradiated at −196°C and, immediately after irradiation, poured into a precipitating solvent at room temperature. The results are shown in Table I. No polymer was obtained in any case. It is evident that the in-source polymerization does not occur at −196°C.

TABLE I
Radiation-Induced In-Source Polymerization of Nitroethylene at −196°C[a]

Code	Sample			Conversion, %
	Monomer, ml	MTHF, ml	Monomer mole-%	
10	1.0	9.0	12.7	0
75	1.5	10.5	15.6	0
76	1.9	9.9	20.0	0
2	3.5	10.5	30.3	0

[a] Dose rate, 3.12×10^4 r/hr; total dose 2.0×10^6 r.

TABLE II
Relation between Polymer Conversion and Postpolymerization Temperature[a]

Code	Monomer concn, mole-%	Polymerization temperature, °C	Conversion, %
90	25.0	−78	0.6
87	25.0	−95	0.7
66	25.0	−120	1.7
64	25.0	−135	2.3
26	11.6	−150	0

[a] Dose rate, 3.12×10^4 r/hr; total dose, 2.0×10^6 r; preirradiation temperature, −196°C; polymerization time, 150 min.

The results of the postpolymerizations at various temperatures are summarized in Table II. Polymer was not obtained at −150°C. In the temperature range between −135°C and −78°C, the polymer yield decreased with increasing postpolymerization temperature.

The effect of the preirradiation dose of the conversion is shown in Figure 2 and Table III. The polymer conversion increased with increasing preirradiation dose, and then leveled off in the dose range above 0.9×10^6 r. The mean value of G(monomer) was calculated to be 2.73×10^2 from the slope of the linear part in Figure 2. The molecular weight of the polymers was not dependent on the dose, even for the preirradiations above 0.9×10^6 r, as shown in Table III.

The polymer yield increased linearly with increasing monomer concentration. Consequently, the polymer conversion was independent of the monomer concentration within the range examined, as shown in Figure 3.

The molecular weight of the polymers obtained was almost proportional to the monomer concentration. Since the concentration of the active species responsible for chain initiation can be derived from the quotient

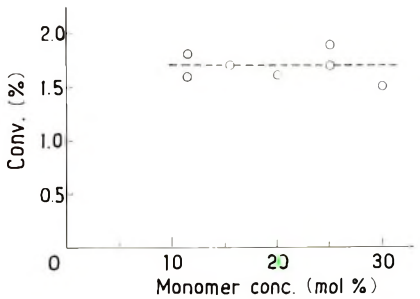

Fig. 3. Relation between polymer conversion and monomer concentration. Dose rate, 3.12×10^4 r/hr; total dose, 2.0×10^6 r; preirradiation temperature, $-196°C$; postpolymerization temperature, $-120°C$, polymerization time, 150 min.

(polymer yield)/(molecular weight), these results indicate that the concentration of the initiating species is independent of the monomer concentration.

TABLE III
Effect of Preirradiation Dose on Polymer Conversion and Molecular Weight of Polymer[a]

Code	Total dose, $\times 10^{-6}$, r	Conversion, %	G (monomer) $\times 10^{-2}$	$\bar{M}_w$ $\times 10^{-4}$
81	0.22	0.46	2.95	—
82	0.47	0.79	2.38	2.87
83	0.68	1.37	2.84	3.28
84	0.88	1.70	2.73	3.11
85	1.43	1.71	1.36	3.24
86	2.68	1.73	0.91	3.09

[a] Dose rate, 3.12×10^4 r/hr; preirradiation temperature, $-196°C$; postpolymerization temperature, $-120°C$; polymerization time, 150 min.; monomer concentration, 24.4 mole-%.

For comparison with the results of the ESR measurements, the effect of photo-bleaching on the postpolymerization was studied. After preirradiation at $-196°C$, the samples were exposed to visible light at the same temperature and then warmed to the postpolymerization temperature. As summarized in Table IV, the polymer yield obviously decreased with photo-irradiation. Similar results were reported for acrylonitrile by Bodard and Marx.[8]

TABLE IV
Effect of Photo-irradiation on the Postpolymerization of Nitroethylene[a]

Code	Monomer concn, mole-%	Postpolymerization temperature, °C	Photo-irradiation[b]	Conversion, %
18	11.6	−120	+	0.7
16	11.6	−120	None	1.6
65	25.0	−120	+	0.5
66	25.0	−120	None	1.7
69	25.0	−120	None	1.9
63	25.0	−135	+	1.0
64	25.0	−135	None	2.3
24	11.6	−150	+	0
26	11.6	−150	None	0

[a] Preirradiation and photo-irradiation temperature, −196°C; dose rate, 3.12×10^4 r/hr; total dose, 2.0×10^6 r; polymerization time, 150 min.

[b] Photo-irradiation by a tungsten lamp for 1 hr.

DISCUSSION

From the viewpoint of studying the initiation process of the radiation-induced polymerization, it is worthwhile to compare the results of the postpolymerization with those of the ESR measurements. The postpolymerization does not occur at below −150°C. Under the same conditions, the anion radicals of nitroethylene formed by the capture of electrons are stably trapped in the glassy mixture. Further, postpolymerization begins in the temperature range between −140°C and −135°C where the ESR spectrum due to the anion radicals disappears. The polymer yield of the postpolymerization decreases with photo-irradiation at −196°C. This fact suggests that the initiating species of the polymerization are deactivated by exposure to visible light. Also the anion radicals in the glassy mixture are bleached out by the photo-irradiation. These correlations indicate that the polymerization is initiated by anion radicals of nitroethylene as predicted by the optical[15] and the mass spectrometric investigations.[16,17] In the experiments of photo-bleaching, the absence of the polymer in the postpolymerization could be expected from the results of ESR measurements. However, the results of Table IV indicate that the photo-irradiation in the conditions used is insufficient for the polymerization system. This may be explained by the fact that the ampoules for the polymerization are much bigger than those for the ESR measurements.

Figure 3 shows that the concentration of the initiating species is independent of the monomer concentration. Further, the ESR study shows that the electrons trapped in the MTHF matrix are easily captured by a small quantity of nitroethylene in the system. These facts indicate that the G value for the production of the anion radicals of nitroethylene is about 2.6, which is the same as that for trapped electrons.[19] In order to deduce the initiating efficiency of the anion radicals for the postpolymerization, it is necessary to estimate the initiation yield G_i. In the present

study, G_i is obtained from the quotient G(monomer)/$\overline{DP}_n$ in the preirradiation dose range below 0.9×10^6 r. Since the average degree of polymerization was obtained as 2.1×10^2 from the results of Table III, the G_i value was estimated to be about 1.3. From these results, it is concluded that the anion radicals formed in the glassy mixture can effectively initiate the postpolymerization of nitroethylene.

The dependence of the preirradiation dose on the polymer conversion (see Fig. 2) indicates that at about 0.9×10^6 r the population of trapped ions reaches a limit beyond which the average distance between ion pairs probably interrupts further trapping. This argument is also supported by the fact that the molecular weights of the polymers obtained in the saturation range are almost the same as those at the dose below 0.9×10^6 r as shown in Table III.

It is not yet clear as to why the polymer yield decreases with increasing postpolymerization temperature in the range between -135°C and -78°C. Recently, Chapiro et al.[10] reported that very fast polymerization occurred in a narrow temperature range a few degrees above the glass transition point. Although the glass transition point in the present system is unknown, it may lie in the temperature range between -140 and -135°C, where the ESR spectrum due to the anion radicals just disappears. If the postpolymerization takes place in a limited temperature range around -140°C, the polymerization time, which means the remaining time in this temperature range, is considered to be inversely proportional to rate of temperature increase. Consequently, the polymer yield at lower temperatures is relatively higher than that at higher temperatures. Alternatively, these results can be explained by the rapid occurrence at elevated temperatures of charge recombination between charged species, which leads to prevent further propagation. From the results of Chapiro et al. and our experimental results that the postpolymerization starts with disappearance of the ESR spectrum due to the anion radicals, the former explanation seems to be more likely for this polymerization system.

In conclusion, the results obtained in the present study support the concept that the radiation-induced polymerization of nitroethylene is initiated by anion radicals and proceeds by a free anionic mechanism.

The authors express their gratitude to Dr. H. Yoshida of Research Reactor Institute, Kyoto University and Mr. K. Tsuji of Sumitomo Chemical Company, Ltd. for their helpful discussions and their collaboration in measuring the ESR spectra.

References

1. Y. Amagi and A. Chapiro, *J. Chim. Phys.*, **59**, 537 (1962).
2. A. Chapiro and M. Pertessis, *J. Chim. Phys.*, **61**, 991 (1964).
3. A. Chapiro and L. Perec, *J. Chim. Phys.*, **63**, 842 (1966).
4. A. Chapiro and S. Nakashio, *J. Chim. Phys.*, **63**, 1031 (1966).
5. A. Chapiro and D. Roussel, in *Macromolecular Chemistry Prague 1965* (*J. Polym. Sci. C*, **16**), O. Wichterle and B. Sedláček, Eds., Interscience, New York, 1967, p. 3011.
6. I. Kaetsu, K. Tsuji, K. Hayashi, and S. Okamura, *J. Polym. Sci. A*, **5**, 1899 (1967).

7. I. M. Balkalov, V. I. Goldanskii, N. S. Enikolopyan, S. F. Terekhova, and G. M. Trofimova, *Vysokomol. Soed.*, **6**, 98 (1964); *Macromolecular Chemistry Paris 1963*, (*J. Polym. Sci. C*, **4**) M. Magat, Ed., Interscience, New York, 1964, p. 909.

8. M. Bodard-Gauthier and R. Marx, in *Macromolecular Chemistry, Prague 1965*, (*J. Polym. Sci. C*, **16**), O. Wichterle and B. Sedlàček, Eds., Interscience, New York, 1968, p. 4241.

9. H. Kamiyama, K. Hayashi, and S. Okamura, *Ann. Rept. Japan Assoc. Rad. Res. Polymers*, **8**, 139 (1966/1967).

10. A. Chapiro, A. M. Jendrychowska-Bonamour, and L. Perec, in *Radiation Chemistry* (*Advan. Chem. Ser.* **82**), American Chemical Society, Washington, D. C., 1968, p. 513.

11. H. Yamaoka, R. Uchida, K. Hayashi, and S. Okamura, *Kobunshi Kagaku*, **24**, 79 (1967).

12. H. Yamaoka, Ff. Williams, and K. Hayashi, *Trans. Faraday Soc.*, **63**, 376 (1967).

13. K. Tsuji, H. Yamaoka, K. Hayashi, H. Kamiyama, and H. Yoshida, *J. Polym. Sci. B*, **4**, 629 (1966).

14. K. Tsuji, H. Yoshida, K. Hayashi, and S. Okamura, *Kobunshi Kagaku*, **25**, 31 (1968).

15. H. Kamiyama, K. Hayashi, and S. Okamura, *Ann. Rept. Japan Assoc. Rad. Res. Polymers*, **7**, 145 (1965/1966).

16. H. Yamaoka, T. Shiga, K. Hayashi, S. Okamura, and T. Sugiura, *J. Polym. Sci. B*, **5**, 329 (1967).

17. T. Shiga, H. Yamaoka, K. Arakawa, and T. Sugiura, *J. Phys. Chem.*, to be published.

18. G. D. Buckley and C. W. Scaife, *J. Chem. Soc.*, **1947**, 1471.

19. D. R. Smith and J. J. Pieroni, *Can. J. Chem.*, **43**, 876 (1965).

Received June 10, 1969
Revised July 30, 1969

JOURNAL OF POLYMER SCIENCE: PART A-1 VOL. 8, 505–514 (1970)

Polymerization and Reaction of Tetraoxane with Various Olefins Catalyzed by $BF_3O\cdot(C_2H_5)_2$

T. MIKI, T. HIGASHIMURA, and S. OKAMURA, *Department of Polymer Chemistry, Kyoto University, Kyoto, Japan*

Synopsis

The copolymerization of tetraoxane with various olefins by $BF_3\cdot O(C_2H_5)_2$ in ethylene dichloride at 30°C has been studied. The gas chromatographic technique was employed for the determination of concentration of each compound. The rate of tetraoxane consumption was decreased by the addition of olefins in the order of; no addition > *trans*-stilbene > styrene > 1,1-diphenylethylene > 2-chloroethyl vinyl ether > cyclohexene ≥ indene ≥ α-methylstyrene. The formation of the methanol-insoluble copolymer of tetraoxane and olefin was not confirmed. However, 4-methyl-4-phenyl-1,3-dioxane and 4,4-diphenyl-1,3-dioxane were formed in the reaction of tetraoxane with α-methylstyrene and 1,1-diphenylethylene, respectively. 4,4-Diphenyl-1,3-dioxane was identified on the basis of the molecular weight measurement, elemental analysis and NMR and infrared spectroscopy. On the other hand, 1,3-dioxane derivatives were not formed in the reaction of tetraoxane with α,β-disubstituted olefins. Monomer composition dependence of the copolymerization of tetraoxane with 1,1-diphenylethylene or α-methylstyrene has been studied. The amount of 4,4-diphenyl-1,3-dioxane formed reached a maximum at a monomer composition of 1:1 in the reaction of tetraoxane with 1,1-diphenylethylene. The formation of cyclic dimer of α-methylstyrene was suppressed by tetraoxane.

INTRODUCTION

It has been found that copolymer could be obtained and that a large amount of 4-phenyl-1,3-dioxane is formed[1] in the copolymerization of tetraoxane with styrene by $BF_3\cdot O(C_2H_5)_2$ in ethylene dichloride at 30°C. In the present study, tetraoxane was copolymerized with various olefins by $BF_3\cdot O(C_2H_5)_2$ in ethylene dichloride at 30°C, and the results were compared with the result obtained in the tetraoxane–styrene system. Olefins used were: α-methylstyrene (αMS), indene, cyclohexene, 2-chloroethyl vinyl ether (CEVE), 1,1-diphenylethylene (DPE), and *trans*-stilbene.

An attempt was made to detect 1,3-dioxane derivatives which are expected to form in view of the formation of 4-phenyl-1,3-dioxane in the tetraoxane–styrene system. 4,4-Diphenyl-1,3-dioxane was isolated in the tetraoxane–DPE system and 4-methyl-4-phenyl-1,3-dioxane was probably formed in tetraoxane–αMS system. No 1,3-dioxane derivatives were observed in other systems. In addition, the monomer composition dependence of the copolymerization reaction was studied in DPE–tetraoxane and αMS–tetraoxane systems.

EXPERIMENTAL

Tetraoxane was purified by recrystallization from acetone solution.[1]

DPE was synthesized by the dehydration over $KHSO_4$ of diphenyl ethyl carbinol which was obtained from bromobenzene and acetophenone[2] and DPE was purified by repeated distillation at reduced pressure. Other materials were purified by distilling commercial products.

The copolymerization procedure was the same as described in the previous paper.[1] The amount of each product in the reaction system at a given period of time was measured by gas chromatography, adopting the internal standard method. Columns used were poly(ethylene glycol) 4000–C 22, dinonyl phthalate–Celite 545, and silicon DC 550–Celite 545; internal standards used were: benzene, *m*-xylene, *p*-cymene, *trans*-decalin, α-bromonaphthalene, and benzyl benzoate.

RESULTS AND DISCUSSION

Effect of Olefins on Polymerization of Tetraoxane

Tetraoxane was copolymerized with various olefins by $BF_3 \cdot O(C_2H_5)_2$ in ethylene dichloride at 30°C. The rates of consumption of tetraoxane and olefin and the rate of formation of trioxane were measured by gas chromatography.[1] The reaction conditions and the results are shown in Table I,

TABLE I
Change in Concentration of Each Component in Polymerization of Tetraoxane (TeX) with Various Olefins[a]

Olefin	$[Olefin]_0$, mole/l.	$[TeX]_{60}$, mole/l.	$[ToX]_{60}$, mmole/l.	$[Olefin]_{60}$, mole/l.
αMS	0.85	0.217	1.7	0.28
Indene	1.03	0.213	2.8	0.28
Cyclohexene	0.99	0.208	3.3	0.94
"	0.50	0.204	4.5	0.45
CEVE	1.08	0.188	11.1	0
DPE	0.48	0.163	10.0	0.29
Styrene	0.75	0.129	16.1	0.24
trans-Stilbene	0.50	0.083	50.0	0.49
None	—	0.046	106	—

[a] $[TeX]_0$, 0.250 mole/l.; $[BF_3 \cdot O(C_2H_5)_2]_0$, 4 mmole/l.; 30°C; reaction time, 60 min.

where the data concerning the homopolymerization of tetraoxane are also included; $[TeX]_{60}$, $[ToX]_{60}$, and $[Olefin]_{60}$ denote the concentrations of tetraoxane, trioxane, and olefin at a reaction time of 60 min.

As is clear from Table I, the rate of consumption of tetraoxane was decreased by the addition of olefins in the order: *trans*-stilbene > styrene > DPE > CEVE > cyclohexene ≥ indene ≥ αMS. This means that olefins interact with the active center produced from tetraoxane and that the

carbonium ions produced from olefines react difficultly with tetraoxane. It was confirmed that almost no cyclohexene was consumed at the reaction time of 60 min on the addition of $BF_3 \cdot O(C_2H_5)_2$ to the cyclohexene solution of 1.0 mole/l. in ethylene dichloride at 30°C. The order of reactivities of these olefins was thus independent of homopolymerizability of olefins.

On the other hand, the amount of trioxane formed at 60 min was also decreased by the addition of olefins in almost the same order as of suppression of the consumption of tetraoxane as shown in Table I, and the ratio of trioxane formed to tetraoxane consumed on the addition of olefins was smaller than that without the addition of olefins. This means that the attack of olefin on the tetraoxane growing chain takes place predominantly before the latter attacks the oxygen atom in its own chain (back-biting reaction) to form trioxane.

The methanol-insoluble polymer was isolated under the experimental conditions (Table I) in indene–tetraoxane, cyclohexene–tetraoxane, CEVE–tetraoxane, styrene–tetraoxane, and *trans*-stilbene–tetraoxane systems. The yield of the methanol-insoluble polymer and the related data are summarized in Table II; the data for the styrene–tetraoxane system were excluded, as they have already been reported.[1] The infrared spectra of the methanol-insoluble polymer obtained in the cyclohexene–tetraoxane and *trans*-stilbene–tetraoxane systems were almost the same as the spectrum of polyoxymethylene, and the infrared spectra of the methanol-insoluble polymer obtained in indene–tetraoxane and CEVE–tetraoxane systems were almost the same as those of polyindene and poly-CEVE, respectively.

Formation of Cyclic Oligomers

In the copolymerization of tetraoxane with styrene catalyzed by $BF_3 \cdot O(C_2H_5)_2$ in ethylene dichloride at 30°C, 4-phenyl-1,3-dioxane was produced.[1]

TABLE II
Methanol-Insoluble Polymer (P) Yield and Related Data in Polymerization of Tetraoxane with Various Olefins[a]

Olefin	P yield, wt-%	ToX yield, wt-%	Total monomer consumption, wt-%	TeX in monomer feed, mole-%	TeX in monomers reacted, mole-%	IR spectrum of polymer[b]
Indene	44.8	0.17	64.5	19.5	4.5	POL
Cyclohexene	0.15	0.25	7.7	20.1	45.5	—
"	1.21	0.35	13.4	33.3	48.5	POM
CEVE	68.3	0.69	84.5	18.8	5.4	POL
trans-Stilbene	5.92	3.75	18.7	33.3	92.5	POM
None	48.3	31.7	81.7	—	—	POM

[a] Reaction conditions are the same as in Table I.

[b] POL, homopolymer of olefin; POM, polyoxymethylene.

According to the mechanism of formation of this compound, various 1,3-dioxane derivatives will be expected to form in the copolymerization of tetraoxane with various olefins, as is shown in eqs. (1) and (2), where I

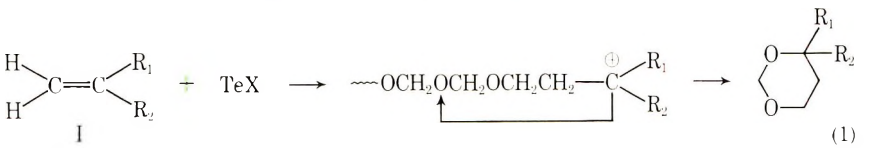

I (1)

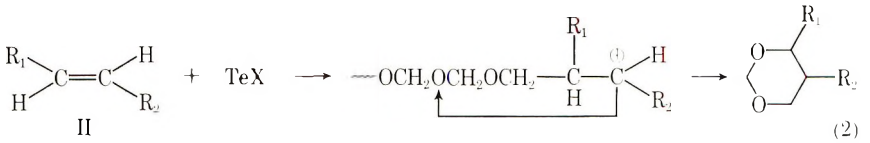

II (2)

denotes α,α-disubstituted olefins including $R_1 = H$ and II denotes α,β-disubstituted olefins, including cyclic olefins. An attempt was made by gas chromatography to detect these 1,3-dioxane derivatives expected to form in all systems mentioned above.

The formation of 4-methyl-4-phenyl-1,3-dioxane has been confirmed in the reaction of αMS with aqueous formaldehyde in the presence of relatively high concentrations of sulfuric acid.[3] 4-Methyl-4-phenyl-1,3-dioxane was likely to form also in the copolymerization of tetraoxane with αMS. Indeed, the amount of this compound produced under the investigated conditions was quite small (see Fig. 4 below) as compared with the amount of 4-phenyl-1,3-dioxane formed during the copolymerization of tetraoxane with styrene under the same conditions.[1]

On the other hand, a white crystalline compound with melting point of 81°C was isolated in the reaction of tetraoxane with DPE and purified by recrystallization from ethanol solution. This new compound was identified as 4,4-diphenyl-1,3-dioxane on the basis of ebullioscopic measurement of molecular weight, elemental analysis, and infrared and NMR spectroscopy. The molecular weight was found to be 245 (calcd, 240.3). The elemental analysis found was H, 6.69%; C, 80.0% (calcd: H, 6.71%; C, 79.97%). Infrared and NMR spectra are shown in Figures 1 and 2, respectively. The infrared spectrum was similar to that of 4-phenyl-1,3-dioxane.[4] The absorption peaks of the NMR spectrum were assigned as shown in Figure 2 on the basis of NMR spectra of 1,3-dioxane and tetrahydrofuran[5] and of the ratio of peak area, found to be 0.98:1.02:1.00:5.00 (= 5-CH_2:6-CH_2:2-CH_2:C_6H_5, from high to low field).

However, the formation of 1,3-dioxane derivatives was not confirmed under our conditions (Table I) by gas chromatography in the *trans*-stilbene–tetraoxane, cyclohexene–tetraoxane, and indene–tetraoxane systems. Then, this may mean that the reaction of eq. (2) takes place with difficulty, compared with the reaction of eq. (1). 1,3-Dioxane derivatives are thought to be formed by the "back-biting" reaction of the growing chain end with depolymerization, as is shown in eqs. (1) and (2). Therefore, the back-

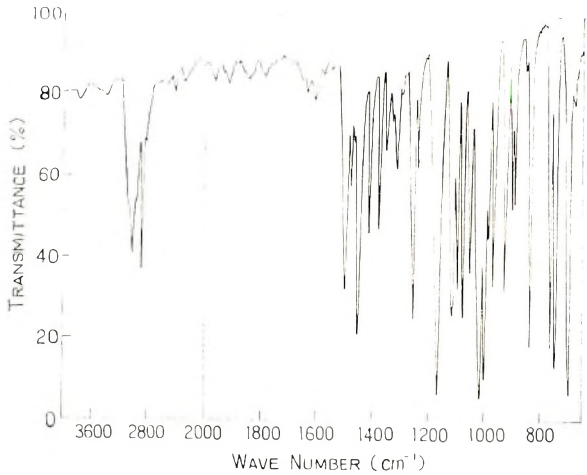

Fig. 1. Infrared spectrum of reaction product 4,4-diphenyl-1,3-dioxane in copolymerization of tetraoxane and 1,1-diphenylethylene by $BF_3 \cdot O(C_2H_5)_2$ at 30°C.

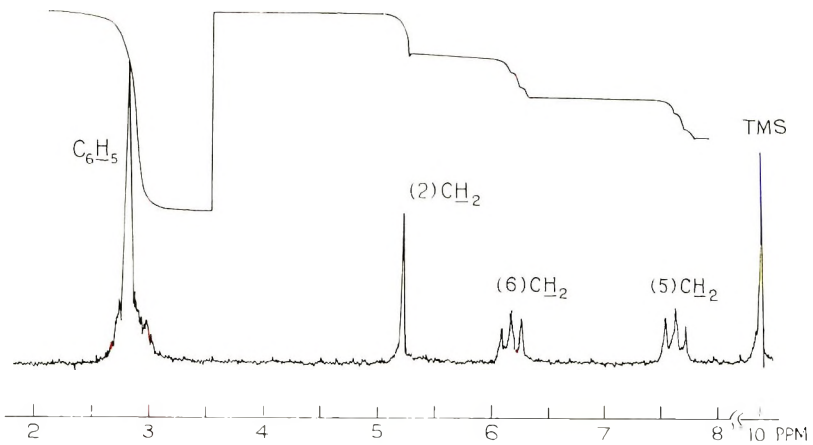

Fig. 2. NMR spectrum of reaction product 4,4-diphenyl-1,3-dioxane in the copolymerization of tetraoxane and 1,1-diphenylethylene by $BF_3 \cdot O(C_2H_5)_2$ (room temperature, 10 wt-% in CCl_4, 60 MHz).

biting reaction of the growing chain end composed of α,β-disubstituted olefin or cyclic olefin takes place with great difficulty, probably due to the limited movement of the growing chain end because of the substituent at the penultimate carbon.

The amount of 4,4-diphenyl-1,3-dioxane formed in the reaction of tetraoxane with DPE will be shown later. The amount of 1,3-dioxane derivative formed in the reaction of tetraoxane only with α-substituted olefins decreased in the order: DPE > styrene > αMS > CEVE; actually no 1,3-dioxane derivative was produced in the tetraoxane–CEVE system. This order among the four olefins is different from the order of suppression of the polymerization of tetraoxane (in the latter case, styrene > DPE >

CEVE > αMS). The order, DPE > styrene > αMS > CEVE, seems to be related to the homopolymerizability of these olefins, in which DPE has the least homopolymerizability. Therefore, it might be concluded that the 1,3-dioxane derivative forms in larger quantities in the reaction of tetraoxane with an α-substituted olefine of poorer homopolymerizability.

Reaction of Tetraoxane with 1,1-Diphenylethylene

As the formation of 4,4-diphenyl-1,3-dioxane was confirmed in the tetraoxane–DPE system, the reaction of tetraoxane with DPE was investigated in detail. The result is shown in Figure 3, where the amount of each component was determined by gas chromatography according to the internal standard method, except for the methanol-insoluble polymer, which was determined gravimetrically. The total consumption of monomers increased markedly to about 50 mole-% with increasing tetraoxane feed. The methanol-insoluble polymer began to form at a tetraoxane feed of more than about 50 mole-%, and the amount of trioxane formed increased slowly with the increase in the tetraoxane feed. On the other hand, the amount of 4,4-diphenyl-1,3-dioxane formed reaches a maximum at a tetraoxane feed of about 50 mole-%, just as the amount of 4-phenyl-1,3-dioxane formed in the copolymerization of tetraoxane with styrene reached a maximum at a tetraoxane feed of about 50 mole-%.[1] The remarkable increase in the total consumption of monomers up to the tetraoxane feed of about 50 mole-% was ascribed to the predominant formation of 4,4-diphenyl-1,3-dioxane.

The ratio of monomers reacted was almost equal to the initial composition of monomer feed, so the relative reactivity of DPE is thought to be similar to that of tetraoxane. The formation of the methanol-insoluble polymer was not so markedly suppressed by the addition of a very small

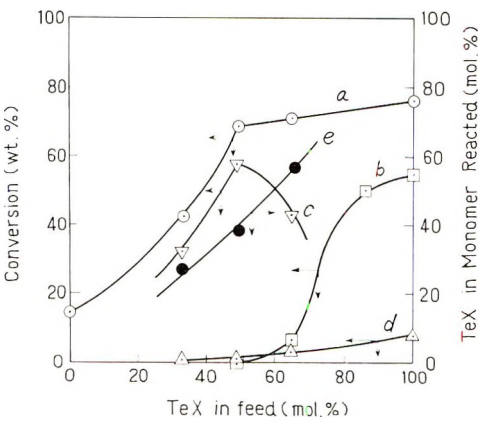

Fig. 3. Monomer-composition dependence of conversion and ratio of monomers reacted at a reaction time of 60 min in the copolymerization of tetraoxane with 1,1-diphenylethylene at 30°C: (○) total monomer consumption; (□) polymer yield; (▽) 4,4-diphenyl-1,3-dioxane yield; (△) trioxane yield; (●) ratio of monomers reacted. $[M]_0$, 0.76 mole/l.; $[BF_3 \cdot O(C_2H_5)_2]_0$, 4.0 mmole/l.

amount of DPE to tetraoxane. So it ought to be expected that the copolymer can be formed in this system. However, infrared spectrum of the methanol-insoluble polymer obtained at a tetraoxane feed of 65.5 mole-% (Fig. 3) was almost the same as that of polyoxymethylene, and the formation of copolymer was not confirmed.

It should be noted that the amount of 4,4-diphenyl-1,3-dioxane formed is almost the entire amount of monomers reacted up to a tetraoxane feed of about 50 mole-% (Fig. 3). This fact means that the formation of this cyclic compound is not due to the acid-catalyzed, formaldehyde–olefin reaction or Prins reaction but due to the eq. (1). According to the Prins reaction, one gram-mole of water is needed for the formation of one gram-mole of 4,4-diphenyl-1,3-dioxane from DPE and formaldehyde which might be derived from tetraoxane. However, the amount of 4,4-diphenyl-1,3-dioxane produced was considerably in excess of the amount of water in the reaction system, which was found to be less than 3 mmole/1. On the other hand, a growing chain end, composed of a few oxymethylene units followed by DPE carbonium ion is necessary for the formation of 4,4-diphenyl-1,3-dioxane according to eq. (1). However, it is not clear at present why the growing chain end attacks preferentially the oxygen atom in its own chain, rather than the oxygen atom of tetraoxane leading to the expectable formation of high molecular weight copolymer. The formation of 4,4-diphenyl-1,3-dioxane is a depolymerization process, so that high molecular weight copolymer might be obtained if the polymerization temperature were lowered or if monomer concentrations were increased. These are subjects of a future work.

Effect of Cyclic Oxygen Compounds on Cyclic Dimerization of α-Methyl Styrene

The effect of the monomer composition was studied in the copolymerization reaction of tetraoxane with αMS catalyzed by $BF_3 \cdot O(C_2H_5)_2$ in ethylene dichloride at 30°C. The result is shown in Figure 4. The homopolymerization of αMS catalyzed by $BF_3 \cdot O(C_2H_5)_2$ takes place very rapidly in ethylene dichloride at 30°C but no methanol-insoluble polymer of high molecular weight is produced. Indeed, αMS was almost completely consumed within 2 min under the investigated conditions, as is shown in Figure 5. In the copolymerization of tetraoxane with αMS, however, αMS was not all consumed even at a reaction time of 60 min under the investigated conditions (Fig. 4). Thus the rate of consumption of αMS was decreased by the addition of tetraoxane. The total monomer consumption has a minimum at a tetraoxane feed of about 65 mole-%. The relationship between composition of monomer feed and ratio of monomers reacted showed that the relative reactivity of αMS is larger than that of tetraoxane. The formation of the methanol-insoluble polymer was markedly suppressed by the addition of a very small amount of αMS to the tetraoxane, just as the formation of methanol-insoluble polymer was hindered by the addition of a very small amount of styrene to trioxane, the relative reactivity of styrene

being larger than that of trioxane.[4] So the formation of copolymer cannot be expected in this system; actually, the infrared spectrum of methanol-insoluble polymer obtained at the tetraoxane feed of 91 mole-% (Fig. 4) was almost the same as that of polyoxymethylene.

On the other hand, a cyclic dimer of αMS, 1,1,3-trimethyl-3-phenylindane, was observed to form in the homopolymerization of αMS with acid at near room temperature.[6] The amount of 1,1,3-trimethyl-3-phenylindane pro-

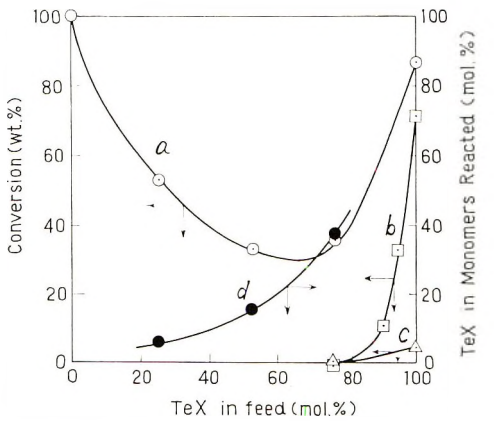

Fig. 4. Monomer–composition dependence of conversion and ratio of monomers reacted at a reaction time of 60 min. in the copolymerization of tetraoxane with α-methylstyrene at 30°C: (○) total monomer consumption; (□) polymer yield; (△) trioxane yield; (●) ratio of monomers reacted. $[M]_0$, 1.00 mole/l.; $[BF_3 \cdot O(C_2H_5)_2]_0$, 4.0 mmole/l.

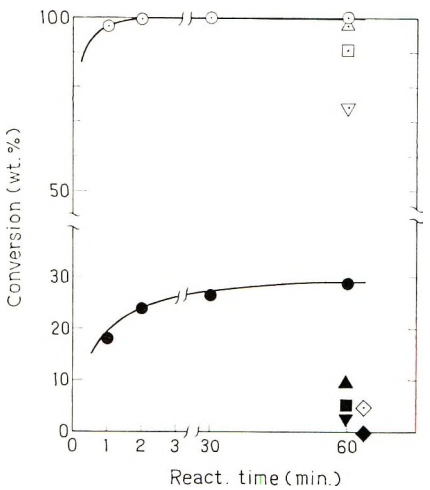

Fig. 5. Polymerization of α-methylstyrene on the addition of 1,4-dioxane catalyzed by $BF_3 \cdot O(C_2H_5)_2$ at 30°C: (⊙, ▽, △, ⊡, ◱) consumption of α-methylstyrene (αMS); (●, ▼, ▲, ■, ◆) yield of cyclic dimer of αMS. Concentrations of 1,4-dioxane added: (⊙, ●) none; (△, ▲) 14.3 mmole/l.; (⊡, ■), 28.5 mmole/l.; (▽, ▼) 57 mmole/l.; (◇, ◆) 400 mmole/l. $[\alpha MS]_0$, 0.685 mole/l.; $[BF_3 \cdot O(C_2H_5)_2]_0$, 4 mmole/l.

duced was measured by gas chromatography by the internal standard method. The result is shown in Figure 5; the yield of the cyclic dimer to αMS charged was about 30 wt-% under the investigated conditions. In the copolymerization of tetraoxane with αMS, however, the cyclic dimer of αMS was not produced under the investigated conditions (Fig. 4).

1,1,3-Trimethyl-3-phenylindane has been considered to be formed by an irreversible cyclization of the dimer cation, which is regarded as an intramolecular alkylation, as is shown in eq. (3).[6] Thus the dimer cation (III)

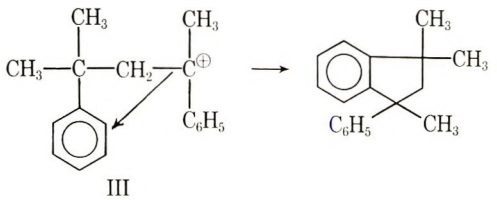

III (3)

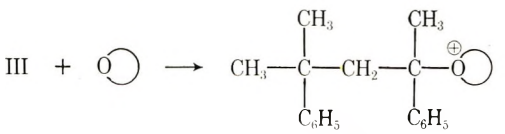

IV (4)

plays an important role in the formation of the cyclic dimer. In the presence of cyclic oxygen compounds like tetraoxane, however, this dimer cation (III) will be solvated selectively by cyclic oxygen compound molecule and transformed to a more stable oxonium ion (IV) which is thought to be less reactive than ion (III), as is shown in eq. (4). This may be the reason why the formation of the cyclic dimer of αMS is suppressed in the copolymerization of tetraoxane with αMS. Moreover, this kind of solvation by cyclic oxygen compounds will be applied not only to the dimer cation (III) but also other cation of various chain lengths. This may be the reason why the rate of consumption of αMS is small in the copolymerization of tetraoxane with αMS, compared with that in the homopolymerization of αMS.

To clarify the mechanism of selective solvation of carbonium ion with cyclic oxygen compounds, 1,4-dioxane was used instead of tetraoxane, because the former cannot be polymerized by acidic catalysts. The effect of addition of 1,4-dioxane on the rate of consumption of αMS and the formation of the cyclic dimer is also illustrated in Figure 5.

As is clear from Figure 5, the rate of consumption of αMS and the amount of the cyclic dimer of αMS formed decreased with increasing the amount of 1,4-dioxane added. The amount of the cyclic dimer of αMS was markedly decreased on the addition of a very small amount of 1,4-dioxane, as compared with that obtained without addition of 1,4-dioxane, while αMS was almost all consumed. This fact might support strongly the mechanism of solvation of carbonium ion with cyclic oxygen compounds suggested in eq. (4).

Furthermore, αMS was copolymerized with DPE, a monomer which has no oxygen atom in the molecule but a relative reactivity similar to tetraoxane. $BF_3 \cdot O(C_2H_5)_2$ in ethylene dichloride at 30°C was used. αMS was all consumed and primarily the cyclic dimer of αMS was produced. The yield of the cyclic dimer to the amount of αMS charged was 21 wt-% at a reaction time of 60 min and at initial concentrations of αMS, DPE, and $BF_3 \cdot O(C_2H_5)_2$ of 0.685, 0.140, and 4×10^{-3} mole/l., respectively. Thus it was shown that an olefin does not as markedly suppress the consumption of αMS and the formation of the cyclic dimer of αMS as a cyclic oxygen compound.

References

1. T. Higashimura, A. Tanaka, T. Miki, and S. Okamura, *J. Polym. Sci. A-1*, **5**, 1937 (1967).
2. *Organic Synthesis Coll. Vol. 1*, H. Gilman and A. H. Blatt, Eds., Wiley, New York, 1941, p. 226.
3. J. F. Walker, *Formaldehyde*, 3rd ed., Reinhold, New York, 1964, p. 422.
4. T. Higashimura, A. Tanaka, T. Miki, and S. Okamura, *J. Polym. Sci. A-1*, **5**, 1927 (1967).
5. F. A. Bovey, *NMR Data Tables for Organic Compounds*, Interscience, New York, 1967.
6. D. J. Worsfold and S. Bywater, *J. Amer. Chem. Soc.*, **79**, 4917 (1957).

Received May 5, 1969
Revised August 1, 1969

JOURNAL OF POLYMER SCIENCE: PART A-1 VOL. 8, 515–521 (1970)

Properties of Nylon 6 Anionically Obtained with $NaAl(LAc)_4$ Catalyst and Polymerization of ϵ-Caprolactam with $NaAl(Lac)_3(OEt)$ Catalyst

T. KONOMI* and H. TANI, *Department of Polymer Science, Faculty of Science, Osaka University, Machikaneyama, Toyonaka, Osaka, 560, Japan*

Synopsis

The *m*-cresol-insoluble polymer of ϵ-caprolactam obtained with $NaAl(Lac)_4$ catalyst is converted to a soluble polymer on treatment with dilute (0.1 wt-%) aqueous hydrochloric acid without any accompanying degradation of polymer chain. Aluminum contained in the polymer was not removed completely by extensive extraction with methanol, regardless of the solubilities of the polymers. This fact suggests the existence of two forms of aluminum in the polymer: one contributes to insolubility of the polymer and the other does not. The polymerization behavior in the case of $NaAl(Lac)_3(OEt)$ was somewhat different from that of $NaAl(Lac)_4$ and of $NaAl(Lac)_3(NHBu)$. These results are considered to reflect a difference in the stability of the Al-O, Al-(Lac), and Al-N bonds in the catalyst.

INTRODUCTION

Anomalous behavior of $MAlEt_4$ catalyst in the high-temperature polymerization of ϵ-caprolactam, in comparison with alkali metal catalyst, was reported in a previous work.[1]

The polymer obtained at 170–200°C was insoluble in *m*-cresol even after treatment with methanol or water for 6–16 hr. The key factor for formation of insoluble polymer is the catalytic behavior of the aluminum component: the solubility of the polymer is determined solely by whether Al caprolactamate has a catalytic activity or not.

In this paper, the effect of treatment of an insoluble polymer with aqueous hydrochloric acid on the content of aluminum remaining attached in the polymer was studied. In addition, the temperature change of the polymerized system in connection with the action of Al lactamate as an initiator and the polymerization with $NaAlEt_3(OEt)$ as a catalyst in comparison with that by $NaAlEt_3(NH\text{-}n\text{-}Bu)$[1] were examined.

* Present address: Katata Research Institute, Toyo Spinning Co., Ltd., Katata Shiga, Japan.

EXPERIMENTAL

Treatment of Polymer with Aqueous Hydrochloric Acid

The polymer used for this experiment was prepared with $NaAl(Lac)_4$ (0.25 mole-%) catalyst at 255°C for 30 min.

For convenience of efficient extraction, the polymer was shaped by lathe turning. Polymer was treated with 0.1 or 0.25 wt-% of boiling aqueous hydrochloric acid (12 ml/0.06 g of polymer) for a given time and then with boiling water for 5 hr.

Determination of Aluminum Remaining Attached in the Polymer After Treatment with Aqueous Hydrochloric Acid

The polymer used was prepared with $NaAl(Lac)_4$ (ca. 5.0 mole-%) at 202°C for 60 min. The polymer was extracted in the same manner as described above. The remaining aluminum content was determined by EDTA or by colorimetry.

Measurement of Temperature Change in the Polymerization System

Temperature change was measured directly with a thermometer inserted in the polymerization system composed of monomer (4.168 g) and Na caprolactamate or $NaAl(Lac)_4$ (0.5 mole-%). The polymerization vessel had an inside diameter of 15 mm; the thickness of wall was ca. 1 mm.

Polymerization of ε-Caprolactam with $NaAl(Lac)_3(OEt)$ as Catalyst

$NaAlEt_3(OEt)$ was prepared by vigorously stirring equimolar amounts of $NaAlEt_4$ and ethanol in benzene at room temperature, and then by evaporating the reaction mixture at 50°C under 4 mm Hg pressure. The reaction of $NaAlEt_3(OEt)$ with ε-caprolactam was carried out at 120°C for 30 min after removal of bubbles formed by the reaction at 121°C under 10 mm Hg pressure. Polymerization of the system thus obtained and after-treatment was done in the same manner as described previously for $NaAl(Lac)_4$.[1]

RESULTS AND DISCUSSION

Solubility and Reduced Viscosity of the Polymer after Treatment with Aqueous Hydrochloric Acid

The effect of the treatment time on the degradation of polymer was studied by the use of 0.1 and 0.25 wt-% aqueous hydrochloric acid (Table I). Hydrolytic degradation of polymer by this acid treatment was observed for both polymers A and B. The degree of degradation was almost the same in both polymers after 120 min treatment, and the change from insoluble to soluble polymer was observed in the first stage of treatment. This fact implies that some acid-labile chemical bond in the polymer struc-

TABLE I
Effect of the Acid-Treatment Time on the Reduced Viscosity of Polymer[a]

Treatment time, min	η_{sp}/c[b]			
	Polymer A[c]		Polymer B[d]	
	0.10 wt-% HCl	0.25 wt-% HCl	0.10 wt-% HCl	0.25 wt-% HCl
0	Insoluble	Insoluble	3.56	—
30	8.64	5.22	3.86	3.07
60	5.58	4.23	3.48	2.37
90	5.72	3.43	3.28	2.31
120	4.76	2.87	3.32	2.10
180	3.97	2.14	2.81	1.43

[a] 0.06 g of polymer was treated with 12 ml of aqueous hydrochloric acid.

[b] From solution viscosity of a solution containing 0.5 g of polymer/100 ml of *m*-cresol at 30°C.

[c] Polymer A: an insoluble polymer prepared by using $NaAl(Lac)_4$ (0.25 mole-%) at 202°C for 2 hr.

[d] Polymer B: a soluble polymer prepared by using Na(Lac) (0.125 mole-%) at 255°C for 30 min.

ture, for example $Al(NH—polymer)_3$, is a key factor for the insolubility of the polymer A.

The relation between aluminum content and solubility of the polymer treated with aqueous hydrochloric acid was studied (Table II). The aluminum content decreases with increasing concentration of the acid used, and the polymer becomes soluble only in the low aluminum content range.

In combining the results shown in Table I and II, there is no obvious correlation between aluminum content remaining after by extraction and the insolubility of the polymer. The aluminum which remains, therefore, must be classified in two different bonding types: one contributes to

TABLE II
Solubilities and the Aluminum Remaining in the Polymers Treated with Hydrochloric Acid[a]

Concn of hydrochloric acid, wt-%	η_{sp}/c	Al remaining in the polymer, mole-%[b]
0	Insoluble	4.25
0.05	Insoluble	2.87
0.50	Insoluble	0.628
1.00	Insoluble	0.167
2.50	1.723	0.004[c]

[a] The polymer used was prepared by using $NaAl(Lac)_4$ (ca. 5.0 mole-%) at 202°C for 60 min. A polymer slab turned in a lathe (thickness, 0.1–0.2 mm; width, 1.0–1.5 mm) was used for the treatment. Hydrochloric acid/polymer = 20 ml/1.1 g.

[b] EDTA method unless otherwise noted.

[c] Colorimetric method.

TABLE III
Extraction of Alkali Metal (Sodium) in Polymer[a]

Extraction time, hr	Amount of sodium metal not extracted, %[b]
0.5	14.5
1.0	19.5
3.0	15.2
5.0	15.2
24.0	9.0

[a] Preparation condition of the polymer used: $NaAl(Lac)_4$, 0.50 mole-%; polymerization temperature, 202°C; time, 60 min.

[b] The value obtained by titration relative to the charged value in the polymerization.

the insolubility of the polymer and the other does not. It is considered that the former is one which binds aluminum to the polymer NH-end group in the initiation reaction, and the latter is one which binds to the amide groups in the polymer chain and or in monomer.

These considerations are inconsistent with the facts that the *m*-cresol-insoluble polymer is formed only under polymerization conditions in which $Al(LAc)_3$ has no catalytic activity and that aluminum is not removed by methanol extraction, in contrast to sodium (remaining metal content is 60–85% for aluminum and only about 10% for sodium) (Table III).

$$(\text{polymer—NH})_3\text{Al} \xrightarrow{H^+} (\text{polymer—NH}_2) + Al^{+++}$$

$$\sim\!\!\sim\!\text{N—C(=O)—Al(Lac)}_2 \xrightarrow{H^+} \sim\!\!\sim\!\text{N(H)—C(=O)} + Al^{+++}$$

On treatment with aqueous hydrochloric acid, the aluminum atom which contributes to the insolubility of the polymer is splitted off from the polymer. Degradation of the polymer chain depends on the concentration of the acid: at a concentration of about 0.1 wt-%, the transformation of insoluble to soluble polymer proceeds without accompanying appreciable degradation, while at concentrations higher than 0.25 wt-%, splitting off of aluminum is accompanied by only slight degradation.

Temperature Change during the Polymerization

If the polymerization were initiated by $Al(Lac)_3$ in the $NaAl(Lac)_4$ catalyst at a temperature lower than that in the case of Na(Lac) catalyst, different temperature versus time curves would be observed between the two polymerizing systems owing to the heat of polymerization. This expectation was actually realized, as shown in Figure 1. At 254°C, no peak was observed in the system of $Na(Lac)_4$ in contrast to the system of Na(Lac). This is due to the consumption of the heat of polymerization in the $Na(Lac)_4$ system causing a temperature rise at a lower temperature than

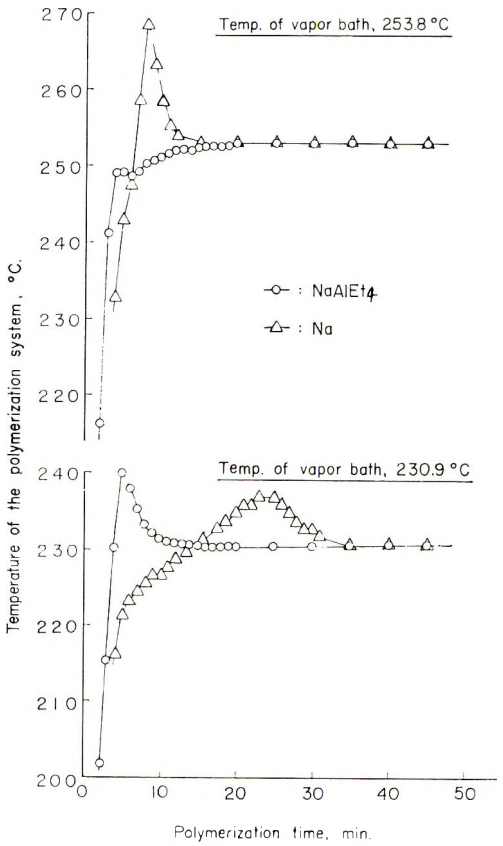

Fig. 1. Temperature change of polymerization system containing $NaAl(Lac)_4$ or Na(Lac). Monomer, 4.164 g; catalyst concentration, 0.50 mole-%.

for the Na(Lac) system. In the same way, the system of $NaAl(Lac)_4$ reached 230°C in a shorter time than the Na(Lac) system. These results support the participation of $Al(Lac)_3$ in the initiation in the presence of Na(Lac) at a relatively high temperature.

Polymerization of ε-Caprolactam with $NaAl(Lac)_3(OEt)$ as a Catalyst

The nature of the aluminum bond is a key factor for producing an insoluble polymer. A soluble polymer was obtained by modifying the $NaAl(Lac)_4$ by replacing one of the Lac groups.[1]

Similarly, the polymerization behavior of $NaAl(Lac)_3(OEt)$ was now investigated (Table IV). The catalytic activity of $NaAl(Lac)_3(OEt)$ is slightly lower than that of $NaAl(Lac)_4$. This tendency is considered to be due to the presence of an equilibrium between ethoxyl anion and lactam anion around both metals.[2-4] All the polymers obtained with $NaAl(Lac)_3(OEt)$ at 231°C were soluble, regardless of the polymerization time. At 202°C, the solubility of polymer depends on the polymerization time:

the polymer is soluble in less than 30 min and changes to an insoluble polymer at longer than 30 min. This difference in the polymerization behavior between $NaAl(Lac)_3(OEt)$ and $NaAl(Lac)_4$ is considered to be due to the difference in the stability between Al-N and Al-O bond.

TABLE IV
Polymerization of ε-Caprolactam with $NaAl(Lac)_3(OEt)$ as Catalyst.[a]

Polymerization temperature, °C	Polymerization time, min	Methanol-soluble part, wt-%	η_{sp}/c
255	10	13.2	4.56
	20	12.9	3.41
	30	12.7	2.54
	60	12.5	1.73
	120	12.8	1.65
231	10	19.8	15.3
	20	12.0	15.2
	30	11.7	12.4
	60	11.3	7.62
	120	11.4	3.51
202	10	95.1	2.73
	20	68.2	3.79
	30	17.3	Insoluble
	60	11.4	Insoluble
	120	11.3	Insoluble
171	10	100	—
	20	98.1	—
	30	97.5	—
	60	95.5	3.31
	120	73.6	9.82

[a] Catalyst concentration, 0.25 mole-%.

TABLE V
Correlation between Solubility of Nylon 6 and Polymerization Time and Temperature for Various Catalysts

Catalyst	Polymerization temperature, °C	Polymerization time, min		
		<30	30	120
Na(Lac)	202	Soluble	Soluble	Soluble
	231	Soluble	Soluble	Soluble
$NaAl(Lac)_4$	202	Insoluble	Insoluble	Insoluble
	231	Insoluble	Soluble	Soluble
$NaAl(Lac)_3OEt$	202	Soluble	Insoluble	Insoluble
	231	Soluble	Soluble	Soluble
$NaAl(Lac)_3(NHBu)$	202	Soluble	Soluble	Soluble
$Al(Lac)_3$	202	a	a	a
	231	Inactive	Inactive	Active

[a] Catalyst is almost inactive.

For the polymerization behavior with $NaAl(Lac)_4$,[1] $NaAl(Lac)_3(NHBu)$,[1] $NaAl(Lac)_3(OEt)$, $Na(Lac)$, and $Al(Lac)_3$, the relation between the solubility of polymer and the catalytic activity of $Al(Lac)_3$ is summarized in Table V.

With $NaAl(Lac)_3(OEt)$ catalyst, a change from soluble to insoluble polymer was observed at 202°C at a threshold time of 30 min; at 231°C, the soluble polymer was formed from the start of polymerization. These results are considered to be due to the existence of an exchange reaction between the alkoxyl group and the lactamate group:

$$X_2Al(OEt) + LacH \rightleftarrows X_2Al(Lac) + HOEt$$

where X denotes a lactamoyl group or polymer. The equilibrium shifts to the left side at higher temperature.

The authors are indebted to Dr. R. Yamadera for the instruction in analyses of aluminum and gratefully thank Mr. F. Yoshida for his enthusiastic assistance in some of the experiments.

Reference

1. T. Konomi and H. Tani, *J. Polym. Sci. A-1*, **7**, 2269 (1969).
2. T. Konomi and H. Tani, *J. Polym. Sci. A-1*, **7**, 2255 (1969).
3. P. Cefelin, E. Sittler, and O. Wichterle, *Coll. Czechoslov. Chem. Commun.*, **24**, 3287 (1957).
4. J. Stehlicek, J. Sebenda, and O. Wichterle, *Coll. Chechoslov. Chem. Commun.*, **29**, 1236 (1964).

Received February 11, 1969
Revised August 18, 1969

JOURNAL OF POLYMER SCIENCE: PART A-1 VOL. 8, 523–532 (1970)

Studies in Cyclocopolymerization. VI. Copolymerization of Trimethylvinylsilane and Dimethyldivinylsilane with Maleic Anhydride

GEORGE B. BUTLER and ALFRED F. CAMPUS, *Department of Chemistry, University of Florida, Gainesville, Florida 32601*

Synopsis

This paper reports the results of copolymerization of trimethylvinylsilane and dimethyldivinylsilane, respectively, with maleic anhydride. The former forms a 1:1 alternating copolymer while the latter, being a 1,4-pentadiene, forms a 1:2 cyclocopolymer. Consistent with the theory that charge-transfer complexes are involved in certain copolymerizations, it has been shown in this work that both of the vinyl silanes studied form charge-transfer complexes with maleic anhydride. The stoichiometric composition of these complexes have been shown by ultraviolet analysis to be 1:1 molar complexes. The equilibrium constants for complexation of trimethylvinylsilane and dimethyldivinylsilane with maleic anhydride have been determined by NMR and are 0.061 and 0.107 l./mole, respectively.

INTRODUCTION

It was reported by Kanazashi[1] that trimethylvinylsilane (Me_3VinSi), dimethyldivinylsilane (Me_2Vin_2Si), triethylvinylsilane (Et_3VinSi) and dimethylphenylvinylsilane ($Me_2PhVinSi$) do not polymerize on heating 24 hr at 150°C in the presence of benzoyl or acetyl peroxide. The lack of formation of high molecular weight polymer from Me_3VinSi may result from the steric hindrance of the large trisubstituted silyl group in the structural unit of the polymer, while the formation of relatively high molecular weight polymer from triethoxyvinylsilane[2] seems to be explained by the free rotation of the ethoxy group around the Si-O bond. More recently, however, a high molecular weight polymer of Me_3VinSi was reported[3] by use of butyllithium as initiator. We repeated the free-radical polymerizations of Me_3VinSi and Me_2Vin_2Si; no high molecular weight polymer was obtained in the case of Me_3VinSi, but we isolated a white powdery polymer, soluble in benzene in the case of Me_2Vin_2Si. We shall discuss the structure of this polymer in another paper. The copolymerizations of Me_3VinSi and $(EtO)_3VinSi$ with styrene and acrylonitrile were studied by Scott and Price;[4] the copolymers obtained always contained much more styrene and acrylonitrile, respectively, than the silane derivative.

The present paper reports the results of a copolymerization study of Me_3VinSi and Me_2Vin_2Si[5, 6] with maleic anhydride. Maleic anhydride, which does not homopolymerize under the usual free-radical conditions, is known to give copolymers with a high regularity. Indeed, previous work from this laboratory[5–11] has shown that certain 1,4-dienes, such as divinylether (DVE), would undergo a bimolecular alternating inter-intramolecular copolymerization with certain alkenes such as maleic anhydride (MA) and fumaronitrile (FN), to give linear cyclocopolymers with a constant composition of diene:alkene equal to 1:2. The 1:2 dimethyldivinylsilane–maleic anhydride copolymer represents one example of a cyclocopolymer previously reported.[5, 6] Such comonomer pairs which form regular 1:2 cyclocopolymers also form charge-transfer complexes and we report elsewhere[12] evidence of the participation of the charge-transfer complex between the comonomers in the mechanism of cyclocopolymerization, particularly in the cases of DVE–MA and DVE–FN.

Examples of alternating free-radical copolymerization of maleic anhydride with electron-rich alkenes are numerous and well known; such comonomer pairs also form charge-transfer complexes, and the participation of the complex in the alternating free-radical copolymerization mechanism has been proposed by different authors[13, 14] and in recent years by Iwatsuki and Yamashita.[15–17]

Such charge-transfer complexes are also observed in the case of Me_3VinSi and Me_2Vin_2Si with maleic anhydride, and we shall thus present together with the results of copolymerization, the results of the study of the charge-transfer complexes.

RESULTS AND DISCUSSION

Formation of a Charge-Transfer Complex between Trimethylvinylsilane, Dimethyldivinylsilane, and Maleic Anhydride

Stoichiometric Composition

By adding to a chloroform solution of MA a solution in the same solvent of Me_3VinSi or Me_2Vin_2Si, there appears in the ultraviolet spectrum of the mixture a new and broad band, whose appearance and position can be attributed to the formation of a charge-transfer or electron-donor–acceptor (EDA) complex. The application of the continuous variation method[18, 19] to these charge-transfer spectra permits the determination of the stoichiometric composition of the complex.

Since maleic anhydride absorbs in the same region as the complex, the measurements had to be run with an identical molar solution of acceptor in the reference beam, and since the maximum in the charge-transfer band could not be observed, the values at longer wavelengths were used to determine the stoichiometric composition of the complexes. The results are shown in Figure 1.

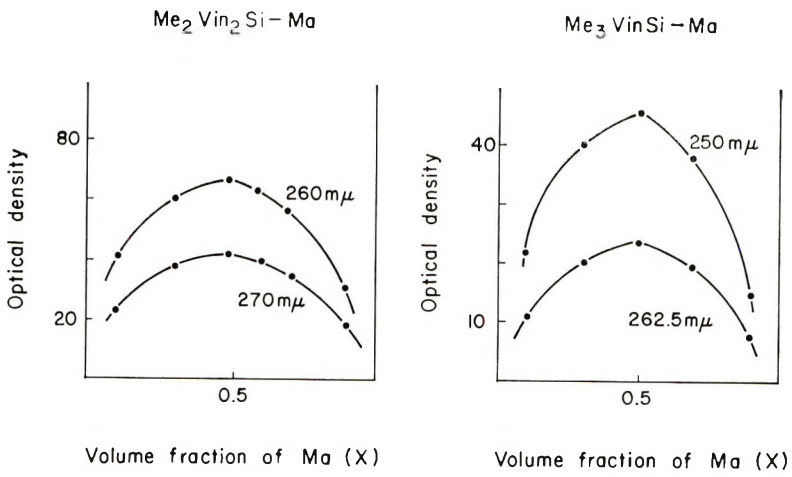

Fig. 1. Ultraviolet determination of the stoichiometric composition of the charge-transfer complexes. Solvent, $CHCl_3$.

In both cases, the maximum absorbance is found to be for a molar fraction of 0.5 in maleic anhydride; hence it can be concluded that the stoichiometry of the complex, even in the case of the divinyl derivative is 1:1. We discuss elsewhere[12] the possibility of the participation of the two double bonds in the complex.

Determination of the Equilibrium Constant of Complexation

The equilibrium constant of the Me_3VinSi–MA and Me_2Vin_2Si–MA complexes were determined by nuclear magnetic resonance by using the equation given by Hanna and Ashbaugh.[20]

$$1/\Delta_{obsd}{}^{A} = (1/Q\Delta_{AD}{}^{A})\,(1/\epsilon_{D}) + (1/\Delta_{AD}{}^{A}) \qquad (1)$$

Here $\Delta_{obsd}{}^{A} = \delta_{obsd}{}^{A} - \delta_{0}{}^{A}$, which is the difference between the shift of acceptor protons in complexing media ($\delta_{obsd}{}^{A}$) and the shift of the acceptor in uncomplexed media; $\Delta_{AD}{}^{A} = \delta_{AD}{}^{A} - \delta_{0}{}^{A}$, which is the difference in the shift of the acceptor protons in pure complex; ξ_D is the concentration of the donor, in this case Me_3VinSi or Me_2Vin_2Si, which is always much greater than the acceptor concentration.

The concentration of MA was kept constant at 0.05 mole/l., while the vinylsilane concentration was increased from 0.33 to 2.97 mole/l. in the case of Me_2Vin_2Si and from 0.69 to 4.60 mole/l. in the case of Me_3VinSi. The shift of the acceptor protons (singlet) was followed and by plotting $1/\Delta_{obsd}{}^{A}$ as a function of $1/\epsilon_D$, we obtained in both cases a straight line (Fig. 2), the slope of which and the intersection with the ordinate permits a first approximation of the equilibrium constant of complexation and of the shift of the acceptor protons in the pure complex.

The application of the method of least squares to eq. (1) gives a more exact determination of K and $\Delta_{AD}{}^{A}$; the results are given in Table I.

TABLE I
NMR Determination of the Equilibrium Constant of Complexation of the Charge-Transfer Complexes of Me_3VinSi–MA and Me_2Vin_2Si–MA with Maleic Anhydride[a]

Complex with maleic anhydride	Δ_{AD}^{A}, cps	K, l./mole
Me_3VinSi–MA	42.3	0.061
Me_2Vin_2Si–MA	29.5	0.107

[a] Solvent, $CDCl_3$; 23°C.

Despite the fact that silicon is less electronegative than carbon, it is able to withdraw π electrons from an unsaturated system to which it is bonded. Such behavior is generally understood as resulting from the fact that silicon is a second-row element and that it thus has vacant d-orbitals which can be the site of the transfer of charge towards silicon. A variety of evidence[21] supports this $d\pi$–$p\pi$ bonding between the silicon atom and a π-electron system; among them are studies of dipole moments and studies of proton magnetic resonance spectra. A detailed study of the NMR spectra of Me_3VinSi and Me_2Vin_2Si as well as phenylvinylsilane derivatives reported by Hobgood and Goldstein[22, 23] concludes that the $d\pi$–$p\pi$ bonding is responsible, at least for a part, of the considerably low position of the shifts of the vinyl protons of silane derivatives compared with the corresponding shifts in hexene-1. This $d\pi$–$p\pi$ bonding leads to a decrease of the electronic density of the double bonds of vinylsilanes, which would decrease the strength of the charge-transfer complexes compared with the carbon analogous, but we do not have at the present time results to report on the complex of 3,3′-dimethyl-1,4-pentadiene and maleic anhydride. By comparison (see Table II) with the charge-transfer complexes studied in the case of ethyl vinyl ether (EVE) and divinyl ether (DVE),[12] we ob-

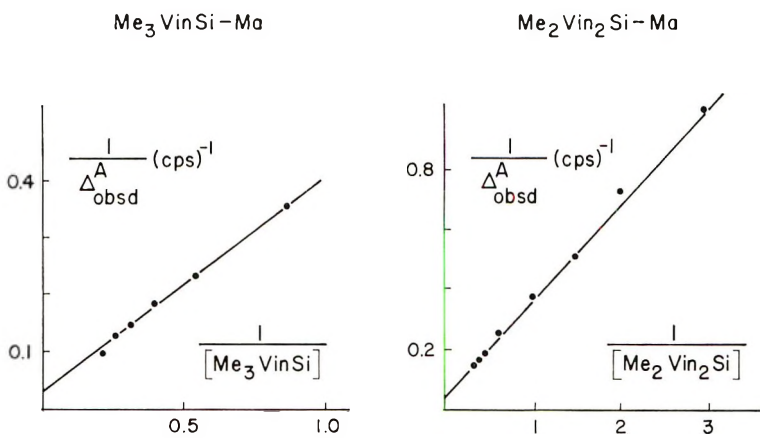

Fig. 2. NMR determination of the equilibrium constant of the charge-transfer complexes. Solvent, $CDCl_3$; 23°C.

TABLE II
Comparison between Vinylsilanes and Vinyl Ethers
Complexes with Maleic Anhydride

Complex	λ_{max}, mμ	K, l./mole
Me_3VinSi–MA	<250	0.061
Me_2Vin_2Si–MA	<250	0.107
EVE–MA	277.5	0.041
DVE–MA	278	0.036

served that the maximum absorptions in the case of vinylsilane complexes are at lower wavelength than those of the vinyl ethers.

Since for a series of complexes of different donors with the same acceptor, λ_{max} is linearly related to the ionization potential of the donor,[24] we conclude that the ionization process requires less energy in the case of vinyl ethers compared with vinylsilanes, which can be well understood by the fact that the double bonds of the vinyl ethers are more electron-rich, due to the delocalization of the nonbonding pairs of the oxygen atom towards the vinyl groups. The opposite effect is observed in the $d\pi$–$p\pi$ bonding in the case of vinylsilanes.

On the other hand, if we compare the stability of these complexes, we observe that the silane complexes are more stable than complexes of the vinyl ethers. This increase in stability can perhaps be attributed to this $d\pi$–$p\pi$ bonding characteristic of compounds containing silicon attached to unsaturated systems.

Investigation of the 3,3-dimethyl-1,4-pentadiene–maleic anhydride complex will give us a better system for comparison.

Copolymerization Studies

Copolymerization of Trimethylvinylsilane with Maleic Anhydride

Table III shows data for copolymerization of trimethylvinylsilane and maleic anhydride.

Over a relatively wide range of initial monomer composition, the molar fraction of MA in the copolymer remains constant and equal to 0.5 except for the most dilute solution in Me_3VinSi where a value of 0.547 was found for m_2. These values are quite consistent with an alternating copolymer. The fact that two monomers give an alternating copolymer while they do not homopolymerize under the same conditions is not new; the first example was reported in 1930[25] in the case of the alternating free-radical copolymerization of stilbene with maleic anhydride.

The copolymers Me_3VinSi–MA were soluble in the polymerization medium (benzene) and were precipitated twice in anhydrous ether before analysis. The structure of the copolymer was verified by infrared spectroscopy; they show a relatively simple spectrum with the characteristic absorptions of the anhydride ring in the carbonyl region between 1900 and

TABLE III
Trimethylvinylsilane (M_1)–Maleic Anhydride (M_2) Copolymers[a]

Run no.	M_2 (monomer mole ratio)	Reaction time, hr	Conversion, %	Rate of polymerization, conversion/time $\times 10^3$	Si, %[b]	m_2
FI	0.8	115	3.0	26	12.93	0.547
FII[c]	0.6	96	8.4	87	14.50	0.492
FIII	0.5	91.25	12.0	122	14.05	0.508
FIV	0.4	96	8.7	91	14.28	0.504
FV[d]	0.2	115	5.6	48	14.04	0.508

[a] Solvent of copolymerization, benzene; 60°C.; initiator, AIBN (1% mole); $[M]_T$ = 4 mole/l. (constant).

[b] The composition of the copolymer is based upon the silicon content; 1:1 copolymer requires 14.15% Si.

[c] $[\eta]$ = 0.06 dl/g (30°C, acetone).

[d] $[\eta]$ = 0.08 dl/g (30°C, acetone).

1700 cm^{-1} and of the trimethylsilyl group[26] at 2955, 1250, and 1410 cm^{-1} (very reduced).

It has been observed by some authors[15–17] that the rate of the alternating free-radical copolymerization is maximum for a monomer feed ratio equal to 1:1, the medium in which the concentration of the charge-transfer complex of 1:1 stoichiometry is higher. Similar behavior is observed in this case (Fig. 3). Such observation can support to some extent the participation of the charge-transfer complex formed between Me_3VinSi and MA in its alternating free-radical copolymerization,[3] which could be re-

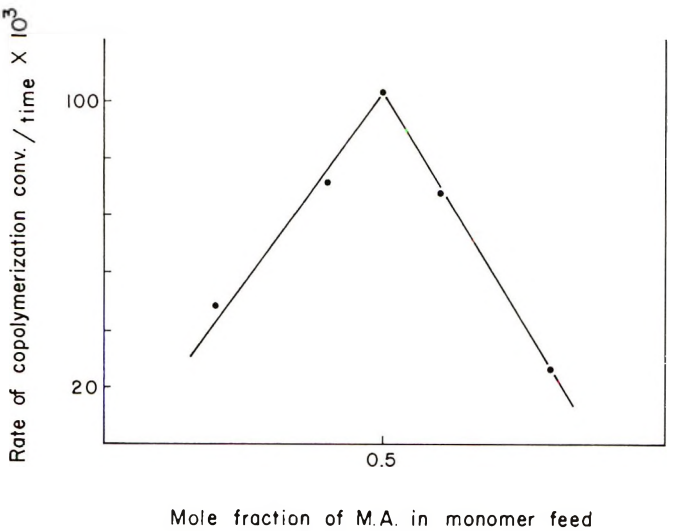

Fig. 3. Dependence of the rate of copolymerization upon the monomer feed ratio in the copolymerization of Me_3VinSi and MA. AIBN, benzene, 60°C.

duced, as it was proposed by Iwatsuki and Yamashita,[15–17] to the homopolymerization of the charge-transfer complex formed between the comonomers.

Copolymerization of Dimethyldivinylsilane with Maleic Anhydride

The data for the copolymerization of dimethyldivinylsilane with maleic anhydride are given in Table IV.

TABLE IV
Dimethyldivinylsilane (M_1)–Maleic Anhydride (M_2) Copolymers[a]

Run no.	M_2 (monomer mole ratio)	Reaction time, hr	Conversion, %	Si, %[b]	m_2	Conversion, %/hr
D1	0.20	27.5	5.3	9.30	0.660	0.194
D2[c]	0.33	27	8.1	9.29	0.660	0.300
D3	0.50	24	7.6	9.12	0.666	0.317
D4	0.60	23	10.8	9.27	0.661	0.469
D5	0.67	22	12.0	8.99	0.672	0.545
D6[d]	0.75	21	10.1	9.13	0.666	0.481
D7	0.80	19	10.6	8.97	0.671	0.558

[a] Solvent of copolymerization, benzene; 60°C; initiator, AIBN (0.5%/mole); $[M]_T$ = 1.3–3.9 mole/l.

[b] The composition of the copolymer is based upon the silicon content; 1:2 copolymer requires 9.11% Si.

[c] $[\eta]$ = 0.13 dl/g (30°C, acetone).

[d] $[\eta]$ = 0.07 dl/g (30°C, acetone).

Over a wide range of initial monomer composition, the molar fraction of maleic anhydride in the copolymer is equal to the predicted value for 2:1 molar alternating copolymers. The copolymers were insoluble in the polymerization medium (benzene), but were soluble in solvents such as acetone and DMF from which they were precipitated twice into anhydrous ether before analysis. The solubility of these copolymers in organic solvents rules out the possibility of formation of a crosslinked polymer. The 1:2 Me_2Vin_2Si:MA content, the nonhomopolymerizability of MA and the absence (based on infrared and NMR studies) of any remaining double bond in the copolymers permit us to rule out such a structure as I for the copolymer:

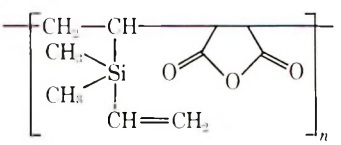

I

On the other hand, the position and the integration of the NMR peaks of the copolymers are quite consistent with the 1:2 Me_2Vin_2Si:MA cyclic

unit as defined previously[5–11] for pairs of monomers such as divinyl ether–maleic anhydride and divinyl ether–fumaronitrile. The structure of the copolymers can thus be as shown by II.

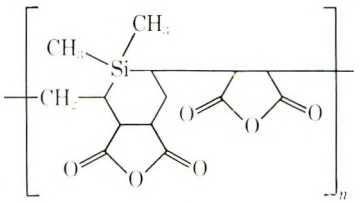

II

Since the ratio of diene to olefin is constantly equal to 1:2 the copolymer composition equation(s) as a function of monomer feed in terms of the reactivity ratio parameters is reduced to $r = 1/2$.

We discuss elsewhere[12] the possibility of the participation of the charge-transfer complex between comonomers in the mechanism of cyclocopolymerization. We showed in the first part that the charge-transfer complexes between vinylsilanes and maleic anhydride, although of weak strength have a relatively high stability, which improves the concentration of the charge-transfer complex in the polymerization medium. The stability of the complex and the regularity of the 1:2 structure seems to be related since in this case we have a very regular 1:2 copolymer while in the case of divinyl ether–fumaronitrile less stable complex, the value of m_2 ranges from 0.55 to 0.63, and in the case of divinyl ether-acrylonitrile, where no obvious interaction of the charge-transfer nature occurred, even less regularity is obtained.

EXPERIMENTAL

Materials

Trimethylvinylsilane and dimethyldivinylsilane were obtained from Peninsular ChemResearch, Inc. and were freshly distilled (under nitrogen) before use; the boiling points are, respectively, 55°C and 80°C. Maleic anhydride was recrystallized from chloroform and then sublimed just before use. Benzene, solvent of copolymerization (Fisher reagent) was dried over sodium and chloroform (spectro-grade) was used for the ultraviolet studies of the complexes; deuterated chloroform, used for the NMR studies of the complexes was obtained from Merk, Sharp and Dohme. Azobis-isobutyronitrile, used as initiator, was recrystallized from methanol.

Copolymerization

For each system, maleic anhydride and AIBN were weighed while vinylsilanes were measured volumetrically and diluted with dry benzene as solvent. The polymerization tubes were evacuated twice and sealed under high vacuum. The reactions were carried out in an oil bath at 60 ±

0.05°C. The polymers were purified twice by precipitation into a nonsolvent (anhydrous ether), filtered through fritted glass filter funnels and dried in a vacuum oven prior to analysis. The copolymer composition was determined upon silicon analysis; analyses were done in duplicate by Galbraith Microanalytical Laboratories, Knoxville, Tennessee.

Charge-Transfer Complexes Studies

The stoichiometric composition of the charge-transfer complexes was determined on a Beckman DK-2A spectrophotometer with chloroform as solvent; 10^{-2} cm cells were used and the concentrations of initial solutions were 2 mole/l. The determinations of the equilibrium constants of complexation were done on a Varian Associates analytical NMR spectrometer, model A-60 with $CDCl_3$ as solvent. The solutions were prepared at room temperature in volumetric flasks and the temperature of the apparatus was kept constant at the same temperature. The concentration of maleic anhydride was kept constant at 0.05 mole/l., while the vinylsilane concentration was increased.

This work was supported predominantly by National Institutes of Health Grant No. CA 06838 for which we are grateful. One of us (AFC) also received financial support for a brief period from a post-doctoral fellowship award made available to the Department of Chemistry through a Science Development Grant from the National Science Foundation. The intrinsic viscosity determinations were made by Mr. C. Lawson Rogers.

References

1. M. Kanazashi, *Bull. Chem. Soc. Japan*, **28**, 44 (1955).
2. B. A. Azbuzov and T. G. Shavska, *Dokl. Akad. Nauk SSSR*, **68**, 859 (1949).
3. N. S. Nametkin, V. S. Khotimskii and S. G. Durgaryan, *Dokl. Akad. Nauk SSSR*, **166**, 1118 (1966).
4. C. E. Scott and C. C. Price, *J. Amer. Chem. Soc.*, **81**, 2670 (1959).
5. G. B. Butler, paper presented at 134th Meeting, American Chemical Society, Chicago, Ill., September 7–12, 1958; *Abstracts of Papers*, p. 32T.
6. G. B. Butler, *J. Polym. Sci.*, **48**, 279 (1960).
7. G. B. Butler, Paper presented at 133rd Meeting, American Chemical Society, San Francisco, California, April 13–18, 1958; *Abstracts of Papers*, p. 6R.
8. J. M. Barton, G. B. Butler, and E. C. Chapin, *J. Polym. Sci. A-1*, **5**, 1265 (1967).
9. G. B. Butler and R. B. Kasat, *J. Polym. Sci. A*, **3**, 4205 (1965).
10. G. B. Butler, G. Vanhaeren, and M. F. Ramadier, *J. Polym. Sci. A-1*, **5**, 1265 (1967).
11. G. B. Butler and K. C. Joyce, in *Macromolecular Chemistry, Brussels-Louvain 1967* (*J. Polym. Sci. C*, **22**), G. Smets, Ed., Interscience, New York, 1968, p. 45.
12. G. B. Butler and A. F. Campus, paper presented to *American Chemical Society, Division of Polymer Chemistry*, Atlantic City, N. J., September 1968; *Preprints*, **9**, 1266 (1968); *J. Polym. Sci. A-1*, in press.
13. P. D. Bartlett and K. Nozaki, *J. Amer. Chem. Soc.*, **68**, 1495 (1946).
14. W. Barb, *Trans. Faraday Soc.*, **49**, 143 (1953).
15. S. Iwatsuki, Y. Yamashita, et al., *Kogyo Kagaku Zassh*, **67**, 1464, 1467, 1470 (1964); *ibid.*, **68**, 1138, 1963, 1967, 2463 (1965); *ibid.*, **69**, 145 (1966).
16. S. Iwatsuki, Y. Yamashita, et al., *Makromol. Chem.*, **89**, 205 (1965); *ibid.*, **102**, 232 (1967).

17. S. Iwatsuki and Y. Yamashita, *J. Polym. Sci. A-1*, **5**, 1753 (1967).
18. P. Job, *C. R. Acad. Sci.* (Paris), **180**, 928 (1925); *Ann. Chim. Phys.*, **9**, 113 (1928).
19. W. C. Vosburgh and G. R. Cooper, *J. Amer. Chem. Soc.*, **63**, 437 (1941).
20. M. W. Hanna and A. L. Ashbaugh, *J. Phys. Chem.*, **68**, 811 (1964).
21. C. Eaborn, *Organosilicon Compounds*, Academic Press, New York, 1960, pp. 91–113.
22. R. T. Hobgood, J. H. Goldstein, and G. S. Reddy, *J. Chem. Phys.*, **35**, 2038 (1961).
23. R. T. Hobgood and J. H. Goldstein, *Spectrochim. Acta*, **19**, 321 (1963).
24. G. Briegleb, *Elektronen-Donator-Acceptor Komplexe*, Springer Verlag, Berlin-Göttingen-Heidelberg, 1961.
25. T. Wagner-Jauregg, *Ber.*, **63**, 3213 (1930).
26. M. Kanazashi, *Bull. Chem. Soc. Japan*, **26**, 493 (1953).

Received December 9, 1968
Revised August 19, 1969

JOURNAL OF POLYMER SCIENCE: PART A-1 VOL. 8, 533–543 (1970)

Effect of Lithium Alkoxide and Hydroxide on Polymerization Initiated with Alkyllithium

H. L. HSIEH, *Research and Development Department, Phillips Petroleum Company, Bartlesville, Oklahoma 74003*

Synopsis

The effects of lithium *tert*-butoxide on rates of initiation, propagation, and polymerization of butyllithium-initiated polymerization of butadiene and styrene were examined. Toluene and cyclohexane were used as solvent and the experiments covered BuLi/-*t*-BuOLi ratios from 1:0 to 1:6. Both polymerization and propagation rates declined in the presence of alkoxide. The initiation rate in cyclohexane increased to a maximum at BuLi/*t*-BuOLi ratio of 1:0.5 and then decreased. A mechanism of rapid dissociation of butyllithium oligomer by alkoxide and multiple complexation of butyllithium with excess alkoxide is proposed. Lithium alkoxide also reduced the copolymerization rate but did not affect the copolymerization characteristics. Water reacted with organolithium compound rapidly to form hydroxide. It was found that the hydroxide reacted very slowly with more organolithium compound in hydrocarbon solution to form oxide. Their effects on polymerization were investigated.

INTRODUCTION

In an anionic polymerization system, where the initiator is a mixture of alkyllithium and sodium to cesium alkoxides, we have shown that the active center is a dynamic tautomeric equilibrium involving the two metals.[1,2] The rate of polymerization, stereochemistry, and copolymerization characteristics reflect this mechanism. Accordingly, one would not expect such changes when the initiator is a mixture of alkyllithium and lithium alkoxide. This was generally found to be true. However, lithium alkoxide is capable of association with organolithium compounds and of affecting anionic polymerization in a different manner. Indeed, Welch[3] reported that lithium *n*-butoxide formed *in situ* decreased the overall polymerization rate of styrene in benzene initiated with butyllithium. Roovers and Bywater reported[4] that in benzene both the initiation rate and the propagation rate of styrene were decreased by the addition of lithium *tert*-butoxide. To obtain more detailed information and a better understanding of the effect of lithium alkoxide on anionic polymerization, we undertook an extensive study of this problem.

The investigation of the effect of lithium alkoxide was extended to lithium hydroxide and lithium oxide as well. The hydroxide and oxide, both formed from the reaction of alkyllithium and water, are undoubtedly the

most common impurities in an anionic polymerization system. Knowledge of their effect, if any, is essential to those who are studying the kinetics of anionic polymerization.

EXPERIMENTAL

The solvents employed, petroleum-derived toluene and Phillips' polymerization grade cyclohexane, were dried by countercurrent scrubbing with prepurified nitrogen, followed by passage over activated alumina. Phillips' special purity butadiene was distilled through sodium dissolved in ethylene glycol before it was condensed and transferred into bottles containing Drierite. Styrene, polymerization grade, was vacuum-distilled first and then refluxed with CaH_2 before another vacuum distillation. *n*-Butyllithium (*n*-BuLi) in heptane was obtained from Foote Mineral Company. The concentration determined was 1.43*M* by total alkalinity, 1.45*M* by disulfide cleavage method[5] and 1.42*M* by liquid chromatographic analysis of *n*-butane after hydrolysis. No butane was found before hydrolysis. The concentration of *n*-BuOH after hydrolysis was only 0.004*M*, indicating only a trace of *n*-BuOLi was present.

The lithium *tert*-butoxide (*t*-BuOLi) solution was prepared by reacting *tert*-butyl alcohol (*t*-BuOH) with an equal mole of *n*-BuLi in cyclohexane to give a 0.5*M* concentration. The alcohol was Baker Analyzed reagent. The solution, after reaction, was purged with prepurified nitrogen for at least 40 min at 3 l./min to remove butane formed. It was analyzed by gas chromatography to make certain that no detectable butane remained. The final concentration was determined by acid titration.

The initiator solution was formed by mixing measured amounts of *n*-BuLi and *t*-BuOLi solutions at room temperature. It was stored for 24 hr before use. For the study of the effect of LiOH, water was added directly to the polymerization solution before the addition of *n*-BuLi.

Polymerization procedure and the procedures used to determine rates of polymerization and propagation were described in our earlier publications.[6,7] Polymerization bottles, after being washed and dried, were rinsed with a cyclohexane solution of dicyclopentenyllithium before use.

Rate of initiation was determined by gas chromatographic analysis for butane after hydrolysis. The principle and general procedure was discussed in our earlier publication.[8] However, the procedure for chromatographic analysis has been modified and improved. For this study the vapor phase was analyzed in contrast to the analysis of the polymerization solution in our earlier work. We found that, while the concentration of butane was much lower in vapor phase than in solution, the values obtained from vapor are more accurate representations of the total butane. Isobutane (Phillips Research Grade) was used as the internal standard.

Analysis of the reaction mixtures was accomplished by using a Hewlett-Packard Model 5754 B chromatography unit equipped with flame and thermal conductivity detectors. Columns were 14-ft lengths of $^1/_8$ in. stain-

less steel packed with 3.9% di-2-ethylhexyl sebacate and 8.1% bis(2-methoxyethyl) adipate on Coast Engineering Laboratories' 80–100 mesh GC-22 support. Piping connections were arranged to allow analysis of the light components on forward flow to the flame detector and heavy component analysis on reverse flow to the thermal conductivity detector. A dual-pen, Mosely recorder with disk integrator was used to measure the amount of each gas present.

Calibration was done by analyzing the vapor of the standard mixtures of solvent, monomer, *n*-butane, and isobutane after equilibration at room temperature. In some cases, it was necessary to prepare several standard mixtures with decreasing ratios of *n*-butane to isobutane in order to determine the extent of change in the factor with different concentrations. For both calibration and experimental samples, the gases were allowed to equilibrate before sampling for analysis.

RESULTS AND DISCUSSION

Lithium Alkoxide

In a polymerization of a mixture of butadiene and styrene in cyclohexane with butyllithium (BuLi), butadiene is preferentially polymerized first. Addition of the sodium, potassium, rubidium, or cesium *tert*-butoxide greatly increased the rate of polymerization and eliminated the break (inflection point) in the time versus conversion curve that is characteristic of block copolymerization.[2] However, addition of lithium *tert*-butoxide (*t*-BuOLi) retarded the rate of polymerization. Furthermore, the inflection point on these time–conversion curves, which can be easily identified by appearance of orangish-yellow color (stryllithium), are positioned at approximately the same conversion. This suggests no additional randomization occurred. Indeed, the styrene inclusion profile is not changed in the presence of various amounts of *t*-BuOLi (Fig. 1). This is further confirmed

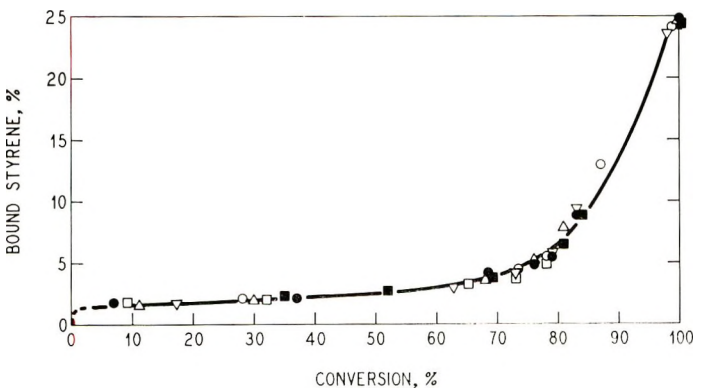

Fig. 1. Styrene incorporation at various conversions from samples prepared at *n*-BuLi/*t*-BuOLi ratios between 1:0 and 1:6.

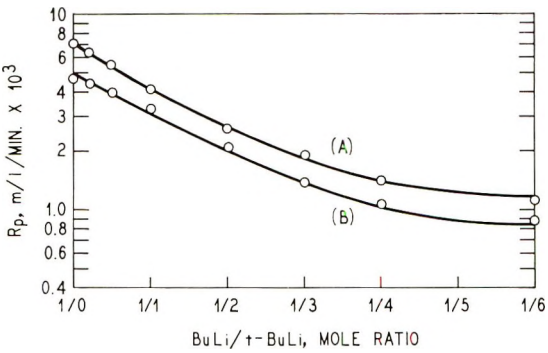

Fig. 2. Rate of propagation R_p of butadiene (1.6M) preinitiated with *sec*-BuLi ($1.55 \times 10^{-3}M$) and variable *t*-BuOLi at 30°C: (*A*) toluene as solvent; (*B*) cyclohexane as solvent.

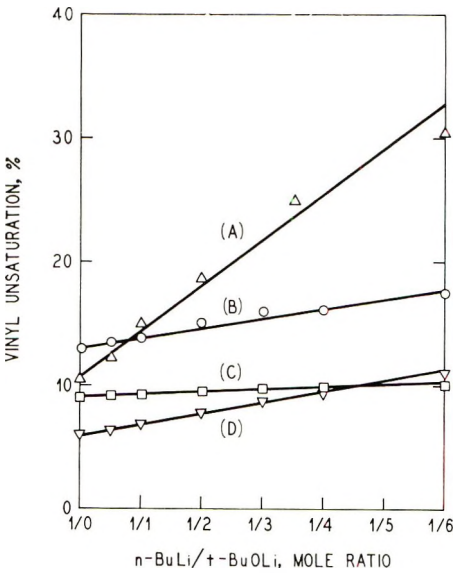

Fig. 3. Effect of lithium alkoxide on vinyl unsaturation of polybutadiene: (*A*) at 30°C in toluene; (*B*) at 70°C in toluene; (*C*) at 70°C in cyclohexane; (*D*) at 30°C in cyclohexane.

by the uniform (18% ± 1) polystyrene contents of all the samples as determined by the oxidative degradation method.[9]

In view of the reduction of the overall polymerization rate of the mixture of butadiene and styrene, the rates of propagation for each monomer were separately studied. Rates of propagation R_p for butadiene, which were completely separated from the initiation reaction by pre-initiation with *sec*-BuLi,[7] are shown in Figure 2.

It is quite apparent that the presence of *t*-BuOLi reduced propagation rates.

Polar compounds, such as ethers, amines, and sulfides, generally affect the stereochemistry of polymerization of dienes with alkyllithium initiators.[10] Lithium *tert*-butoxide had an effect like a very weak polar material in this regard, as shown by the increase of vinyl unsaturation in polybutadiene (Fig. 3).

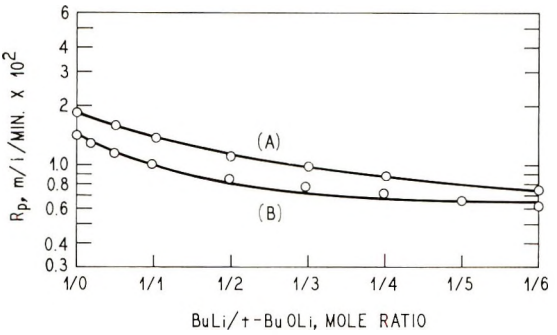

Fig. 4. Rate of propagation of styrene (0.70M) preinitiated with *sec*-BuLi ($1.55 \times 10^{-3}M$) at 30°C: (*A*) in toluene; (*B*) in cyclohexane.

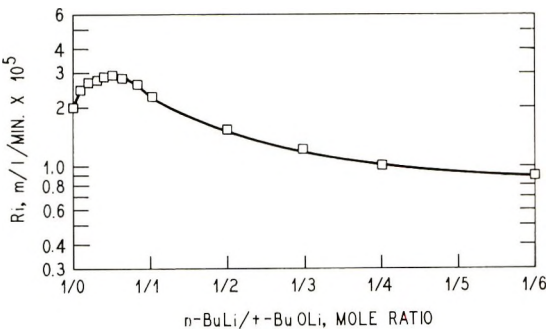

Fig. 5. Rate of initiation R_i of styrene (0.86M) with *n*-BuLi ($2.7 \times 20^{-3}M$) and variable *t*-BuOLi in cyclohexane at 30°C.

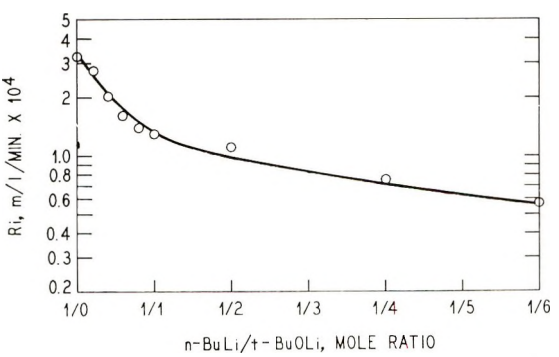

Fig. 6. Rate of initiation R_i of styrene (0.44M) with *n*-BuLi ($2.7 \times 10^{-3}M$) and variable *t*-BuOLi in toluene at 30°C.

The rates of propagation and initiation of styrene with BuLi and variable amounts of *t*-BuOLi were then examined. Again, both toluene and cyclohexane were used as solvent (Figs. 4–6).

The maximum initiation rate R_i in cyclohexane increased to a maximum at the ratio of BuLi/*t*-BuOLi of about 1:0.3 to 1:0.5. At the ratio of 1:1, the rate is about the same as the control. Beyond that the rate decreased continuously. The maximum rate of initiation in toluene did not show an initial increase.

In either solvent, the rate of propagation (maximum rate) for both monomers decreased with the presence of *t*-BuOLi. It is assumed that the alkoxide coordinates with the polymer lithium to form the mixed aggregates which are less reactive toward monomer than the polymer-lithium itself. The coordination of the alkoxide to the polymer-lithium would serve to block the sites at which reaction with the monomer occurs.

In cyclohexane the initiation rate increased at low *t*-BuOLi concentrations and then decreased as the concentration of the alkoxide was increased. On the other hand, in toluene the rate decreased even at very low alkoxide levels. To present a concise mechanism involving alkoxide is difficult. The initiation reaction with alkyllithium is extremely complex, and the exact mechanism is not known.[11] However, we wish to propose the following explanations at this time. Initially the presence of *t*-BuOLi disrupts the butyllithium hexamer to give very reactive dissociated product, probably a coordinated dimer, and some unreactive mixed associated. Glaze and Adams,[12] in their study of pyrolysis of *sec*-BuLi, proposed a prior, rapid dissociation of the alkyllithium oligomer by alkoxide. When more alkoxide is added, the multiple complexation decreases the rate of reaction. Complexes such as $(n\text{-BuLi}\cdot t\text{-BuOLi})_n$ have been reported.[13] When a large excess of alkoxide is available, further complexation causes crowding which makes very unreactive species. In toluene there is a relatively high concentration of the dissociated product to start and therefore no initial increase in rate can be observed.

The initiation rate in toluene is much faster than in aliphatic solvent.[8] Furthermore, there is a noticeable induction period in aliphatic solvent but not in toluene. Our assumption that there is a significant difference in concentration of the very reactive butyllithium dimer at the start in the two solvents is consistent with these facts. Rover and Bywater[14] reported the presence of *t*-BuOLi eliminated the induction period of isoprene polymerization with *sec*-BuLi in hexane.

Lithium Hydroxide

The first experiment was carried out by adding BuLi to a solution of cyclohexane, butadiene and water at 50°C. The conversions at various times were obtained (Table I). Water was expected to react with BuLi rapidly to form LiOH and if no further reactions occur, then all the four runs (A to D) had identical amounts of initiator with variable RLi/LiOH ratios.

TABLE I
Effect of Lithium Hydroxide on Polymerization: First Experiment[a]

Run	$[n\text{-BuLi}]_0$, $M \times 10^3$	$[H_2O]_0$, $M \times 10^3$	Time, min	Conversion, %	Inherent viscosity[b]	$\bar{M}_n \times 10^{-3}$[b]
A	3.6	0	16	18	0.53	25
			30	57		
			50	77		
			70	88		
			100	95		
			180	100		
B	4.5	0.9	16	16	0.63	32
			30	48		
			50	74		
			70	86		
			100	94		
			180	100		
C	5.4	1.8	16	16	0.73	38
			30	48		
			50	74		
			70	86		
			100	93		
			180	100		
D	7.2	3.6	16	15	1.20	76
			30	42		
			50	68		
			70	81		
			100	87		
			180	89		
			240	98		

[a] $[Bd]_0 = 1.6M$; 50°C.
[b] On the final samples.

From the analytical data, it is quite clear that these four runs did not have same amounts of initiator. The inherent viscosity and number-average molecular weight $\bar{M}_n$ are progressively higher from runs A to D with the biggest jump at run D (D had the lowest BuLi/H_2O ratio). The final sample from run D had $\bar{M}_n$ three times that of the control. In other words, the number of active growing chain-ends in run D is on the average only about one-third of that in run A during the polymerization. Reaction between LiOH and RLi, which can be BuLi as well as polybutadienyllithium, must have occurred. The formation of salts was observed as precipitate. The rate of polymerization was also slowest for run D.

The second experiment was carried out by adding BuLi to the polymerization solvent containing water but not monomer at 50°C. Butadiene was added 30 min later. Rate of polymerization and analytical data on the final polymers were again obtained (Table II).

With additional reaction time between BuLi and water, even less BuLi was available for initiation in runs B, C, and D. The final sample from run D had $\bar{M}_n$ eleven times that for the control, indicating as much as 90%

TABLE II
Effect of Lithium Hydroxide on Polymerization: Second Experiment[a]

Run	$[n\text{-BuLi}]_0$, $M \times 10^3$	$[H_2O]_0$, $M \times 10^3$	Time, min	Conversion, %[b]	Inherent viscosity[c]	$\bar{M}_n \times 10^{-3}$
A	3.6	0	16	18	0.53	25
			30	51		
			50	77		
			70	88		
			100	95		
			180	100		
B	4.5	0.9	16	12	0.66	33
			30	45		
			50	72		
			70	84		
			100	93		
			180	100		
C	5.4	1.8	16	12	0.81	44
			30	43		
			50	70		
			70	82		
			100	92		
			180	100		
D	7.2	3.6	16	12	2.63	287
			30	34		
			50	54		
			70	66		
			100	80		
			180	95		
			240	96		
			960	96		

[a] $[Bd]_0 = 1.6M$; 50°C.
[b] After BuLi and water were prereacted for 30 min at 50°C.
[c] On final samples.

of the BuLi remaining from the initial 30-min reaction with water was consumed by further reaction with LiOH. Run D did not ever reach quantitative conversion, evidence that the "living" chain-ends which were relatively few to begin with, were ultimately terminated by reaction with LiOH before all monomer was polymerized. These data indicated that one mole of water reacted with two moles of organolithium compound. That run D reached even 96% conversion suggested that reaction between RLi and LiOH must be quite slow. The rate of polymerization is much slower in Run D than the control; this must be due to the very low initiator level and, to a lesser degree, the continuous termination reaction during polymerization.

To confirm that two kinetically distinguishable steps exists,

$$\mathrm{RLi} + \mathrm{HOH} \xrightarrow{\text{fast}} \mathrm{RH} + \mathrm{LiOH}$$
$$\mathrm{RLi} + \mathrm{LiOH} \xrightarrow{\text{slow}} \mathrm{RH} + \mathrm{Li_2O}$$

TABLE III
Reactions of Butyllithium and Water at 30°C

Run	$[n\text{-BuLi}]_0$, $M \times 10^3$	$[H_2O]$, $M \times 10^3$	Time, min	[Butane], $M \times 10^3$
A	3.6	0	1	0.08
			73	0.20
			205	0.20
B	4.5	0.9	12	0.90
			17	0.96
			35	1.12
			60	1.28
			210	2.00
C	5.4	1.8	17	1.54
			40	1.66
			65	1.88
			220	3.24
			400	3.60
D	7.2	3.6	24	3.00
			45	3.50
			71	4.00
			95	5.68
			266	6.32
			415	7.00

BuLi and H_2O were mixed in cyclohexane and the butane generated, which represents the reacted BuLi, was quantitatively measured by gas chromatography. The results are shown in Table III.

Results from runs B, C and D verified the surmise that one mole of water ultimately reacted with two moles of BuLi and the second step is very slow. Even at 50°C, it was found that it took 4 hr completely to destroy 7.2×10^{-3} mole BuLi with 3.6×10^{-3} mole water in one liter solution. This coincides with the time required to completely terminate the polymerization for run D in Table II. Equally noteworthy is the fact that at the end of 30 min at 50°C there was still about 0.4×10^{-3} mole BuLi left in solution, which agrees with the actual amount of initiator calculated from $\bar{M}_n$ of the final polymer for run D in Table II.

The final question is whether lithium oxide (Li_2O) formed from the complete reactions of BuLi and water affects the polymerization. Three independent rate studies were made. The control used BuLi concentration of $3.6 \times 10^{-3}M$. The second one used $7.2 \times 10^{-3}M$ BuLi along with $3.6 \times 10^{-3}M$ water prereacted at 50°C for 4 hr. Gas chromatographic analysis showed that all of the BuLi was consumed in this time, so that Li_2O must have been formed. To this an additional $3.6 \times 10^{-3}M$ BuLi was added as initiator before the addition of butadiene. The ratio of BuLi/Li_2O was therefore 1:1. The fact that at the end of 4 hr all BuLi had been consumed was further verified by showing no detectable amount of polymerization occurred when monomer was added. The third study used $10.8 \times 10^{-3}M$ BuLi and $3.6 \times 10^{-3}M$ water prereacted at 50°C for 4 hr before the addi-

tion of butadiene. In this case the ratio of BuLi/Li_2O is again 1:1, with Li_2O formed in the presence of BuLi. All three cases of course had identical amounts of unreacted BuLi initiator. The conversion versus time curves showed that the rates are identical (Fig. 7). Inherent viscosity and $\overline{M}_n$ for the final polymers are also the same within experimental error.

Our data showed conclusively that lithium hydroxide deactivates the organolithium compound in 1:1 mole ratio. Fujimoto, Ozaki, and Nagasawa[15] observed a similar reaction in the anionic polymerization of α-methylstyrene in tetrahydrofuran. The product, lithium oxide, has no effect on the polymerization.

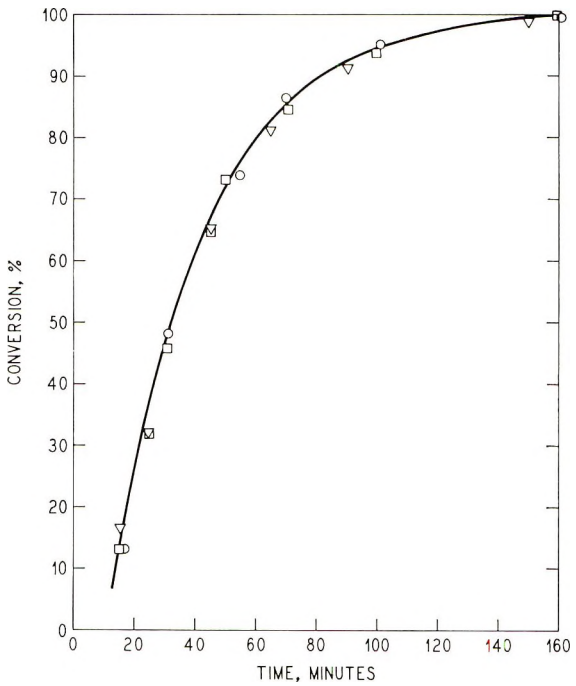

Fig. 7. Rate of polymerization of butadiene (1.6M) in cyclohexane at 50°C with n-BuLi ($3.6 \times 10^{-3}M$); (□) no Li_2O; (○) $Li_2O = 3.6 \times 10^{-3}M$; (▽) $Li_2O = 3.6 \times 10^{-3}M$, formed in the presence of n-BuLi.

In a recent publication, Guyot and Vialle[16] reported that LiOH up to 50 mole-% in excess of BuLi greatly reduced the apparent initiation rate constant of isoprene with *sec*-BuLi. These authors analyzed hydrolyzed polymerization solutions by gas chromatography. However, the amount of butane measured after hydrolysis would represent not only the unreacted BuLi but also the part of BuLi reacted with LiOH. Unless the amount of butane was measured before hydrolysis also, neither the exact amount of unreacted BuLi nor the concentration of the true initiator is known.

References

1. H. L. Hsieh and C. F. Wofford, *J. Polym. Sci. A-1*, **7**, 449 (1969).
2. C. F. Wofford and H. L. Hsieh, *J. Polym. Sci. A-1*, **7**, 461 (1969).
3. F. J. Welch, *J. Amer. Chem. Soc.*, **82**, 6000 (1960).
4. J. E. L. Roovers and S. Bywater, *Trans. Fraday Soc.*, **62**, 1876 (1966).
5. C. A. Uraneck, J. E. Burleigh, and J. W. Cleary, *Anal. Chem.*, **40**, 327 (1968).
6. H. L. Hsieh, *J. Polym. Sci. A*, **3**, 153 (1965).
7. H. L. Hsieh, *J. Polym. Sci. A*, **3**, 173 (1965).
8. H. L. Hsieh, *J. Polym. Sci. A*, **3**, 163 (1965).
9. I. N. Kolthoff, T. S. Lee, and C. W. Carr, *J. Polym. Sci.*, **1**, 429 (1946).
10. A. V. Tobolsky and C. E. Rogers, *J. Polym. Sci.*, **40**, 73 (1959).
11. T. L. Brown, Advan. *Organometal. Chem.*, **3**, 365 (1965).
12. W. H. Glaze and G. M. Adams, *J. Amer. Chem. Soc.*, **88**, 4659 (1966).
13. L. Lochmann, J. Pospisil, J. Vodnansky, and D. Lim, *Coll. Czechoslov. Chem. Commun.*, **30**, 2187 (1965).
14. J. E. L. Roovers and S. Bywater, *Macromolecules*, **1**, 328 (1968).
15. T. Fujimoto, N. Ozaki, and M. Nagasawa, *J. Polym. Sci. A*, **3**, 2259 (1965).
16. A. Guyot and J. Vialle, *J. Polymer Sci. B*, **6**, 403 (1968).

Received June 9, 1969
Revised August 19, 1969

JOURNAL OF POLYMER SCIENCE: PART A-1 VOL. 8, 545–561 (1970)

Studies in Cyclocopolymerization. V. Further Evidence for Charge-Transfer Complexes in Cyclocopolymerization

GEORGE B. BUTLER and ALFRED F. CAMPUS, *Department of Chemistry, University of Florida, Gainesville, Florida 32601*

Synopsis

Previous work from this laboratory has shown that certain 1,4-dienes which readily undergo cyclocopolymerization with certain alkenes also form charge-transfer complexes with the same alkenes. The results observed and the proposed cyclocopolymerization mechanism are consistent with participation of the charge-transfer complex as a distinct species in the copolymerization. It was the purpose of this investigation to determine whether there was a dilution effect on the relative reactivities of the monomers in support of the charge-transfer participation concept, and whether the results of a suitable terpolymerization study would also support this postulate. In the divinyl ether–fumaronitrile system, the maximum rate of copolymerization occurred at a monomer feed ratio of 1:2 and the composition of the copolymer was also 1:2 at a total monomer concentration of 3 mole/l. However, when the concentration was progressively lowered to 0.5 mole/l. at the same monomer feed ratio, the fumaronitrile content of the copolymer decreased in a linear manner. In a series of terpolymerization experiments with the divinyl ether–maleic anhydride–acrylonitrile system, it was shown that the divinyl ether–maleic anhydride ratio in the terpolymer was always less than 1:1 and had an upper limit of 1:2, regardless of the feed ratio of the termonomers. These results are consistent with the participation of the charge-transfer complex of divinyl ether and maleic anhydride in a copolymerization process with either maleic anhydride or acrylonitrile as the comonomer.

In an attempt to explain the alternating free-radical copolymerization between styrene and maleic anhydride, Bartlett and Nozaki[1] proposed that the molecular complex formed between the comonomers might participate in the mechanism of the copolymerization. This explanation was supported later by Barb,[2] while other authors[3,4] explained the alternating free-radical copolymerization as resulting from an electron-transfer interaction between the growing radical and the monomer in the transition state of propagation. Styrene is not the only monomer leading to a 1:1 copolymer structure; examples of compounds which form such polymers with maleic anhydride, fumaronitrile, etc. include also ethylene,[5,6] vinyl ethers,[7–10] and ω-phenylalkenes,[11,12] as well as many others. The copolymerization of styrene and maleic anhydride in different solvents was recently reinvesti-

gated[13] and the formation of charge-transfer complexes between the comonomers and their participation in the alternating free-radical copolymerization was extensively studied by Iwatsuki and Yamashita.[7–9] These authors conclude that the alternating copolymerization could be reduced to a homopolymerization of the charge-transfer complex formed between the comonomers and that the terpolymerization of these alternating copolymerizable monomers with a third monomer which has little or no interaction with either monomer of the pair could be reduced to a copolymerization of the charge-transfer complex formed between the alternating copolymerizable monomers and the third monomer.

On the other hand, previous work from this laboratory[14–18] has shown that certain 1,4-dienes would undergo a bimolecular alternating inter–intramolecular copolymerization with certain alkenes as illustrated in eqs. (1).

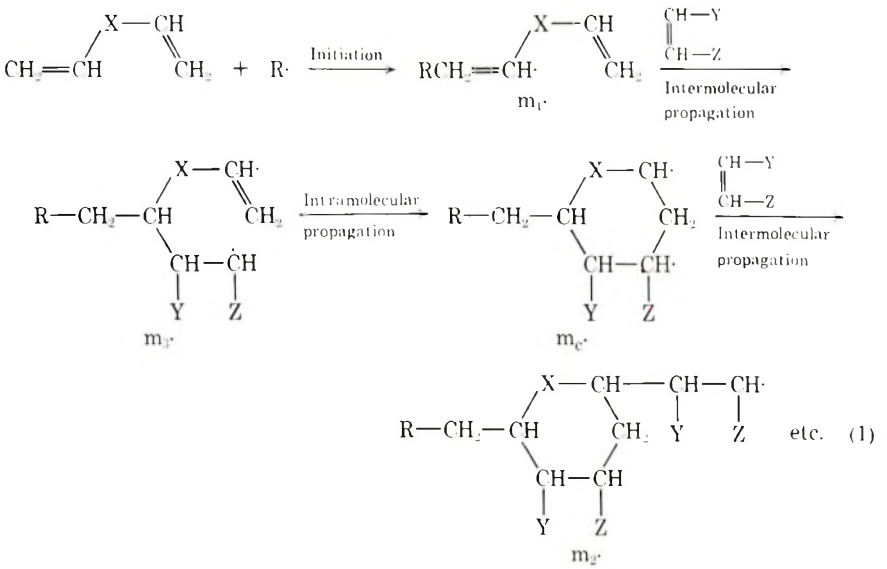

Several systems have been investigated and the 1:2 composition of the copolymers obtained is quite consistent with this mechanism. It was observed[18] that divinyl ether as well as certain other vinyl ethers, forms a charge-transfer complex with certain electron-deficient alkenes such as maleic anhydride and fumaronitrile with which it readily undergoes cyclocopolymerization.

The present study was undertaken to provide further evidence of the formation of the charge-transfer complex between the comonomers and of its participation in the cyclocopolymerization. The 1,4-diene used was divinyl ether (DVE) and the monoolefins were maleic anhydride (MA) and fumaronitrile (FN). Acrylonitrile (AN) was used as the third monomer in the terpolymerization experiments. For comparison, the results of a com-

plex study of styrene–maleic anhydride and ethyl vinyl ether (EVE)–maleic anhydride are also reported.

RESULTS AND DISCUSSION

Determination of the Stoichiometric Composition and the Equilibrium Constant of Complexation of Different Charge-Transfer Complexes Formed between Comonomers Which Undergo Cyclocopolymerization

Stoichiometric Composition

When a solution of maleic anhydride (or fumaronitrile) in chloroform (or DMF) is added to a solution of a 1,4-diene (DVE) or ethyl vinyl ether (EVE) in the same solvent there appears in the ultraviolet spectrum of the mixture a new and broad band whose appearance and position can be at-

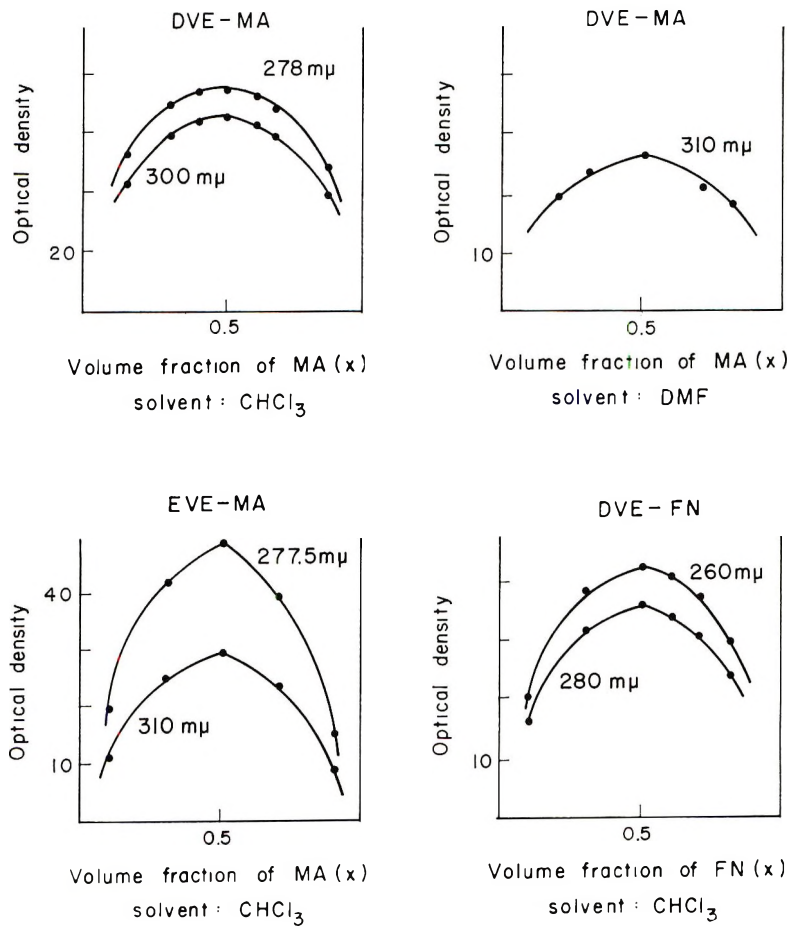

Fig. 1. Ultraviolet determination of the composition of the charge-transfer complexes.

tributed to the formation of electron-donor–acceptor (EDA) complexes. The interpretation of the spectra of these complexes permits the determination of their stoichiometric composition by the continuous variation method.[19,20] The results are shown in Figure 1.

Since MA or FN absorbs near the maximum absorption of their complexes, the experiments had to be run with an identical molar solution of acceptor in the reference beam. The charge-transfer band maximum is at 278 mμ for the DVE–MA complex, and at 260 mμ for the DVE–FN complex. In the case of EVE–MA, the maximum is observed at 277.5 mμ. In all the cases, the maximum absorbance is found to be for a molar fraction of 0.5 in acceptor; hence it can be concluded that the stoichiometry of the complexes DVE–MA (in $CHCl_3$ and DMF), DVE–FN, and EVE–MA is 1:1. We report elsewhere[21] the 1:1 complex formation of trimethylvinylsilane (Me_3VinSi) and dimethyldivinylsilane (Me_2Vin_2Si) with maleic anhydride as acceptor, together with their radical copolymerization. As for the oxygen and the carbon series, the silicon series gives an alternating 1:1 copolymer in the case of Me_3VinSi–MA and 1:2 cyclocopolymer in the case of Me_3VinSi–MA. The geometry of these complexes is unknown as well as whether one or both double bonds of the diene are involved in the complex; however, the structures I and II may be considered:

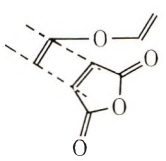

I

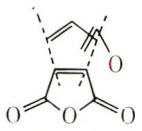

II

We shall report some observations which could be of interest in the understanding of the structure of the complex. It was reported[22] that alkyl vinyl ethers, as well as other electron-rich alkenes, react with tetracyoethylene (TCNE) in order to give a 1:1 addition product having a 1,1,2,2-tetracyanocyclobutane structure. While the reaction of ethyl vinyl ether (EVE) with TCNE is very fast, the reaction of DVE–TCNE is much slower and only the 1:1 addition product could be isolated. The DVE–TCNE adduct was determined by NMR to have the structure III.

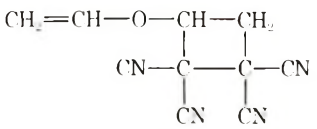

III

This structure is analogous to the structure of the adduct of EVE–TCNE, without the second olefinic bond being involved; the remaining double bond of the DVE–TCNE adduct does not react with an additional amount of TCNE. Moreover, the e value given[23] for EVE ($e = -1.6$) is greater than that observed in the case of DVE ($e = -1.3$). Such observations lead to

the conclusion that the electron density of the double bond is greater for EVE than for DVE, which is easily explained by the effect of the ethoxy group.

On the other hand, in the charge-transfer complex theory it is well known[24] that, when different donors interact with the same acceptor, the charge-transfer energy varies linearly with the ionization potential of the donors and since the ionization potential for alkene derivatives is directly related to the electron density of the double bond, it is reasonable to expect that the DVE–MA complex will not absorb at a significantly longer wavelength than the EVE–MA complex. The results are given in Table I.

TABLE I
Maximum Absorption of the Charge-Transfer Complexes between Vinyl Ethers and Maleic Anhydride[a]

Complex	Absorption maximum, mμ
EVE–MA	277.5
DVE–MA	278
Furan–MA	291

[a] Solvent: $CHCl_3$.

These observations show that the maximum absorption of the DVE–MA complex compared with the EVE–MA complex is not found at a significantly longer wave-length, which suggests that the DVE–MA complex must have some other configuration than that of the EVE–MA complex and that the presence of both double bonds would have some effect on the charge-transfer interaction. Since the cyclic structure is known to appear in the copolymer, it is highly probable that the donor (DVE) in the complex has a pseudo-cyclic structure, analogous to the furan molecule. As shown in Table I, the furan–MA complex has its maximum at 291 mμ, a longer wavelength than the noncyclic ethers. These observations do not establish the absolute configuration of the complex, but since all of them substantiate each other, it can reasonably be postulated at the present time that both double bonds of DVE participate in complex formation with maleic anhydride in a more or less pseudo-cyclic form similar to the furan structure.

Determination of the Equilibrium Constant of Complexation

It is known that it is possible to determine the equilibrium constant of charge-transfer complexes either by ultraviolet spectroscopy by using the Benesi-Hildebrand equation[25] or by nuclear magnetic resonance as was reported in the literature recently.[26–29] The NMR method, where it is applicable, is more accurate and easier, since in the case of weak complexes the ultraviolet absorption maximum is often near that of one of the components. In all the cases the shift of the acceptor protons (singlet) was followed; the concentration of the acceptor was kept constant while the

concentration of the donor was increased; the donor is always in large excess compared to the acceptor. The equation given by Hanna and Ashbaugh[29] was used:

$$1/\Delta^{A}_{obsd} = (1/Q\Delta^{A}_{AD})\,(1/\xi_D) + (1/\Delta^{A}_{AD}) \qquad (2)$$

where $\Delta^{A}_{AD} = \delta^{A}_{obsd} - \delta^{A}_{0}$ is the difference between the shift of the acceptor protons in complexing media (δ^{A}_{obsd}) and the shift of the acceptor is uncomplexed form (δ^{A}_{0}); $\Delta^{A}_{AD} = \delta^{A}_{AD} - \delta^{A}_{0}$ is the difference in the shift of the acceptor protons in pure complex; ξ_D is the concentration of the donor, which has always to be much greater than the acceptor concentration in order that $Q = K$, the equilibrium constant of complexation and that the quotient $\gamma_{AD}/\gamma_A\gamma_D$ remains constant over the range of solutions studied.

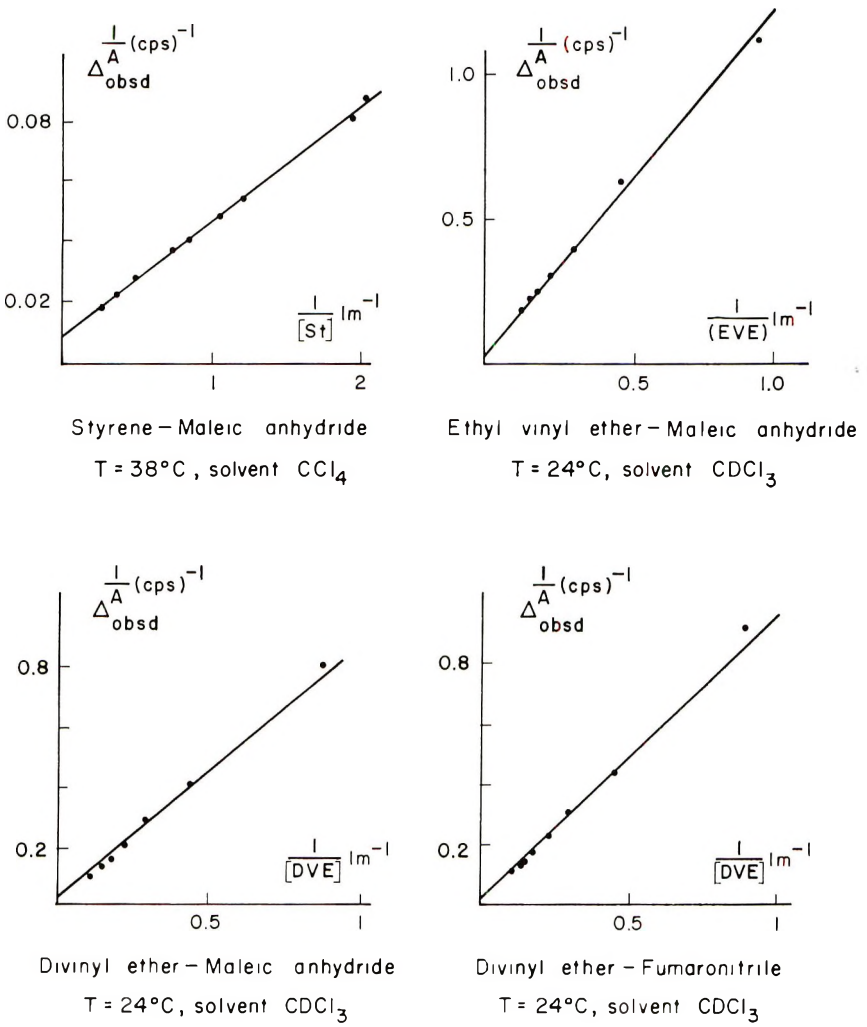

Fig. 2. NMR determination of the equilibrium constant of complexation of the charge-transfer complexes.

TABLE II
NMR Determination of the Equilibrium Constants of Charge-Transfer Complexes

Complex	Solvent	Temp, °C	Δ^{A}_{AD} cps	K, l./mole
St–MA	CCl_4	38	125.0	0.216
EVE–MA	$CDCl_3$	24	21.3	0.041
DVE–MA	$CDCl_3$	24	33.5	0.036
DVE–FN	$CDCl_3$	24	127.5	0.008

In these experiments the acceptor concentration was kept constant at 0.05 mole/l., while the donor concentration was increased from 0.3 to 9 mole/l. By plotting $1/\Delta^{A}_{obsd}$ as a function of $1/\xi_D$, in every case a straight line was obtained; the slope of the line and its intersection with the ordinate permit a first approximation of the equilibrium constant of complexation and of the shift of acceptor protons in the pure complex. For comparative purposes, the equilibrium constant of the complex styrene–maleic anhydride was also determined by this method (Fig. 2).

For a more exact determination of K and Δ^{A}_{AD}, the method of least squares was applied to eq. (2), and the results obtained are summarized in Table II.

As expected, the values of K are relatively low; however they are real; for comparison, the value reported by Foster and Fyfe[28] for the complex between benzene and trinitrobenzene in CCl_4 at 35.5°C is 0.31 l./mole.

Dilution Effect on the Copolymerization of Divinyl Ether with Fumaronitrile

Some authors,[3,4] in the case of alternating free-radical copolymerization, opposed the postulate of participation of the molecular complex in the mechanism of reaction because of the absence of a dilution effect on the monomer reactivities. If we represent by A the acceptor concentration, by D the donor concentration, and by K the equilibrium constant of formation of the molecular complex C, one can write the reaction for formation of this complex as follows:

$$A + D \overset{K}{\rightleftharpoons} C \tag{3}$$

the complex concentration being

$$[C] = K[A][D] \tag{4}$$

By diluting the reaction solution by a factor of two, the concentration of the complex in the new medium will be decreased by a factor of four:

$$[C]' = K([A]/2)([D]/2) = [C]/4 \tag{5}$$

If the molecular complex is responsible to some extent for the regularity of the 1:2 structure in the cyclocopolymer, it is quite reasonable to expect a decrease of this regularity by dilution, since the dilution will decrease the relative concentration of the complex.

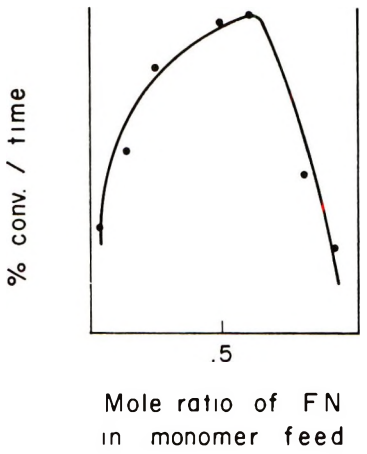

Fig. 3. Rate of copolymerization of DVE–FN.[17]

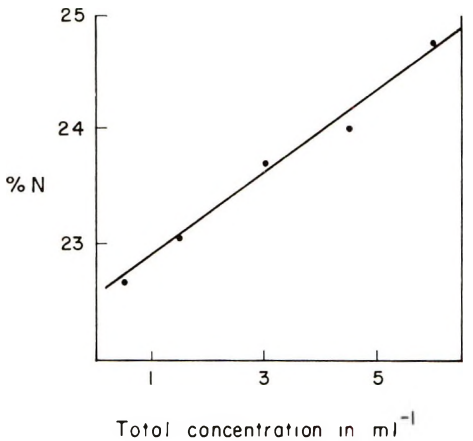

Fig. 4. Effect of dilution on the copolymerization of divinyl ether (M_1) with fumaronitrile (M_2).

The copolymerization of divinyl ether with fumaronitrile has been reported from this laboratory.[17] While in alternating copolymerization, a maximum in the rate of polymerization for an initial monomer feed of 1:1[7–9] (medium in which the concentration of complex is highest) is observed, in this case (Fig. 3) a polymerization rate maximum for a monomer feed of DVE–FN equal to 1:2, similar to the composition of the polymer obtained, is observed; recall however, that the stoichiometry of the complex is 1:1. The two steps of cyclocopolymerization, namely the formation of the cyclic radical and the addition of the electron-poor monomer to this cyclic radical, seem thus to be dependent upon the electronegativity difference between the two monomers, which is responsible for the complex formation. For the optimal monomer feed for DVE–FN (1:2), copolymerizations were carried out for different total concentrations in the same

TABLE III
Dilution Effect on the Copolymerization of Divinyl Ether (M_1) with Fumaronitrile (M_2)[a]

Run no.	Total concentration, mole/l.	N, %[b]	M_2	$[\eta]$, dl/g[c]
CDII	6	24.74	0.660	
CDI6	4.5	24.00	0.642	0.13
CDI3	3	23.68	0.630	0.11
CDI2	1.5	23.05	0.615	
CDI5	0.5	22.66	0.600	

[a] Solvent, DMF; 60°; DVE/FN = 1:2; initiator, AIBN (1 mole-%).
[b] Nitrogen percentage was corrected on the basis of 95% found for polyacrylonitrile.
[c] In acetone, 30°C.

solvent (DMF), in order to determine whether there was a dilution effect in this system. The results are given in Table III and Figure 4.

Upon diluting the medium of copolymerization, not only was a decrease of the rate of polymerization observed, as expected, but also a decrease in the nitrogen content of the copolymer and consequently in the fumaronitrile content. The upper limit of FN content in the copolymer corresponds thus to the 1:2 structure (III) previously described:[14–18]

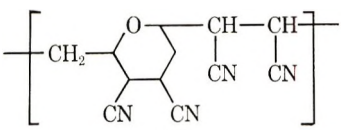

III

Since by dilution, the nitrogen content decreases, this 1:2 regularity of the copolymer must also decrease. NMR and infrared studies, however, do not show any detectable change in the spectra of the copolymers and particularly in their unsaturation content; such structures as, IV must thus be unimportant.

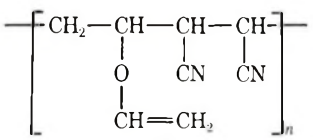

IV

Two remaining possibilities which can explain the decrease of FN in the copolymer are (1) the decrease of selectivity of addition to the cyclic radical and (2) homopolymerization of a limited number of divinyl ether units. Both require addition of vinyl ether radicals to vinyl ether double bonds. This has been shown to occur in a homopolymerization study of DVE;[30] however the rate of this homopolymerization has been shown to be very low compared to its copolymerization with FN, but in the absence of suffi-

cient FN this alternative course would be favored. The first possibility would lead to a limited sequence of units having the structure V.

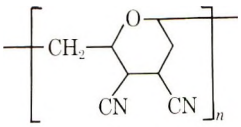

V

The second possibility would lead to a limited sequence of structure VI units:[30]

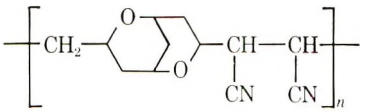

VI

The structure of the copolymer can thus be represented as III_x-V_y-VI_z, in which $x \rangle\rangle\rangle y,z$. Consequently, it can be concluded that addition to the cyclic radical is less selective than the cyclization step. An analogous effect has also been observed in the case of terpolymerization (discussed in the following section).

Radical Terpolymerization of Divinyl Ether, Maleic Anhydride, and Acrylonitrile

The copolymerizations of DVE:MA and DVE:AN were reported earlier by this laboratory.[14] While the copolymer DVE–MA has a true 1:2 structure, the copolymer DVE–AN is generally richer in acrylonitrile than the 1:2 composition expected; however, in this case also, the divinyl ether enters into the copolymer in a six-member ring form by copolymerization with AN. The high concentration in AN in the copolymer can be explained by the fact that AN can readily homopolymerize by a free radical mechanism while MA does not.

Another explanation could be found in the fact that the polymerizable double bond of acrylonitrile is less electron-deficient (e = 1.20)[31] compared with the values of maleic anhydride (e = 2.25) and fumaronitrile (e = 1.96); the molecular association between AN and DVE will thus be much less stable than the association of DVE–MA, and thus the effect of this association on the polymerization mechanism, if any, will be greater in the case of MA and FN than in the case of AN. We were indeed unable to detect any obvious molecular association between DVE and AN, while we showed in the first part that DVE and MA form a stable charge-transfer complex. On the other hand, acrylonitrile (M_1) copolymerizes only to a small extent, if at all, with maleic anhydride (M_2). The values of the reactivity ratios given in the literature[32] are $r_1 = 6$, $r_2 = 0$(60°C).

In the first series of experiments the donor acceptor ratio was kept constant at the optimal value of 1:2, the donor being divinyl ether, and the acceptor being the sum of maleic anhydride and acrylonitrile; in every ex-

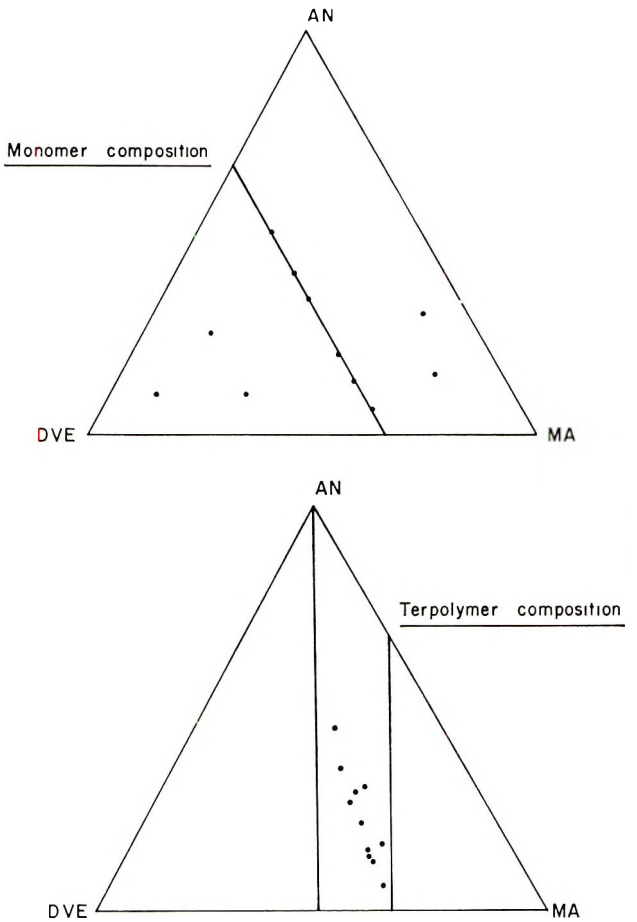

Fig. 5. Radical terpolymerization of divinyl ether (DVE)-maleic anhydride (MA)-acrylonitrile (AN).

periment the relative molar concentration in MA and AN was varied, their sum being always twice the molar concentration of DVE. In a second series of experiments different ratios of DVE:MA:AN, were used, the total concentration being the same in all the experiments and equal to 6 mole/l. The results are given in Table IV and Figure 5.

From these experiments, it was observed that when the donor/acceptor ratio was kept constant (1:2), while varying the relative concentration in MA and AN, a terpolymer was obtained, soluble in DMF, acetone, etc., and containing a ratio DVE:MA always less than 1:1 and having as a limit the value 1:2. Also, the terpolymer was always richer in MA and always poorer in AN than the monomer feed, although AN can homopolymerize readily by a free radical mechanism. NMR and infrared studies showed no detectable remaining double bond in the terpolymer. In all the experiments regardless of the composition of the monomer

TABLE IV
Terpolymerization of Divinyl Ether–Maleic Anhydride–Acrylonitrile[a]

Run no.	Monomer composition			Conversion, %	Polymer composition[b]			[η], dl/g[c]
	AN, %	MA, %	DVE, %		AN, %	MA, %	DVE, %	
T II 3RE	6.6	60.0	33.3	6.32	6.6	60.8	32.6	
T II 1R3	13.3	53.3	33.3	3.24	13.9	53.9	32.1	0.12
T II 4 RE	20.0	46.6	33.3	6.54	15.2	53.5	31.2	
T II 5 RE	33.3	33.3	33.3	7.50	27.2	43.6	29.2	
T II 2R3	40.0	26.6	33.3	3.29	35.7	36.9	27.4	0.13
T II 6	50.0	16.6	33.3	4.22	45.2	31.3	23.7	
T II 7B	10.0	10.0	80.0	9.37	22.0	48.6	29.4	
T II 8	10.0	30.0	60.0	8.42	16.6	55.8	27.6	0.19
T II 9	25.0	15.0	60.0	4.90	30.5	45.1	24.3	
T II 10	15.0	70.0	15.0	2.64	12.3	55.6	32.1	0.09
T II 11	30.0	60.0	10.0	2.16	29.8	43.7	26.5	

[a] Solvent, DMF; 60°C; initiator, AIBN (1 mole-%); total initial monomer concentration, 6 mole/l.
[b] Based upon nitrogen and carboxyl content.
[c] In DMF, 30°C.

feed used, the ratio DVE:MA in the terpolymer was always less than 1:1 and had the 1:2 structure as an upper limit. Since the ratio DVE:MA in the terpolymer varies from 1:1 to 1:2, and MA does not homopolymerize nor copolymerize with AN under the conditions used, one has to conclude that every molecule of DVE in the terpolymer chain is cyclized by a MA molecule to form the DVE:MA cyclic unit represented by X·:

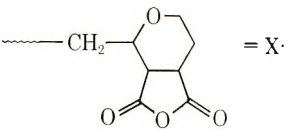

If X· reacts with another molecule of MA

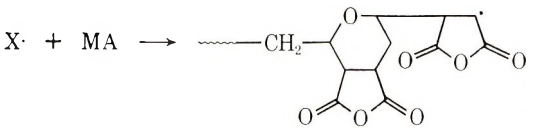

in order to give the 1:2 DVE:MA structure, this step, because of the non-reactivity of the MA radical with another molecule of MA or with AN, must be followed by an addition of a new DVE–MA couple.

If X· reacts with acrylonitrile,

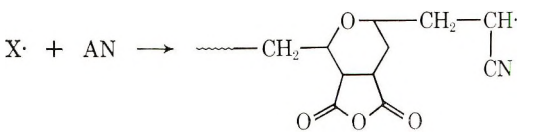

one obtains a growing chain terminated by an acrylonitrile radical; this AN radical can react either with a DVE–MA couple or with another molecule of AN. The homopolymerization of the acrylonitrile radical will result in a sequence of AN units within the chain of the terpolymer, which will increase the nitrogen content of the terpolymer and decrease the 1:2 regularity of the monomer pair DVE–MA, just like in the copolymerization of DVE–AN discussed above. The terpolymer can thus be represented by the structure VII:

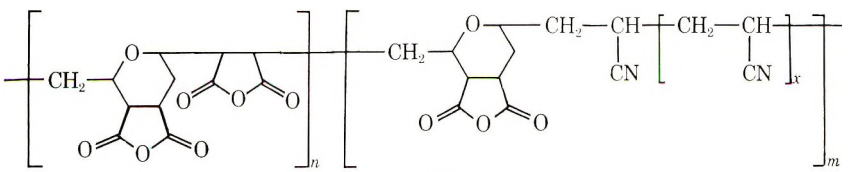

VII

where n represents the 1:2 DVE–MA unit in the cycloterpolymer, and m the unit containing acrylonitrile. In the series of terpolymerizations in which the donor/acceptor ratio was kept constant to the 1:2 value, it was

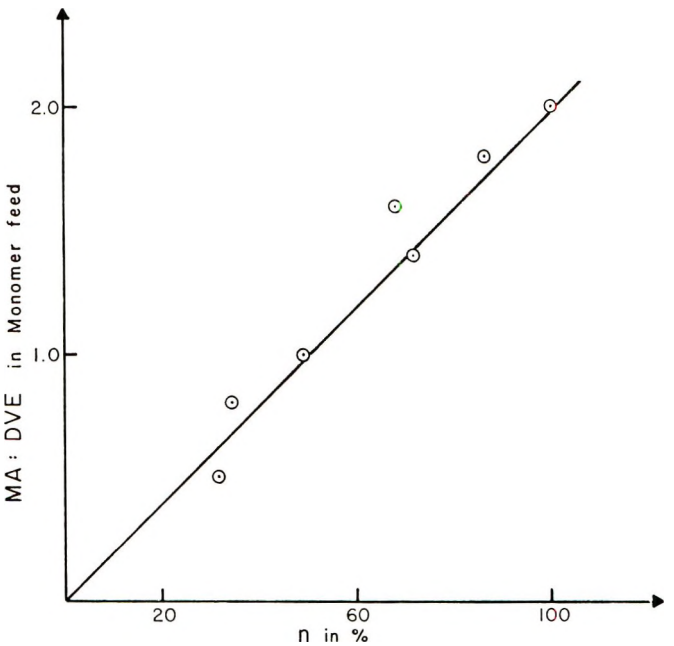

Fig. 6. Variation of the 1:2 DVE–MA content on the terpolymer (n) vs. the MA:DVE ratio in the monomer feed.

observed that the value of n decreased with the decrease of the MA:DVE ratio in the monomer feed. The results are given in Table V and Figure 6. Here again in the terpolymerization system, it was observed that by diluting the polymerization solution, a decrease in the selectivity of the monomer

TABLE V
Variation of the 1:2 DVE–MA Content in the Terpolymer (n) with the MA:DVE Ratio in the Monomer Feed

Run no.	MA:DVE in monomer feed	n, %
T II 3 R E	1.8	86.5
T II 1 R 3	1.6	67.9
T II 4 R E	1.4	71.5
T II 5 R E	1.0	49.3
T II 2 R 3	0.8	34.7
T II 6	0.5	32.1

addition was observed (Table VI). Indeed, for a monomer feed of DVE:-MA:AN equal to 1:1:1, the value of the 1:2 DVE–MA content in the terpolymer (n) decreased with dilution, while the AN content increased for the same content of DVE.

TABLE VI
Dilution Effect on the Terpolymerization of Divinyl Ether–Maleic Anhydride–Acrylonitrile[a]

Run no.	Total initial monomer concentration, mole/l.	Conversion, %	Polymer composition[b] AN, %	MA, %	DVE, %	n, %
T II 5RE	6	7.5	27.2	43.6	29.2	49.3
T II 5dl	1.2	8.8	31.3	39.7	29.0	36.9

[a] Solvent, DMF; 60°C; initiator, AIBN (1 mole-%); ratio DVE:MA:AN = 1:1:1.
[b] Based upon nitrogen and carboxyl content.

Thus, it is shown in these cycloterpolymerization experiments that divinyl ether reacts preferably with maleic anhydride in order to give a cyclopolymer. This verifies the statement that was made above, that the molecular association between maleic anhydride and divinyl ether, being greater (e value greater) than the association between divinyl ether and acrylonitrile, has a greater effect in controlling the composition of the terpolymer. This molecular association, being of the nature of a charge-transfer complex, thus has a remarkable effect on the cyclocopolymerization mechanism. It was also observed that while the cyclization step is very selective (DVE–MA), the next step, the addition of the monoalkene to the cyclic radical is only slightly so, which allows the inclusion of AN units in the terpolymer chain.

EXPERIMENTAL

Materials

Divinyl ether, obtained from Merck, Sharp and Dohm, and ethyl vinyl ether obtained from Carbide Chemicals, were freshly distilled (under nitrogen) before reaction. Maleic anhydride was recrystallized first from chloroform and then sublimed before use. Fumaronitrile and dimethylformamide (Fisher reagent) used as solvent were purified as reported in the literature.[17,33] Acrylonitrile was distilled under nitrogen, and azobisisobutyronitrile (AIBN) used as initiator was recrystallized from methanol.

Polymerization

For each system, the monoolefin (MA or FN) was weighed; divinyl ether and acrylonitrile were measured volumetrically into volumetric flasks and diluted to volume with solvent. The concentration of AIBN was 1% per mole of total monomer concentration. The solution was transferred to glass tubes, and the tubes were evacuated twice and sealed under high vacuum. The polymerizations were carried out at 60 ± 0.01°C, and the polymers were purified by precipitations into a nonsolvent, filtered

through fritted glass filter funnels and dried in a vacuum oven prior to analysis. The fumaronitrile copolymers were precipitated into methanol and purified by reprecipitation from acetone into dry pentane. The maleic anhydride terpolymers were preicipitated into dry diethyl ether and purified by reprecipitation from acetone into dry pentane.

Analysis

The composition of the copolymers and terpolymers were calculated from their nitrogen (FN,AN) and carboxylic (MA) content. The nitrogen analyses were done in duplicate by Galbraith Microanalytical Laboratories, Knoxville, Tennessee. The maleic anhydride content was determined by high frequency titration, using a Sargent Chemical Oscillometer, Model V.

Stoichiometric Composition of the Charge-Transfer Complexes

Spectrophotometric studies of the complexes were run on a Beckman DK-2A spectrophotometer using chloroform (or DMF) as solvent. The concentrations of the initial solutions were 2 mole/l.; 10^{-2} cm cells were used.

NMR Determination of the Equilibrium Constant of Complexation

The NMR studies were done on a Varian Associates analytical NMR spectrometer, model A-60. The solutions (in $CDCl_3$) of 1,4-dienes–monoolefins were prepared at room temperature in volumetric flasks and the temperature of the NMR spectrometer was kept constant at the same temperature. In the case of styrene–maleic anhydride, the solutions (in CCl_4) were prepared at 38°C, normal temperature of the apparatus. The concentration of the acceptor was kept constant at 0.05 mole/l., while the donor concentrations (at least 10 times higher) was increased.

This work was supported predominantly by National Institutes of Health, Grant No. CA 06838 for which we are grateful. One of us (AFC) also received financial support for a brief period from a post-doctoral fellowship award made available to the Department of Chemistry through a Science Development Grant from the National Science Foundation. The intrinsic viscosity determinations were made by Mr. C. Lawson Rogers.

References

1. P. D. Bartlett and K. Nozaki, *J. Amer. Chem. Soc.*, **68**, 1495 (1946).
2. W. Barb, *Trans. Faraday Soc.*, **49**, 143 (1953).
3. F. M. Lewis, C. Walling, W. Cummings, E. R. Briggs, and F. R. Mayo, *J. Amer. Chem. Soc.*, **70**, 1519 (1948).
4. C. Walling, E. Briggs, K. Wolfstirn, and F. R. Mayo, *J. Amer. Chem. Soc.*, **70**, 1537 (1948).
5. L. H. Flett and W. H. Gardner, *Maleic Anhydride Derivatives, Reactions of the Double Bond*, Wiley, New York, 1952, p. 26.
6. W. E. Hanford, U. S. Pat. 2,378,629 (1945); *Chem. Abstr.*, **39**, 4265 (1945).
7. S. Iwatsuki, Y. Yamashita et al., *Kogyo Kagaku Zasshi*, **67**, 1464, 1467, 1470 (1964); *ibid.*, **68**, 1138, 1963, 1967, 2463 (1965); *ibid.*, **69**, 145 (1966).

8. S. Iwatsuki, Y. Yamashita et al., *Makromol. Chem.*, **89**, 205 (1965); *ibid.*, **102**, 232 (1967).
9. S. Iwatsuki and Y. Yamashita, *J Polym. Sci. A-1*, **5**, 1753 (1967).
10. R. D. Kimbrough, *J. Polym. Sci. B*, **2**, 85 (1964).
11. M. M. Martin and N. P. Jensen, *J. Org. Chem.*, **27**, 1201 (1962).
12. C. Aso and T. Kunitake, *Bull. Chem. Soc. Japan*, **38**, 1564 (1965).
13. E. Tsuchida, Y. Ohtani, H. Nakadai, and I. Shinohara, *Kogyo Kagaku Zasshi*, **70**, 573 (1967).
14. G. B. Butler, *J. Polym. Sci.*, **55**, 1967 (1961).
15. J. M. Barton, G. B. Butler, and E. C. Chapin, *J. Polym. Sci. A*, **3**, 501 (1965).
16. G. B. Butler and R. B. Kasat, *J. Polym. Sci. A*, **3**, 4205 (1965).
17. G. B. Butler, G. Vanhaeren, and M. F. Ramadier, *J. Polym. Sci. A*, **5**, 1265 (1967).
18. G. B. Butler and K. C. Joyce, in *Macromolecular Chemistry, Brussels-Louvain 1967*, (*J. Polym. Sci. C*, **22**), G. Smets, Ed., Interscience, New York, 1968, p. 45.
19. P. Job, *C. R. Acad. Sci.* (Paris), **180**, 928 (1925); *Ann. Chim. Phys.*, **9**, 113 (1928).
20. W. C. Vosburgh and G. R. Cooper, *J. Amer. Chem. Soc.*, **63**, 437 (1941).
21. G. B. Butler and A. F. Campus, *J. Polymer Sci. A-1*, in press.
22. J. K. Williams, D. W. Wiley, and B. C. McKusick, *J. Amer. Chem. Soc.*, **84**, 2210 (1962).
23. C. C. Price and T. C. Schwan, *J. Polym. Sci.*, **16**, 577 (1955).
24. G. Briegleb, *Elektronen-Donator-Acceptor Komplexe*, Springer Verlag, Berlin-Göttingen Heidelberg, 1961.
25. H. A. Benesi and J. H. Hildebrand, *J. Amer. Chem. Soc.*, **71**, 2703 (1949).
26. M. W. Hanna and A. L. Ashbaugh, *J. Phys. Chem.*, **68**, 811 (1964).
27. A. A. Sandoval and M. W. Hanna, *J. Phys. Chem.*, **70**, 1203 (1966).
28. R. Foster and C. A. Fyfe, *Trans. Faraday Soc.*, **61**, 1626 (1965).
29. R. Foster, C. A. Fyfe, and M. I. Foreman, *Chem. Comm.*, **1967**, 913.
30. C. Aso and S. Ushio, *Kogyo Kagaku Zasshi*, **65**, 2085 (1962).
31. G. E. Ham, *Copolymerization*, Interscience, New York, 1964.
32. F. R. Mayo, F. M. Lewis, and C. Walling, *J. Amer. Chem. Soc.*, **70**, 1529 (1948).
33. *Organic Syntheses*, **30**, 46 (1950).

Received December 9, 1968
Revised August 20, 1969

JOURNAL OF POLYMER SCIENCE: PART A-1 VOL. 8, 563–576 (1970)

Synthesis and Characterization of Polyiminobenzothiazoles

ROBERT C. EVERS, *Polymer Branch, Nonmetallic Materials Division, Air Force Materials Laboratory, Wright-Patterson Air Force Base, Ohio 45433*

Synopsis

A series of polyiminobenzothiazoles was synthesized by the polymerization of either 2,6-dichloro- or 2,6-diphenoxybenzobisthiazole with a number of aromatic diamines. A polymer was also obtained from the self-condensation of either 2-chloro- or 2-phenoxy-6-aminobenzothiazole. The polymers were characterized by their elemental analysis and infrared spectra. Thermogravimetric analysis, differential thermal analysis, and softening under load were used to evaluate their thermal properties. The polymers were found to be light tan to brown powders which showed only slight softening below their decomposition temperatures. Onset of breakdown under thermogravimetric analysis in a nitrogen atmosphere generally occurred at 375–400°C. The polymers were sparingly soluble in organic solvents and had inherent viscosities in the range of 0.11–0.55.

INTRODUCTION

Over the past decade, a number of new aromatic-heterocyclic polymers of superior thermal stability have been synthesized. Among these are the polybenzothiazoles, which have been prepared in high molecular weight by several methods.[1–5] These polymers show good thermal stability in both air and in nitrogen. They are soluble, however, only in concentrated sulfuric acid and are infusible in their final cyclized form.

This paper describes the preparation and characterization of a new polymer system which is analogous to the polybenzothiazole system but contains an imino group between the 2-position of the benzothiazole ring and the aromatic nucleus. The hetero linkage would be expected to detract from the thermal stability of the polymer but to increase the solubility and fusibility of the system over that of the polybenzothiazoles. This class of polymers will be referred to here as polyiminobenzothiazoles and can be represented by the general structure:

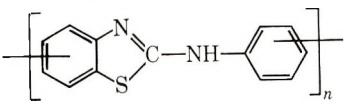

The preparation of a number of polyiminobenzothiazoles by both solution and melt polymerization techniques is described below.

TABLE I
Polymerization Conditions

Trial no.	Monomers	Reaction medium	Acid acceptor	Reaction temp, °C	Reaction time, hr	Soluble, %	η_{inh} (solvent)[a]
1	2,6-Dichlorobenzobis-thiazole + benzidine	TMS	DEA	150–160	24	65	0.31 (DMAC)
2	"	TMS	NMP	170	2.5	95	0.13 (DMAC)
3	2,6-Dichlorobenzobis-thiazole + 4,4′-diamino-diphenylsulfone	TMS	DEA	150	2	40	0.55 (DMAC)
4	"	TMS	NMP	130	18	100	0.11 (DMAC)
5	2,6-Dichlorobenzobis-thiazole + 4,4′-diamino-diphenylether	TMS	DEA	150	2	0	—
6	"	TMS	NMP	230	0.25	95	0.24 (DMAC)
7	"	TMS	NMP	120	18	100	0.18 (DMAC)
8	2,6-Dichlorobenzobis-thiazole + 4,4′-diamino-diphenylmethane	TMS	NMP	140–150	2	100	0.24 (HMP)

9	2,6-Diphenoxybenzobis-thiazole + benzidine	Melt	—	150–200	6	100	0.14 (DMAC)
10	"	Melt	—	170–200	2	100	0.21 (DMAC)
11	2,6-Diphenoxybenzobis-thiazole + 4,4′-diamino-diphenylmethane	Melt	—	200	2	40	0.32 (HMP)
12	2-Chloro-6-aminobenzo-thiazole	NMP	NMP	180	3	100	0.19 (DMAC)
13	"	TMS	NMP	140–200	22	95	0.49 (DMAC)
14	"	TMS	NMP	170	3.5	95	0.18 (DMAC)
15	"	TMS	DEA	215	48	100	0.14 (DMAC)
16	2-Phenoxy-6-aminobenzo-thiazole	Melt	—	260–280	1	100	0.19 (DMAC)
17	"	Melt	—	290	0.5	70	0.29 (HMP)

[a] Values obtained at solution concentrations of 0.2–0.4 g/100 ml at 25°C.

DISCUSSION

A survey of the literature revealed that a number of methods are known for the preparation of benzothiazoles containing an imino group in the 2-position of the heterocyclic ring. The preparation of a number of model compounds by some of the more promising methods indicated that the nucleophilic displacement reactions of aromatic amines with various 2-chloro- or 2-phenoxy-benzothiazoles proceeded smoothly and in high yield. The scope of the present work, therefore, was limited to the preparation of aromatic polyiminobenzothiazoles via the polycondensation of various aromatic diamines with 2,6-dichloro- or 2,6-diphenoxybenzobisthiazole. The self-condensation of 2-chloro- and 2-phenoxy-6-aminobenzothiazole was also studied. These polymerization reactions are described below and are summarized in Table I.

Polymerization Reactions

Polymerization of Aromatic Diamines with 2,6-Dichloro- and 2,6-Diphenoxybenzobisthiazole. The solution polymerization of 2,6-dichlorobenzobisthiazole with a number of aromatic diamines (benzidine, 4,4′-diaminodiphenylsulfone, diaminodiphenyl ether, and diaminodiphenylmethane) was investigated with the use of tetramethylene sulfone (TMS) as a solvent and either diethylaniline (DEA) or *N*-methylpyrrolidone (NMP) as acid acceptors:

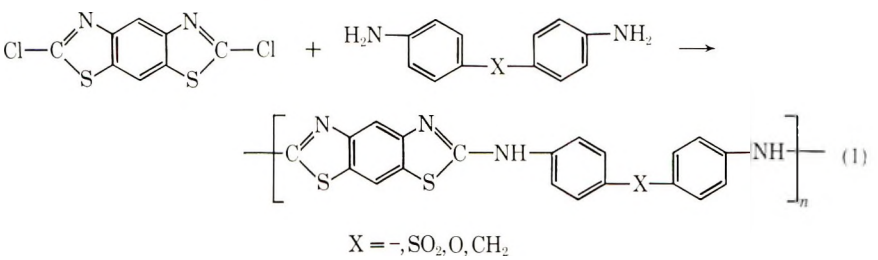

(1)

X = –, SO_2, O, CH_2

The resulting polymers had various degrees of solubility in DMAC or hexamethylphosphoramide (HMP) and the inherent viscosities of the insoluble portions ranged from 0.11 to 0.55. Most of the insoluble portions were readily soluble in cold concentrated sulfuric acid or warm methanesulfonic acid, but tests indicated that concurrent degradation of the polymer also occurred. As the inherent viscosities increased, the proportion of soluble polymer usually decreased. Yields were in the range of 40-80 percent. Considerable loss of material (presumably low molecular weight polymer) occurred during purification of the products by a dissolution-reprecipitation process and/or Soxhlet extraction. This was especially true in those cases in which DEA was used as an acid acceptor.

Attempts to advance the molecular weights of the polymers by secondary solid-phase reactions for 2–4 hr at temperatures of less than 225°C did not lead to an increase in molecular weight. Heating at temperatures above

225°C for a similar length of time resulted in polymers which were insoluble in organic solvents. It is not known whether this insolubility was due to cross-linking or to an increase in the degree of polymerization of the polymer. It is interesting to note, however, that appreciable swelling of the insoluble portions occurred in DMAC or HMP. This might be taken as evidence that crosslinking did occur in addition to any possible increase in the degree of polymerization. The crosslinking would probably result from attack of imino groups in the polymer chain upon unreacted chloro endgroups. Due to the relatively low nucleophilicity of the imino groups, one would expect that temperatures in excess of 225°C would be necessary for reaction (crosslinking) to take place.

The reaction of *N,N'*-diethylbenzidine, or *N,N'*-diphenylbenzidine with 2,6-dichlorobenzobisthiazole resulted in products of low molecular weight whose elemental analyses were completely inconsistent with the proposed structures.

The melt polymerization of 2,6-diphenoxybenzobisthiazole with benzidine or 4,4'-diaminodiphenylmethane proceeded readily at 180–190°C and yielded polymers with inherent viscosities of 0.14–0.32. If reaction temperatures greater than 225°C were used, substantial portions of insoluble polymer resulted.

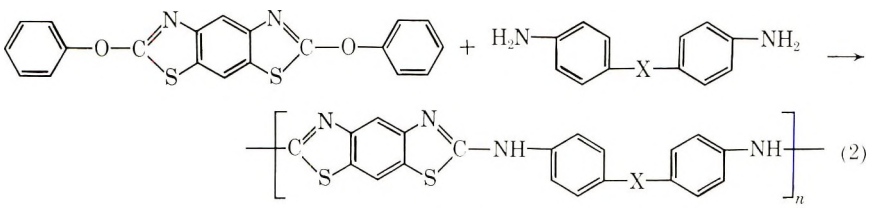

(2)

X = –, CH_2

Neither 4,4'-diaminodiphenylsulfone nor *N,N'*-diethylbenzidine would react to any extent with the diphenoxy derivative in the melt at temperatures up to 320°C. This lack of reactivity can be attributed to the lower nucleophilicity of these diamines as compared to benzidine and 4,4'-diaminodiphenymethane.

Self-Condensation of 2-Chloro- and 2-Phenoxy-6-aminobenzothiazole. A number of attempts to prepare a polyiminobenzothiazole by the solution polymerization of 2-chloro-6-aminobenzothiazole met with varying degrees of success.

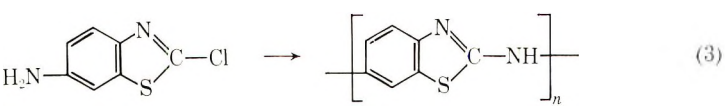

(3)

The highest viscosities (up to 0.49) were obtained in those cases in which TMS was used as a solvent and NMP as an acid acceptor. However, elemental analyses indicated the presence of chlorine in the polymers in considerable excess over that which would be expected from unreacted end-

groups. Attempts to purify the polymers were only partially successful. Other solution polymerizations with DEA as the acid acceptor generally yielded only very low molecular weight material and a low yield of polymer. No polymer could be isolated from reactions in which either HMP or dimethyl sulfoxide was used as a solvent.

In order to prepare a pure polymer, the melt polymerization of 2-phenoxy-6-aminobenzothiazole was investigated. This polymer evolved phenol at 260°C to give high yields of polymer with inherent viscosities of 0.19 and 0.29. If the reaction temperature was increased to 290°C for 1 hr, a substantial portion of the polymer was insoluble in organic solvents. The elemental analysis of the polymer agreed fairly well with the calculated values.

Model Compounds

Four model compounds (I–IV) were prepared in order to serve as a reference for the determination of structure of the polyiminobenzothiazoles. 2-Anilino-

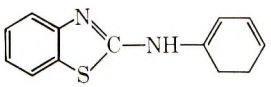

I

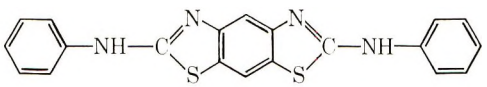

II

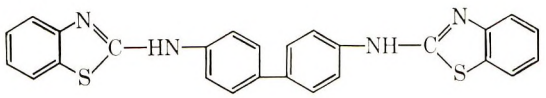

III

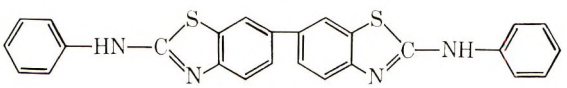

IV

benzothiazole (I) and 2,6-dianilinobenzobisthiazole (II) were prepared by several synthetic routes but the method of choice[6,7] was the reaction of aniline with 2-chlorobenzothiazole and 2,6-dichlorobenzobisthiazole or the corresponding phenoxy- derivatives. Yields of 85–90% were obtained. 4,4′-Bis(2-iminobenzothiazolyl)biphenyl (III) was prepared in a similar manner from 2-phenoxybenzothiazole and benzidine. 2,2′-Dianilino-6,6′-bibenzothiazole (IV) was prepared in low yield from 3,3′-dimercaptobenzidine and phenylisothiocyanate.

These compounds were white crystalline or powdery solids which were soluble in a number of polar organic solvents and could be recrystallized from glacial acetic acid or dilute ethanol. They could be hydrolyzed by gentle warming in concentrated sulfuric or hydrochloric acid.

Physical Properties of Polymers

The physical properties of the polyiminobenzothiazoles are discussed below and are summarized in Table II.

TABLE II
Physical Properties of Polymers

Trial no.	Structure	Appearance	η_{inh} (solvent)[a]	Analysis: Calcd for DP = ∞, (Found) C, %	H, %	N, %	S, %	O, %	Inversion points, °C: Softening curve[b]	TGA curve[c]	DTA transition, °C[d]
2	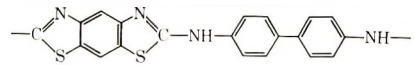	Light brown powder	0.13 (DMAC)	64.52 (63.20)	3.23 (3.40)	15.05 (14.64)	17.20 (17.30)	—	240	470	None observed
4	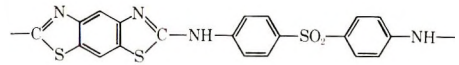	Brown powder	0.11 (DMAC)	55.05 (53.55)	2.75 (3.33)	12.83 11.71	22.02 21.85	7.34 (8.30)	320	420	365, 470
6	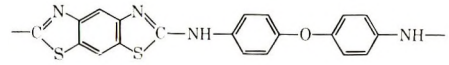	Brown powder	0.24 (DMAC)	61.56 (61.78)	3.09 (3.87)	14.43 (12.51)	16.49 (16.51)	4.12 (5.30)	200	470	290
11	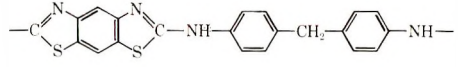	Tan powder	0.32 (HMP)	65.20 (65.39)	3.63 (3.68)	14.51 (13.80)	16.58 (15.62)	—	260	420	184, 249
17	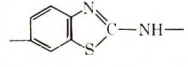	Greenish powder	0.29 (HMP)	56.76 (57.42)	2.70 (3.45)	18.92 (17.21)	21.62 (20.21)	—	250	420	175

[a] Values determined on a solution concentrations of 1.2–0.4 g/100 ml at 25°C.
[b] ΔT = 150°C/hr in an air atmosphere.
[c] ΔT = 180°C/hr in a nitrogen atmosphere.
[d] ΔT = 20°C/min in an air atmosphere.

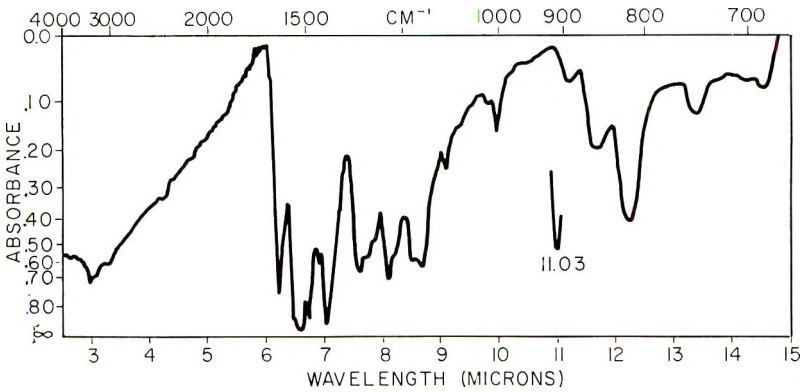

Fig. 1. Infrared spectrum of polymer prepared from 2,6-diphenoxybenzobisthiazole and benzidine (KBr pellet).

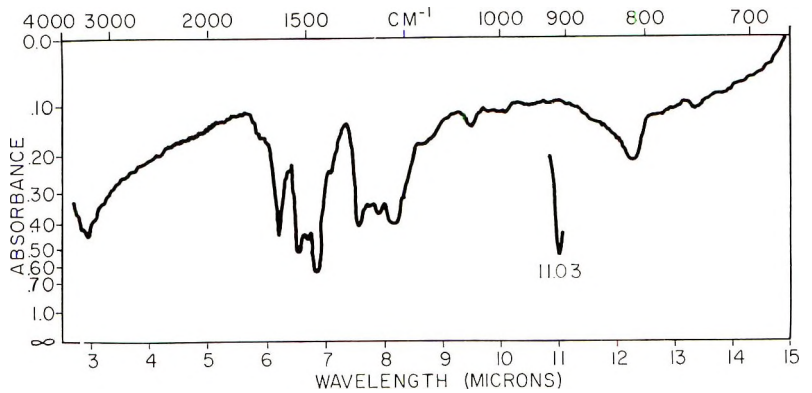

Fig. 2. Infrared spectrum of polymer prepared from 2-phenoxy-6-aminobenzothiazole (KBr pellet).

General Appearance. The polymers were light tan to brown-colored powders with the exception of the polymer from 2-phenoxy-6-aminobenzothiazole which was a yellowish-green powder. They were only sparingly soluble in organic solvents such as DMAC or HMP. In no cases, would they form concentrated solutions in these solvents. The polymers dissolved readily in concentrated sulfuric acid but appeared to hydrolyze rather rapidly in that medium.

Molecular Weight. The polymers exhibited inherent viscosities of 0.11–0.55 in either DMAC or HMP. Vapor-pressure osmometric determinations of molecular weight on several of the polyiminobenzothiazoles prepared from 2,6-dichlorobenzobisthiazole produced values of 2300–2600 for polymers with inherent viscosities of 0.11–0.18. These values would correspond to approximately 6 to 7 repeating units in the molecule. It was not possible to obtain values for the polymers of higher inherent viscosity due to their low solubility in organic solvents. Extrapolation of the present

results, however, indicate that an inherent viscosity of 0.5 corresponds to a molecular weight of approximately 10,000.

Infrared Spectra. The infrared spectra of the polymers were consistent with their assigned structures and corresponded well with the spectra of the model compounds. In all cases, the polymer spectra had bands at

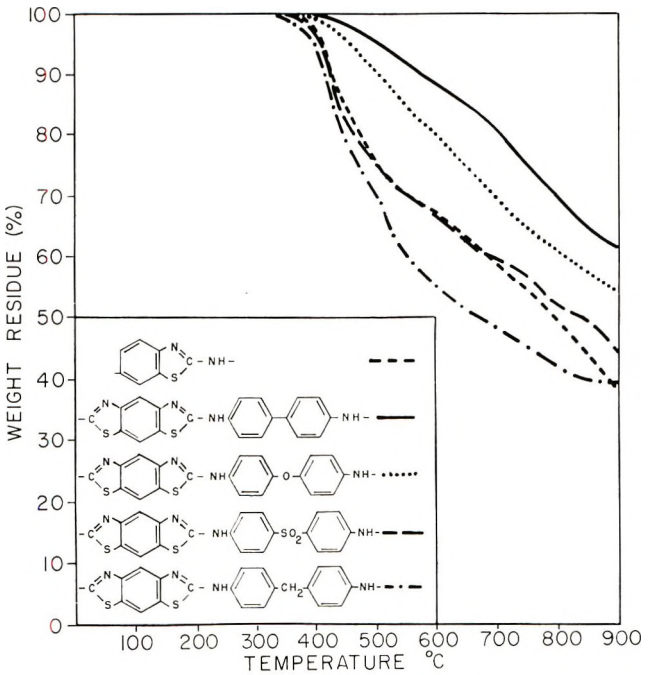

Fig. 3. Composite TGA plots. ΔT = 180°C/hr, in N_2.

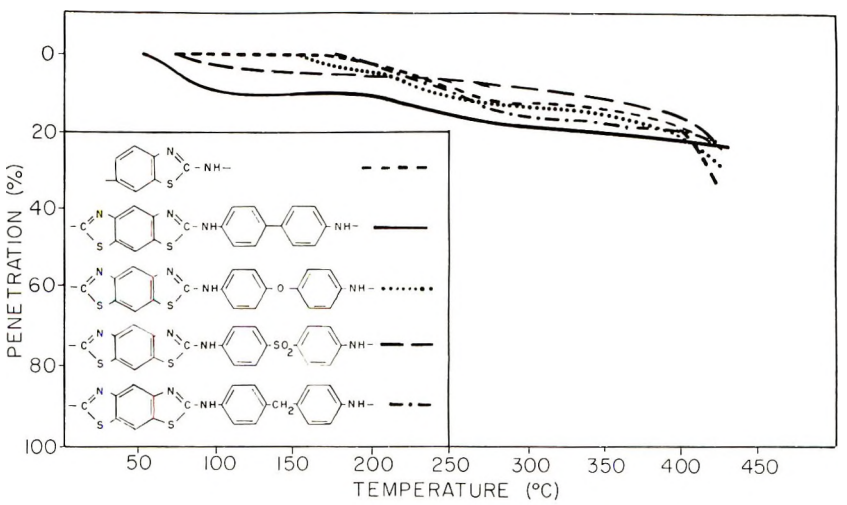

Fig. 4. Composite softening curves. ΔT = 150°C/hr, in air.

~1440 and 1490 cm^{-1} attributable to phenyl groups and a band at 1600–1620 cm^{-1} characteristic of —C=C— and —C=N— stretching vibrations.[8] The spectra also exhibited bands at 815–830 cm^{-1} attributable to benzothiazole ring deformation[2] and at 3300–3500 cm^{-1} indicative of the imino linkage in the polymer.[8] Several representative polymer spectra are shown in Figures 1 and 2.

Elemental Analysis. The elemental analyses of the polymers were fairly consistent with the proposed structures. In all cases, the hydrogen content was higher than the theoretical value and excess oxygen was shown to be present in some of the polymers. This could be taken as evidence of water being present in the materials and would help to explain the generally low values for the other elements in the polymers. This presence of water is further indicated by the considerable increase in the hydrogen content of the polyiminobenzothiazoles upon their remaining open to the air at room temperature for several hours.

Thermal Properties. The thermal properties of the polymers were evaluated by means of thermogravimetric analysis (TGA), differential thermal analysis (DTA), and softening under load.[9] Composite TGA curves and softening under load curves are shown in Figures 3 and 4. The polyiminobenzothiazoles began to soften in the temperature range of 150–200°C but showed only a limited softening up to the decomposition point of 400°C. Within this general softening range, these polymers exhibited distinct DTA endotherms. The only DTA transition formed outside the softening ranges was a decomposition endotherm at 470°C exhibited by the polymer with a sulfone linkage (trial 4). TGA curves of the samples run under nitrogen show initial breakdown in the region of 375–400°C with weight losses of 37–60% being recorded at 900°C. A TGA run in an air atmosphere on the polymer from 2-phenoxy-6-aminobenzothiazole indicated catastrophic breakdown commencing at 300°C with no residue at 900°C.

The polyiminobenzothiazoles were of lower thermal stability than polybenzothiazoles of similar molecular weights. For example, the product from 2-phenoxy-6-aminobenzothiazole (η_{inh} = 0.29 in HMP) exhibited initial breakdown under nitrogen at 375°C with the inversion point of the TGA curve being at 420°C. A 40% weight residue remained at 900°C. In contrast, the TGA curve (obtained under identical conditions) of poly-2,2′-(*p*-phenylene)-6,6′-bibenzothiazole[1] (η_{inh} = 0.35 in H_2SO_4) showed initial breakdown at 410°C and an inversion point of 540°C. A 67% weight residue remained at 900°C.

EXPERIMENTAL

Intermediates, Solvents, and Monomers

The polymerization solvents and acceptors were obtained from standard commercial sources and were purified by vacuum distillation over phosphorus pentoxide with only the center fraction being retained. The purified materials were stored over molecular sieves in amber-colored bottles.

N,N'-Diphenylbenzidine, benzidine, 4,4'-diaminodiphenyl ether, 4,4'-diamino-diphenylmethane, and 4,4'-diaminodiphenylsulfone were obtained from standard commercial sources and recrystallized twice from the following solvents: *N,N'*-diphenylbenzidine, toluene; benzidine, absolute ethanol; 4,4'-diaminodiphenylether, dilute ethanol; 4,4'-diaminodiphenylmethane, benzene; 4,4'-diaminodiphenylsulfone, methanol. 3,3'-Dimercaptobenzidine[10] and *N,N'*-diethylbenzidine[11] were prepared by methods previously reported in the literature.

The remaining chemicals were obtained from standard chemical sources and used as received.

2-Phenoxybenzothiazole. 2-Chlorobenzothiazole (5.07 g, 0.03 mole) and phenol (2.82 g, 0.03 mole) were heated under nitrogen at 150°C with stirring. The temperature was gradually raised to 250°C over the course of 4 hr. The product was distilled, yielding 5 g of water-white product, bp 149–150°C/0.03 mm.

ANAL. Calcd: C, 68.72%; H, 3.96%; N, 6.17%; S, 14.10%. Found: C, 68.42%; H, 3.90%; N, 6.30%; S, 14.03%.

2,6-Dichlorobenzobisthiazole. This monomer was prepared in low yield by a modification of the procedure given by Grandolini.[7]

2,6-Dimercaptobenzobisthiazole[7] (10.0 g) was added slowly with vigorous stirring and cooling to sulfuryl chloride (60 ml). The brown slurry was stirred at room temperature for 18 hr and then poured onto 300 ml of cracked ice. The precipitate was isolated by filtration and dried in a vacuum desiccator. The dry brown powder (4.60 g) was slurried in 300 ml of ether and poured on a column of alumina (activity grade II). The ether soluble portion was eluted through the alumina with 300 ml of ether which was treated with charcoal and reduced in volume to 50 ml. The white precipitate was filtered off and upon drying yielded 1.0 g of snow-white product, mp 182–183°C (lit.[7] 179–183°C).

ANAL. Calcd: C, 36.78%; H, 0.77%; N, 10.73%; S, 24.52%; Cl, 27.20%. Found: C, 36.72%; H, 0.80%; N, 10.10%; S, 24.78%; Cl, 27.22%.

2,6-Diphenoxybenzobisthiazole. 2,6-Dichlorobenzobisthiazole (0.5 g) was added to molten phenol (8 g) and this solution was stirred and heated at reflux under nitrogen until no more hydrogen chloride gas could be detected by litmus (4 hr). The cooled solution was added to 100 ml of 50% methanol. The precipitate was isolated by filtration and recrystallized from methanol to yield 0.4 g of silvery plates, mp 185–186.5°C.

ANAL. Calcd: C, 63.83%; H, 3.19%; N, 7.45%; S, 17.02%. Found: C, 63.76%; H, 3.42%; N, 7.82%; S, 17.40%.

2-Chloro-6-aminobenzothiazole. 2-Chloro-6-aminobenzothiazole could be prepared readily by the procedure given by Katz.[12] Recrystallization from dilute ethanol gave a 54% overall yield of white needles, mp 155–156°C (lit.[11] 155–157°C).

2-Phenoxy-6-aminobenzothiazole. 2-Chloro-6-nitrobenzothiazole (10.7 g, 0.05 mole) was dissolved in 500 ml of 95% ethanol. To the hot solution was added phenol (7.0 g, 0.075 mole) and potassium hydroxide (4.2 g, 0.075 mole) dissolved in 50 ml of water. The solution was refluxed overnight and treated with charcoal. The charcoal was removed by filtration and about 200 ml of water added to the filtrate. The volume was reduced until crystallization was imminent. Cooling of the solution followed by filtration yielded 12 g of 2-phenoxy-6-nitrobenzothiazole as orange needles, mp 114–115°C (lit.[13] 116–117°C).

Powdered iron (25 g) and glacial acetic acid (7.0 ml) were heated in 150 ml of water at 85°C for 15 minutes. Then finely powdered 2-phenoxy-6-nitrobenzothiazole (12.0 g) was added portionwise over 30 min and the mixture heated and stirred at 90°C for 1 hr. The reaction mixture was cooled to 0°C and filtered. The dried residue was extracted with hot benzene. The benzene solution was treated with charcoal and then washed with dilute potassium hydroxide solution followed by water. After the colorless solution was dried over anhydrous sodium sulfate, hydrogen chloride gas was passed through it precipitating the white hydrochloride salt (mp 233°C with decomposition). It was isolated by filtration, dried, and dissolved in water. The aqueous solution was filtered and the free amine precipitated with dilute potassium hydroxide solution. Approximately 7.0 g of light-tan powder was collected, mp 78–79°C. It could be recrystallized from benzene–ligroin but this did not seem to improve the sample purity.

Anal. Calcd: C, 64.46%; H, 4.13%; N, 11.57%; S 13.22%. Found: C, 64.45%; H, 4.11%; N, 11.38%; S, 13.37%.

Preparation of Model Compounds

2-Anilinobenzothiazole. The procedure given by Hoffmann was used for the preparation of this compound.[6] 2-Chlorobenzothiazole (1.69 g, 0.01 mole) and aniline (1.86 g, 0.02 mole) were heated under nitrogen at 150°C for 1 hr. The grey-colored solid was recrystallized from dilute ethanol to give 1.95 g (87% yield) of white needles, mp 159.5–161°C (lit.[6] 159°C).

Anal. Calcd: C, 69.03%; H, 4.47%; N, 13.39%; S, 14.61%. Found: C, 69.49%; H, 4.66%; N, 12.88%; S, 13.98%.

2,6-Dianilinobenzobisthiazole. This model compound was prepared by the procedure given by Grandolini.[7] 2,6-Dichlorobenzobisthiazole (0.261 g, 0.001 mole) and aniline (0.558 g, 0.006 mole) were heated under nitrogen to 190°C for 30 min. The cooled reaction mixture was recrystallized from dilute ethanol to give 0.33 g (89% yield) of white crystals with a mp of 288–290°C (lit.[7] 288–289°C).

Anal. Calcd: C, 64.17%; H, 3.74%; N, 14.97%; S 17.11%. Found: C, 64.18%; H, 3.84%; N, 14.76%; S, 17.40%.

4,4′-Bis(2-iminobenzothiazolyl)biphenyl. 2-Phenoxybenzothiazole (1.13 g, 0.0050 mole) and benzidine (0.46 g, 0.0025 mole) were heated under nitrogen at 150°C for one hour. The product was recrystallized from glacial acetic acid to give 0.95 g (85% yield) of a white powder, mp 343.5–345°C.

ANAL. Calcd: C, 69.33%; H, 4.00%; N, 12.44%; S, 14.22%. Found: C, 68.84%; H, 3.97%; N, 12.39%; S, 14.41%.

2,2′-Dianilino-6,6′-bibenzothiazole. 3,3′-Dimercaptobenzidine (1.24 g, 0.005 mole) and phenyl isothiocyanate (1.35 g, 0.010 mole) were heated under nitrogen in a reaction tube at 150°C for one hour. The temperature was raised to 325°C and heating continued for 1 hr. A reduced pressure of 0.03 mm was applied for the final 30 min. Approximately 0.40 g (18% yield) of white sublimate with mp 328–330°C was obtained.

ANAL. Calcd: C, 69.33%; H, 4.00%; N, 12.44%; S, 14.22%. Found: C, 70.09%; H, 4.08%; N, 12.45%; S, 14.45%.

Preparation of Polymers

The following are representative polymerization procedures for the preparation of polyiminobenzothiazoles.

Solution Polymerization of 4,4′-Diaminodiphenyl Ether and 2,6-Dichlorobenzothiazole. 4,4′-Diaminodiphenyl ether (0.500 g, 0.0025 mole) and 2,6-dichlorobenzobisthiazole (0.652 g, 0.0025 mole) were dissolved in 30 ml of TMS and 5 ml of NMP. This polymerization mixture was heated with stirring under dry nitrogen at 230°C for 25 minutes at which time a yellow precipitate formed. The slurry was added to methanol and the polymer isolated by filtration. It was extracted in a Soxhlet with methanol for 84 hr and dried at 180°C in a vacuum oven for 8 hr. Approximately 0.7 g of a tan powdery material was obtained. The DMAC-soluble portion (95%) had an inherent viscosity of 0.24 in that solvent at 25°C.

ANAL. Calcd: C, 61.86%; H, 3.09%; N, 14.43%; S, 16.49%; Cl, 0.00%. Found:* C, 61.78%; H, 3.87%; N, 12.51%; S, 16.51%; Cl, 0.00%.

Thermal Polymerization of 4,4′-Diaminodiphenylmethane and 2,6-Diphenoxybenzobisthiazole. Equimolar quantities of 4,4′-diaminodiphenylmethane (0.691 g, 0.0035 mole)and 2,6-diphenoxybenzobisthiazole (1.312 g, 0.0035 mole) were mixed well in a polymer tube. Heating was commenced under nitrogen in a preheated aluminum block at 150°C and the temperature gradually increased. At 190°C, reaction occurred with the evolution of phenol and solidification of the polymerization mixture. After 1 hr, the polymer was taken out, ground to a fine powder, and then heated at 200°C for 1 hr. It was extracted in a Soxhlet with methanol for 48 hr and dried for 6 hr at 180°C in a vacuum oven. Approximately 1.2 g of a light-brown powder was obtained. The HMP-soluble portion (40%) had an inherent viscosity of 0.32 in that solvent at 25°C.

* Values found for the combined soluble and insoluble portions.

ANAL. Calcd: C, 65.28%; H, 3.63%; N, 14.51%; S, 16.58%. Found:* C, 65.39%; H, 3.68%; N, 13.80%; S, 15.62%.

Melt-Polymerization of 2-Phenoxy-6-aminobenzothiazole. The monomer (5.0 g) was heated under nitrogen in a polymer tube. At approximately 280°C, evolution of phenol occurred with subsequent solidification of the polymerization mixture. The yellow solid was heated for 1 hr at 280°C, at which time it was taken from the polymer tube, finely crushed, and then heated for 30 min at 280°C. It was 70% soluble in DMAC and the filtered solution was added dropwise to a tenfold excess of methanol. The precipitate was isolated by filtration, dried, and finely ground. It was extracted with methanol in a Soxhlet for 100 hr and dried in a vacuum oven at 150°C for 8 hr. The greenish-yellow powder (2.8 g) had an inherent viscosity of 0.29 in HMP at 25°C.

ANAL. Calcd: C, 56.76%; H, 2.70%; N, 18.92%; S, 21.62%. Found: C, 57.42%; H, 3.45%; N, 17.21%; S, 20.21%.

The author wishes to thank Dr. G. F. L. Ehlers for information and advice concerning the thermal properties of the polymers.

References

1. E. Brumfield, A. V. DiGiulio, P. M. Hergenrother, R. D. Lake, B. Rudney, and S. C. Temin, ASD-TDR-63-249 (1963).
2. Y. Imai, I. Taoka, K. Uno, and Y. Kuakura, *Makromol. Chem.*, **83**, 167 (1965).
3. Y. Imai, K. Uno, and Y. Iwakura, *Makromol. Chem.*, **83**, 179 (1965).
4. P. M. Hergenrother, W. Wrasidlo, and H. H. Levine, *J. Polym. Sci. A*, **3**, 1665 (1965).
5. P. M. Hergenrother and H. H. Levine, *J. Polym. Sci. A*, **4**, 2341 (1966).
6. A. W. Hoffmann, *Ber.*, **12**, 1130 (1879).
7. G. Grandolini, *Gazz. Chim. Ital.*, **90**, 1221 (1960).
8. L. J. Bellamy, *The Infra-red Spectra of Complex Molecules*, 2nd Ed., Methuen, London; Wiley, New York, 1958.
9. G. F. L. Ehlers and W. M. Powers, *Materials Res. Stds.*, **4**, 298 (1964).
10. Houben-Weyl, *Methoden der Organischen Chemie*, E. Miller, Ed., George Thieme, Stuttgart, 1955, Vol. IX, p. 39.
11. R. Rabjohn, Ed., *Organic Syntheses, Coll. Vol. IV*, Wiley, New York, 1963, p. 283.
12. Leon Katz, *J. Amer. Chem. Soc.*, **73**, 4007 (1951).
13. H. Taniyama, *J. Pharm. Soc. Japan*, **67**, 123 (1947).

Received June 9, 1969
Revised September 11, 1969

Contents (continued)

The *Journal of Polymer Science* publishes results of fundamental research in all areas of high polymer chemistry and physics. The *Journal* is selective in accepting contributions on the basis of merit and originality. It is not intended as a repository for unevaluated data. Preference is given to contributions that offer new or more comprehensive concepts, interpretations, experimental approaches, and results. Part A-1 *Polymer Chemistry* is devoted to studies in general polymer chemistry and physical organic chemistry. Contributions in physics and physical chemistry appear in Part A-2 *Polymer Physics*. Contributions may be submitted as full-length papers or as "Notes." Notes are ordinarily to be considered as complete publications of limited scope.

Three copies of every manuscript are required. They may be submitted directly to the editor: For Part A-1, to C. G. Overberger, Department of Chemistry, University of Michigan, Ann Arbor, Michigan 48104; and for Part A-2, to T. G Fox, Mellon Institute, Pittsburgh, Pennsylvania 15213. Three copies of a short but comprehensive synopsis are required with every paper; no synopsis is needed for notes. Books for review may also be sent to the appropriate editor. Alternatively, manuscripts may be submitted through the Editorial Office, c/o H. Mark, Polytechnic Institute of Brooklyn, 333 Jay Street, Brooklyn, New York 11201. All other correspondence is to be addressed to Periodicals Division, Interscience Publishers, a Division of John Wiley & Sons, Inc., 605 Third Avenue, New York, New York 10016.

Detailed instructions in preparation of manuscripts are given frequently in Parts A-1 and A-2 and may also be obtained from the publisher.